Andrzej Golenko

Fundamentals of Machine Design

A Coursebook for Polish and Foreign Students

Reviewed by Dr Michał Banaś, Wroclaw University of Technology

2010

Contents (part 1: units 1 to 15)

4

Andrzej GOLENKO

FUNDAMENTALS OF MACHINE DESIGN
A Coursebook for Polish and Foreign Students

Foreword

This coursebook has been designed and written to support the learning process in the Fundamentals of Machine Design course. It is therefore limited and dedicated to topics included in the syllabus of the course only. The arrangement of lectures is also governed by assignments offered concurrently in the design class and experiments conducted in the laboratory.

Each chapter comprises the body of a lecture together with illustration material. Some of the drawings shall be completed concurrently with my explanations during the lecture. These are denoted by a dark triangle (stub drawings). Whenever I expect student's participation in the solving of a problem, you will find a question mark. To enhance practical skills of the student, most of the lectures are provided with relevant numerical problems (NP) and a few numerical problems to be solved at home (HW). Model solutions to these problems are available at my office.

Notation and symbols: As the majority of student attending this course are those Polish students who are willing to learn and practice their skills in technical English, symbols, subscripts and superscripts in this course book relate mostly to Polish textbooks. There is no separate list of symbols used. These are explained either directly in the text or in the accompanying drawings.

The content of this coursebook is split into two parts, 15 lecture units for the fall and spring semesters in each part. Some of the units may, however, need more than 2 lecture hours while other, less than 2 hours.

There is a short glossary of technical terms at the end of each chapter. Those students who do not feel sufficiently confident with English may use a word-per-word translation of this coursebook offered to those students who register this course with Polish as the language of instruction.

The quality of the English language in this couresbook is the sole responsibility of the author.

Course presentation, objectives and learning outcomes

The Fundamental of Machine Design is a two-semester course that synthesises all the previous courses of the mechanical engineering curriculum: Engineering Drawing, Materials Science, Strength of Materials, Mechanics, etc. The main objective of this course is to provides rules for the design of general-purpose machine elements such as joints, shafting, coupling & clutches, roller contact and sliding bearings (the first semester) and transmissions (the second semester). Excluded are specific machine elements such as pump rotors, engine

pistons etc, which are covered in specialized courses. After the successful completion of the course, the student shall be able to cover all steps of the analysis stage of the design process with a special stress on its embodiment (detailed) phase, i.e. the selection of form and dimensions. The mastering of topics discussed in this course is a precondition to a successful design, but the course itself, unfortunately, is only part of the whole design process.

Textbooks recommended

1. Dziama A., Osinski Z. Podstawy Konstrukcji Maszyn, WNT, 1999
2. Dietrych J., Kocańda S., Korewa W.: Podstawy Konstrukcji maszyn, WNT, Warszawa, 1966
3. Shigley J.E.: Standard Handbook of Mechanical Engineering, McGraw Hill Book Company, 1996
4. Mott R.L.: Machine Elements in Mechanical Design, Prentice Hall, 2003

A detailed list of references is included at the end of the coursebook

Course completion requirements

Acceptance of the lecture: regular attendance, submission of homework assignments
Acceptance of the course:
Attendance: 10 points
Homework assignments (5 assignments min.): 15 points
Final examination (75 points)
(Make-up examinations only upon presentation of a medical certificate!)

Grading rules (ECTS equivalents in brackets):
Less than 40: 2.0 (F)
40 to 60: 2.0 (F+)
60 to 75: 3.0 (D to C)
75 to 80: 3.5 (CC)
80 to 85: 4.0 (B)
85 to 90: 4.5 (A)
over 90: 5.0 (AA)

In the case of an F+ note one additional (a re-sit) examination will be administered if the total number of points after the final examination is not less than 40.

Contact: office no 206, building B-5, Łukasiewicza 7/9; andrzej.golenko@pwr.wroc.pl

Office hours:

1. The Design Process

1.1. General

There are many models that aim at the description of the actual design process. Most of them are multi-stage schemes with many feedbacks, complicated loops etc. trying to reflect the way an idea (an abstract) is converted into a reality (an artefact). What we need right now is a simple flow-chart (Fig. 1.1) that we shall follow during the design class.
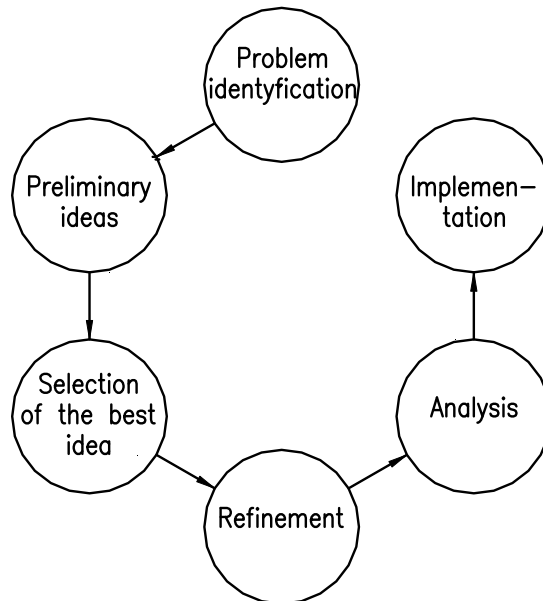
Fig. 1.1. The design process [6]

1.2. Problem identification

The first four steps of this scheme shall be termed as conceptual design, and these shall be more broadly discussed in advanced Design Methodology courses. The next step (Analysis) is termed as the embodiment phase or detailed design. Following a definition given by J. Dietrych [1], the embodiment design consists in the selection of geometry (form and size) and materials together with some initial loading that is inherent with a failure-free operation of a designed object. This phase together with design classes is the core of the Fundamentals course. The last step (Implementation) deals with the preparation of assembly and working drawings. These topics have already been discussed in engineering drawing courses but, if necessary, shall be discussed again during design classes.

Let's start with the conceptual design phase. There is a need to perform some useful work. Within the scope of the first stage we have to identify the problem, i.e. determine the external load, limitations in terms of geometry, manufacturing methods, etc. (design specifications). Let our problem be the replacement of an automobile tire. Be it a medium size car, the mass of which is approx. 1200 kg (Fig. 1.2).
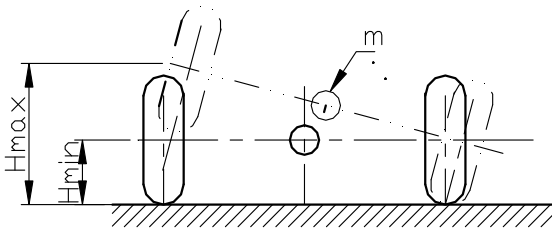
Fig. 1.2. Jacking a car

If the car is jacked at the centre of gravity, the load shall be divided by two. Taking some allowance for additional load conditions, we may assume F_{max} = 8 kN (to be applied somewhere at the end of the first part of the total travel of the jack). The minimum and maximum height (rise) of the jack shall be 150 mm and 400 mm respectively. These data are usually given directly in the student's assignment sheet.

1.3. Preliminary ideas

In certain fields of technology (hydraulics, electronics) it is possible to find and apply an algorithm of the solution finding process. It is more difficult in mechanical engineering, though some attempts have been done, especially in the Theory of Machines and Mechanisms. Certain complex problems call for an inter-disciplinary co-operation. The brainstorming approach has been widely known and employed in practice. In most cases, however, new solutions grow on old ones. We rely on our experience, observations and common sense. At this stage the solution must be free hand sketched or by using simple drawing conventions. It must be viable from the point of view of kinematics!

Let's discuss a few possible solutions of our problem (these are typical drawings presented by the students at this phase).

a)   b)   c)
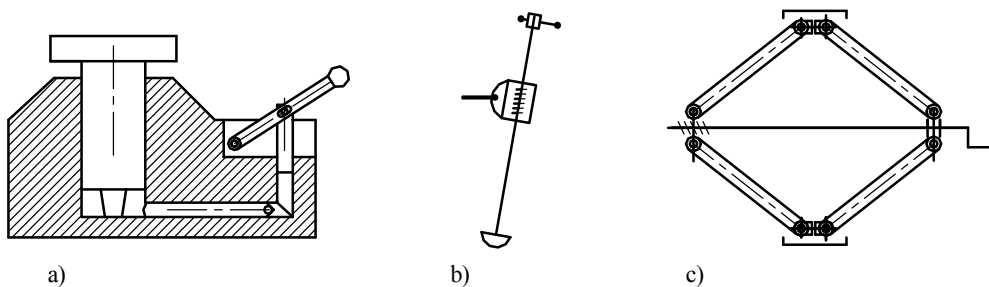
Fig. 1.3. Preliminary ideas. An hydraulic (a), tower (b), and scissors jacks (c)

A minimum requirement to accept the idea of a hydraulic jack (Fig. 1.2a) is to include a non-return valve in the hydraulic line. With the tower jack (Fig. 1.2b), it is important to provide a pin at the connection of the nut body with the lifting bar. The last idea (Fig. 1.2c) is usually redundant in mobility. Students forget to constrain this mobility by adding toothed sections at the bottom and upper transverse bars.

1.4. Selection of the best idea

Which solution is the best? No decision is possible until a set of criteria have been established. Some of them, however, are more important than the others so needed are quantifiers (weights). Let's have the following criteria: price (low price), weight, and convenience of usage (universality). We shall compare them on a zero/one basis to appropriate relevant weights (a criteria weighing method [3]):

Table 1.1. Weighing the criteria

Criteria				Weight
Price	1	0		1/3
Weight	0		0	0
Universality		1	1	2/3

Thus the first criterion (price) is assigned with a weight of 1/3; the second is meaningless–nil, and the third–2/3. In the next step, we confront all ideas with regard to each criterion separately.

Table 1.2. Selecting the best idea

Idea no	price (x 1/3)			∑	Universality (x 2/3)			∑	Overall
Hydraulic	0	0		0	1	0		2/3	2/3
Tower	1		1	2/3	0		0	0	2/3
Scissors		1	0	1/3		1	1	4/3	5/3

The winner is the scissors jack! Figures put into theses tables are for illustration purposes only. The actual decision making process is usually time consuming and difficult.

1.5. Refinement

The selected idea has to be refined in order to meet the assumed (set) specifications. This procedure consists in the selection of an arrangement of the component elements, link lengths, angles etc., and it is done either analytically, or – my recommendation – by a scaled drawing. We have to use drawing instruments (CAD recommended) at this stage!

In a scissors jack we have to limit the minimum angle between links (be it 15º: excessive stresses) and the maximum angle (75º: poor stability). We check if the maximum height meets the speciation (it does not; the maximum height is too big). The length of the links was

reduced to 220 mm and now the maximum height agrees with the target value. The scheme obtained (Fig. 1.4) is a basis for the analysis stage of the design process.
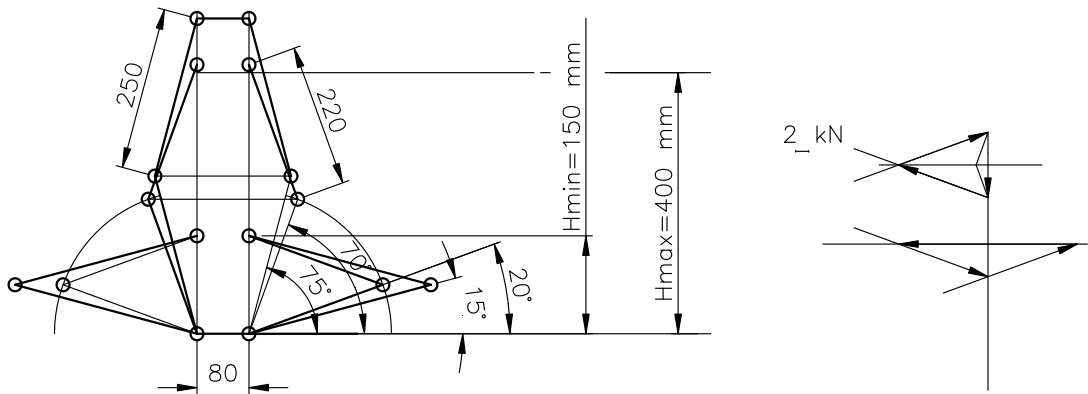

Fig. 1.4. The refinement of parameters of the selected solution

1.6. Analysis

This is the core of the design process, and at the same time, the core of our lecture. The analysis stage consists, as explained earlier, in the selection of geometry (shape and dimensions), materials and of some dynamic properties for the selected solution. Let's discuss more in detail the first two criteria.

Prior to the design stage, the force analysis has to be done. I'd recommend a graphical approach. The selected structure of our scissors jack is being loaded with a centrally located load identified in the first stage of the process and the resolution of this force into the two arms is quite simple; either by the analytical or graphical method (see Fig. 1.4).

Selection of shape. The shape should be best suited to the load transferred. There is no problem with the power screw (though we have to decide about the thread form) and pins. These are standardised. The problem is with the links. What shape is good for a compressed member (buckling)? A channel (roll-formed), a double flat bar arrangement will do.

Selection of material. The power screw must be flexible yet tough. Medium carbon plain or alloy steel might be a good choice. Links: as buckling depends on the section modulus only, low carbon steel is the best choice. Finally pins (resistance to wear): high carbon steel.

Selection of dimensions. There is a distinct difference in the way problems are solved in the Strength of Materials and Design courses. In the strength course all dimensions are usually given, and controlled are actual stresses in an element. For a simple round bar with a cross-section A subjected to a tensile load F we have: $\sigma = F / A \le k_r$; where $k_r = R_e/FS$ (R_e = the yield strength; FS = the factor of safety.)

In the design approach, assumed are limiting stresses and calculated are dimensions, here: $d \ge \sqrt[2]{4F /(\pi k_r)}$ .Unfortunately, this approach is not always possible. If given are all the necessary data (tensile/compressive load, torque), we use a complex stress formula (e.g. Huber, Mises-Hencky). In the design approach, we usually know only the tensile load. The

diameter is calculated based upon a simple formula for tensile stress, but using a very high value of the factor of safety or a correction factor to make up for additional load.

1.7. Implementation

The implementation stage consists in the preparation of assembly and working drawings. These issues were discussed in the Engineering Drawing course. A model solution of this problem is shown in Fig. 1.5.

Fig. 1.5. A scissors jack [Jiaxin Datong]

Of the many feedback and loops omitted in the presented scheme, the most important is a correlation between the last two stages of the design process. Some machine elements cannot be analysed until at least preliminary scaled drawing of them has been done. To calculate pins for bending, necessary is an arrangement of the mating links with the calculated pin. Again, these topics will be discussed in the design course.

Glossary

appropriate	przydzielić
conceptual design	projektowanie
concurrent	równoczesny
design specifications	warunki techniczne
design stress	naprężenie dopuszczalne
embodiment/detailed design	konstruowanie
enhance	podnieść (w sensie jakości)
feedback	sprzężenie zwrotne
force polygon	wielobok sił
implementation	wdrożenie
jack	podnośnik
non-return valve	zawór zwrotny
off-set	przesunięty
piston	tłok
power screw	śruba mechanizmowa
quantifier	waga
re-sit examination	egzamin poprawkowy
roller contact bearing	łożysko toczne
rotor	wirnik
sliding/ journal bearing	łożysko ślizgowe
tension	rozciąganie
truncated cone	ścięty stożek

2. Fatigue Analysis

2.1. Combined static load

The Strength of Materials course provided you with basic information on how to handle elements subjected to static loading, be it a simple load (tension, compression, torsion), combined load (tension plus bending), or complex load (tension/bending plus torsion). Let's discuss, for the sake of our first design assignment, a case of combined normal load as in the following numerical problem:

NP 2.1. Find values and plot the distribution of stresses over the cross-section of an upright shown (points A, B, and C; locate point C!). Data: F = 50 kN; l = 35 mm; b_1 = 30 mm; b_2 = 20 mm; w_1 = 85 mm; w_2 = 70 mm. Material: cast iron, grade 200. Find the value of the factor of safety (FS).
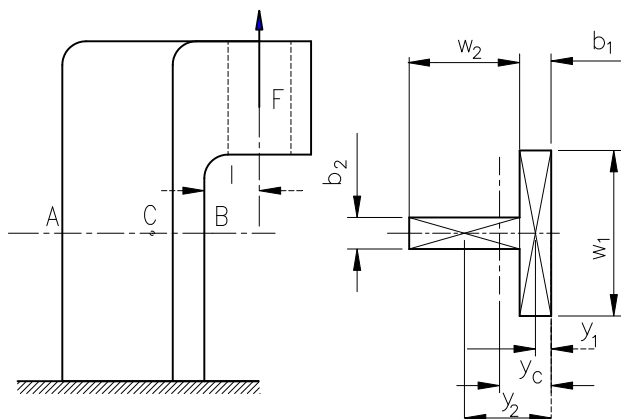
a) Centroid of the cross-section: $y_C = \dfrac{A_1 y_1 + A_2 y_2}{A_1 + A_2} = \dfrac{b_1 w_1 y_1 + b_2 w_2 y_2}{b_1 w_1 + b_2 w_2} = \dfrac{30 \cdot 85 \cdot 15 + 20 \cdot 70 \cdot 65}{30 \cdot 85 + 20 \cdot 70} = 32.75$ mm

b) Equivalent bending load: $M = F(l + y_C) = 50 \cdot 10^3 (35 + 32.75) = 3387500$ Nm

c) Component stresses. The direct stress: $\sigma_r = \dfrac{F}{A} = \dfrac{50 \cdot 10^3}{3950} = 12.65 \ \dfrac{\text{N}}{\text{mm}^2}$; the bending stress:

- moment of inertia of the cross-section: $I_{xx} = \dfrac{w_1 b_1^3}{12} + w_1 b_1 \left(y_C - \dfrac{b_1}{2} \right)^2 + \dfrac{b_2 w_2^3}{12} + b_2 w_2 (b_1 + 0.5 w_2 - y_C)^2 =$

$\dfrac{85 \cdot 30^3}{12} + 85 \cdot 30 (32.75 - 0.5 \cdot 30)^2 + \dfrac{20 \cdot 70^3}{12} + 20 \cdot 70 (30 + 0.5 \cdot 70 - 32.75)^2 = 3022413.5$ mm^4

- Section modulus of the cross-section (point A; CA = 67.25 mm):

$$W_{xx}^A = \frac{I_{xx}}{CA} = \frac{3022413.6}{67.25} = 44942.9 \quad \text{mm}^3$$

- Section modulus (point B; CB = 32.75 mm): $W_{xx}^B = \frac{I_{xx}}{CB} = \frac{3022413.6}{32.75} = 92287.4 \quad \text{mm}^3$

- Bending stress (point A): $\sigma_g^A = \frac{M}{W_{xx}^A} = \frac{3387500}{44942.9} = 75.4 \quad \frac{\text{N}}{\text{mm}^2}$

- Bending stress (point B): $\sigma_g^B = \frac{M}{W_{xx}^B} = \frac{3387500}{92287.4} = 36.7 \quad \frac{\text{N}}{\text{mm}^2}$

d) Maximum stress (points A & B):

$$\sigma_{max}^A = \sigma_r - \sigma_g^A = 12.6 - 75.4 = \ -62.8 \quad \frac{\text{N}}{\text{mm}^2}; \qquad \sigma_{max}^B = \sigma_r + \sigma_g^B = 12.6 + 36.7 = 49.3 \quad \frac{\text{N}}{\text{mm}^2}$$

e) Factor of safety: $FS = \frac{R_m}{\sigma_{max}^B} = \frac{200}{49.3} = 4.06$ (cast iron grade 200 means that its ultim. strength is 200 MPa!)

2.2. Fluctuating load

Most of the machine elements are subjected to variable, fluctuating loading. This type of loading is very dangerous not only because limiting stresses are considerably lower than those established for static loading, but also because of the nature of material failure, which is abrupt, without any traces of yielding. The phenomenon was first discovered still in the 19th century by observing poor service life of railroad axles designed based upon static design limits.

The origins of some of the most spectacular aircraft crushes of the previous decades in Poland (Iljushin 62M) and abroad (Aloha flight # 243) were in the fatigue of material (turbine shaft, fuselage subjected to repetitive pressurisations: see Fig. 2.1).

Fig. 2.1. Aloha flight # 243
[Aircraft Accident Report]

A fluctuating load (stress)

4-28-1988 After 89,090 flight cycles on a 737-200, metal fatigue lets the top go in flight.

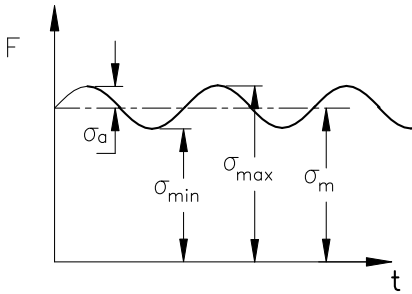pattern (Fig. 2.2) is characterised by two parameters:

Fig. 2.2. A typical load pattern

The mean stress is: $\sigma_m = (\sigma_{max} + \sigma_{min})/2$

and the amplitude stress is: $\sigma_a = (\sigma_{max} - \sigma_{min})/2$.

The ratio of the mean stress over the amplitude stress is denoted by $\chi = \sigma_m/\sigma_a$. There are two characteristic load patterns: one with $\chi = 1$, the load is pulsating; and one with $\chi = 0$, the load is reversed. The latter one is the most dangerous form of load variation.

The stress limit for fluctuating loading (the endurance limit) is defined as a value of stress that is safe for a given specimen irrespective of the number of load repetitions. It stays usually in a close relationship to the ultimate stress limit (see Table 2.1).

Table 2.1. Endurance limit vs. the ultimate strength in MPa

Type of loading/material			St 3[1]	45[2]	35HM[3]
Reversed bending	Z_{go}	0.42 R_m	170	280	500
Reversed tension/compression	Z_{rc}	0.33 R_m			
Reversed torsion	Z_{so}	0.25 R_m	100	170	260
Pulsating bending	Z_{gj}	0.7 R_m	300	480	700
Pulsating torsion	Z_{sj}	0.5 R_m	200	340	550

1) low carbon steel; 2) medium carbon steel (enhanced properties); 3) medium carbon alloy steel (chromium)

2.3. Wőhler diagram

How to establish a safe value of the limiting stress for a given load pattern? It is usually done using a testing machine (MTS, Instron). A specimen with given standard dimensions is subjected to reversed loading starting at first from a relatively high level (Z_c, Fig. 2.3.)
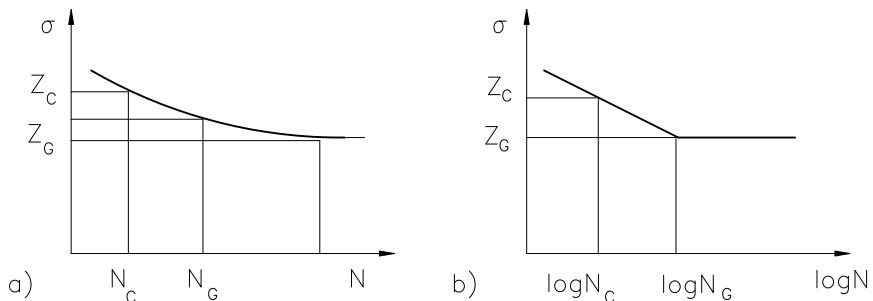

Fig. 2.3. Wöhler diagrams

The number of cycles to breakage (N_c) is being recorded. Next, the maximum stress is reduced until the specimen stays safe irrespective of the number of load cycles. The safe number of cycles is denoted as N_G, and the safe value of stress is denoted by Z_G. The testing procedure should be repeated for each load pattern and for each value of the coefficient χ. Usually, the latter is done for reversed and pulsating load only. The Wőhler diagram in the logarithmic scale is a straight line (Fig. 2.3b.)

2.4. Fatigue diagrams

The results of testing for the endurance limit are summarised in fatigue diagrams. These are plotted either in the σ_{max}, σ_{min} (ordinate); σ_m (abscissa) coordinate system (Smith) or in the σ_a (ordinate) and σ_m (abscissa) coordinate system (Haigh, Soderberg,). The latter ones are shown in Fig. 2.4.

Fig. 2.4. Construction of fatigue diagrams: Haigh (dashed line), Soderberg
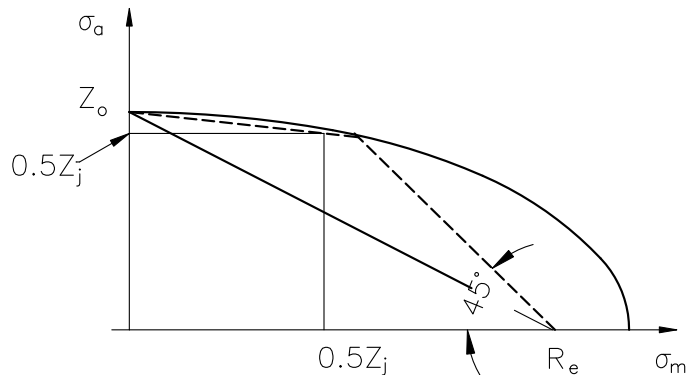
The ordinate axis represents a reverse cycle, and the limiting stress value is that of the endurance limit Z_o for a given type of load (tension, bending, torsion). The abscissa represents static loading, and the limiting stress value is that of the ultimate stress R_m or, to be on the safe side – the yield stress R_e. Each of the two plots represents a simplification of the actual plot (an ellipsis quadrant) and is on the "safe side". In the Haigh's diagram (a dashed line), the safe area is limited by two lines: one is traced from Z_o through a point with coordinates $0.5Z_j$, $0.5Z_j$ and the second line is traced at an angle of 45° from R_e. The Soderberg line is the most conservative simplification: it joins directly Z_o and R_e and best serves my teaching objectives (qualitative understanding of the problem rather than quantitative accuracy at the expense of more complex formulas).

2.5. Endurance limit for a machine element (modification factors)

Machine elements are significantly different to a tested specimen in terms of size, surface quality, shape, and the presence of so called "stress risers". These are all abrupt changes in the cross-section, discontinuity in the material geometry (small holes) or structure (case hardening) that form the nucleus of the propagating fatigue crack.

The stress concentration factor α_k gives a ratio of the maximum stress over the medium stress in a cross-section of a e.g. flat bar shown in Fig. 2.5: $\alpha_k = \sigma_{maz}/\sigma_n$. This stress concentration can be attributed to combined loading of extreme fibres of the bar (see Fig. 2.5b) and is a function of geometrical parameters of a stress riser (r, R, ρ for the bar in Fig. 2.5).
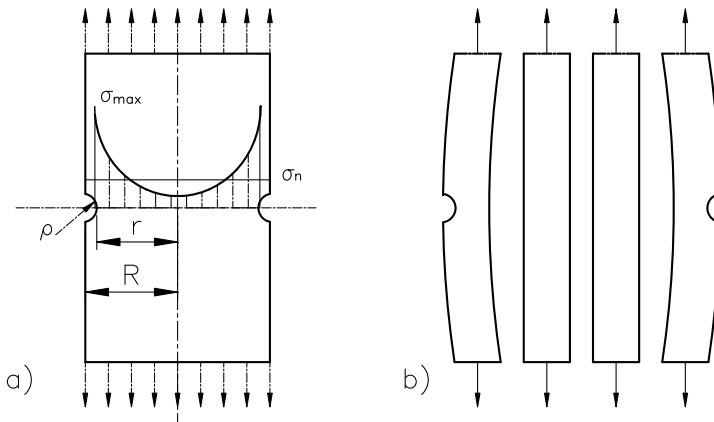
Fig. 2.5. Stress concentration factor

It has been established that the actual influence of the stress concentration factor is not as high as one might have expected. This is due to a different response of materials against stress risers. Some materials are highly sensitive to stress concentration (glass), some of them are altogether insensitive (cast iron; discontinuities inherent to the internal structure of the material). This sensitivity to stress risers is expressed by the sensitivity factor η_k. A sensitivity modified stress concentration factor is: $\beta_k = 1 + \eta_k(\alpha_k - 1)$. If surface finish is accounted for, the resultant stress concentration factor is: $\beta = \beta_k + \beta_p - 1$. The last factor that in a quantitative way modifies the endurance limit is the size factor (γ, $1/\varepsilon$). The larger is the element, the lower is the limit. Other factors are assessed in a qualitative way. Series notches, shot penning, surface hardening, case hardening (carbonisation) improve the endurance limit due to compressive stresses present at the surface of an element. Parallel notches, corrosion, galvanic coating (tensile stresses), reduce the limit. A collection of different stress concentration diagrams is provided in Appendix 1.

As the effect of stress concentration is valid for fluctuating load only, a usual approach is to reduce the endurance limit at the ordinate axis of the Soderberg diagram, and to leave the abscissa unchanged. We obtain thus a diagram valid for a machine element. The best solution, however, is to test actual machine elements under load pattern registered during real operational conditions. This is done in the aircraft and automobile industry but the application range of such testing is limited to the tested element only.

2.6. Safety factor

The factor of safety (*FS*) represents a ratio of the safe stress (deformation, stability) to its actual value. The less we know about the actual load and material the higher the factor of safety. In some applications it may be as high as 7, in other, as low as 1.1. By the introduction of design stresses (k_r, $k_g = R_e/FS$.) all European engineers had been spared the trouble of selecting the factor of safety. Sufficient is not to exceed the safe value of the design stress. In the USA, in each problem the factor of safety must be either assumed or controlled and compared to a safe value.

Fig. 2.6. Factor of safety: a graphical representation

For any given fluctuating load cycle the factor of safety is defined as a ratio of the maximum safe stress (point L) to the actual maximum stress (point C):

$$FS = \frac{OL' + LL'}{OC + CC'} = \frac{OL}{OC}$$

Based on the above proportion, any cycle can be transformed into an equivalent reversed cycle (its amplitude shown with the leader line). The formula for the *FS* is:

$$FS = \frac{Z_o}{\beta\gamma(\sigma_{aC} + \tan\psi \cdot \sigma_{mC})}; \quad \text{where}: \ \tan\psi = \frac{Z_o}{\beta\gamma \cdot R_e}$$

NP 2.2. The beam shown has a circular cross-section and supports a load of $F = 15$ kN that is repeated (zero-maximum). The beam is machined from AISI 1020 (20) steel, as rolled. Determine the diameter d if $\rho = 0.2\ d$ $(\rho = 0.4\ r$ in diagram A1.2; page 162$)$, the shoulder height is $0.25d$ ($R/r = 1.5$ in A1.2)) and $FS = 2$. Draw to scale Soderberg's diagram for this problem. Data: $a = 200$ mm; $b = 400$ mm; $l = 150$ mm; $R_e = 360$ MPa; $R_m = 450$ MPa; $Z_{go} = 228$ MPa.

Reactions: $R_A = 10$ kN; $R_B = 5$ kN

Bending moment in section I-I: $M = R_A l = 10 \cdot 10^3 \ 150 = 1500 \cdot 10^3$ Nmm

Theoretical stress concentration factor (Appendix: Fig. 1.2A): $\alpha_k = 1.5$ $(R/r=1.5; \rho/r = 0.4)$

Notch sensitivity factor (Appendix: Fig. 1.5A): $\eta = 0.65$

Stress concentration factor: $\beta_k = 1 + \eta(\alpha_k - 1) = 1 + 0.68(1.5 - 1) = 1.34$

Surface finish factor: $\beta_p = 1.15$ (Appendix: Fig.1.7A). See that the abscissa (R_m) is still in obsolete units (kG/mm^2; multiply by 10 to get MPa. Material is considered as rolled but after rough turning.)

Resultant stress concentration factor: $\beta = \beta_k + \beta_p - 1 = 1.34 + 1.15 - 1 = 1.45$

As the problem is of design nature, the size factor shall be omitted, i.e. we assume $\gamma = 1$.
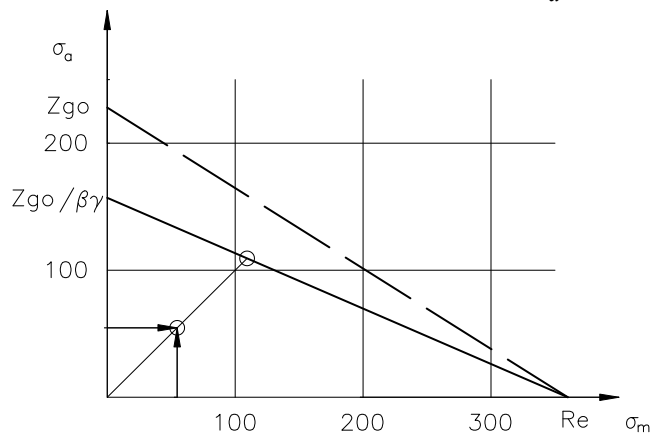
Amplitude stress (as a function of the beam diameter) : $\sigma_a = \sigma_m = \dfrac{\sigma_{max}}{2} = \dfrac{M}{2 \cdot Z_{xx}} = \dfrac{1500 \cdot 10^3 \cdot 32}{2 \cdot \pi \cdot d^3} = \dfrac{7639437}{d^3}$

Inclination of the Soderberg line: $\tan \Psi = \dfrac{Z_{go}}{\beta \gamma R_e} = \dfrac{228}{1.45 \cdot 1 \cdot 360} = 0.437$

From the formula for FS we isolate d:

$$d = \sqrt[3]{\dfrac{7639437 \cdot \beta \gamma \cdot FS(1 + \tan \psi)}{Z_{go}}} = \sqrt[3]{\dfrac{7639437 \cdot 1.45 \cdot 1 \cdot 2(1 + 0.437)}{228}} = 51.7 \, \text{mm}$$

Actual value of the amplitude (mean) stress (assumed d = 52 mm): $\sigma_a = \sigma_m = \dfrac{7639437}{d^3} = \dfrac{7639437}{52^3} = 54.3 \, \dfrac{\text{N}}{\text{mm}^2}$

2.8. Selection of shape for fatigue life

Design for fatigue will be explained in detail wherever applicable in this coursebook. For illustration, Fig. 2.7 shows a design feature that is the most vulnerable for against fluctuating loading, i.e., a shaft shoulder.
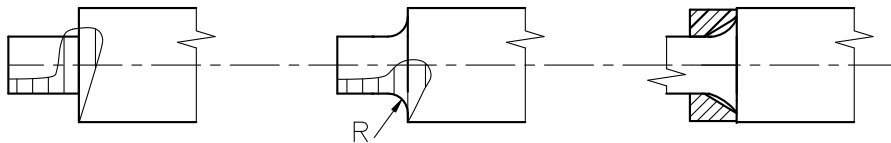
Fig. 2.7. Shaft shoulder design for fatigue

A fillet with a large radius will lower stresses at the shoulder of a shaft. This will reduce, however, the effective shoulder surface for the mounted elements. A solution may be a short distance sleeve.

HW 2.1. In a C-clamp frame shown, calculate the necessary thickness t based upon the allowable design stress in static bending k_g = 180 N/mm^2. Data: F = 3 kN; w = 25 mm; L = 50 mm. Plot the distribution of stresses over the cross-section of the frame.

Hints:
- Calculate the direct and secondary stresses
- Find the maximum stress
- Isolate t from the maximum stress formula

Answer: 8.7 mm

HW 2.2. A steel road as shown (steel 40) Q&T has been coarse machined to the following dimensions: D =25 mm; d = 20 mm; ρ = 3 mm. What may be the maximum pulsating (zero-maximum) torque for FS = 1.4? Draw to scale the Soderberg diagram. Data: R_m = 620 MPa; R_e = 390 MPa (yield limit in torsion is $R_{e\tau}$ = 0.6 R_e, i.e 234 MPa!); Z_{go} = 260 MPa; Z_{so} = 160 MPa.
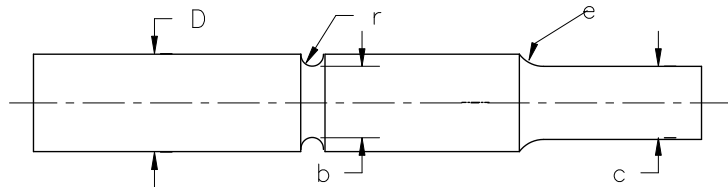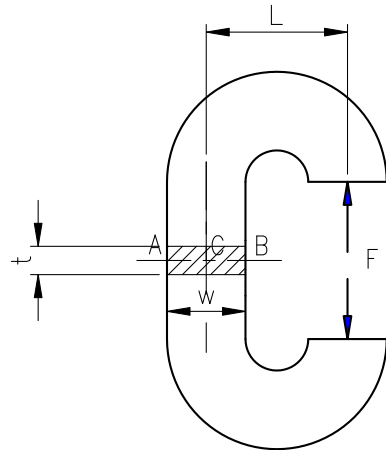
Answer: Approx. T = 173 Nm

Glossary

abrupt	nagłe	in terms	w funkcji
abscissa	odcięta	limit stress	naprężenie dopuszczalne
beam	belka	load pattern	sposób obciążenia
breakage	złamanie	mean	średnie
case hardening	utwardzanie powierzchni	notch	karb
combined	złożony	ordinate	rzędna
complex	j.w.	ratio	stosunek
compression	ściskający	sensitivity	czułość
crack	pęknięcie	series notches	karby szeregowe
crush	katastrofa	shot peening	śrutowanie
endurance limit	wytrzymałość zmęczeniowa	specimen	próbka
failure	zniszczenie	stress riser	karb
fatigue diagram	wykres zmęczeniowy	surface quality	jakość powierzchni
fluctuating	zmienny	tensile	rozciągający
fuselage	kadłub samolotu	torsion	skręcający
centroid	środek ciężkości	ultimate	tu: doraźna

3. Power Screws

3.1. Efficiency, general considerations

Power screws constitute a group of mechanisms transferring rotation into rectilinear motion (and vice-versa, though not always!). The most distinctive feature of any mechanism (power screws included) is its efficiency. Let's have a mechanism for which the output power P_2 and friction losses P_f are constant irrespective of the direction of power flow.
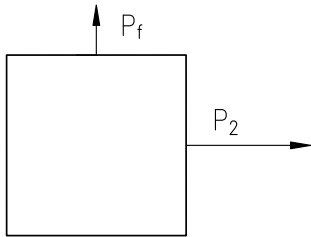

Fig. 3.1. Model of a mechanism with constant friction losses

The efficiency in the direction 1 to 2 is:

$$\eta_{12} = \frac{P_2}{P_2 + P_f} = \frac{1}{1 + \dfrac{P_f}{P_2}} \Rightarrow \frac{P_f}{P_2} = \frac{1}{\eta_{12}} - 1.$$

The efficiency in the direction 2 to 1 is: $\eta_{21} = \dfrac{P_2 - P_f}{P_2} = 1 - \dfrac{P_f}{P_2}$. If we substitute the last

term in the second equation with its value from the first equation we will get: $\eta_{21} = 2 - 1/\eta_{12}$.

What is the meaning of this formula? If the efficiency in the direction 1 to 2 is less than 0.5, then the efficiency in the direction 2 to 1 is equal to zero. This condition is known as "a self-locking condition": To drive any mechanism in the self-locking direction needed is positive power given to both the input and output of the mechanism (in other words: if you lower your car using a screw jack then there are two power inputs: the first from the gravity forces of the lowered vehicle, the other – from your hand: all power is being transformed into heat).
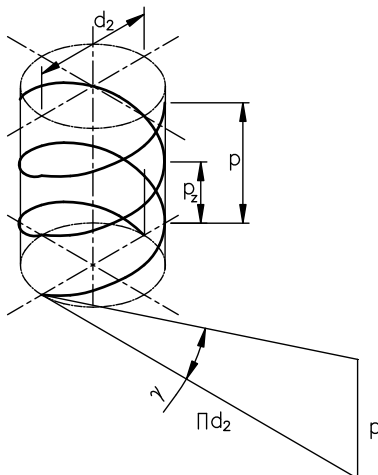
3.2. Thread basics

Fig. 3.2. Thread basics

The thread surface is a surface generated by a straight line moving at a constant pace along the axis of the cylinder. The line is inclined at a constant angle to the horizontal (different for different thread types). Any thread line is characterised by its pitch (p_z = the distance between any two consecutive thread crests), lead (p = the distance a screw thread advances axially in one turn), helix angle and sense (left- and/right-hand).

The thread line shown in Fig. 3.2 is a two-start thread line. This is possible when the helix angle is high. For small values of this angle, one start thread is only possible. In such cases the helix angle is given by: $\tan\gamma = p/(\pi d_2)$; where d_2 is the medium diameter of the thread profile. The thread form may be triangular (M); square (a non-standard form); trapezoidal (Acme) (Tr), buttress (S), round (R). The thread line may be wound on a cylinder or cone. An important conclusion: for any standard values of the pitch diameter available are different pitches. A trapezium thread Tr 16 is available with two pitches: 4 mm and 2 mm. The lower is the pitch, the lower is the helix angle!

3.3. Distribution of forces in a screw-nut mechanism

Before we start discussing the distribution of forces in a screw-nut mechanism, let me introduce a notion of the friction angle, which will be useful in the explanation of the problem, and a notion of the lead angle.

Fig. 3.3. The notion of the friction angle

The item 1 will not move rightwards until the loading force has not been tilted opposite to the direction of movement by an angle ρ, which is equal to the arctangent of the coefficient of friction (μ). The normal force of reaction (F_{21}) combines with the friction force ($F_{21}\mu$) into the resultant reaction force F_r. This will help us in answering the following question: How to determine the horizontal force (torque) in order to overcome a vertical force acting on the nut if friction between the screw and the nut is accounted for? In the further analysis this vertical force has been assigned with a subscript a, which stands for axial to avoid confusion with those power screws that operate in the horizontal position (your design project!). An assumption was also made that the thread form is a rectangular one.
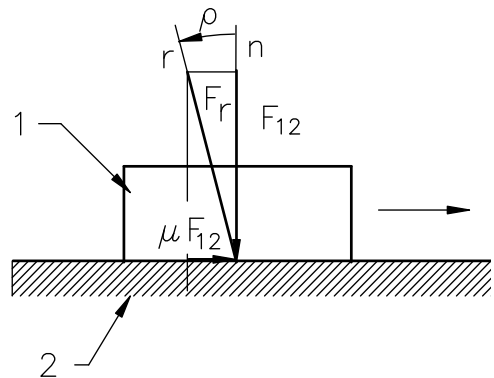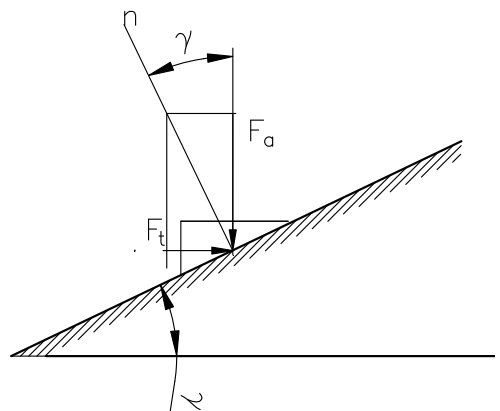
3.3.1. Upward nut movement (no friction losses).

The situation is presented in Fig. 3.4.

Fig. 3.4. Distribution of forces on a helical surface (no friction)

The only possible line of force action between items 1 and 2 is perpendicular to the surface of contact. If we project the end of force F to the normal direction we shall obtain the

resultant force, which in this case is the same as the normal force. When we project the resultant force to the horizontal direction, we shall obtain the sought, horizontal component of the resultant force. Its value is equal: $F_t = F_a \tan \gamma$.

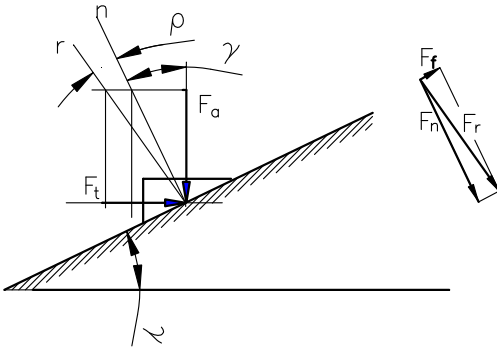### 3.3.2. Upward movement (friction losses included)

Fig. 3.5. Distribution of forces (↑, friction forces included)

The starting point is the same. This time the resultant direction is tilted by an angle ρ counter clockwise to the normal direction. The horizontal force is larger than that in the no-friction case discussed above. Again, the resultant force is made up of the normal force and the friction force. Its value is equal to: $F_t = F_a \tan(\gamma + \rho)$.

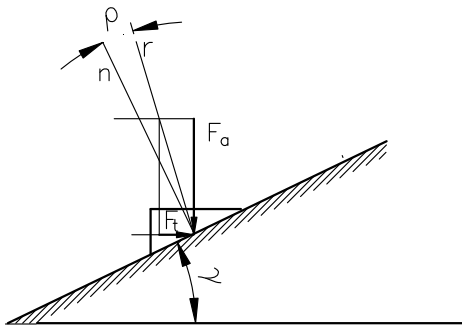### 3.3.3. Downward movement (friction losses included, no self-locking condition)

Fig. 3.6. Distribution of forces (friction losses included, no self-locking condition)

Following the same procedure but tilting this time the resultant force in the clockwise direction we shall find the horizontal force, which is less than that in the no-friction case. The formula is: $F_t = F_a \tan(\gamma - \rho)$.

3.3.4. Downward movement (friction losses included, self locking condition)

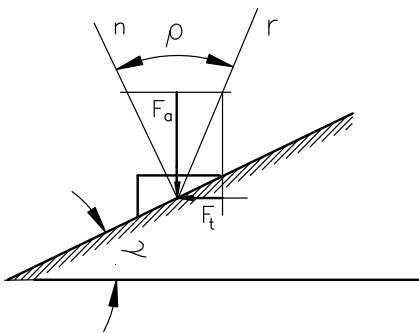Fig. 3.7. Distribution of forces (friction losses included, self locking condition

The situation is the same as above, but the friction angle is so large that the horizontal component changes its sign. The formula is the same as above.

The actual thread form is different to a rectangular one: If the surface of action is inclined not only in the axial cross-section but also in the transverse cross-section (Fig. 3.8),

then the distribution of forces is more complex and needs a three-dimensional analysis. It is possible to by-pass these difficulties by artificially increasing the coefficient of friction by a factor which is equivalent to a ratio between the resultant transverse force for a V-thread form and the vertical force for a rectangular thread form. As

Fig. 3.8. Force distribution at the surface of contact in a V-type thread

$F_n/F_a = cos\ \alpha/2$ then $\mu' = \mu/cos\ \alpha/2$ and

consequently, $\rho = \rho/cos\ \alpha/2$.

Thus the symbol ρ in the formulas given above must be assigned with an apostrophe.
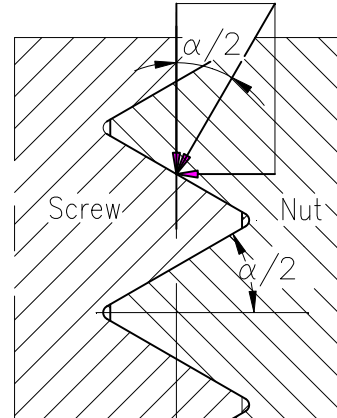
3.4. Torque

When the horizontal force has been established, it is easy to calculate the torque that has to be applied to the screw to obtain the desired motion. The force has to be multiplied by the medium thread radius. Some friction losses are also generated at the point where the thrust exerted by the screw must be transferred to the supporting structure via a thrust washer or bearing. This term in power screws depends upon individual solutions. Sometimes it is absent altogether (see a numerical problem below). For a majority of solutions, where the thrust is taken by a plain washer with the mean diameter d_m, the formula is: $T_C = F_a \mu d_m / 2$; where μ is the coefficient of friction between the two bearing surfaces. Eventually, the formula takes the following form: $T = F_a \left[\dfrac{d_2}{2} \tan(\gamma \pm \rho) + \mu \dfrac{d_m}{2} \right]$ (plus for rising and minus for lowering the load). **This formula is of uttermost importance in the first part of our lecture**.

3.5. Efficiency of a power screw mechanism

Raising the load

Input: the horizontal force acting along the circumference of the mean screw diameter. Output: the vertical force acting along one pitch of the thread (one-start threads).Taking into consideration the relation between the forces and that of the helix line geometry (Fig. 3.2) the efficiency is given by:

$$\eta_r = \frac{F_a p}{F_t \pi d} = \frac{F_a \pi d_2 \tan\gamma}{F_a \tan(\gamma + \rho')\pi d_2} = \frac{\tan\gamma}{\tan(\gamma + \rho')}$$

Lowering the load (similarly): $\eta_l = \dfrac{F_t \pi d_2}{F_a p} = \dfrac{\tan(\gamma - \rho')}{\tan \gamma}$

The design of self-locking power screws (selection of the thread form, nut form and dimensions) will be explained in the design classes offered concurrently). The design of power screws for maximum efficiency (feed mechanisms in machine tools etc.) is explained in detail in specialised courses on machine tool design. The same is valid for the most effective method for the reduction of losses in power screws, i.e. ball screws shown in Fig. 3.9.
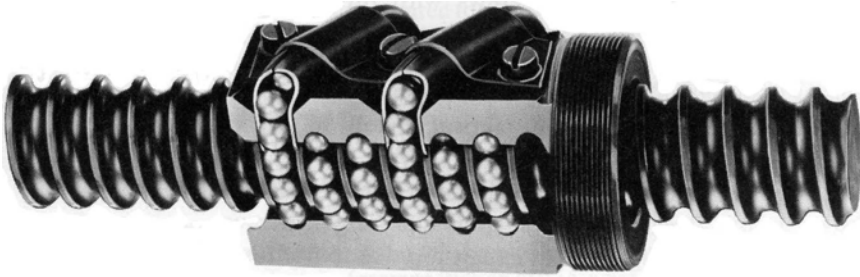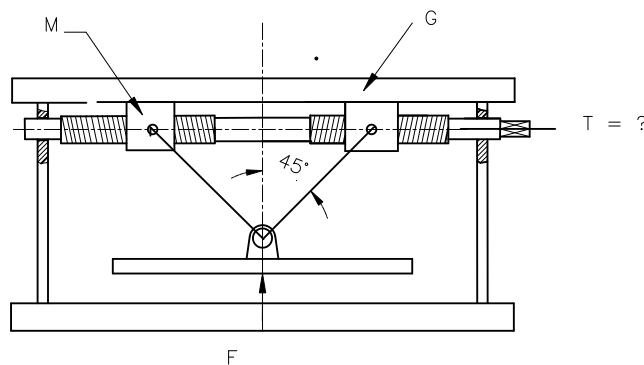

Fig. 3.9. A ball screw [Nook Industries]

NP 3.1. Find the torque that is required to exert a vertical force of $F = 3$ kN in a press shown. The coefficient of friction between the nut M and the body G is equal to 0.15, and between the screw thread and the nut, 0.1. The thread form is Tr 16x2, for which $d_2 = d - 0.65\ p;\ \beta = \pi/2$.

General hints to all power screw problems:

1. Find the force that loads axially the power screw (graphical, analytical solution). For the problem given in NP 3.1, find the vertical and horizontal components of this force. The horizontal component is equivalent to the axial force (see the lecture notes), whereas the vertical component will give additional friction.
2. Calculate the helix angle and the friction angle
3. Identify the collar friction (if any)
4. Calculate the torque

Force in the link L; $F_L = \dfrac{F}{2\cos\beta/2} = \dfrac{3000}{2\cos\pi/4} = 2121.3\,\text{N}$

Force in the screw; $F_a = F_L \sin\beta/2 = 2121.3 \cdot \sin\beta/4 = 1500\,\text{N}$

Bearing of the screw against the frame; $F_v = F_L \cos\beta/2 = 2121.3 \cdot \cos\pi/4 = 1500\,\text{N}$

Torque needed at the handle:

- Thread data (the helix angle): $\gamma = \arctan\dfrac{p}{\pi\,d_2} = \arctan\dfrac{2}{\pi\cdot 14.7} = 2.47°$

- Friction angle: $\rho = \arctan\mu = \arctan 0.1 = 5.7°$ (the transverse inclination of the thread surface neglected)

- Torque: $T = 2\left(F_a + \mu F_v\right)\dfrac{d_2}{2}\tan(\gamma+\rho) = 2(1500 + 0.15\cdot 1500)\dfrac{14.7}{2}\tan(2.47+5.7) = 3641\,\text{Nmm}$

HW 3.1. Calculate the torque that must be applied at the square end of the power screw in the position shown to overcome the resistance moment M applied to arm K. Data: $M = 10$ kNm; $\beta = 30°$; thread form Tr 16x2 (left and right hand at both ends; $d_2 = 15$mm, profile angle $\alpha = 30°$); $\mu = 0.1$; radius of arm K: $R = 0.5$ m.

Answer: $T = 19$ Nm
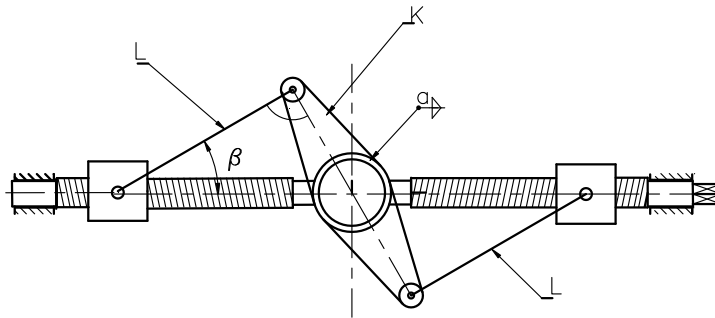
Glossary

efficiency	sprawność
friction angle	kąt tarcia
friction losses	straty tarcia
gravity	ciążenie
irrespective	niezależnie
power flow	przepływ mocy
power screws	mechanizmy śrubowe
rectilinear	liniowy
self locking	samohamowny
substitute	podstawić
thread form	zarys gwintu
torque	moment (powodujący ruch obrotowy)

4. Bolted Connections: part 1

4.1. Load tangent to the plane of contact (loose bolts)

Loose (through) bolted joints are the most common type of non-permanent connections. They are cheap in manufacture and easy in assembly. We shall consider first calculations for one bolted connection (or a group of bolts) that is loaded centrally, i.e. the load passes through the centroid of the bolt pattern and then we will discuss an approach used for the calculation of a group of bolts loaded non-centrally.
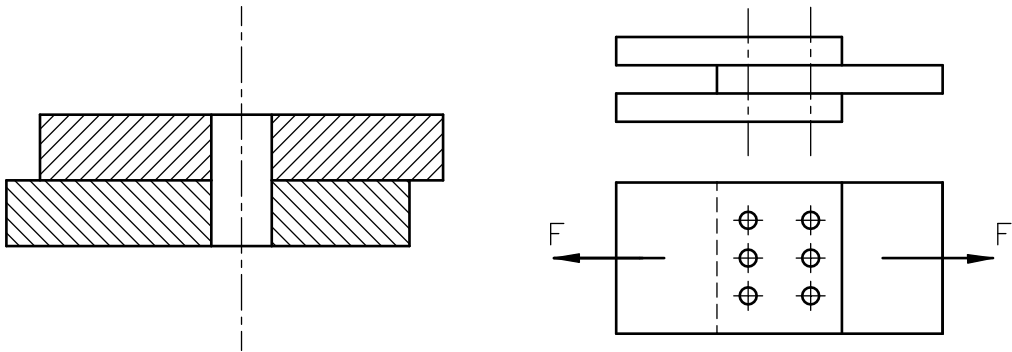
Fig. 4.1. A loose (through) bolted connection (friction-type joints); a group of bolts loaded centrally (▲)

4.1.1. A single bolted connection or a group of n bolts loaded centrally

Calculations are quite simple: in through bolts, the axial load in a bolt must be sufficient to generate a friction force that is greater than the load transferred. For a joint with n bolts, each loaded with a normal force F_n, i friction surfaces with the coefficient of friction μ between the contacting surfaces the grip force: $F_n \cdot n \cdot i \cdot \mu \geq F$. Isolating the normal force: $F_n \geq \dfrac{F}{ni\mu}$.

The coefficient of friction shall be assumed anywhere between 0.16 and 0.4 depending upon contacting surfaces finish (maximum values for sand blasted surfaces in structural engineering). Assume however the lower value to be on the safe side!

For a group of centrally loaded bolts an assumption is made that all bolts are loaded uniformly. Once the normal load has been isolated from the above formula and calculated, we can calculate the necessary bolt diameter using a simple formula for tension with an ample value of the F.S. (a design approach) or you can use a factor of 1.13 to make up for additional torsion: $d = 1.13\sqrt{4F_n /(\pi k_r)}$. Use formulas from chapter 3 to calculate the necessary amount of torque to tighten the connection (collar friction shall be accounted for). Special torque wrenches are used to apply precisely that amount of loading that is prescribed by calculations. Depending upon the torsional elasticity of a connection (soft, hard), a torque wrench may display a so called "mean shift", i.e. a spread in the actual values of normal load in the bolt.

4.1.2. A group of bolts loaded non-centrally

For eccentrically loaded group of bolts, according to the rules of static, we shall transfer the direct load to the centroid (the primary load) and apply an additional moment, i.e. a product of the direct load and a distance from the actual position of the load to the centroid, (the secondary load).
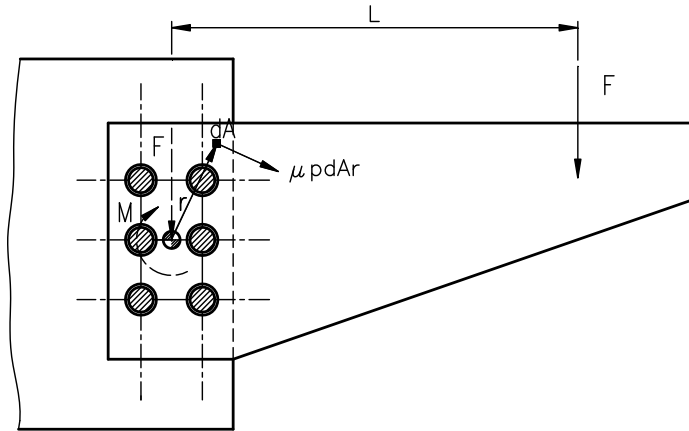

Fig. 4.2. A group of bolts loaded non-centrally

The primary load is distributed evenly among all bolts whereas the secondary load is transferred by elementary friction forces, the amount of each of them is proportional to a distance from this force to the cetroid of the contact area. The primary load $(F_n^{'})$ can be calculated from a formula given in the preceding chapter. The secondary load can be found based upon the following equations:

$$dM = pdA\mu r \ \Rightarrow M = p\mu \int_A rdA = p\mu S_o$$

where S_o is the static (first) moment of the contact surface with respect to its centroid.

$$\text{As } p = \frac{nF_n^{''}}{A} \text{ then } F_n^{''} = \frac{MA}{n\mu S_o}$$

The two forces $(F_n, F_n^{''})$ are summed algebraically and we proceed then as explained in chapter 4.1.1.

4.2. Load tangent to the plane of contact (fitted bolts)

The application range of fitted bolts is restricted due to the higher accuracy in machining needed and costs involved (reaming).
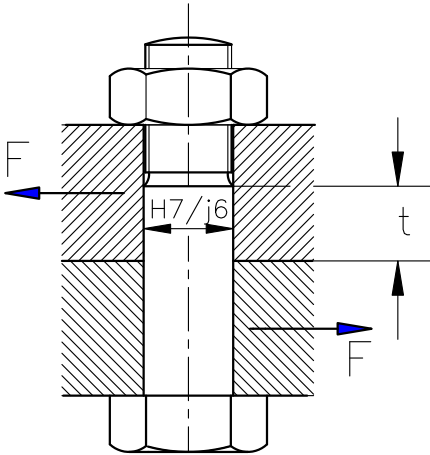
Fig. 4.3. A fitted bolt

4.2.1. A single bolted connection or a group of bolts loaded centrally

A fitted bolt under tangent load represents actually a pin that is calculated for shear and bearing pressure. Similarly treated is a group of bolts centrally loaded (the uniform transfer of load is assumed).

The shearing condition for one bolt sheared in one plane is: $F/A \le k_t$ and the bearing condition is: $F/(d \cdot t) \le p_{all}$. The allowable shearing stress depends upon the type of loading and bolt material: $0.42R_e$ for static loading, $0.3R_e$ for pulsating and $0.16R_e$ for reversed loading. The same is true for bearing pressure. Usually $p_{all} = 2.2\ k_t$. For a group of centrally loaded bolts we need to account for the number of bolts and the number of surfaces subjected to shear i (similarly to loose bolts).

4.2.2. A group of non-centrally loaded bolts (non-regular bolt pattern)

The bolt layout is the same as that shown in Fig. 4.2 but there is no gap between the shank of a bolt and its seat in the cantilever plate.
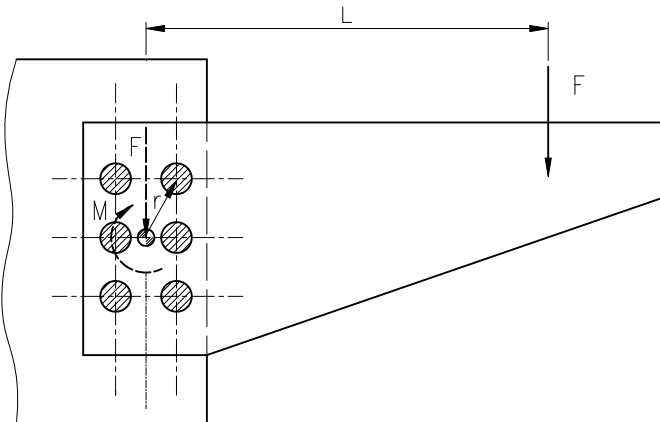

Fig. 4.4. A group of non-centrally loaded bolts (▲)

The primary load is distributed evenly among all bolts: $F_t^{'} = F/n$

The secondary load is proportional to the distance from a bolt in question to the centroid of the bolt pattern:

$$\frac{F_i}{r} = \frac{F_{max}}{r_{max}} = const \quad \Rightarrow F_i = \frac{F_{max} r_i}{r_{max}}$$

The sum of partial moments shall be equal to the secondary load (moment):

$$M = \sum F_i r_i = \sum \frac{F_{max} r_i^2}{r_{max}}; \quad \text{hence: } F_{max} = \frac{M r_{max}}{\sum r_i^2} \quad (F_t'' = F_{max})$$

The vectorial summation of the two components (F_t', F_t'') will yield the maximum load. Proceed then as in the case of a single fitted bolt explained in chapter 4.2.1.

NP 4.1. Two plates 10 mm in thickness and subjected to a tensile load of $F = 4000$ N are connected by 4 bolts as shown in the sketch. Compute the diameter of the bolts if the plates are connected by: a) loose (through) bolts ($\mu = 0.2$) and b) fitted bolts ($p_{all} = 200$ MPa); $t = 7$ mm (see Fig. 4.3 for the symbol). Assume material and the factor of safety.
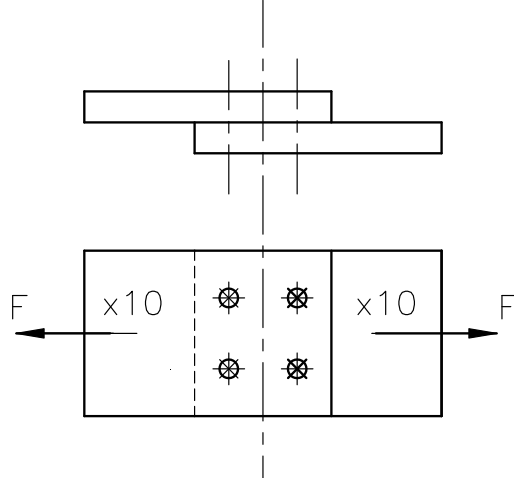
Loose bolts. The normal force required in one bolt: $F_n = \dfrac{F}{n\mu i} = \dfrac{4000}{4 \cdot 0.2 \cdot 1} = 5000$ N \

Assumed is a 5.6 mechanical class bolt. That means that the yield stress is equal to 500 MPa x 0.6 = 300 MPa. Assuming the factor of safety FS = 1.75 we have the design stress for tensile load $k_r = 170$ MPa.

The bolt diameter: $d \geq 1.13\sqrt{\dfrac{4F_n}{\pi k_r}} = 1.13\sqrt{\dfrac{4 \cdot 5000}{\pi \cdot 170}} = 6.92$ mm

Fitted bolts. Force for one bolt: $F_n' = \dfrac{F_n}{ni} = \dfrac{4000}{4 \cdot 1} = 1000$ N .

Assumed is the design stress for shear at a level of 50% of the design stress for tensile load, i.e. $k_t = 85$ MPa.

Diameter of the bolt shank (shear): $d \geq \sqrt{\dfrac{4F_n'}{\pi k_t}} = \sqrt{\dfrac{4 \cdot 1000}{\pi \cdot 85}} = 3.87$ mm

Diameter of the bolt shank (bearing pressure): $d \geq \dfrac{F_n'}{p_{all} t} = \dfrac{1000}{200 \cdot 7} = 0.7$ mm (negligible)

From a table in Appendix 3 we select an M8 bolt for which the root diameter $d_3 = 6.47$ mm.

4.3. Locking means

Fig. 4.5 shows different nut locking means. These are positive (a to d, g) and frictional (the others). Notice a spring washer (e). It was invented by an American railroad worker named Grover and you may find it named after its inventor.
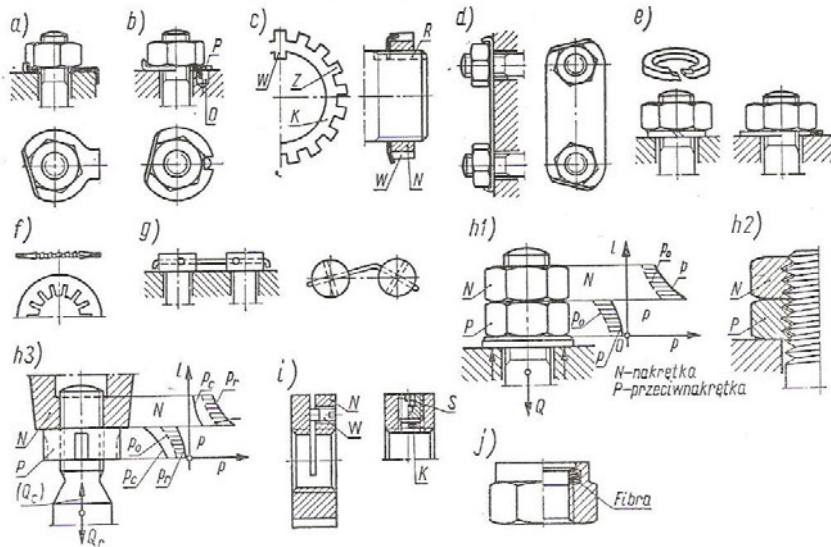
Fig. 4.5. Nut locking means [10]. Legend: nakrętka = nut; przeciwnakrętka = counternut; fibra = fiber

HW 4.1. What amount of moment (torque) shall be applied to screws A (6 of them) to transfer a torsional moment of $T = 100$ Nm from the flange K onto the hub Z. Data: screw M8x1.25; $d_2 = 7.19$ mm (mech. class 8.8), the coefficient of friction $\mu = 0.15$ (faying surfaces). Take all the necessary dimensions from the drawing ([7]) (the pitch diameter of the bolt arrangement $d_p = 38$ mm; scale in the drawing approx. 1 : 2).
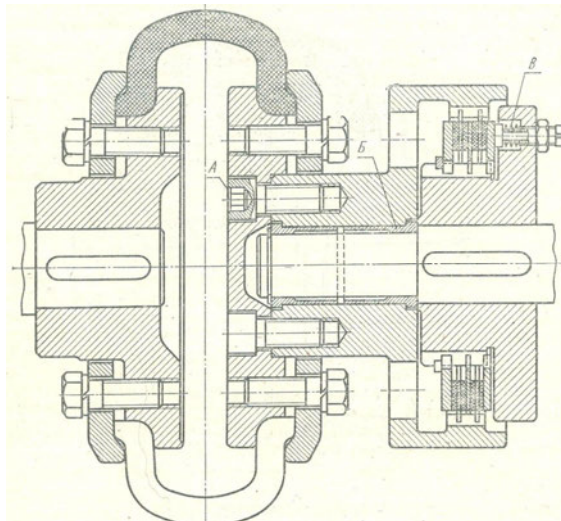
Answer: Approx. 6.5 Nm

(Usually the screw is torqued to 0.75 of the proof stress. For a lubed 8.8 mechanical class screw the maximum torque shall not be greater than approximately 16 Nm).

HW 4.2. Find the resultant force on the most loaded bolt in the group of eccentrically loaded bolts shown and check it for shear and bearing pressure. Shank diameter $d = 10$ mm; plate thickness (each) $t = 10$ mm; $k_t = 80$ MPa; $p_{all} = 200$ MPa. $F = 10$ kN; $L = 400$ mm; $a = 100$ mm; assume $t = 6$ mm.
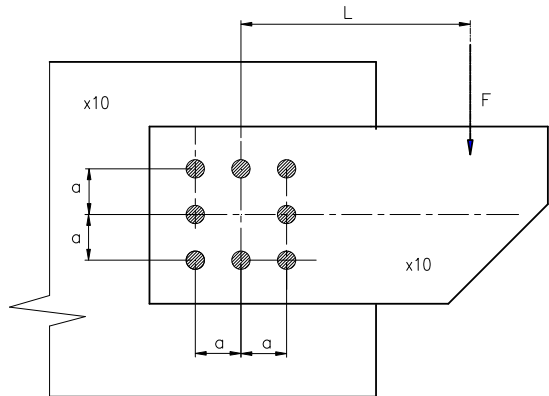
Answer: 5653 N

Glossary

bearing pressure	nacisk powierzchniowy
bolted connection	połączenia śrubowe
cantilever	wysięgnik
collar friction	tarcie kołnierzowe
faying surface	powierzchnia styku
fitted/reamed bolts	sruby pasowane
flange	kołnierz
grip force	tu: siła tarcia
locking means	elementy zabezpieczające
loose/through joints	połączenia luźne
lubed	posmarowany olejem
mean shift	odchylenie od wartości średniej momentu zakręcania
pin	sworzeń
positive	tu: kształtowy
reaming	rozwiercanie
sand blasting	piaskowanie
shank	niegwintowana cześć śruby

5. Bolted connections: part 2

5.1. Load normal to the contact plane (preload)

<u>5.1. 1. A set of two springs analogy</u>

There are two springs in an arrangement shown in Fig. 5.1 that are loaded with a load of 50 N each. Then an external load of 50 N is being applied from the left side. What will be the resultant load in the left and the right spring if the two spring constants are assumed to be the same? A common sense answer: 100 N and 0 N is wrong. Let's analyse this problem in a more detail; this time spring constants of the two springs are different.
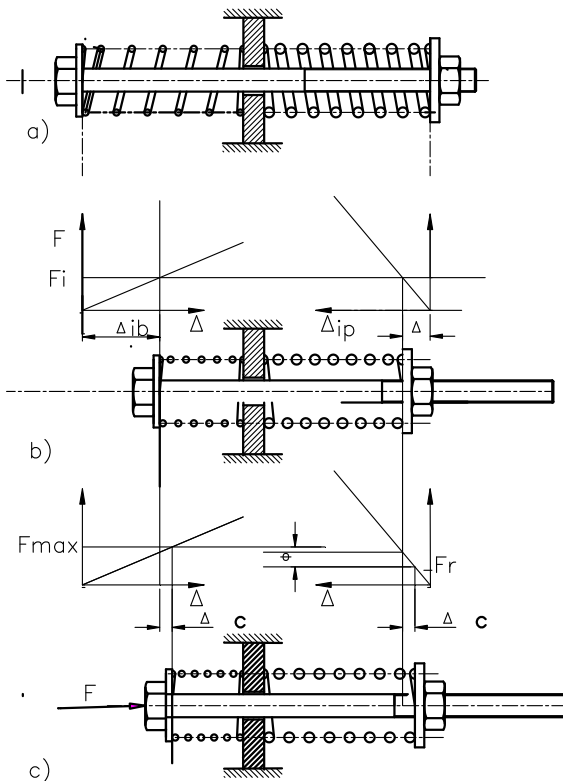

Fig. 5.1. A two spring set analogy of preload

Fig.5.1a shows the starting situation: the two springs are fully extended with no load inside. Then the nut on the right side is being tightened to introduce a certain amount of compression (Fig. 5.1b). This initial compression is termed as preload and denoted further as F_i. The spring constant of the left spring is C_b (represents a bolt in a real joint), and that of the right side, C_p (parts). Under this initial load each spring deforms in agreement with its spring constant: The left spring more than the right one. At this stage the force in each spring is the same but deformations are different. The left spring $\Delta_{ib} = F_i/C_b$. The right spring $\Delta_{ip} = F_i/C_p$

Now we apply the external load F giving an additional load to the left spring and relieving the right one (Fig. 5.1c). This time the deformation Δ is the same (the spindle moves to the right) but the amount of additional load to the left spring and the amount of load relieved from the right one depends upon individual spring constants. A difference between the left and right loading of the two springs shall be equal to this external load F. We can write:

$$\Delta_c C_b + \Delta_c C_p = F \quad \text{hence:} \quad \Delta_c = \frac{F}{C_b + C_p}$$

The two force /deformation diagrams from Fig. 5.1 are combined into one (Fig. 5.2) with the two stiffness lines intersecting at the point of the initial loading (preload).

Fig. 5.2. Construction of the force-deformation diagram (a joint diagram)

In this diagram, the additional force in the bolt is denoted as T_b; whereas the loss of force in the parts, T_p. So:

$$T_b = C_b \Delta_c = F \frac{C_b}{C_b + C_p} \text{; and}$$

$$T_p = C_p \Delta_c = F \frac{C_p}{C_b + C_p}$$
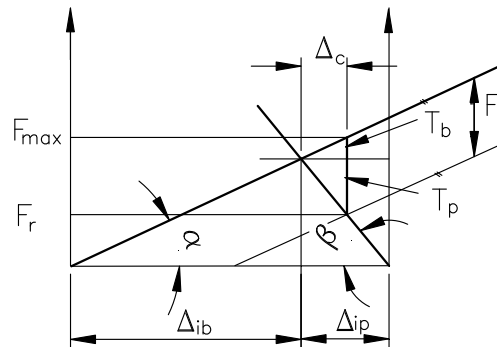
The maximum load (bolt) is $F_{max} = F_i + T_b$ and the residual load (parts): $F_r = F_i - T_p$.

Going back to our first problem; if $C_b = C_p$ then $T_b = T_p = 0.5 F = 25$ N. So finally, the left spring will be loaded with 75 N, and the right spring, with 25 N. How to construct a joint diagram?

1. Trace (to scale) the bolt stiffness line (this requires the assumption of the force and deformation scales).
2. Trace a horizontal line representing preload.
3. At a point of intersection with the bolt stiffness line trace the collar stiffens line.
4. Trace a line that is parallel to the bolt stiffness line and at a distance that is equal to the external load.
5. In the point of intersection with the collar stiffness line trace a vertical line to the intersection with the bolt stiffness line. The lower intersection point is the residual force in the collar, the upper intersection point is the maximum load in the bolt.

5.1 3. Actual bolted connection (spring constants)

The discussed system of springs represents an actual bolted connection where the left spring represents a bolt, which is additionally loaded under an external load, and the right spring represents a collar, which is relieved under this external load. In pressure piping systems the minimum, residual load determines the minimum pressure on the gasket (tightness). The maximum load is necessary for the calculations of bolts.

The calculations of the bolt spring constant (stiffness) is relatively simple: we use the Hook's law and find the resultant stiffness as calculated for a series system of cross-sections of different lengths.

Fig. 5.3. Spring constant for a bolt

$$\frac{1}{C_b} = \frac{1}{\frac{EA_1}{l_1}} + \frac{1}{\frac{EA_2}{l_2}} + \dots$$
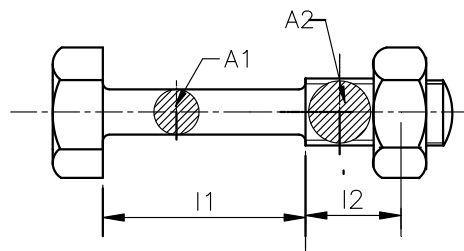
This problem is more complex in the case of a collar. How to define its cross-section? There are many models. Most of them employs a truncated cone traced starting from a point under the bolt head where the distance is equal to the opening of a spanner (span across flats) and at an angle of 45 degrees. This truncated cone is replaced by an equivalent hollow cylinder, the stiffness of which is easy for calculations.
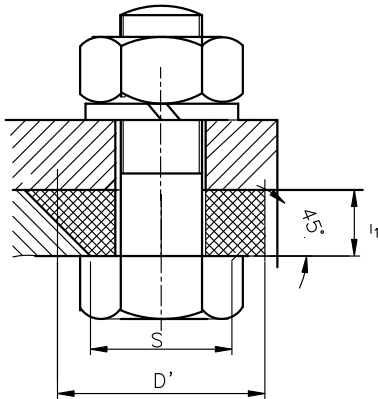
Fig. 5.4. Spring constant for parts

$$D^{'} = S + l_1$$

5.1.4. Advantages of preload

If we set the time axis at the point of intersection of the two stiffness lines (Fig. 5.2) then it is possible to determine the load pattern of the bolt: this load fluctuates between the preload and the maximum value. Without preload the load would vary between zero and the external load. If we compare the two fluctuating load patterns we may say that the latter has a high amplitude and a low mean value whereas the former has a high mean value but a low amplitude. If you remember the Soderberg diagram you will find out that with preload the factor of safety becomes higher. There is one more advantage: the deformation of bolts under the external load is two to three times smaller than it would be in a no-preload case.

Let's discuss the influence the preload parameters on the values of maximum and residual force in a joint. Given is the preload, external load. Bolt stiffness is constant and there are two values of the collar stiffness. How does a change in the collar stiffness influence the maximum and minimum load in the joint? Make a graphical solution (Fig. 5.5, left side). The same problem shall be solved for one value of the collar friction and two values of the bolt stiffness (Fig. 5.5, right side).
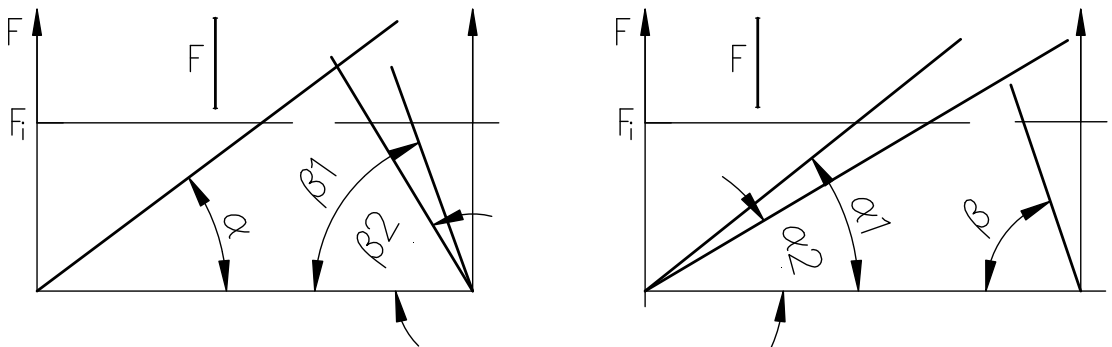
Fig. 5.5. Influence of the bolt stiffness on the value of the maximum and residual loads in a joint (▲)

As flexible bolts are advantageous for the operation of the joint we can achieve this either by making them hollow or by giving a distance sleeve.

Practical recommendations (in terms of the yield limit): preload $F_i = 0.6$ to 0.8 of R_e. Gasketed joints (stiffness): 128 to 188 MPa/mm for asbestos gaskets and 1100 MPa/mm maximum for metal jacketed gaskets. Important! To obtain the stiffness, these values shall be multiplied by the contact area per one bolt.

NP 5.1 Find the maximum and residual forces in a bolted non-gasketed joint of a pipeline flange shown. Data: internal pressure $p_i = 2.0$ MPa; $D = 150$ mm; $t_1 = t_2 = 25$ mm; $l_1 = 20$ mm; $l_2 = 10$ mm; $l_3 = 25$ mm; $d_s = 7$ mm; $d_o = 10$ mm; initial tension $F_i = 10$ kN. Draw to scale the joint diagram (force–deformation diagram).
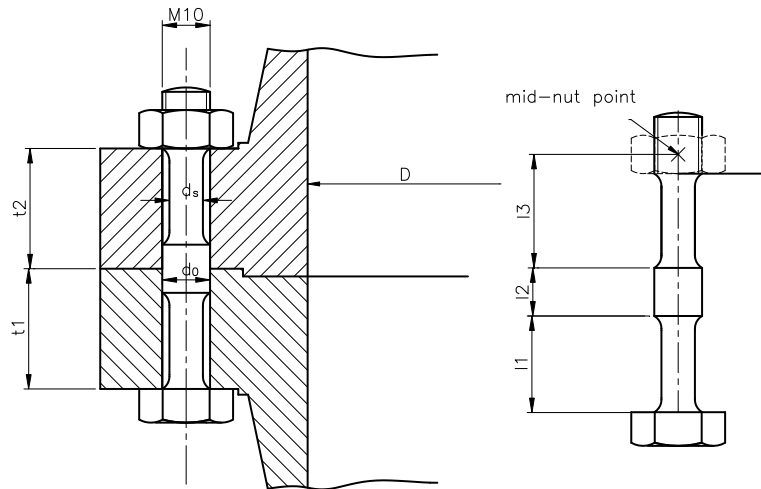
Spring constants (bolt): $A_1 = \dfrac{\pi d_s^2}{4} = \dfrac{\pi \cdot 7^2}{4} = 38.48 \text{ mm}^2$ $\quad C_{b1} = \dfrac{EA_1}{l_1} = \dfrac{2 \cdot 10^5 \cdot 38.48}{20} = 384845.1 \dfrac{\text{N}}{\text{mm}}$

Analogously $C_{b2} = 1570796$ N/mm and $C_{b3} = 307876.1$ N/mm
For a series system of springs:

$$\frac{1}{C_b} = \frac{1}{C_{b1}} + \frac{1}{C_{b2}} + \frac{1}{C_{b3}} = \frac{1}{384845.1} + \frac{1}{1570796.3} + \frac{1}{307876.1} = \frac{1}{154246.5} \Rightarrow C_b = 154246.5 \frac{\text{N}}{\text{mm}}$$

Parts: $D'_{p1} = S + t_1 = 17 + 25 = 32 \text{ mm}$. As $d_0 = 10$ mm then $A_{p1} = 725.7 \text{ mm}^2$

$$C_{p1} = \frac{EA_{p1}}{t_1} = \frac{2 \cdot 10^5 \cdot 725.7}{25} = 5805663 \frac{\text{N}}{\text{mm}} \; ; C_{p1} = C_{p2}. \text{ Hence the resultant spring constant for}$$
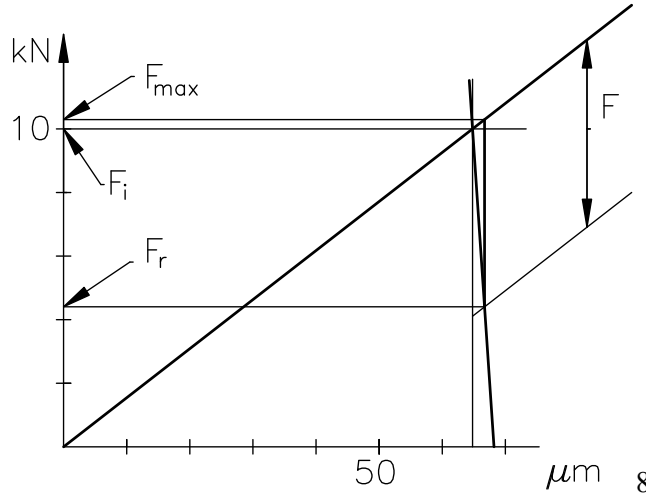
parts: $C_p = \dfrac{C_{p1} C_{p2}}{C_{p1} + C_{p2}} = \dfrac{C_{p1}}{2} = \dfrac{5805663}{2} = 2902831.6 \dfrac{\text{N}}{\text{mm}}$

The external load: $F = p_i \dfrac{\pi D^2}{4} = 2 \dfrac{\pi \cdot 150^2}{4} = 35342.9 \text{ N}$; the external load for one bolt:

$F = \dfrac{F_\Sigma}{n} = \dfrac{35342.9}{6} = 5890.5 \text{ N}$. Finally, the residual load:

$$F_r = F_i - F \frac{C_p}{C_p + C_b} = 10 \cdot 10^3 \cdot 5890.5 \frac{2902831.6}{2902831.6 + 154246.5} = 4397.7 \text{ N}$$

and the maximum load: $F_{\max} = F_i + F \dfrac{C_b}{C_p + C_b} = 10 \cdot 10^3 + 5890.5 \dfrac{154246.5}{2902831.6 + 154246.5} = 10297.7 \text{ N}$

To construct a joint diagram, needed are scales for forces and deformations (a common mistake made by students: as in a shortened script $C_b = tan\ \alpha$ and $C_p = tan\ \beta$, students return an actual value of the spring constants with units and the two angles become very close to 90 degrees). Let's have 1 mm in the diagram = 0.2 kN in force and 0.001mm in deformation. So the initial deformation of the bolts and parts in the diagram is 64.8 mm and 3.4 mm respectively

5.2. A group of bolts under normal load

A bracket shown in Fig. 5.6 is one of the many possible applications for a group of bolts under normal load.
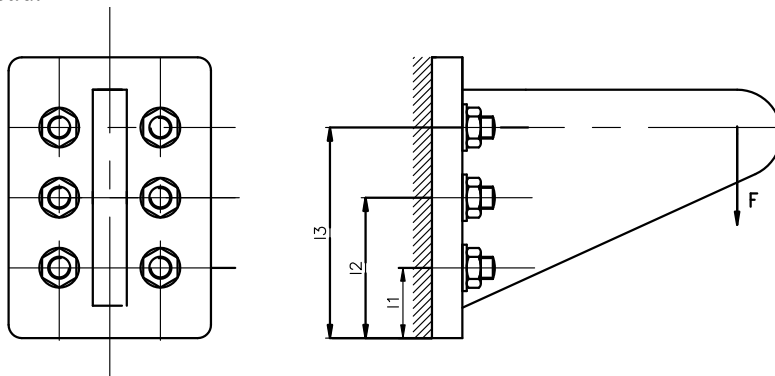

Fig.5.6. Group of bolts under normal, non-central load

As in all cases of non-central loading we first reduce the load to the centroid, which gives a direct load and a moment.

All bolts are initially loaded and then loaded externally with this moment. Contrary to the case discussed above, this load is not the same for all bolts. An assumption is made that the moment related load is proportional to a distance from the line of action to the possible pivot point of the whole bolt group. This is the lower edge of the bracket. Similarly, the summation of all individual moments shall give the input moment. The formula for the maximally loaded bolt (the top row) is the same as the formula obtained for the maximally loaded fitted bolt discussed in chapter 4.2. The only difference is that r_i is replaced with l_i (Fig. 5.6), i.e. $F_{\max} = Ml_{\max}/(\Sigma l_i^2)$. This formula can be employed for cases where the initial load is very small e.g. anchor bolts.

HW 5.1. Find the value of the stiffness constant for parts C_p in a bolted connection with a preload of $F_i = 2000$ N so that under an external load of $F = 1000$ N the maximum force in the bolt is 1.75 times greater than the residual force. The spring constant for a bolt $C_b = 100$ kN/mm. Draw the joint diagram (to scale). Find values of F_{max} and F_r.

Answer: 200000 N/mm

HW 5.2. A woodworking clamp shown is attached to a workbench by four lag screws. Calculate the maximum pulling force if the external load $F = 3$ kN; $a = 250$ mm; $b = 100$ mm; c = 50 mm.

Answer: 3450 N
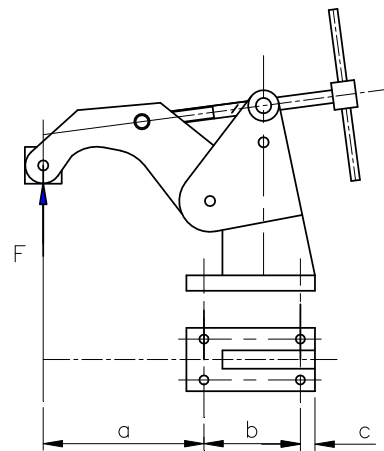
Glossary

across span	wymiar pod klucz
collar/flange	kołnierz
gasket	uszczelka
hollow	wydrążony
initial loading	napięcie wstępne
lag screw	śruba do drewna
piping systems	systemy rurociągów
preload	zacisk wstępny
relieve	odciążyć
residual force	zacisk resztkowy
spanner opening	wymiar pod klucz
stiffness	sztywność
tightness	szczelność
truncated cone	stożek ścięty

38

6. Welded Connections

6.1. Stress analysis

Detailed explanation of the welding processes is given in other courses. For the sake of our course we have to distinguish between butt joints (Fig. 6. 1) and fillet joints (Fig. 6.2).

Fig. 6.1. Butt joints [Corus Constr.]

Fig. 6.2. Fillet joints [Roymech]

The design stress for welded materials is reduced, depending upon the type of loading and welding quality.

$$k' = z_o z k_r$$

where: z_o is a coefficient of static strength (for fillet welds use $z_0 = 0.65$)
z is a weld quality factor (0.5 for a normal weld, 1 – for a strong weld)
k_r is the design stress under tensile loading

With butt joints, follow the rules that you have already learned in the Strength course. That means that if loading is complex, you need to employ the Huber-Mises-Hencky theorem.

The use of the Huber-Mises-Hencky theorem is justified only in those cases where normal and tangent stresses act at the same point. This is not true for fillet welds. Therefore, for general purpose fillet welds you are allowed to summarise stresses vectorially. Irrespective of their true nature we shall name and denote them all as shear stresses and the resultant stress shall not be greater than the allowable shearing stress.

Notice! In many fields of engineering (piping systems, pressure systems) engineers must follow strictly rules given in the relevant Codes!

We shall discuss now a few cases of fillet joints. All joints are subjected to eccentric loading: In all cases stick to the following procedure:

1. Find the fillet weld area subjected to load and its centroid.
2. Find the equivalent load (direct load, bending or/and torsion)
3. Find the area and section modulus (bending or/and torsion)
4. Find the component stresses
5. Locate the maximally loaded point
6. Find the resultant stress; compare with the allowable value.

.

Component stresses:

$$\tau_F = \frac{F}{A}; \quad \tau_M = \frac{M}{W_{xx}} = \frac{Fl}{\dfrac{a(h-2a)^2}{6}}$$

Resultant stress:

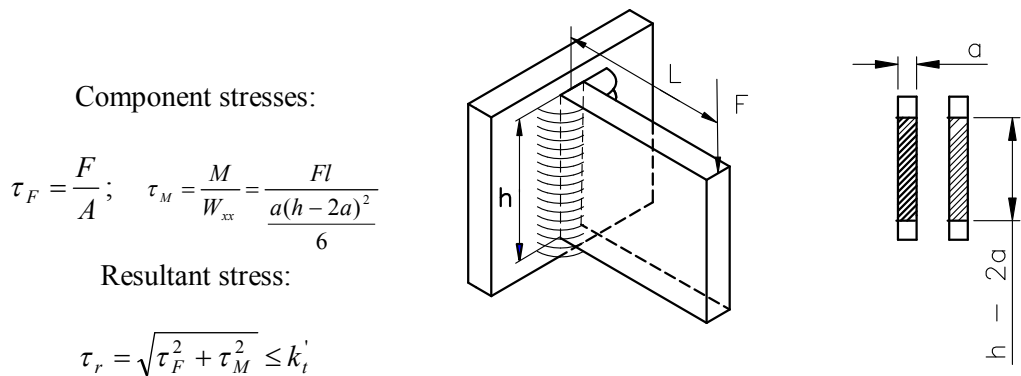$$\tau_r = \sqrt{\tau_F^2 + \tau_M^2} \le k_t'$$

Fig. 6.3. A bracket (direct load and bending) (▲)

In the case of arc welding the length of the weld seam may be reduced by a doubled value of the fillet weld throat (initial and final craters).

Area and the centroid?

$$\tau_F = \frac{F}{A}; \quad \tau_M = \frac{FL}{W_0} \quad \vec{\tau}_r = \vec{\tau}_F + \vec{\tau}_M \le k_t'$$
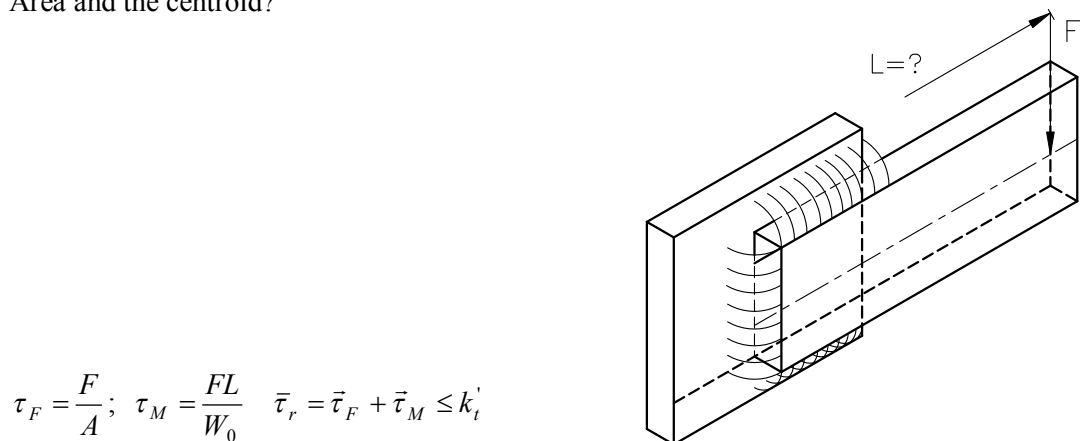
Fig. 6.4. Bracket (direct load and torsion) (▲)

Point 1 of the recommended procedure (the centroid) may pose here a certain problem. Once found, we follow the same sequence of tasks, i.e. the direct stress, the secondary stress (tangent to the radius from the considered point to the centroid and finally, the vectorial summation of the resultant stress.
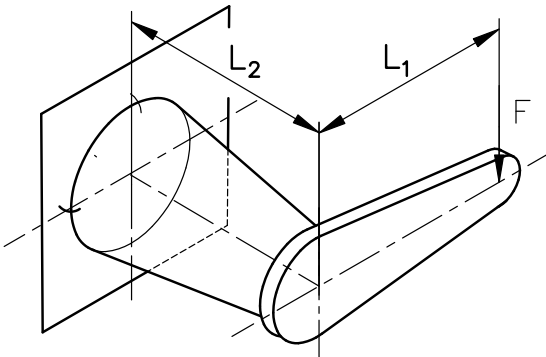

Fig. 6.5. A handle (direct load, bending and torsion) (▲)

There are two problems in a welded handle shown in Fig. 6.5. Both problems will be solved in the class.
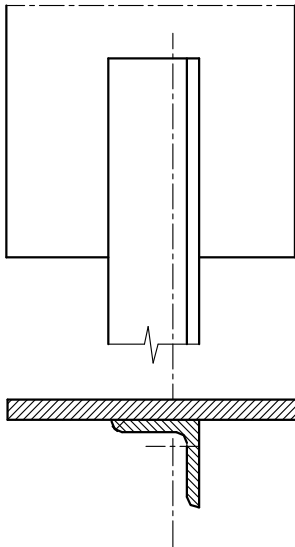
6.2. Design of welded joints

Fig. 6. 6. Design of an angle with a gusset plate (▲)

Design recommendation for welded joints will be explained using foils. Specifically, try to locate the centroid of the fillet weld area in the line of loading. How to design a welded connection of an angle with the gusset of a truss to be in agreement with this recommendation (Fig.6.6)?

NP 6.1.Find the value of the maximum stress in a fillet weld shown if the weld is made with an E600 rod (k_r = 120 MPa). The weld quality factor $z = 0.8$ (static load). Data: F = 10 kN; L= 50 mm; b = 40 mm; c = 60 mm; a = 3 mm (throat).
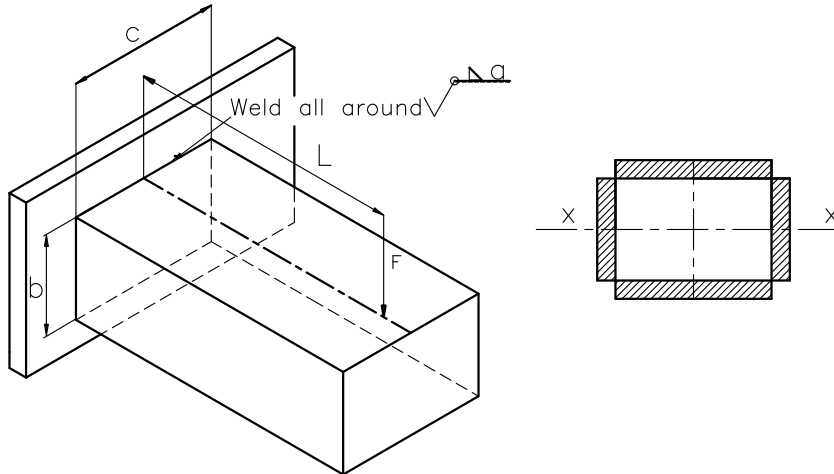
Bending moment: $M = FL = 10000 \cdot 50 = 500000 \, Nmm$

Area subjected to load: $A = 2(b + c)a = 2(40 + 60)3 = 600 \, mm^2$

Moment of inertia (x-x):

$$I_{x\ x} = \frac{(c + 2a)(b + 2a)^3}{12} - \frac{cb^3}{12} = \frac{(60 + 6)(40 + 6)^3}{12} - \frac{60 \cdot 40^3}{12} = 215348 \, mm^4$$

Section modulus: $Z_{x\ x} = \dfrac{I_{x\ x}}{a + b/2} = \dfrac{215348}{3 + 40/2} = 9363.0 \, mm^3$

Direct shearing stress: $\tau'_F = \dfrac{F}{A} = \dfrac{10000}{600} = 16.6 \, \dfrac{N}{mm^2}$

Stress due to the bending moment: $\tau'_M = \dfrac{M}{Z_{x\ x}} = \dfrac{500000}{9363} = 53.4 \, \dfrac{N}{mm^2}$

Maximum stress (upper or lower seam): $\tau_r = \sqrt{(\tau'_F)^2 + (\tau'_M)^2} = \sqrt{16.6^2 + 53.4^2} = 55.9 \, \dfrac{N}{mm^2}$

Allowable stress: $k_t = z_0 z k_r = 0.65 \cdot 0.8 \cdot 120 = 62.4 \, \dfrac{N}{mm^2}$. The seam is safe!

HW 6.1. Localize and calculate the shearing stress at the most loaded point of a fillet weld shown. Data: $F = 10$ kN; $d = 40$ mm; $D = 150$ mm; $a = 4$ mm
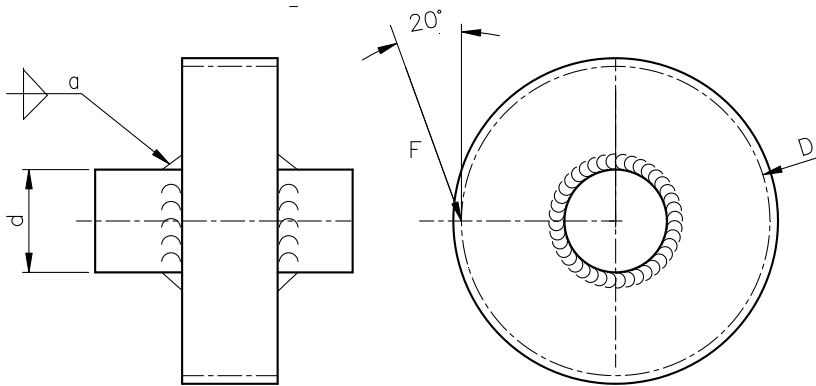
Answer: 41.2 MPa

HW 6.2. Localize and calculate the shearing stress at the most loaded point in a bracket shown. Data: $F = 50$ kN, weld quality factor $z = 0.85$ (static load); throat $a = 7$ mm; $H = 250$ mm; $b = 50$ mm; $L = 200$ mm.
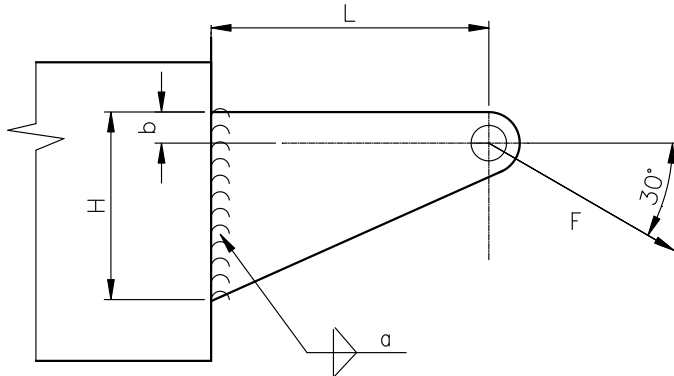
Answer: 64.8 MPa

How to redesign the bracket to minimize shearing stresses due to the bending moment?

Glossary

bracket	wspornik
butt weld	spoina czołowa
code rules	przepisy dozoru
fillet weld	spoina pachwinowa
gusset	blacha węzłowa
moment of inertia	moment bezwładności
seam	szew/spoina
section modulus	wskaźnik średnicowy
truss	kratownica

7. Shaft-Hub Connections

7.1. Introduction

As we move slowly towards the main task of mechanical engineers, i.e. the transfer of power, it is time to discuss possible methods of connections between shafts and the hubs of elements mounted onto them (toothed wheels, sheaves, coupling flanges etc.). The connections are broadly divided into two groups: those which use the force of friction and those which use positive engagement. In rare cases, used are both methods. It is also a good time to discuss fits and tolerances. You need to know how to calculate the minimum clearance (allowance) or the maximum clearance or, in the case of pressed fits, interference min., max.).

7.2. Positive engagement

The most widely used hub-shaft connections are parallel key ones shown in Fig. 7.1a. A usual fit between the shaft and the hub is H7/k6, i.e. a transition fit. The higher is the speed and the larger is the shaft, the more tight fit is recommended. Woodruff keys (Fig 7.1b) are used for high volume applications (cheap in manufacture).
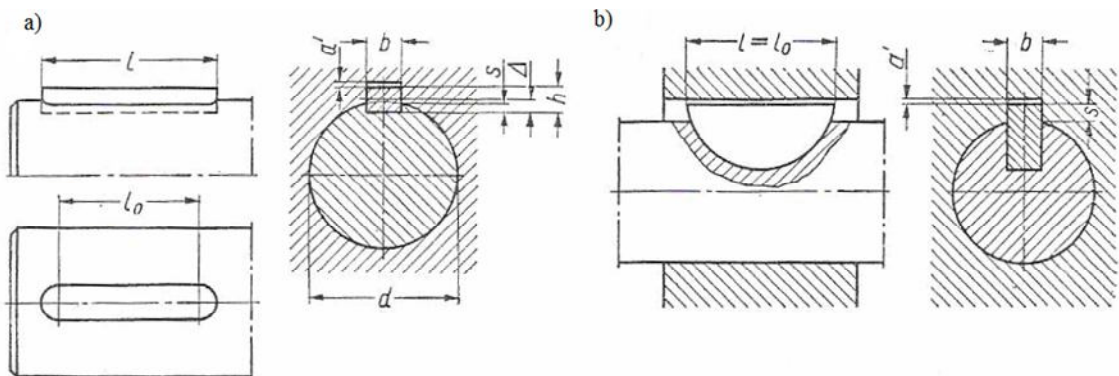

Fig. 7.1. Keyed connections (parallel, Woodruff) [10]

The calculations of positive engagement connections are quite simple, and take into account either the allowable pressure between the key and the weaker of the two elements (which is usually the hub; see Table 7.1) or the allowable shearing stress. A usual mode of failure is deformation first, and then, shearing. As the cross section of a key (bxh) is governed by the diameter of the shaft, the designer is responsible for the length (l) of the engagement only (subject to standardization). This will be illustrated in the following numerical example.

NP 7.1. A 45 mm shaft is transmitting 30 kW at 1500 rpm. Find the necessary length of the key in a connection shown in Fig. 7.1a if the hub is made of cast iron (p_{all} = 50 MPa; see Table 7.1); and the key is made of AISI 1060 steel (St6, k_t = 80 MPa, static load). Data: bxh = 9x14 mm; $\varDelta$ (see Fig. 7.1; t_l in PN-70M/85005) = 5.5 mm.

Torque transmitted: $T = \dfrac{30P}{\pi n} = \dfrac{30 \cdot 30 \cdot 10^3}{\pi \cdot 1500} = 191.0 \text{ Nm}$

Tangential force: $F = \dfrac{2T}{d} = \dfrac{2 \cdot 191 \cdot 10^3}{45} = 8488 \text{ N}$

Key length (shear): $l = \dfrac{F}{bk_t} = \dfrac{8488}{9 \quad 80} = 11.8 \text{ mm}$

and bearing pressure $l = \dfrac{F}{(h - \Delta)p_{all}} = \dfrac{8488}{(14 - 5.5)50} = 20.0 \text{ mm}$

The nearest standard value is 22 mm but a usual practice is to assume the nearest standard value closest to the length of the hub. The length of the hub is, again practice, equal to the shaft diameter. Hence l = 40 mm.

Table 7.1. Allowable pressure (p_{all}) in keyed connections [10]

Materials		Stationary hub	Sliding hub
Key	Hub	MPa	MPa
St6* St7	cast iron	30 to 50	
St6 St7	steel	60 to 90	20 to 40
St7	case hardened journal and hub	200 to 300	case hardened surfaces 120 to 200

*St6, St7 are plain high carbon steel grades; Lower values for the fluctuating mode of loading

Parallel keys are also a good chance to explain differences between the hole and shaft basis fitting systems. In some applications the hub needs a freedom in its axial displacements. Had it been fitted on the hole basis rule, then the key should have been machined to different widths across its height (Fig. 7.2a to b). The shaft base rule allows avoiding this inconvenience (Fig. 7.2c to d).
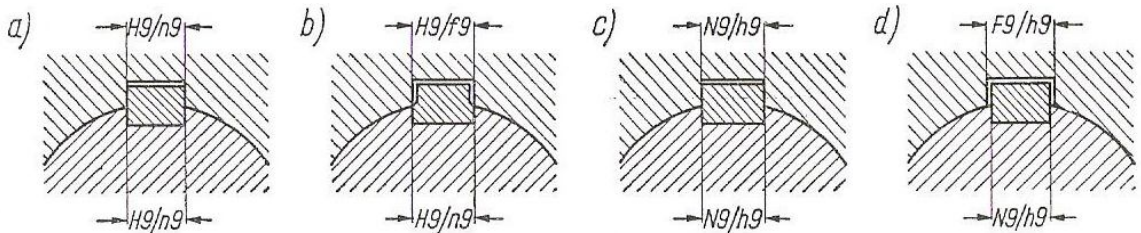

Fig. 7.2.   Hole basis vs. shaft basis rule when fitting a parallel key [10]

A similar situation (the base shaft rule) is in fitted knuckle pin connections (Fig. 7.3). The pin is toleranced to h6 and the hole receiving the pin in the fork and in the eye, based on our choice, is toleranced to P7 or F7 respectively.

Fig. 7.3. A fitted knuckle pin connection [10]

Where pressure is too high and even a doubled key is not sufficient, used are splined connections (Fig. 7.4a). The two elements are centered on the shaft diameter d. For a stationary connection recommended is an H7/h6 fit and for a sliding hub, H7/f7 one. The width of one spline is toleranced to H10/f8 (stationary) or H10/c9 (sliding). The choice of these fits is governed by accuracy in angular positions of all splines. The outer diameter (D) is toleranced to H11/a11 (an ample amount of clearance). In applications where space is limited, used are serrated connections (Fig. 7.4b). A typical application is a connection of a half-axle with the elastic coupling in the drive-line of an automobile. For maximum load carrying capacity used are involute splined connection shown in Fig. 7.4c. Properties of the involute line will be discussed in detail in the next semester. In calculations we assume that 75% of all splines are active in the transfer of torque.
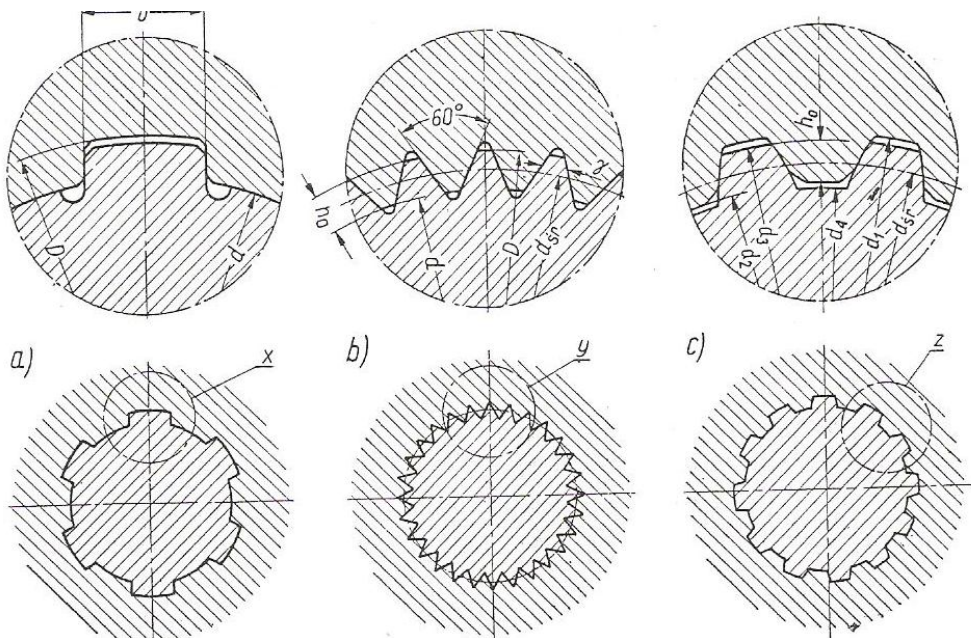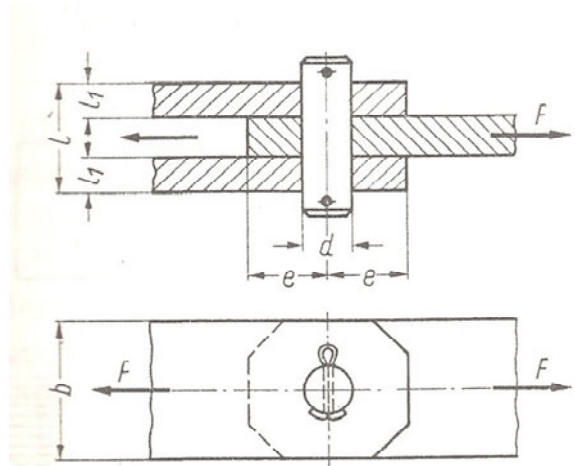

Fig. 7.4. Splined and serrated connections [10]

Tapered keys shown in Fig. 7.5 are used mostly at shaft extensions and for limited speed applications due to a small eccentricity of the hub with respect to the shaft after mounting.
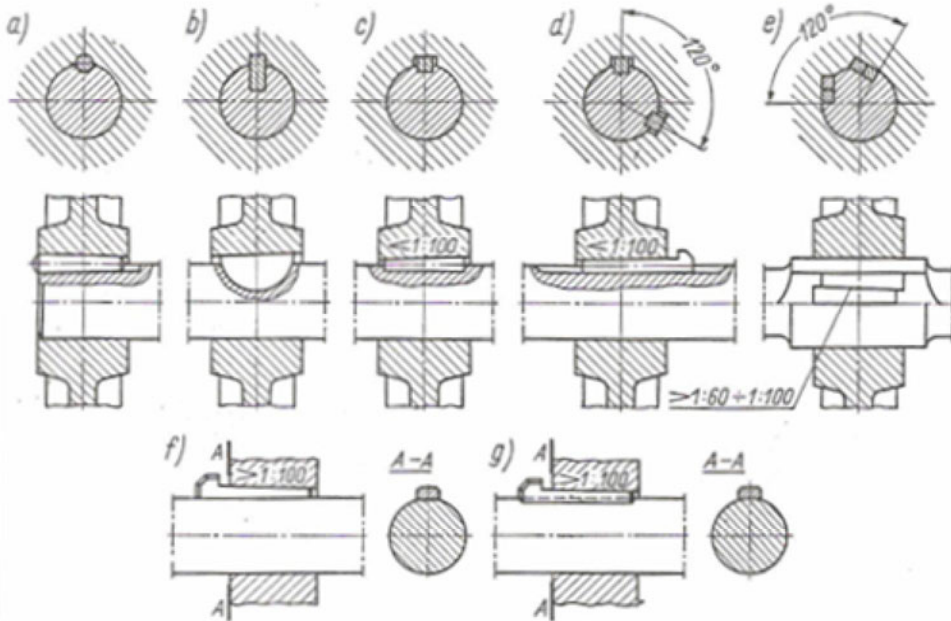

Fig. 7.5. Tapered key connections [10]

7.3. Connections by friction

In many applications the position of the hub on the shaft must be freely related to another element (in terms of their angular positions). Connections by friction allow achieving this goal. Let's start with cone connections (cylindrical press-fit connections will be discussed in the next lecture). Direct cone connections (Fig. 7.6) are used at shaft extensions, also for mounting heavy barrel bearings on plain shafts (without shoulders).
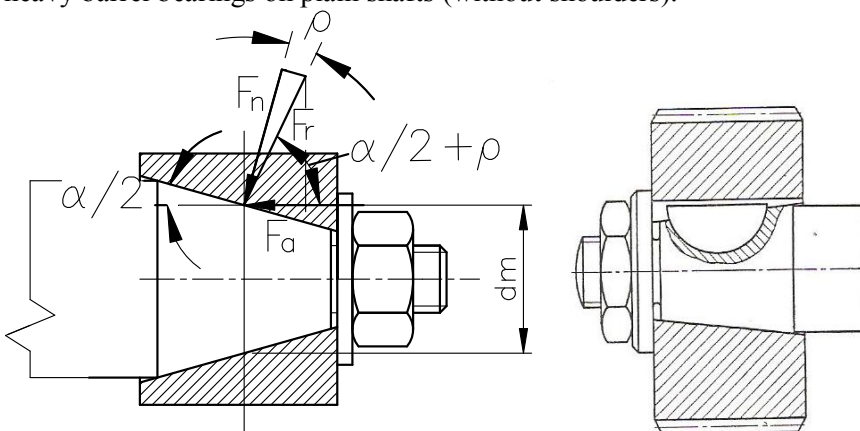

Fig. 7.6. A direct cone connection [10]

The problem here is similar to that discussed in the chapter on power mechanisms. What shall be the amount of the axial force at the threaded shaft extension to generate a friction force sufficient to transfer a given amount of torque? In power screw mechanisms given was the axial force in the screw. In our case we can calculate the normal force that is necessary for the transfer of the torque. The resultant force will be tilted by the angle ρ against the direction of mounting. Its value may be obtained by projecting a line parallel to the surface of the cone from the end of the normal force. The horizontal component of the resultant force will yield the sought horizontal force (force in the screw).

$$F_n \mu \frac{d_m}{2} = T \; ; \; F_r = F_n / \cos \rho \; \text{ and } \; F_a = F_r \sin(\alpha / 2 + \rho)$$

$$\text{hence;} \; F_a = \frac{2T}{d_m \mu} \frac{\sin(\alpha / 2 + \rho)}{\cos \rho}$$

When we know the axial force, it is easy to calculate the necessary amount of the tightening torque. Fig. 7.6b shows a combination of a friction and positive engagement that is adopted in situations where the loss of friction may result in the total damage to the engaged elements (gearing).

A variation of the discussed connection is an indirect tapered connections used in the mounting of barrel roller bearings (Fig. 7.7).
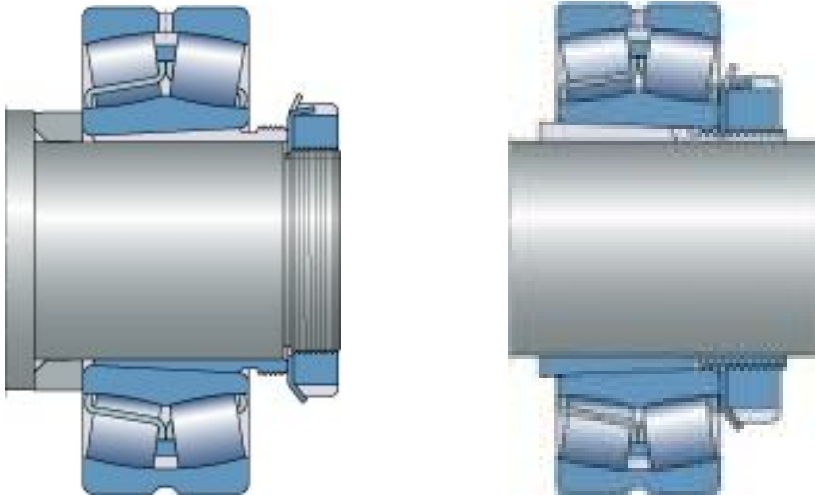

Fig. 7.7. Mounting of a double barrel bearing on a withdrawal (left) and adapter sleeve (right) [SKF]

The tapered sleeve has a large longitudinal gap. When pushed (or pulled in the case of adapter sleeves) the gap closes and the sleeve wedges against the shaft and the inner ring. In this application, the shaft journal must be machined within tight limits for out-of roundness or out of cylindricity tolerances (IT 5) whereas tolerance for its diameter is very large (IT9 or

48

even more). This type of a joint is actually the only solution to high overall size application with the shaft diameter close to 500 mm.

Fig. 7.8 shows other methods of shaft-hub connections using friction forces. Tapered rings shown in these drawings are known by their brand name of Federrings
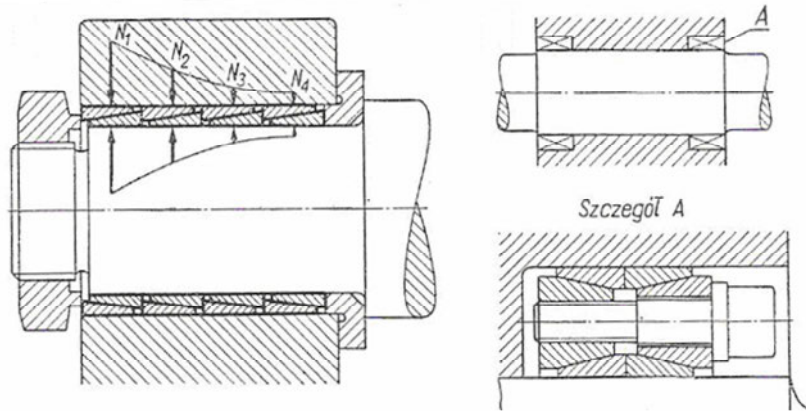

Fig. 7.8. Tapered rings in shaft-hub connections [10]. Legend: szczegół = detail

HW 7.1. Find the maximum, minimum and mean value of clearance or interference in a keyed shaft-hub connection shown in Fig. 7.1 if the keyway-key fit is: D9/h9 (hub) and the keyseat-key fit is N9/h9 (shaft). Data: b = 8 mm; EI =-38 μm (N9); ES = 76 μm (D9), Tolerance zone for the 9th class of accuracy IT9 = 36 μm. Draw the bar diagram.

Glossary

allowance	tu: luz minimalny
bar diagram	rysunek położenia pól tolerancji
barrel roller bearing-	łożysko baryłkowe
base hole	podstawowy otwór
base shaft	podstawowy wałek
broaching	przeciąganie
cone connection	połączenie stożkowe
coupling flange	piasta sprzęgła kołnierzowego
fit	pasowanie
high volume application	zastosowanie masowe
hub	piasta
interference	wcisk
plain shaft	wał gładki
positive engagement	sprzężenie kształtowe
serrated connection	połączenie wielozębkowe
shaping	dłutowanie
sheave	kółko pasowe
shoulder	odsadzenie na wale
spline	wielowypust

8. Press-fit Connections

8.1. Formulation of the problem

The most widespread friction type shaft-hub connections are press fit ones. When designing a press-fit connection, the problem is to find such an interference fit that:

1) the minimum interference is large enough to produce a friction force sufficient to transfer the load applied, be it in tension or torsion, and this part of the problem had been discussed at length before one of your laboratory experiments. A short summary of formulas for a cylindrical shaft (d in diameter and l in length): The minimum pressure required to transfer an axial force/torque is respectively:

$$p_{min} = \frac{F}{\pi d l \mu} \quad \text{and} \quad p_{min} = \frac{2T}{\pi d^2 l \mu}$$

2) the maximum interference shall not produce stresses dangerous to the weaker element, which is usually the hub. And here the problem becomes a little bit more complex. We start from the point to which you had been instructed in the Strength course when discussing thick walled cylinders.

8.2. Stress and strength analysis

Let's have a hollow shaft and a hub, the geometry of which is given by two indices: for the hub: $\delta_h = \dfrac{d_o^2 + d^2}{d_o^2 - d^2}$ and for the shaft: $\delta_s = \dfrac{d^2 + d_i^2}{d^2 - d_i^2}$.

Fig. 8.1. Distribution of stresses in a thick-walled cylinder (Lame's theory) (▲)

There are two principal stresses: the tangential one and the radial one. The radial stress is simple to find. At the surface of contact it is p (compression) and it decreases to zero at the outer surface, both in the hub and the hollow shaft. The tangential stresses at the surface of contact (point 2 and 3) are given by simple formulas:
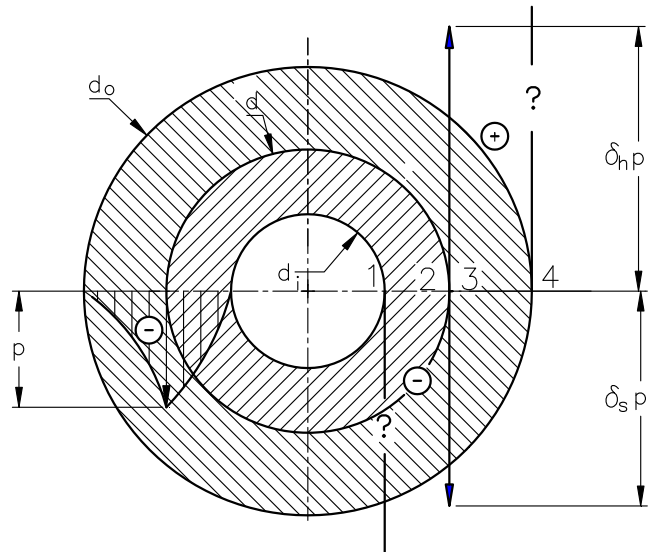
$$\sigma_{t2} = -\delta_s \, p \; ;$$

$$\sigma_{t3} = \delta_h \, p$$

The Lame's theory says that the sum of tangential and radial stresses at each point of the cross section is always constant. Using this formula, try to determine stresses at the periphery of the joint, i.e. at points 1 and 4, both in the shaft and in the hub.

$$\sigma_{t1} = ?$$

$$\sigma_{t4} = ?$$

The maximum tangential stress occurs at the inner surface of the hollow shaft. As shafts are usually made of ductile materials, this stress shall not be greater than the yield stress (in pressed fits we allow a small amount of permanent deformation, therefore the limiting stress in not divided by the factor of safety): $\sigma_{t1} \le R_e$.

To check stresses at the surface of contact of the hub, we need to employ the strength theorems: H-M-H for ductile hub, St-Venant (Rankine) for brittle materials ($\sigma_3 = 0$):

$$\text{H-M-H: } \sigma_r = \sqrt{\frac{1}{2}\left[(\sigma_1 - \sigma_2)^2 + \sigma_2^2 + \sigma_1^2\right]}$$

$$\text{St. Venant: } \sigma_r = \sigma_1 - v\sigma_2$$

So the resultant stress at the surface of the hub (ductile):

$$p\sqrt{\delta_h^2 + \delta_h + 1} \le R_e \Rightarrow p_{max} \le \frac{R_e}{\sqrt{\delta_h^2 + \delta_h + 1}}$$

If the hub is made of a brittle material (e.g. cast iron), then:

$$p\delta_h + vp \le k_r \Rightarrow p_{mam} \le \frac{k_r}{\delta_h + v_h}$$

8.3. Selection of a fit

As the result we have two limiting values of pressure. To find the relevant amount of deformation, needed is the general Hook's law:

$$\varepsilon = \frac{1}{E}\left(\sigma_1 - v\sigma_2\right)$$

So for the surface of contact (points 2 and 3):

$$\Delta d_{\min} = p_{\min} d\left[\frac{\delta_h + v_h}{E_h} + \frac{\delta_s - v_s}{E_s}\right]$$

$$\Delta d_{\max} = p_{\max} d\left[\frac{\delta_h + v_h}{E_h} + \frac{\delta_s - v_s}{E_s}\right]$$

When selecting a fit, the calculated deformation shall be modified by a small amount resulting from the levelling of surface irregularities of the hub and shaft (C_f; in micrometers). The minimum amount of interference ($W_{\min}$) shall be not less than:

$$W_{\min} \geq \Delta d_{\min} + 1.2\left(R_{z1} + R_{z2}\right)$$

and the maximum interference ($W_{\max}$) shall not be greater than

$$W_{\max} \leq \Delta d_{\max} + 1.2\left(R_{z1} + R_{z2}\right)$$

where R_{z1} and R_{z2} are numerical values of surface irregularities of the hub and shaft (ten point mean roughness; in micrometers. For smooth turning $R_z = 10$ µm and for fine/rough grinding $R_z = 3.2$ to 6.3 µm).

Using fit and tolerance tables in Appendix 2 a fit shall be found such that the above formulated criteria are met. The procedure is explained in the attached numerical example. Finally, the force of pressing is:

$$F = \pi d l p_{\max} \mu$$

where l is the length of the pressed connection. These engagement and disengagement processes will be illustrated in a laboratory experiment. When seeking the pulling force for a bearing puller, the manufactures of roller contact bearings recommend the following correction factor accounting for surface finish:

$$\Delta d_{eff} = \frac{d}{d + 3}\Delta d$$

NP 8.1. A bronze nut is pressed into a steel holder (a plain carbon steel section of a pipe, see your design project for illustration). Find a press fit such that the friction force developed on the cylindrical surface is alone

sufficient to resist the friction on the surface of the thread. Data: $T = 10$ Nm; $d_o = 40$ mm; $d = 28$ mm; $d_i = 15$ mm; $l = 25$ mm; $E_s = 2.1 \cdot 10^5$ MPa; $E_b = 1.14 \cdot 10^5$ MPa; $v = 0.3$ (steel/bronze); $\mu = 0.1$; R_e (bronze) $= 90 - 120$ MPa.
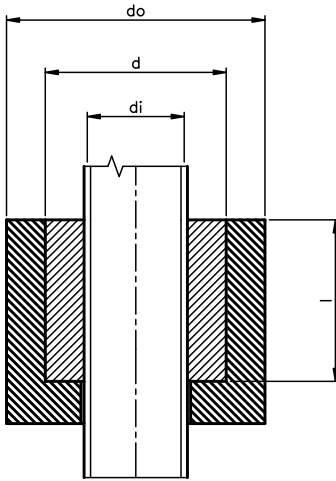
Diametric indices:

$$\delta_h = \frac{d_o^2 + d^2}{d_o^2 - d^2} = \frac{40^2 + 28^2}{40^2 - 28^2} = 2.92 \text{ and}$$

$$\delta_s = \frac{d^2 + d_i^2}{d^2 - d_i^2} = \frac{28^2 + 15^2}{28^2 - 15^2} = 1.8$$

Minimum pressure:

$$p_{min} = \frac{2T}{\pi d^2 \mu L} = \frac{2 \cdot 10 \cdot 10^3}{\pi \cdot 28^2 \cdot 0.1 \cdot 25} = 3.25 \frac{N}{mm^2}$$

Maximum pressure (strength of the bronze insert at the inner surface):

$$p_{max} \le \frac{R_e}{\delta_s + 1} = \frac{100}{1.8 + 1} = 35.7 \frac{N}{mm^2}$$

Deformation at the surface of contact (minimum)

$$\frac{\Delta d_{min}}{d} = p_{min} \left[\frac{\delta_h + v_h}{E_h} + \frac{\delta_s - v_s}{E_s} \right] = 3.25 \left[\frac{2.92 + 0.3}{2.1 \cdot 10^5} + \frac{1.8 - 0.3}{1.14 \cdot 10^5} \right] = 92.6 \cdot 10^{-6} ;$$

$\Delta d_{min} = 0.0026$ mm   and the maximum deformation:

$$\frac{\Delta d_{max}}{d} = p_{max} \left[\frac{\delta_h + v_h}{E_h} + \frac{\delta_s - v_s}{E_s} \right] = 35.7 \left[\frac{2.92 + 0.3}{2.1 \cdot 10^5} + \frac{1.8 - 0.3}{1.14 \cdot 10^5} \right] = 0.00102 ; \Delta d_{max} = 0.028 \text{ mm}$$

Correction factors for surface finish: Correction factor: surface finish for the outer surfaces of the bronze insert $R_z = 6.3$ μm (rough grinding) and the inner surface of the steel holder $R_z = 10$ μm (fine turning). Then: $C_f = 1.2(R_{zh} + R_{zs}) = 1.2(6.3 + 10) = 0.018$ mm. Finally, the effective minimum and maximum deformations required are:

$$\Delta d'_{min} = \Delta d_{min} + C_r = 0.0027 + 0.018 = 0.0207 \, \mu m ; \quad \Delta d'_{max} = \Delta d_{max} + C_r = 0.028 + 0.018 = 0.046 \, \mu m$$

If we assume that the base hole rule in the 7th grade of accuracy H7 (EI = 0; ES = 21μm, then the first tolerance position for the bronze insert giving the required amount of interference (see the attached tables) is t (the lower deviation $ei = 41$ μm and the upper deviation (6th grade of accuracy) $es = 54$ μm. A practical solution: based upon additional friction developed on the frontal surface of the sleeve, we may assume an H7/s6 fit for this connection.

Fig. 8.2 shows a few hints for the design of shaft journals in press fit joints: the hub longer than the shaft journal (a); a circumferential groove adjacent to the connection (b), and an incision into the frontal hub surface (c).
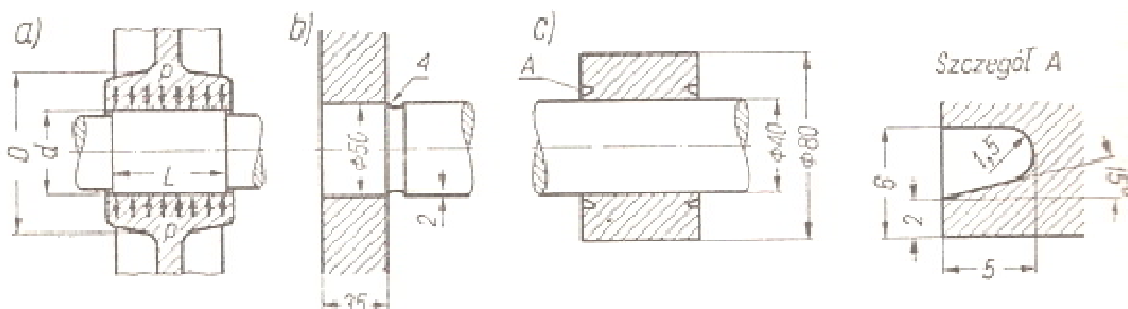

Fig.8.2. Design recommendations for the fatigue design of press fits [10]. Legend: szczegół = detail

HW 8.1. Find the necessary amount of force to mount and dismount a deep groove ball bearing (6310) onto a Φ 50 shaft journal toleranced to m5. Data: bearing width w = 27 mm; inner ring external diameter d_o = 68 mm; μ = 0.1/0.15 (mounting/dismounting); upper shaft deviation es = 20 μm; inner bearing ring deviations ES = 0; EI = -12 μm; steel vs. steel i.e. E = 2.1 10^5 MPa; ν = 0.3.

Hint: When calculating the mounting force (p_{max}), take the theoretical amount of deformation (Δd_{max} = Wmax). When calculating the dismounting force, this deformation shall be reduced (Δd_{eff}).

Answer: F = 13.2/18.4 kN

Glossary

brittle	kruchy
bronze insert	wkładka z brązu
deep groove ball bearing	łożysko kulkowe
ductile	ciągliwy
fine turning	toczenie dokładne
hollow shaft	wał drążony
hub	piasta
press fit	połączenie wtłaczane
radial stress	naprężenie promieniowe
rough grinding	szlifowanie zgrubne
steel holder	oprawa stalowa
strength theorem	hipoteza wytrzymałościowa
tangential stress	naprężenie styczne

9. Shafting

9.1. Introduction

Shafts are designed for the transfer of motion whereas axles are usually (though not always) stationary. That means that the latter are loaded in bending only and the former, in bending and in torsion. Shafts are our first machine elements that need a thorough fatigue analysis (failures occurring to car axles under a load significantly lower than the assumed safe load started at the end of 19th century the fatigue analysis). This is also the first element to which the strength criterion is usually not the most important. Controlled are dynamic and static stability (ability to perform without the loss of shape: bending, deformation, vibrations). To reduce the latter, all shafts need to be balanced, statically and dynamically. Vibrations and balancing problems are discussed in a laboratory experiment given concurrently to the lecture and are omitted in this coursebook.

9.2. Design approach for shafts

9.2.1. Preliminary shaft diameter.

The most important information, which is bending loading, is usually not available at the beginning of the design process. The only information that may be used for the design of a shaft is the torque transferred. We use a simple formula for torsion with an ample value of the factor of safety (4 to 5). (Alternately, we can use the formula for permissible torsional deformation, which is also very simple.)

$$d = \sqrt[3]{\frac{T}{0.2k_s^*}} \; ; \; k_s^* = \; 15 - 20 \text{ MPa} \qquad\qquad d = \sqrt[4]{\frac{32T}{\pi G \varphi_{perm}}} \; ; \; \varphi_{perm} = 0.004 \text{ rad/m}$$

9.2.2. Shaft layout.

When a preliminary diameter has been calculated, all elements can be located on the shaft (usually, the width of a hub is the same as the shaft diameter or by 50% longer). This will allow us to locate all elements and obtain a scheme for the calculation of bending. In the next step we need to determine all external forces loading the shaft. At this stage a chance for a mistake, based upon my experience, is the highest, especially in cases involving helical or bevel toothed gears. As forces act in three dimensions we need to single out all forces acting in two planes (longitudinal forces are usually neglected), which are the horizontal and vertical planes. Up to this moment the procedure is similar to that explained in the Strength course. We have still to learn how to handle combined action of torsion and bending under dynamic conditions.

9.2.3. Combined torsion and bending.

Here is a problem: how to combine fluctuating bending and torsional stresses. As the H-M-H theorem is valid for static loading only, needed is a formula based upon experiments.

Fig. 9.1. Combined reversed torsion and bending

Fig. 9.1 shows the results of testing under simultaneous combined reversed torsion and bending for a steel specimen. The abscissa represents the ratio of the amplitude stress and the endurance limit in bending and the ordinate represents the same limiting values in torsion.
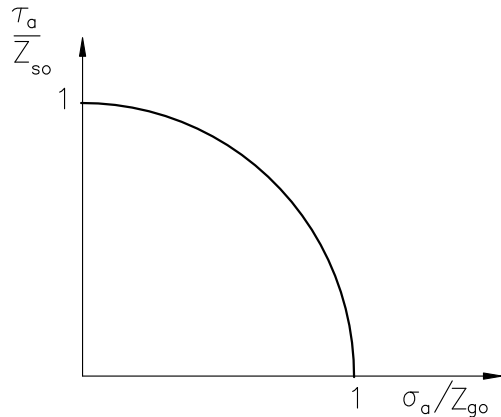
The limiting value in both cases is 1.The equation of a circle with a radius equal to 1 is:

$$\left(\frac{\sigma_a}{Z_{go}}\right)^2 + \left(\frac{\tau_a}{Z_{so}}\right)^2 = 1 \text{ hence} : \sigma_a^2 + \left(\frac{Z_{go}}{Z_{so}}\tau\right)^2 = \left(Z_{go}\right)^2.$$

In a more general form, the left side of the above formula reads: $\sigma_r = \sqrt{\sigma_g^2 + (\alpha\tau)^2}$ and shall be not greater than the design endurance stress, i.e. $Z_{go}/FS = k_{go}$. The coefficient α is equal to 1.7 (reversed bending & torsion, a similarity to the Huber-Mises Hencky theorem) and 0.83 (reversed vending & pulsating torsion – the most frequent case).

For a round cross section the section modulus for torsion is twice as big as that for bending. The above formula can be expressed in terms of moments. This formula is very similar to the H-M-H formula.
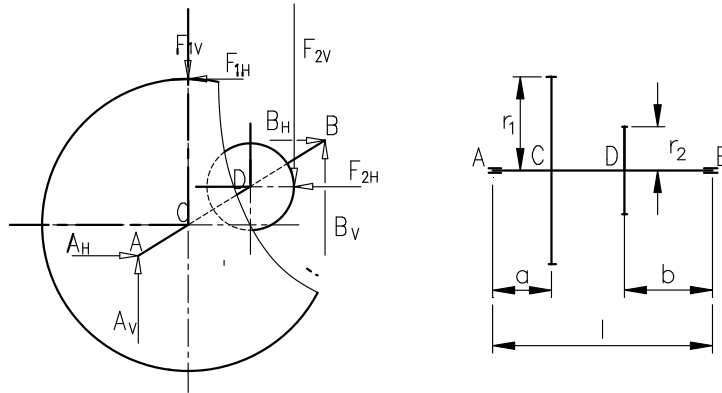
$$\sigma_r = \frac{1}{W_x}\sqrt{M_g^2 + (\frac{\alpha}{2}T)^2} \leq k_{go}$$

As $W_x \approx 0.1d^3$ it is easy to isolate the shaft diameter and to obtain a design formula:

$$d \geq \sqrt[3]{\frac{M_r}{0.1k_{go}}}$$

.

Let's illustrate the shaft design problem with a numerical example (an intermediary shaft in a gear transmission).

NP 9.1. Find the necessary diameter of the shaft shown using the complex stress formula. Data F_{1v} = 1092 N; F_{1H} = 3000 N; F_{2H} = 3640 N; r_1 = 200 mm; r_2 = 60 mm; a = 80 mm; b = 120 mm; l = 300 mm; AISI 1035 steel (k_{go} = 60 MPa).

56

At this point of our lecture you are responsible for the torsional moment equilibrium:

(?) $F_{2V} =$

The loading scheme and bending moment diagrams: The vertical plane: $A_v = 4801$ N; $B_v = 6291$ N $M_v^C = 384080$ Nmm; $M_v^D = 754920$ Nmm The horizontal plane: $A_H = 36456$ N; $B_H = 2984$ N $M_H^C = 292480$ Nmm; $M_H^D = 358080$ Nmm Resultant reactions: $A = 6034$ N; $B = 6962$ N Resultant bending moment $M_c = 482465$ Nmm; $M_D = 835539$ Nmm Torque: $T = 600\,000$ Nmm Resultant moment (bending +torsion) at point D; $M_r = 871852.3$ Nmm Maximum shaft diameter: $d = \sqrt[3]{\dfrac{M_r \cdot}{0.1 \cdot k_{go}}} = \sqrt[3]{\dfrac{871852.3}{0.1 \cdot 60}} = 52.4$ mm	

This shape is known as the parabola of equal strength. For the input and output shafts the diameter is different to zero from the input and output terminal points respectively. The actual shape of the shaft shall be circumscribed on this parabola. This step will be explained in detail during the design class. Some recommendations are given in Fig. 9.4.

9.3. Checkout calculations

When the shaft is designed, all other calculations are of a checkout nature (a strength approach). The fist step is to control deformations at points of location of power transferring elements (toothed gears) and angular deformation (slope) at the position of bearings. A detailed analysis is very time-consuming as the shaft is not of the same cross-section along its length. Graphical methods had been used in the pre-computer era. Now we have dedicated software. You can, however, make a simplified analysis assuming the uniform cross-section shaft (which diameter?) and control it for deformation. If the diameter of this simplified shaft is safe, the actual shaft will also be safe.

Permissible deformation under a toothed gear: f = (0.005 – 0.01) m; m = module
Permissible slope (in radians) at a location of a bearing:
0.001   –   self-adjusting sliding bearings
0.0016   –   tapered roller bearings
0.025   –   deep groove ball bearings

9.4. Fatigue analysis

Fig. 9.2. Strength under combined simultaneous reversed bending and torsion

We use here a modified version of Fig. 9.1. Point C represents the actual bending and torsional stress in the shaft. Graphically, the factor of safety represents a ratio of distance 0L to distance OC. This is given by the following formula:

$$FS = \frac{FS_\sigma FS_\tau}{\sqrt{(FS_\sigma)^2 + (FS_\tau)^2}}$$

To find the actual value of the factor of safety, you have to determine separately the *FS* in bending and in torsion using the same approach that you had already employed when preparing your first homework assignment in fatigue. Fig.9.4 shows fatigue design recommendations for shafts.
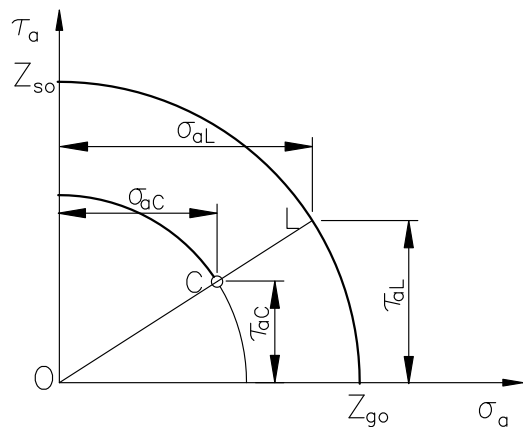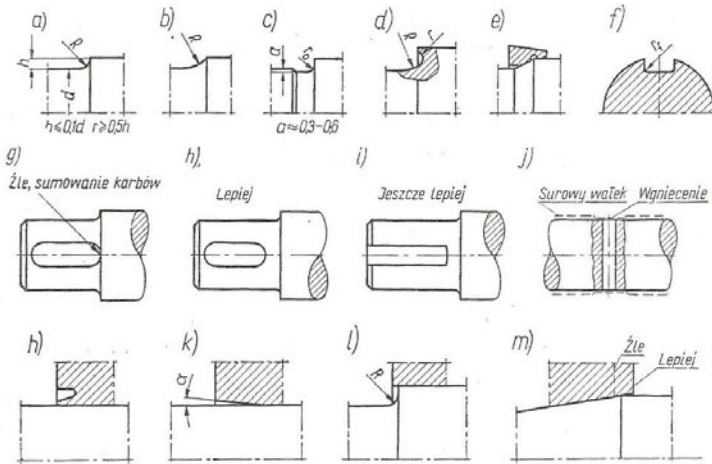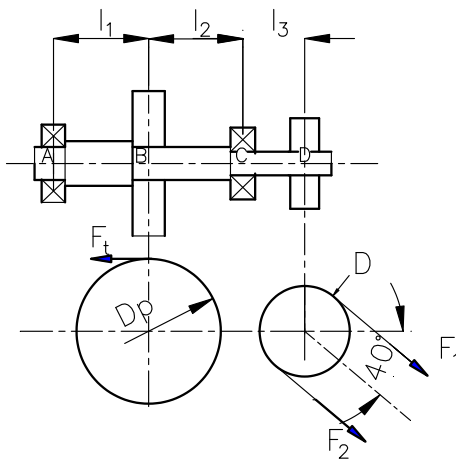
Fig. 9.3. Fatigue recommendations for shafts [10].

Legend: źle = wrong; sumowanie karbów = summation of stress risers; lepiej = better; jeszcze lepiej = still better; surowy wałek = row material; wgniecenie – local deformation/dent

HW 9.1. For the shaft shown (automated transfer system in a metal stamping plant), find the maximum diameter using the combined load formula (bending + pulsating torsion). Draw the necessary diagrams. Data: F_t = 3200 N; F_r = 1164 N; F_2 = 330 N; D_p = 400 mm; D = 250 mm $l_1 = l_2$ = 250 mm; l_3 = 150 mm; material AISI 1040 steel (R_e = 406 MPa; Z_{go} = 240 MPa); assume FS = 4.

Answer: d = 53 mm

Glossary

| balancing	wyważanie
reversed bending	wahadłowe zginanie
bevel gearing	kola zębate stożkowe
car axle	os wagonu kolejowego
circumscribe	opisać
dedicated	tu: opracowane dla potrzeb
helical gearing	koła zębate skośne
layout	tu: rozplanowanie elementów osadzonych na wale
locus	miejsce geometryczne
ordinate	rzędna
self-adjusting	samonastawne
single out	wydzielić
slope	kąt pochylenia
stamping plant	kuźnia
tapered roller bearings	łożyska stożkowe

10. Couplings

10.1. Equivalent (reflected) inertia

As the idea of equivalent inertia systems shall be explained in the course of the Theory of Machine and Mechanisms, allow me to limit this paragraph to the main points only. The criterion of equivalency is the equality of the kinetic energy of the actual and equivalent systems. Therefore:

- Any inertia (e.g. 0.9 kgm^2) that rotates in the actual system (e.g. 500 rpm) slower than in the equivalent system (1500 rpm) must be reduced by a factor equal to the square of the transmission ratio between the two shafts (($1500/500)^2 = 3^2 = 9$). The reduced inertia will be 0.1 kgm^2. This procedure applies usually to the driven side.

- Any inertia that rotates in the actual system faster than in the equivalent system must be increased by the square of the relevant transmission ratio.

- Elements in linear motion shall be reduced based on the ratio of the linear and angular speeds with the discussed above transmission ratio in mind.

NP 10.1. Find the equivalent mass moment of inertia for the first coupling (motor/input to the transmission gear) and the second coupling (output shaft from the transmission gear) used in the transmission system of a belt conveyor shown. Data: $I_m = 0.0025$ kgm^2; $J_1 = 0.0005$ kgm^2 (the pinion) $J_2 = 0.002$ $kgm^{2)}$; (the gear); $J_d = 0.65$ kgm^2; $m = 100$ kg; $D = 200$ mm; $u = 2.15$.
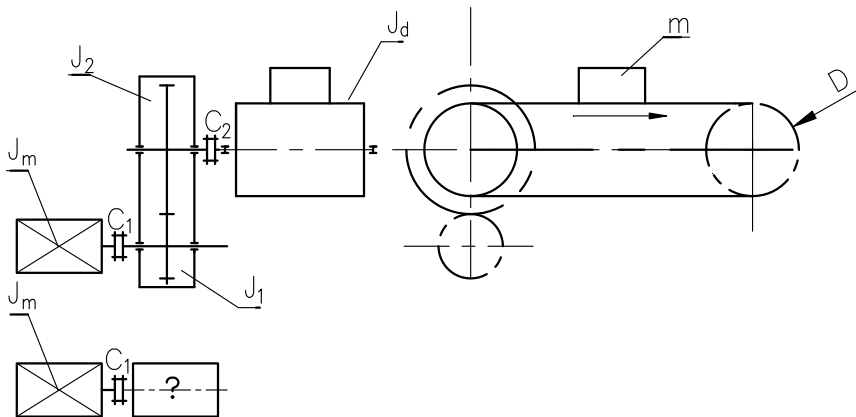
Kinetic energy of the driven elements: $E_2 = \frac{1}{2}\left[J_1\omega_1^2 + J_2\omega_2^2 + 2J_d\omega_2^2 + mv^2\right]$; since $v = D\frac{\omega_2}{2}$ and $\omega_2 = \omega_1/u$

then: $E_2 = \frac{1}{2}\omega_1^2\left[J_1 + \frac{J_2}{u^2} + \frac{2J_d}{u^2} + m\left(\frac{D}{2u}\right)^2\right]$. The term in the square brackets is the sought equivalent inertia.

$J_{2e} = J_1 + \frac{1}{u^2}\left[J_2 + 2J_d + m\left(\frac{D}{2}\right)^2\right] = 0.0003 + \frac{1}{2.15^2}\left[0.002 + 2\cdot0.21 + 100\left(\frac{0.2}{2}\right)^2\right] = 0.091\,kgm^2$

The inertia of the transmission gear is negligible!

10.2. Selection of a coupling

Nearly all of the couplings are subject to standardization. The selection procedure is based upon the rated torque (T_n) and the service factor k, a factor which takes into account the mode of operation of the driver and the driven elements: $T = kT_n$

The smoother is the operation of the driver and driven elements, the lower is the service factor. The limiting cases are three phase electrical motors vs. smooth operating machinery (fans, conveyor belts etc.) with the service factor nearing 1 and one cylinder diesel engine vs. crushing machinery with the factor nearing 3.5. Another factor important in the selection procedure is related to possible errors in the position for the two coupled shafts shown in Fig. 10.1.
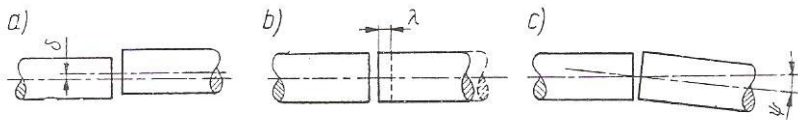

Fig. 10.1.Parallel (off-set), axial and angular misalignments in the position of two shafts [10]

10.3. Rigid couplings

Rigid couplings do not allow for any misalignment or off-set of the connected shafts. Some of them are shown in Fig. 10.2 to 10.4.
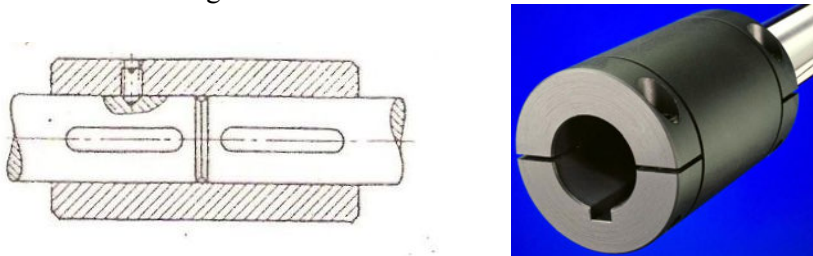

Fig. 10.2. Sleeve coupling [10, Stattford Manufacturing Corporation]
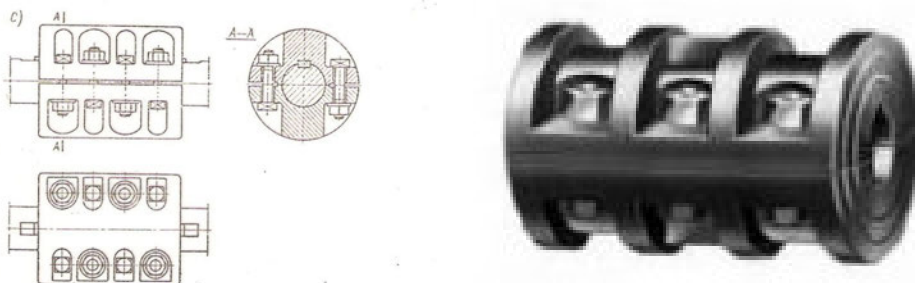

Fig. 10.3. Ribbed (split), clamp coupling [10, Brance-Krachy Co.]
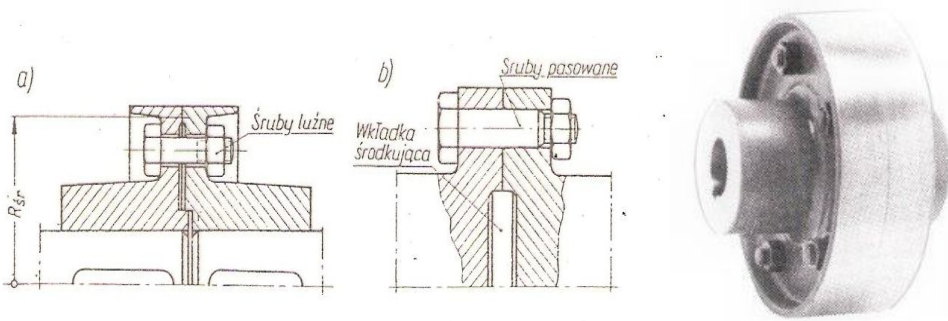
Fig. 10.4. Flanged coupling [10, Royersford]. Legend: śruby lużnie = loose bolts; wkładka centrująca = centring piece; śruby pasowane = fitted bolts

10.4. Flexible couplings

Flexible couplings allow for a certain amount of misalignment and/or offset. An example is an Oldham coupling shown in Fig. 10.5.

Fig. 10.5. Oldham coupling (offset only) [10, Ruland Mfg. Co. Legend: tuleja centrująca = centring piece

A gear coupling shown in Fig. 10.6 has found a widespread application in hoisting machinery.

Fig. 10.6. Gear coupling (misalignment & offset) [10, Rexnord Industries]

A universal joint shown in Fig. 10.7 is a base element of transmission systems used in any vehicle.
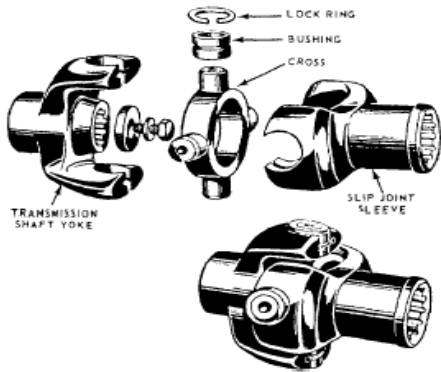
Fig. 10.7. A universal joint [from Engine Mechanics]

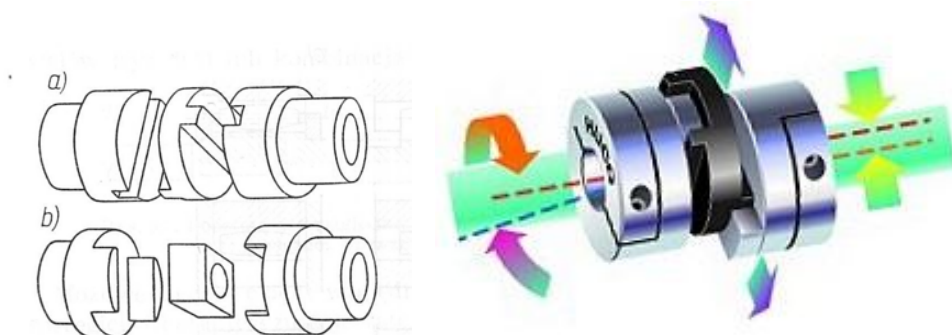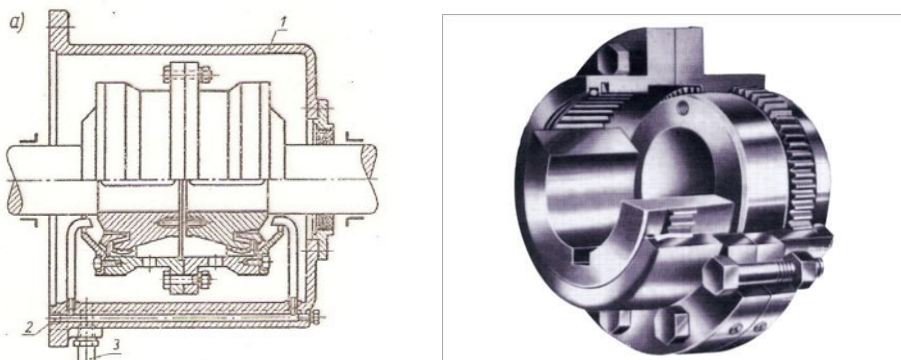The speed of the output shaft will vary depending upon the misalignment angle and position of the yoke ear. Match schemes given in Fig. 10.8 (the upper row) with the two formulas given below.

$$\omega_{2\,min} = \omega_1 \cos\psi \; ;$$

$$\omega_{2\,max} = \frac{\omega_1}{\cos\psi}$$
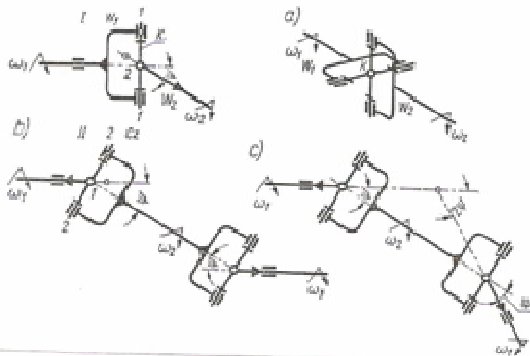
Fig. 10.8. Possible arrangements of constant speed universal joints [10]

Arrangements shown in the bottom row (an intermediary shaft with the two yokes in the same plane!) provide for the constant velocity of the output shaft. By reducing the size of the intermediate shaft (Fig. 10.9a) a homokinetic (or a constant velocity) joint can be obtained. One of the many solutions proposed by a Ford engineer named Rzeppa is depicted in (Fig. 10.9b) and in a photography (Fig. 10.11). The joint has found the most widespread application in the front transmission system of automobiles.
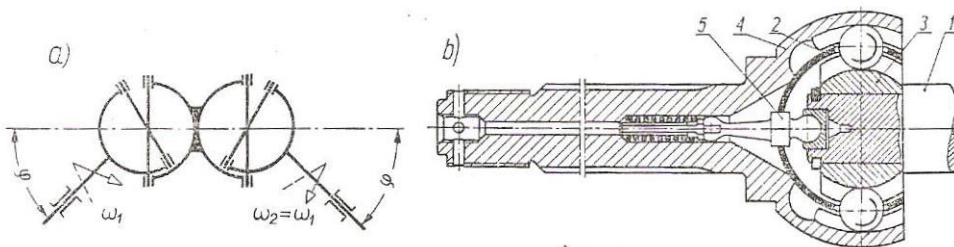
Fig. 10.9. Constant speed universal joint (a) and the Rzeppa joint (b) [10]

Fig. 10.10. The Rzeppa joint, a design embodiment [Wikipedia]
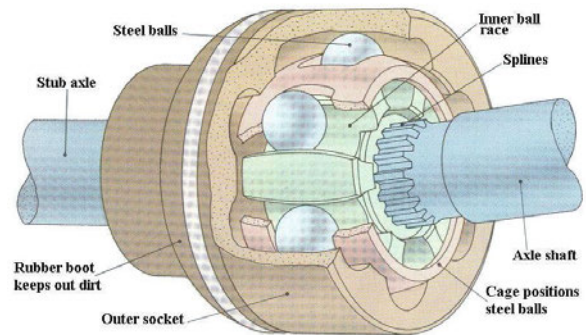
10.5. Elastic couplings

Apart of connecting two shafts and correcting for misalignment, elastic couplings significantly modify the dynamic behaviour of the whole transmission system (torsional vibrations, damping). Their primary duty is to absorb peak loading during the starting or transitional phases of motion. The secondary duty is to damp torsional vibrations in the transmission system. This is possible due to the hysteresis of rubber used widely in this type of couplings. Of the many possible solutions, Fig. 10.11 to 10.13 show the most typical ones.
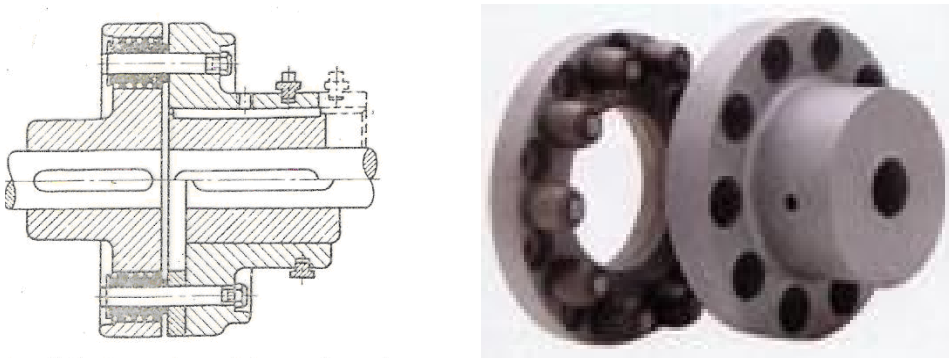
Fig. 10.11. Flanged coupling [10, Hangzhou]
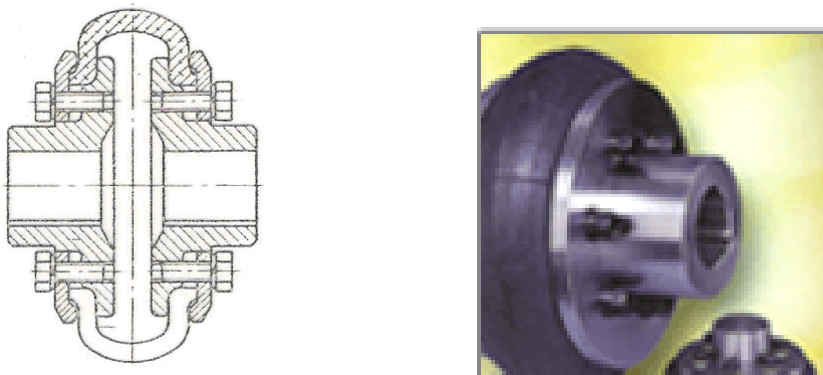
Fig. 10.12. Tire (torus) coupling [10, Swastica Industires]

The Bibby coupling, named after its inventor Dr. James Bibby in 1917 and shown in Fig. 10.12, features a strong progressive characteristic.
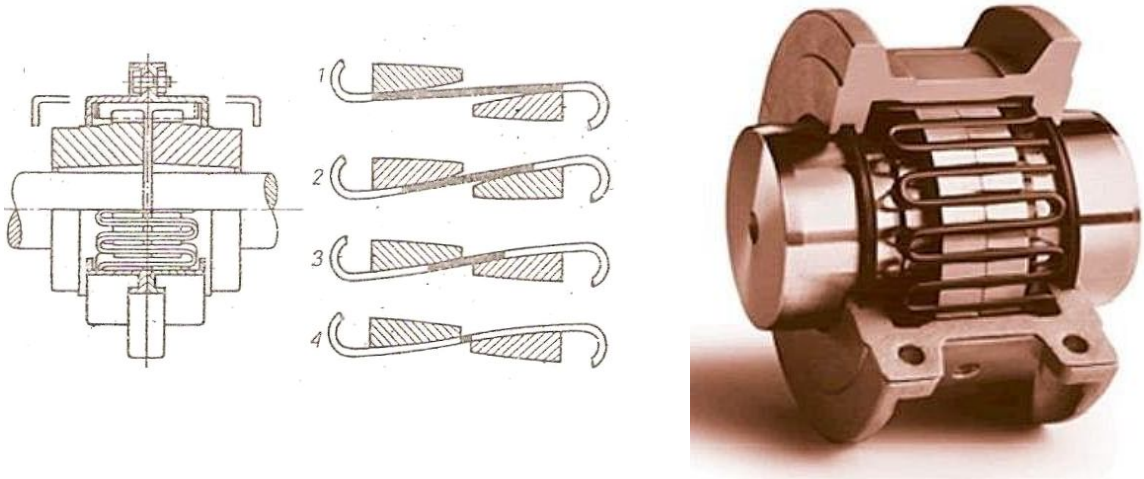
Fig. 10.13. A spring loaded elastic coupling (Bibby coupling) [10, Bibby Transmissions]

HW 10.1. Find the equivalent inertia system for the second coupling (C2) in NP 10.1.

Answer: driver side: $J_{1e} = 0.014$ kgm^2; driven (load) side: $J_{2e} = 2.3$ kgm^2

Glossary

belt conveyor	przenośnik taśmowy
constant speed joint	sprzęgło homokinetyczne/równobieżne
crushing machinery	kruszarki
damping	tłumienie
elastic coupling	sprzęgło podatne skrętnie
equivalent inertia	równoważna bezwładność
fan	wentylator
flanged coupling	sprzęgło kołnierzowe
flexible couplings	sprzęgła podatne giętnie
gear	duże/napędzane koło zębate
misalignment	niewspółosiowość
offset	przestawienie poprzeczne wałów
pinion	małe koło zębate/zębnik
rated torque	moment nominalny
ribbed/clamp coupling	sprzęgło łubkowe
service factor	współczynnik nadwyżek dynamicznych zewnętrznych
sleeve coupling	sprzęgło tulejowe
tire coupling	sprzęgło oponowe
universal joint	sprzęgło Cardana

11. Clutches

11.1. General

There are two types of clutches; those operating by positive engagement (an example is a gear coupling converted into a clutch Fig. 11.1), and those operating on the friction rule (disk, multi-disk) shown in Fig. 11.2 and 11.3. The former may be used only when the speed of the two shafts is the same. The latter are the dominant ones, and we shall discuss a few topics related to their operation.
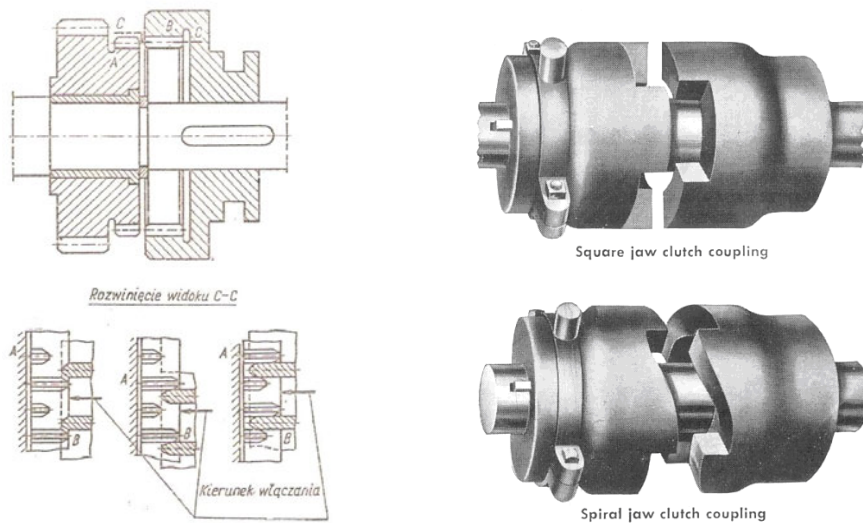
Fig. 11.1. Positive (gear, jaw/dog) clutches [10, Wallace]. Legend: Rozwinięcie widoku…= Development of view C-C; Kierunek włączania …= Direction of engagement
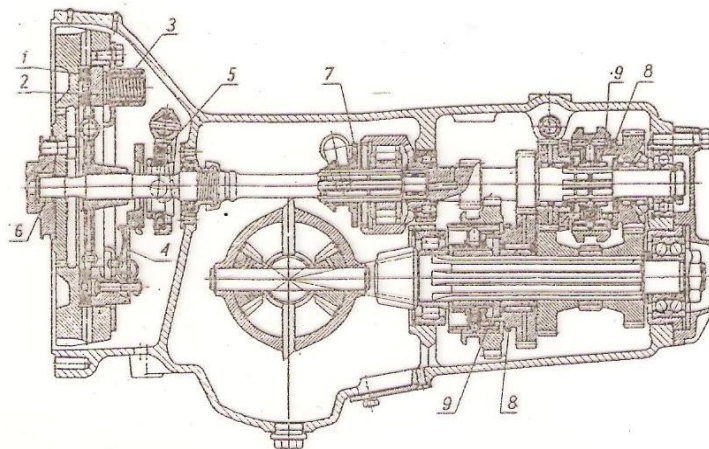
Fig. 11.2. An automobile friction clutch (1 to 3) [10]
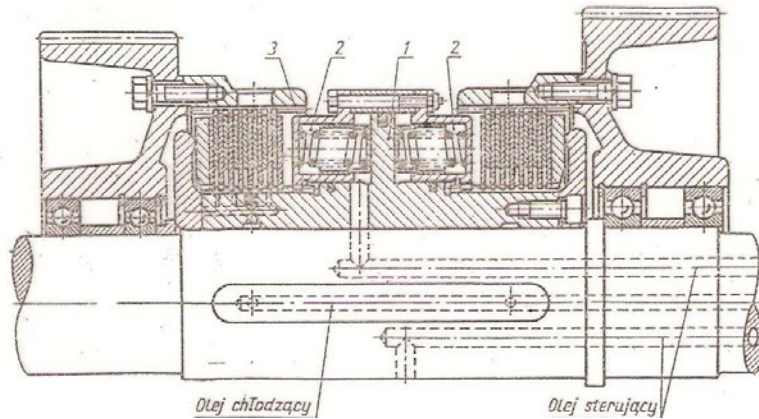
Fig. 11.3. A machine tool friction clutch [10]. Legend: olej chłodzący = cooling oil; olej sterujący = control oil

11.2. Starting analysis

When starting the engagement process, the speed of the driver shaft drops slightly and the speed of the driven shaft accelerates rapidly from zero to a certain speed, common with the driver shaft. This is on an assumption that the inertia of the driver side is very large as compared to the inertia of the driven side. The connected shafts accelerate then to the rated speed (Fig. 11.4a). (This condition is not always true in actual transmission systems: in automobile vehicles the inertia of the driver side is only two to three times as large as the inertia of the driven side. If the clutch pedal were depressed all of a sudden than the speed of the engine would drop below the level of stalling and the engine would stall.

a)   b)   c)
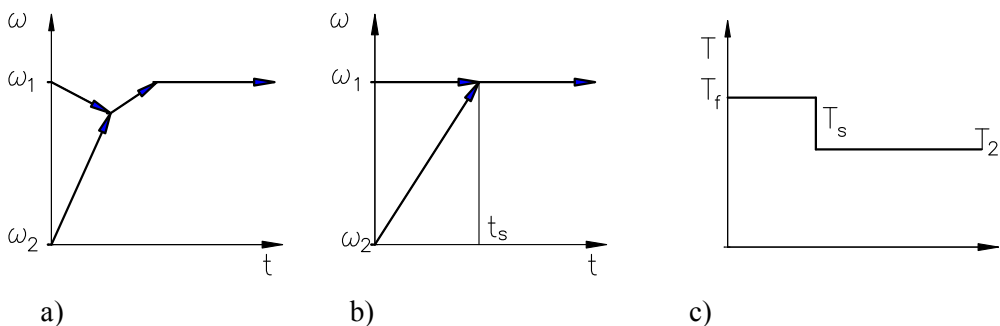
Fig. 11.4. Speed of the two shafts vs. time

Starting time and friction losses (assumed infinite inertia of the driver side Fig. 11.4b). The torque that must be developed on the friction surfaces must be by the service factor greater than the rated torque: $T_f = kT_2$ (Fig. 11.4c). The rated torque is the torque that is necessary to run a system under rated conditions (rolling resistance, grade resistance in the case of an automobile; resistance given by machining forces in the case of machine tools etc.). The difference (T_s) is left for acceleration: $\varepsilon = T_s / J_e$. As $\varepsilon = \omega_1 / t_s$ then finally, the starting time:

$$t_s = \frac{\omega_1 J_e}{T_s} = \frac{\omega_1 J_e}{T_2(k-1)}$$

Clutches are the first machine elements discussed in this course that need detailed thermal calculations. The idea is to balance heat generated during each starting process with heat dissipated during the operation of a clutch. For each starting cycle we have to compare the work delivered by the driver side (Fig. 11.4b): $L_s = T_f \omega_1 t_s$ and the work delivered to the driven shaft:

$$L_2 = \int_0^{t_s} T_f \omega_2 dt = \int_0^{t_s} T_f \frac{\omega_1}{t_s} t dt = \frac{1}{2} T_f \omega_1 t_s \text{ ; hence: } L_f = L_s - L_2 = \frac{1}{2} L_s$$

Each engagement cycle generated a loss of 50% of the energy involved. This must be accounted for in heat balance calculations. The problem will be discussed in more detail during design classes (assignment no 2).

11.3. Friction torque vs. design parameters

An assumption was taken that the mean radius of contacting surfaces is a simple arithmetic average of the minimum and maximum diameters of contact. Textbook formulas are usually more complex (uniform pressure vs. uniform wear).

Fig. 11.5. Friction torque in a multi-disc clutch

$$T_f = F_n \mu \frac{d_m}{2} i = pA\mu \frac{d_m}{2} i$$

$$\text{let}: \Psi = \frac{b}{d_m} \text{ and } A \approx \pi d_m b \text{ then}$$

$$d_m = \sqrt[3]{\frac{2T_f}{\pi p_{all} \Psi \mu i}}$$
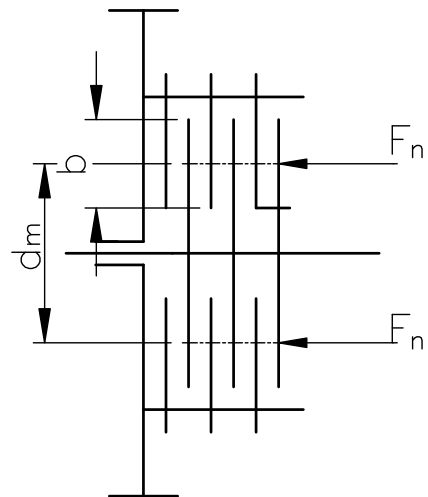
The allowable pressure and the coefficient of friction are dependent upon the type of clutch (wet, dry). Numerical values will be offered with the design assignment no 2.

11.4. Actuation systems

Clutches can be operated by mechanical (need adjusting), hydraulic (troubles with inertia forces), pneumatic or electrical principles. A mechanical system (a set of three levers shown in Fig. 11.6 (the top row) will be discussed in a numerical problem. Solutions in the middle row are so called toggles (when engaged, the linkage is in a dead position). Electromagnetic and hydraulic actuation systems are shown in the bottom row.
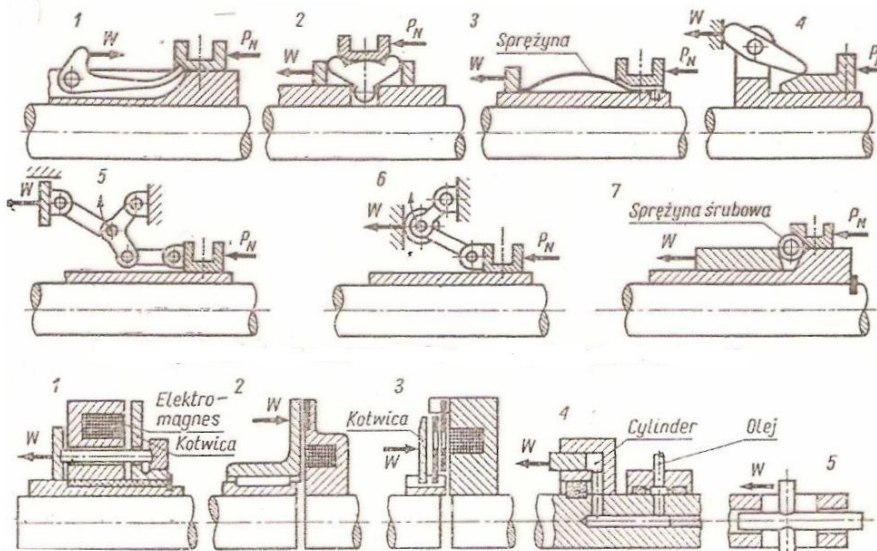
Fig. 11. 6. Different actuation systems [10] Legend: sprężyna śrubowa = coil spring; elektromagnes = electromagnet; kotwica = armature; olej = oil

Let's go back to Fig. 11.3 (hydraulic actuation). To remove oil from a cylinder when a clutch is disengaged, needed is a set of two springs. The selection of their spring constant, preload etc. is a classical problem of preload discussed in chapter 5. The external force is a force that is needed to overcome the inertia of the oil confined in its respective cylinder. Maximum displacement of the compressed spring shall not eliminate gaps between the coils, and finally, under this maximum displacement the opposite spring shall maintain a certain amount of residual tension.

11.5. Operating modes

The operation of a friction clutch may be governed by a certain sequence set in the actuator or by the will of a human being. Friction clutches may also be operated by other principles, e.g. speed, torque, direction of rotation, slip. Exemplary design solutions are shown in the following drawings.

Centrifugal clutches shown in Fig. 11.7 (powder and shoe types) are designed for smooth starting. Possible applications: blowers, conveyor systems, motor-bikes etc.
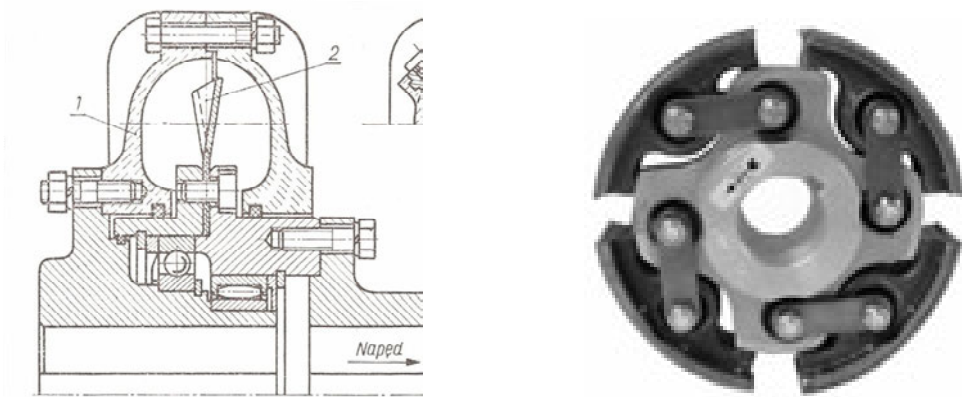
Fig. 11.7. Centrifugal force operated clutches ([10],The Hilliard Corporation). Legend: napęd = driven side

Shear pin clutches (permanent disengagement) and torque limiters (temporary disengagement) shown in Fig. 11.8 are designed for overload protection. Possible applications: crushing, milling, agricultural machinery.
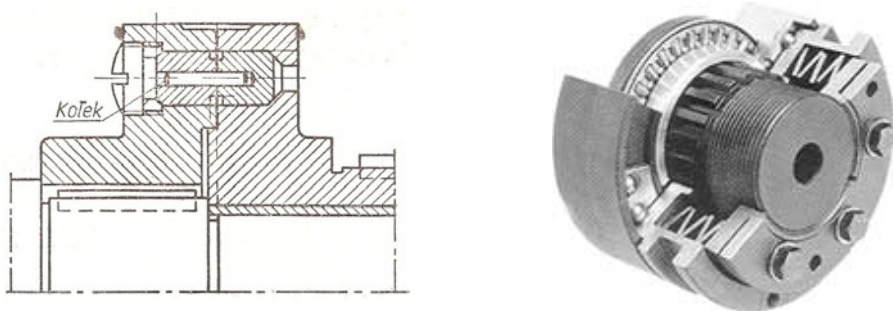
Fig. 11.8. Torque: a ball and dent safety clutch (torque limiter) [Cross + Morse]. Legend: kołek = shear pin

An overrun clutch shown in Fig. 11.9 (a bike hub) is designed for the unidirectional transmission of power (a bike hub).
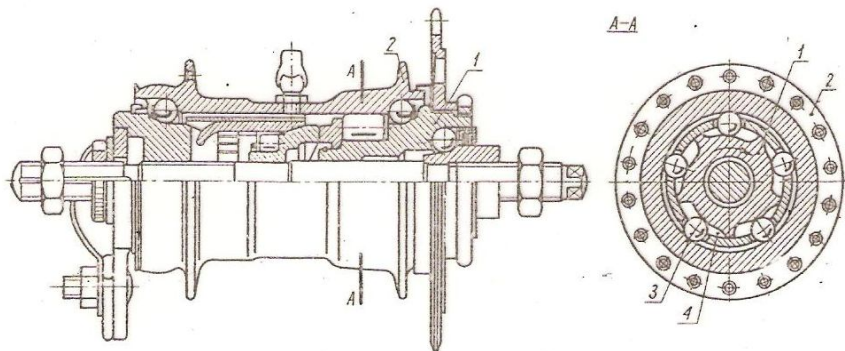
Fig. 11.9. Direction of rotation: an overrun clutche [10]

Fig. 11.10 shows a slip operated hydraulic coupling for application in e.g. earth moving machinery.
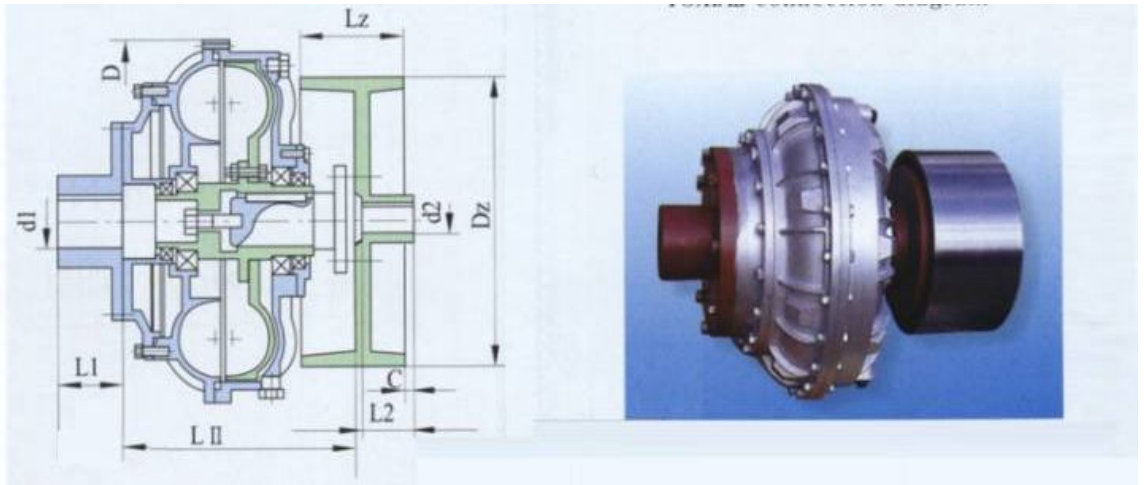
Fig. 11.10. Slip: a hydraulic (fluid) coupling. Application area: earth moving machinery
[Hangzhou Ever-Power Transmissions Co. Ltd]

The turbine impeller in a hydraulic coupling lags behind the pump impeller. This difference is termed as slip: $s = (n_p - n_t)/n$. As the input torque is the same as the output torque, the efficiency of this coupling: $\eta = 1 - s$, i.e. the higher the slip the lower is efficiency. Under normal operating conditions s = 2% to 5%.

NP 11.1 Compute the actuating force F_a in a mechanically actuated multi-disc clutch designed for $T_2 = 100$ Nm. The service factor $k = 1.5$; $\mu = 0.1$ (the graphical method); $d_i = 80$ mm; $d_o = 105$ mm; $\alpha = 30º$
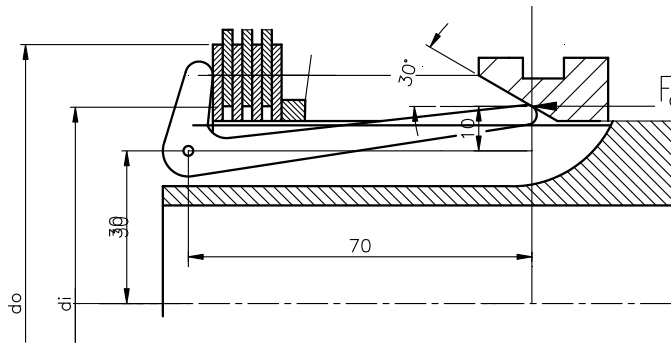
The design friction torque: $T_f = kT_2 = 1.5 \cdot 100 = 150$ Nm. There are six friction surfaces ($i = 6$)

The mean diameter (an approximate formula): $d_m = \dfrac{d_i + d_o}{2} = \dfrac{80 + 105}{2} = 92.5$ mm

The disk engaging force: $F_n = \dfrac{2T_f}{d_m \mu i} = \dfrac{2 \cdot 150 \cdot 10^3}{92.5 \cdot 0.1 \cdot 6} = 5405.4$ N

To construct the force polygon, use dimensions given directly in the drawing. The actuating force at the wedged glider (friction forces neglected): $F_a = 0.8$ kN
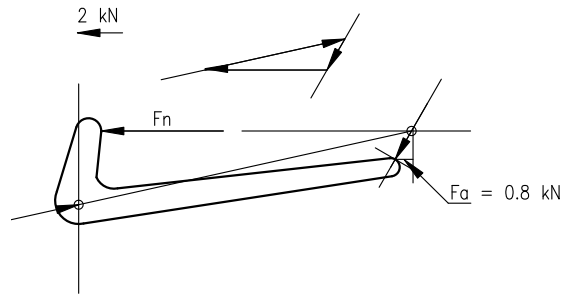
HW 11.1. Explain the operation of a friction clutch shown. Calculate the cone angle α to make the transfer of torque from the shaft (the driver element) to a toothed gear (the driven element) possible. The coefficient of friction between the thread coils and on the conical surface $\mu = 0.1$. Data: $d_2 = 72$ mm (pitch diameter of the thread); d_m =125 mm (mean cone diameter); $\gamma = 14.58°$ *(Tr* 80x20; three start thread). Friction in the longitudinal direction on the cone surface when engaging the two cones, as explained in the lecture, shall be neglected!

Answer: 25°

Hints: Study the distribution of forces in a power screw thread and those in a cone clutch. Compare the axial components of the two force layouts
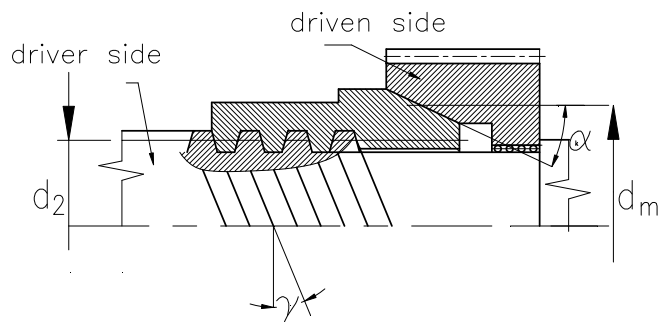
Glossary

actuation	włącznie
back-stop	hamulec zwrotny
engagement process	proces włączania
gear coupling	sprzęgło zębate
grade resistance	opory wzniesienia
machine tool	obrabiarka
overrun clutch	sprzęgło jednokierunkowe
rolling resistance	opory toczenia
safety clutch	sprzęgło bezpieczeństwa
stalling	zadławienie się
thread coils	zwoje gwintu
three start thread	gwint trójzwojny
toggle	mechanizm dwupołożeniowy
wedged glider	przesuwka ze ściętą krawędzią

12. Brakes

12.1. General

A drum brake shown in its base arrangements (Fig. 12.1a) is the most popular braking device. Solutions shown in Fig. 12.1b and 12.1d are more effective in terms of braking effort (no trailing shoe) but of little practical use. A solution shown in Fig. 12.1c provides for uniform distribution of pressure (articulation at the shoes support point) and is the most widespread in the automobile industry.
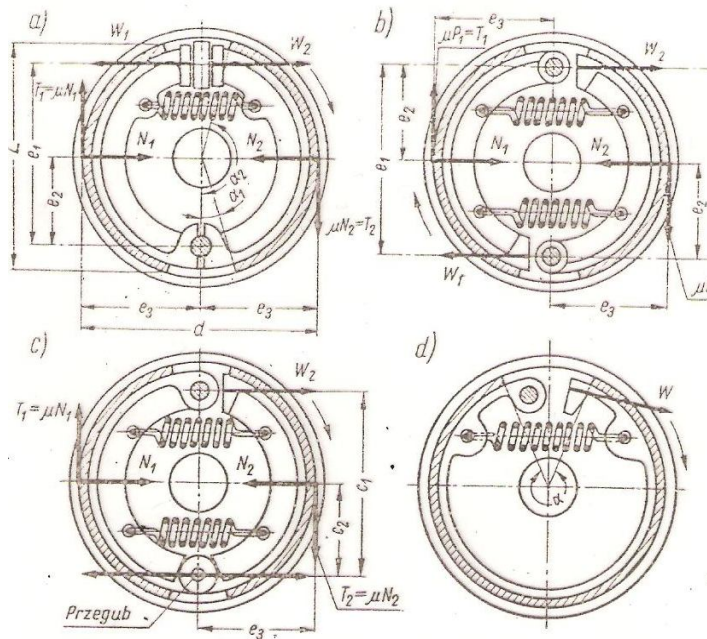
Fig. 12.1. A drum brake with different arrangements of the leading and trailing shoes [10]
Legend: przegub = articulation
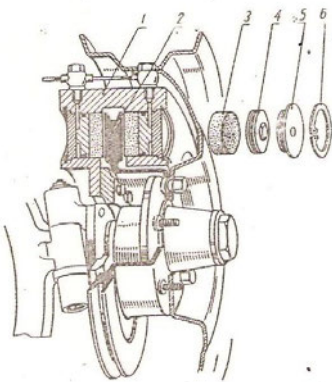
Fig. 12.2 Disk (caliper) brake [10]

The most important performance feature of a brake is its ability to transfer heat produced during braking cycles. Caliper type brakes (Fig. 12.2) are superior to drum brakes in this aspect.

Analytical formulas for the two brake types are discussed in the laboratory course. We shall discuss at length only two types of brakes, a cone brake and a band brake; the latter not because its application is so widespread but because the formulas governing its performance are the same as those used in the calculation of belt transmissions.

12.2. A cone brake

Any friction clutch may easily be converted into a brake by simply fixing its driven element to a stationary supporting structure (vehicle body, machine tool body etc.). An example is a cone brake shown in Fig. 12.3 for application in a shaping machine tool.

Fig. 12.3. A combined multidisc clutch and a cone brake [10]
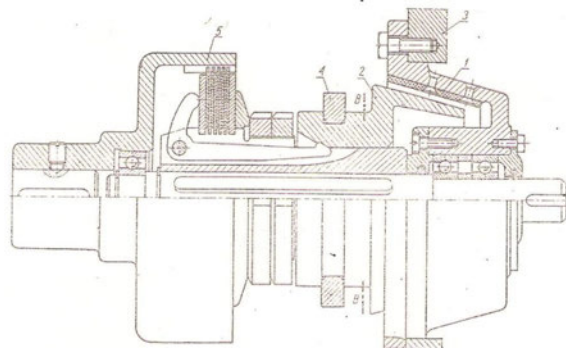
See the formula for a cone shaft-hub connection and put there the friction angle $\rho = 0$. (Friction is a directional phenomenon. If friction is involved in the transmission of the circumferential force, then its value in the axial direction is nil.) The actuating force is then given by:

$$F_a = \frac{2T \sin \dfrac{\alpha}{2}}{d_m \mu}$$

where F_a is the axial actuating force; d_m is the mean cone diameter, and $\alpha/2$ is the half-cone angle.

12.3. Band brakes

Fig. 12.4 shows two base arrangements of a band brake: simple and differential ones.
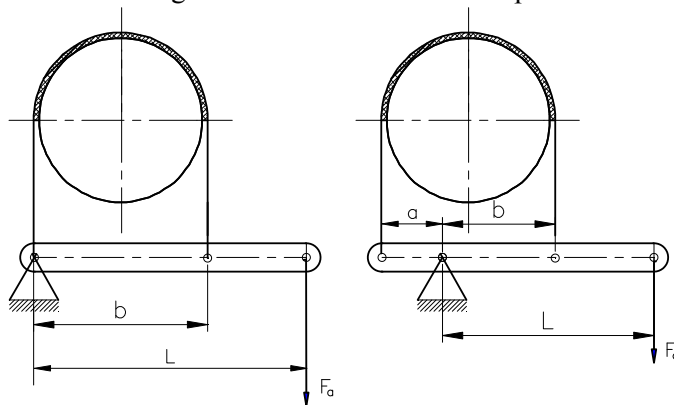
Fig. 12.4. A simple (a) and differential (b) band brake (▲)

Forces in the tension (F_1) and slack side (F_2) of the band are related in agreement with the Euler's equation: $F_1/F_2 = e^{\mu\alpha}$, where α is the wrap angle in radians. Using the equation of static equilibrium: $F_1 - F_2 = F = 2T_f/D$ we have:

$$F_1 = F\frac{e^{\mu\alpha}}{e^{\mu\varepsilon}-1} \text{ and } F_2 = F_1 - F$$

The term $e^{\mu\alpha}$ is denoted usually as *m*. Now let's establish the equation of equilibrium for the actuating lever in both cases shown in Fig. 12.4 (Indicate all active forces acting on this lever!)

A simple band brake (a): $F_a L - F_2 b = 0$ hence $F_a = F_2\frac{b}{L}$

A differential brake (b): $F_a L + F_1 a = F_2 b$ hence $F_a = \frac{F_2 b - F_1 a}{L} = F_2\frac{b - ma}{L}$

Fig. 12.5. A backstop device
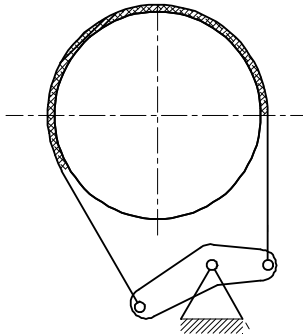
If the arm b is equal to the term "ma", then the actuating force is equal to zero (a self-locking condition). That means that this brake can easily be converted into a back-stop (Fig. 12.5). The backstop shown is disabled when the drum rotates in the CW direction. If, due to an emergency condition (e.g. a power outage), the drum starts rotating in the CCW direction, the back-stop activates and stops the drum.

NP 12.2. Find the actuating force F_a needed to develop a friction power of $P = 7$ kW at a speed of 1000 rpm in a band brake shown. The coefficient of friction $\mu = 0.3$. Data $a = 75$ mm; $\alpha = 30°$; $L = 600$ mm
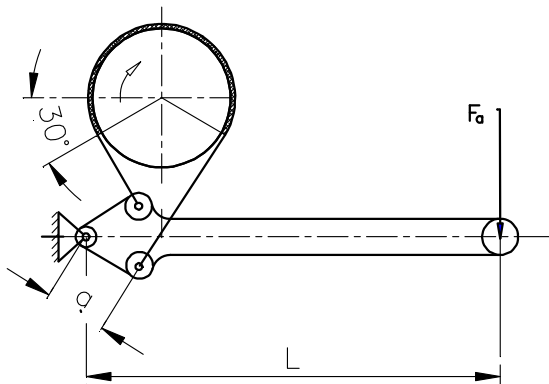
Friction torque: $T_f = \dfrac{P}{\omega} = \dfrac{7\cdot10^3\cdot30}{\pi\cdot1000} = 66.8$ Nm

Rated (nominal) force:

$$F_n = \frac{2T_f}{D} = \frac{2\cdot66.8\cdot10^3}{200} = 668.0 \text{ N}$$

Tension forces (tension side):

$$F_1 = F\frac{e^{\mu\alpha}}{e^{\mu\varepsilon}-1} = 668.0\frac{e^{0.3\cdot1.33\cdot\pi}}{e^{0.3\cdot1.33\cdot\pi}-1} = 934.1 \text{ N}$$

and the slack side: $F_2 = F_1 - F_n = 934.1 - 668.4 = 265.7$ N

Actuating force: $F_a = \dfrac{(F_1 + F_2)a}{L} = \dfrac{(934.1 + 265.7)75}{600} = 150$ N

HW 12.1. Find the actuating force F_a needed to develop a friction torque of 1000 Nm in a band brake shown. Data $\mu = 0.2$; $a = 75$ mm; $b = 225$ mm; $D = 400$ mm.

A hint:

By establishing an equation of equilibrium for the pin joining the slack side of the upped band with the pulling link and the tension side of the lower band you will get a missing fourth equation for the four unknown forces (slack and tension side in the upper and lower band).

Answer: 2146.6 N
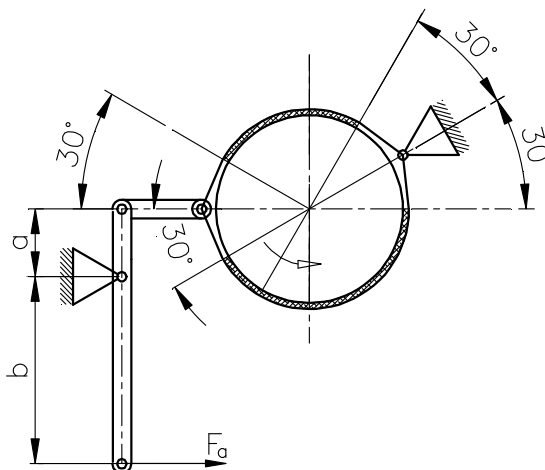
Glossary

back-stop	hamulec zwrotny
band brake	hamulec taśmowy
belt transmission	przekładnia pasowa
calliper	hamulec tarczowy
convert	zamienić
directional phenomenon	zjawisko kierunkowe
involved	brać udział
leading edge	strona atakujaca
power outage	wyłączenie prądu
shoe brake	hamulec bębnowy
slack side	strona luźna, bierna taśmy
stationary	nieruchomy
trailing edge	strona spływająca
wrap angle	kąt opasania

13. Roller Contact Bearings

13.1. Roller contact vs. plain surface (journal) bearings

There are clearly defined areas of application for roller and plain surface bearings though in some instances both types will do equally well. In the table below listed are numerous criteria and the two types of bearing are compared with respect to each other (x denotes the priority choice):

Table 13.1.   Contact vs. plain surface bearings

Criterion	Roller contact	Plain surface
Friction at starting	x	
Servicing and maintenance	x	
Load carrying capacity		x
Noise level		x
Dynamic load		x
Split design		x
Standardisation	x	
No need for running in	x	
High quality, ease of replacement	x	
High thrust load		x
Extreme speed		x

13.2. General description
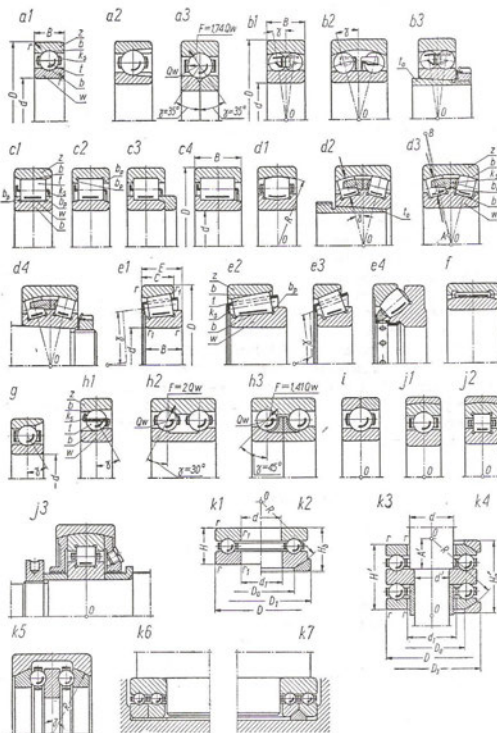
Fig. 13.1. Roller contact bearings [10]

Depending upon the type of loading, ball and roller contact bearings fall into one of the following groups: Radial load only: Cylindrical roller bearings (Fig. 13.1 c1 to c7, f). Radial load and/or small amount of axial load: deep groove ball bearings, designation: 6-(load series, 0, 2, 3, 4)—journal diameter divided by 5 (a1 to a3). Combined radial and axial load: angular contact ball bearings (g1, g2), taper roller bearings (e1 to e4), and self-aligning double row ball and roller bearings (b1 to b3, d1 to d4). Axial load only: thrust bearings (ball and roller types, k1 to k7). There are other lines of division: misalignment (spherical design), space limitations (needle bearings) etc.

Roller contact bearings are highly specialized products (FŁT, SKF, AG, TIMKEN, KOYO, TORRINGTON) and a designer's duty is limited to the proper selection the type and dimensions for a given application. Among the many possible modes of failure: surface fatigue, pitting, wear, seizure, brinnelling, corrosion, breakage, only the first is accounted for in calculations.

13.3. Selection of the service life

The base formula for the calculation of the service life is: $L = \left(\dfrac{C}{P}\right)^p$

where: C = the dynamic (basic) load rating, in N, i.e. the highest load at which at least 90% of tested bearings will rotate 1 mln revolutions (500 hours at 33 rpm) without traces of surface failure,

P = the equivalent radial load (if combined axial and radial action), in N, (roller bearing manufacturers still stick to this obsolete notation of force),

p = the exponent of the equation (p = 3 for ball bearings and p = 10/3 for roller contact bearings).

If the load is increased two times, the service life will decrease 8 times! As the service life is better grasped when expressed in hours, we have the following formula:

$$L_h = \frac{10^6}{60n}\left(\frac{C}{P}\right)^p$$

Agriculture machinery: 5000 hrs
Transmission gears: 20 000 hrs
Machinery operating round the clock: 100 to 200 thousand hours

(For non-standard operating conditions there are a few coefficients which take into account temperature, reliability, material, lubrication, etc.)

13.4. Calculation of the equivalent load

For a combined radial and axial load needed is an equivalent load which, if applied, would initiate the surface fatigue after the same number of revolutions as under actual conditions of loading. The usual form is:

$$P = XF_r + YF_a$$

For deep groove ball bearings the calculations are based upon the static load rating (usually lower than the dynamic rating) and the ratio of the axial load to the reaction in the bearing. See the Appendix for one page of the catalogue to find the necessary data. You need to assume a bearing, select its static capacity, compare with the axial load and select the coefficient "e". If the ratio of the axial load to the radial load is smaller than "e", then the axial load may be neglected. If, not, select the Y coefficient. The procedure is different for different types of bearing, and quite complex for taper roller bearings.

13.5. Bearing arrangements

Deep groove ball bearings: Fig. 13.2 shows a short shaft arrangement and a long shaft arrangement: the latter one is a typical arrangement in which one bearing is held stationary while the other one floats permitting for short displacements due to thermal expansion.
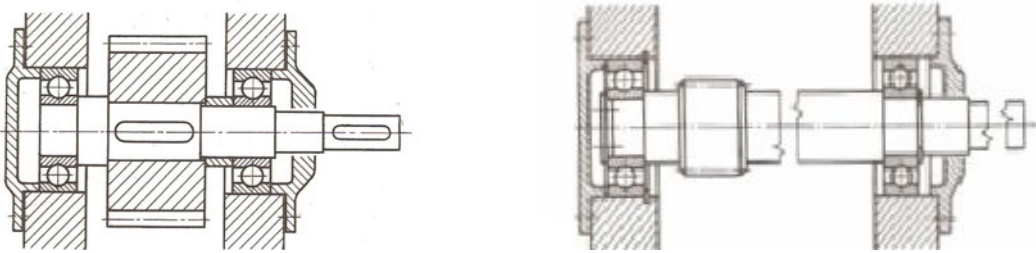
Fig. 13.2. Bearing arrangements for deep groove ball bearings:
a) a short shaft; b) a long shaft [16]

Tapered roller bearings: back to back arrangement (for overhung arrangements, pinion in Fig. 13.3) and face to face arrangements (the crown gear, a typical arrangement where space is not at stake.)
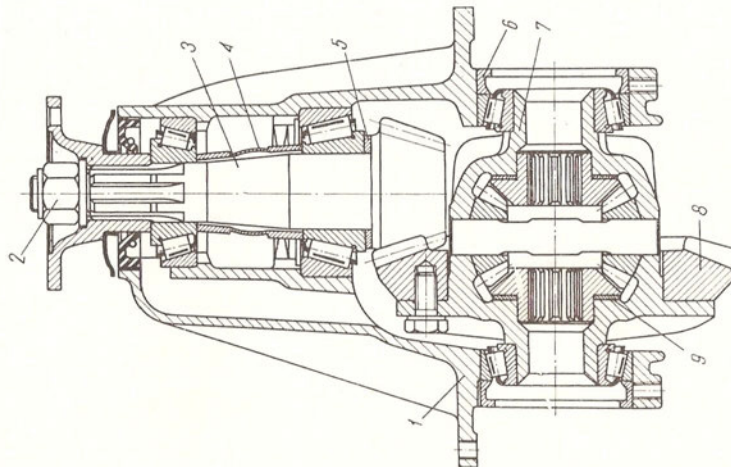
Fig. 13.3. Bearing arrangements for tapered roller bearings (the final drive) [19]

13.6. Selection of fits

Fig. 13.4. Positions of the tolerance zone (T) in roller contact bearings [10]

The rule is that the stationary rings (more generally: the ring that is loaded at one point only) takes a transition fit, the rotating ring (again, the ring that is loaded in turn at each point on the circumference) takes an interference fit.

Positions of the tolerance zone for the inner ring (KB) and outer ring (hB) in roller contact bearings are shown in Fig. 13.4. As a result, a shaft toleranced to m6 (still a transition fit in the hole base system) makes a press fit wit the inner ring. The higher is the speed, and the more severe conditions, the higher is the interference. Usual fits (rotating shaft): HB/m6, stationary housing: F7/hB; H8/hB.
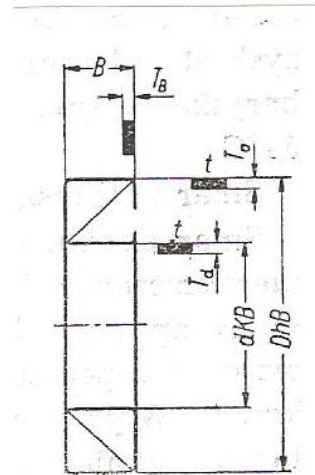
13.7. Lubrication and sealing

Grease: normal speed, temperature and operating conditions. The empty space filled up to 30 to 50%, no more (friction losses!). Oil: high speed and temperature, adjacent elements lubricated with oil.

There are many types of sealing. The dominant ones are:
- felt seals , and
- lip seals [Simmerring] shown in Fig. 13.5
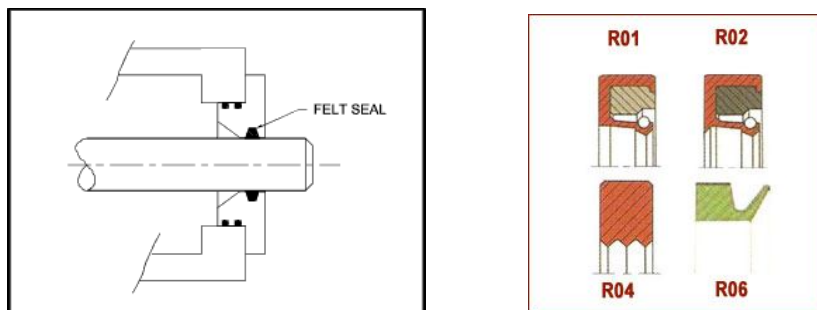
Fig.13. 5. Sealing types (felt and a lip seal) [Roymech]

Felt seals are used for low speed, lip ring, for high speed. Under adverse conditions, combinations of a labyrinth and felt are widely employed (Fig. 13.6).
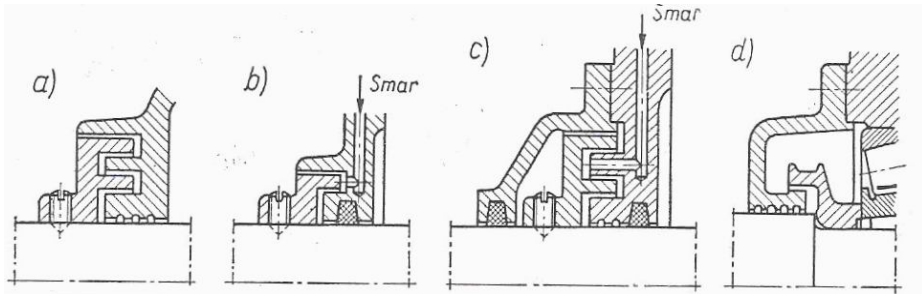
Fig. 13.6. Labyrinth seals [10] Legend: smar = grease

NP 13.1. Find a deep groove ball bearing for the left (A – locating) and right (C – non-locating) bearing support. Find the bearing life if the shaft rotates at a speed of 800 rpm. Data D = 105 mm; F_t = 1500 N; F_r = 582 N; F_a = 430 N. The expected service life: 20000 hrs
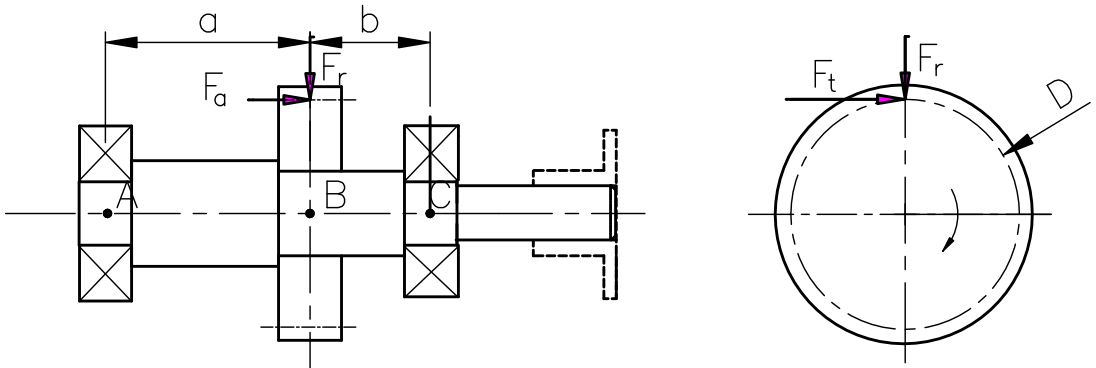
Reactions: R_A = 732.6 N; R_C =1001.7 N. Based upon calculations of the shaft diameter it was assumed: d_A = d_C = 30 mm. The selection procedure for a deep groove ball bearing subjected to a small axial load (bearing A) is a recurrent one. Let's select a medium size bearing, the designation of which is 6206. From an SKF catalogue we find: C_o (static load rating) = 10147N; C (dynamic load rating) = 15137 N. Calculation factor F_a/C_o = 430/10147 = 0.042. Factor e = 0.24 (see a table in the catalogue). The axial load vs. radial load ratio F_a/F_r = 430/732.6 = 0.58 > e. From the table (catalogue) we find: X = 0.56; Y = 1.8. So the equivalent load:

$$P = XF_r + YF_a = 0.56 \cdot 732.6 + 1.8 \cdot 430 = 1184.2 \text{ N}$$

Actual service life of the selected bearing:

$$L_h = \frac{10^6}{60n}\left(\frac{C}{P}\right)^p = \frac{10^6}{60 \cdot 800}\left(\frac{15137}{1184.2}\right)^3 = 43511.4 \text{ hrs} \rangle 20000 \text{ hrs}$$

Since the equivalent load for the right bearing is smaller (Y = 0), we can assume the same bearing size.

HW 13.1. A cross section through an industrial car and the loading for one axle are shown below. Find the expected service life of the left and right bearing (6310) at a speed of 310 rpm.
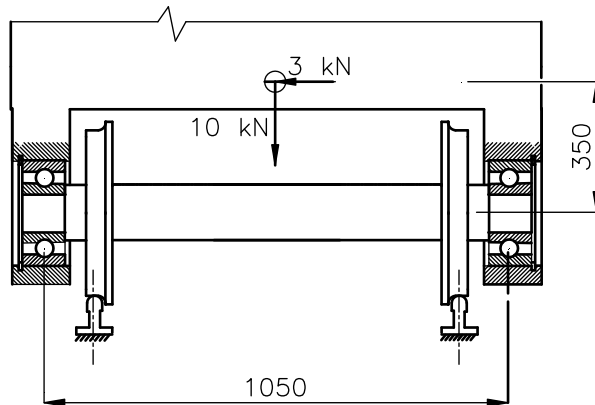
Answer: 21500 hrs (right), 26600 hrs (left)

Hint: It's a short shaft arrangement. Identify first which bearing is the locating one!

Glossary

angular contact	kulkowe skośne
back to back	tu: układ „O"
breakage	wykruszenia
brinneling	wgniecenia pow. na skutek obc. udarowych
exponent	wykładnik
face to face	tu: układ „X"
felt seal	uszczelnienie filcowe
floating bearing	łożysko pływające
grease	smar plastyczny
lip seal	uszczelnienie wargowe (Simmering®)
locating, fixed bearing	łożysko ustalające
lubrication	smarowanie
needle arrangements	złożenia igiełkowe
overhung	wspornikowy
pitting	Pitting/zmęczenie powierzchniowe
reliability	niezawodność
running in	docieranie
seizure	zatarcie
self aligning double row	samonastawne dwurzędowe
service life	trwałość
short shaft arrangement	krótki wał
split design	dzielona konstrukcja
surface fatigue	zmęczenie powierzchni
thrust load	obciążenie osiowe
wear	zużycie

14. Friction and Lubrication

14.1. Coefficient of friction: the Bowden's theory

Fig. 14.1 shows an enlarged cross-section through two surfaces in the frictional contact. Their relative motion is possible on condition that the friction force is sufficient to break the positive contact between the protruding parts of the two surfaces.
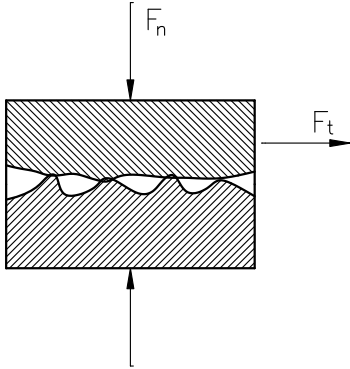
Fig. 14.1. The coefficient of friction

$$F_t = AR_t$$

where A = area of contact
R_t = shear strength

The normal load is a product of the actual contact area and contact pressure:

$F_n = Ap$; where p = contact pressure;

The coefficient of friction: $\mu = \dfrac{F_t}{F_n} = \dfrac{R_t}{p}$

If the value of the coefficient of friction is to be low, the shearing resistance of the two contacting materials shall be low and the resistance to pressure, high. The material of the upper part, which is usually the shaft, is made of a hard material. If the material of the lower part is very soft (low R_t - Fig, 14.2a), the upper part is embedded deep into the lower part and the value of μ is high. If the material of the lower part is also very hard (high p), the area of contact is small but resistance to shear, and consequently – a value of μ, is again very high. The best solution is a pressure resistant base with a thin lining made of soft material (Fig. 14.2c).

a)   b)   c)
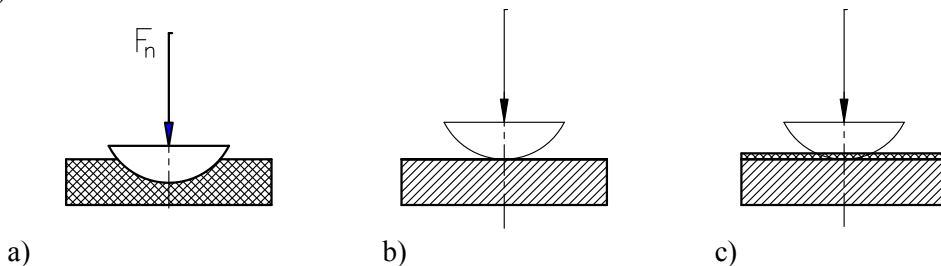
Fig. 14.2. Hard, soft mating material vs. the coefficient of friction

This is what has been adopted for the design of bearing shells. Hard base made of steel or bronze is lined with soft materials like white metals (tin).

14.2. Properties of bearing materials

There are two main bearing materials: tin based and bronze based. These are compared based upon the following criteria: ability to run in, seizure, resistance to corrosion, price, allowable pressure, embeddability (an ability to absorb hard solid particles) etc.

Tin: excellent run in properties, high resistance to seizure, high price; low allowable pressure. The best known tin based alloy is Babbitt (89.3% Sn, 8.9% Sb, and 1.8 % Cu, patented in 1839). Temperature sensitive. Extensive research has been done to limit the amount of expensive tin (lead, cadmium) in the alloy, but to no avail as yet.

Bronze— high hardness, allowable pressure (Diesel engines!). Additions of lead improve its seizure resistance. Brass and gun meal have poor bearing properties

Aluminium**:** excellent anti-corrosion properties. Inferior in the other aspects.

Porous materials (sintered): Filled with oil, good for mixed friction and poor maintenance conditions.

Plastics: food processing industry (no need for a mineral lubricant), poor dimensional stability. Fillers such as graphite, molybdenum disulphide (MoS_2) significantly improve tribological properties of plastics (polyamide mostly).

Graphite, rubber, wood (water lubricated) and dozens of other materials.

14.3. Bearing parameter (the Stribeck curve)

Fig. 14.3 shows a diagram that you have discussed recently during a laboratory experiment. The left, steep branch represents boundary and mixed-film lubrication; the right branch – full-film (hydrodynamic) lubrication. Put some figures into this plot (numerical values of the friction coefficient).
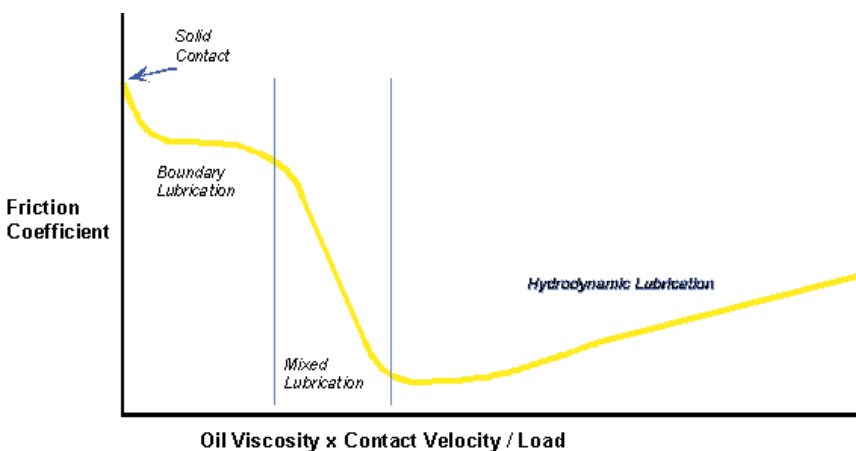
Fig. 14. 3. The Stribeck curve (▲) [from: BHR web site]

Mixed lubrication bearings are designed for the pV parameter. It reflects an ability of a mixed-friction bearing to maintain the thermal balance during operation. Typical values are anything between: 2.5 MPa at a speed of 10 to 60m/s and 15 MPa at a sped of less than 6 m/s.

The fundamentals of the full-film lubrication were laid down by Petroff, Tower and Reynolds.

14.4. The Petroff's equation

A simplified model of a fully hydrodynamic bearing was presented by Petroff in 1883. He assumed the following assumptions:
- the journal is in the central position with respect to the shell,
- the distribution of velocities is linear,
- there are no slips between the lubricant and the surfaces of the journal and the shell.
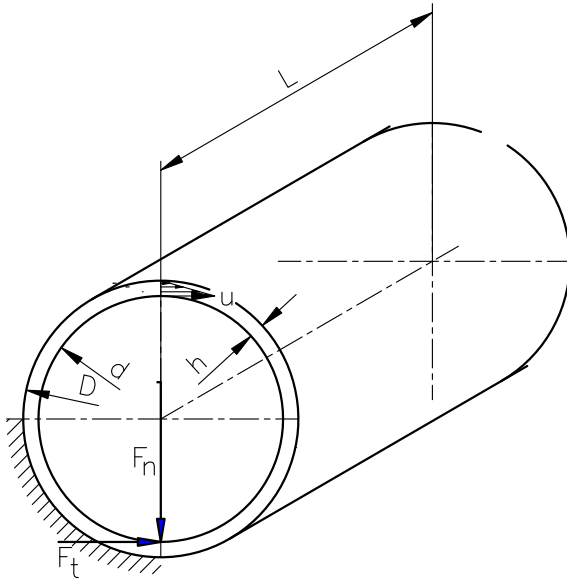
Fig. 14.4. To the Petroff's equation

From the Newton's equation:

$$\tau = -\eta \frac{du}{dy} = -\eta \frac{u}{h}$$

so the shearing force F_t:

$$F_t = \pi L D \tau = -\pi L D \eta \frac{u}{h}$$

The normal load acting on the bearing:

$$F_n = p_m L D$$

but $u = \dfrac{D\omega}{2}$; assuming h = Δ/2 and Δ = D - d; Ψ = Δ/D

the coefficient of friction: $\mu = \dfrac{F_t}{F_n} = \dfrac{-\pi L D \eta D \dfrac{\omega}{2}}{p_m L D \dfrac{\Lambda}{2}} = \pi \dfrac{\eta \omega}{p_m \Psi}$

and its relative value: $\dfrac{\mu}{\Psi} = \pi \dfrac{\eta \omega}{p_m \Psi^2} = 2\pi^2 \dfrac{\eta n^{"}}{p_m \Psi^2} = 2\pi^2 S$

where $S = \dfrac{\eta n''}{p_m \Psi^2}$ is the Sommerfeld number.

This equation provides means to calculate friction losses in lightly loaded sliding bearing, for which the assumption of the central position of the journal is still valid.

NP 14.1. A very lightly loaded 360° bearing 150 mm in diameter and 200 mm long, consumes 1.5 kW in friction when running at 1200 rpm. Radial clearance is 0.15 mm. Find the temperature of oil film using SAE 10 grade**.**

The equation for the power transferred together with the Petroff equation provides the necessary data to calculate the viscosity of the oil, and using the oil chart, its temperature.

Friction power: $P_f = T_f \omega = F_n \mu \dfrac{D}{2} \omega = p_m D L \mu \dfrac{D}{2} \omega$; hence

$$\mu = \frac{2P_f}{D^2 L p_m \omega} = \eta \frac{\omega \pi}{\Psi p_m} \text{ (Petroff equation)}$$

where: $\Psi = \dfrac{\Delta}{D} = \dfrac{2 \cdot h}{D} = \dfrac{2 \cdot 0.15}{150} = 0.002$ and $\omega = \dfrac{\pi n}{30} = \dfrac{\pi \cdot 1200}{30} = 125.6$ rad/s

Finally: $\eta = \dfrac{2 P_f \Psi}{\pi D^2 L \omega^2} = \dfrac{2 \cdot 1500 \cdot 0.002}{\pi \cdot 0.15^2 \cdot 0.2 \cdot 125.6^2} = 0.027 \dfrac{\text{Ns}}{\text{m}^2}$

Using the viscosity chart (see Appendix 5) we can find that for the SAE 20 oil this viscosity corresponds to a temperature of approx. 55 ^{o}C. (See that we are not able to calculate the coefficient of friction at the moment. For the Petroff type of bearing the Sommerfeld number is close to 10. We will discuss again this problem when already in chapter 15!)

HW 14.1. Calculate the coefficient of friction and power consumed in a high-speed bearing of the axial compressor in a jet engine. Data; the radial load $F = 500$ N; shaft diameter $D = 50$ mm; bearing length $L = 50$ mm; the radial clearance $h = 0.05$ mm; speed n = 20 000 rpm; oil viscosity $\eta = 0.01$ Pa·s at a temperature of 68 ˚C (SAW 10W).

Answer: 4.3 kW

Glossary

bearing shell//bushing	panew łożyskowa
embedded	wgłębiony/wcisnięty
gun metal	spiż
journal	czop
lead [wymowa!]	ołów
lining	wyłożenie/wylanie
protruding	sterczące
run in	dotarcie
seizure	zatarcie
sintered	spiekane
tin	cyna

15. The Full Film Lubrication

15.1. The Reynolds equation

Based upon the equilibrium of an elementary volume of lubricant (Fig. 15.1), Reynolds (1866) derived the following equation:
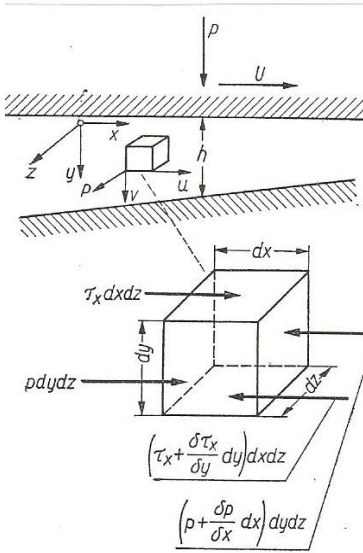
Fig. 15.1. To the Reynolds equation [10]

$$\frac{1}{6\eta}\left[\frac{\partial}{\partial x}\left(h^3\frac{\partial p}{\partial x}\right)\right]+\left[\frac{\partial}{\partial z}\left(h^3\frac{\partial p}{\partial z}\right)\right]=(U_0-U_1)\frac{\partial h}{\partial x}+h\frac{\partial(U_0+U_1)}{\partial x}+2V_1$$

Positive pressure is possible only if any of the three terms on the right side is of a non-zero value. These three conditions are depicted in Fig. 15.2.
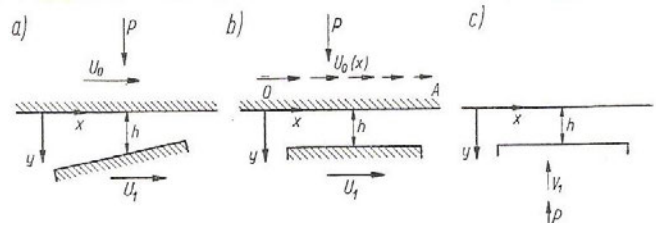
Fig. 15.2. Wedge, shrinking and squeeze conditions for the creation of full-film [10]

The first term is defining a so called wedge action: needed is a difference in the speed of the two plates and a non-zero derivative of the gap height after x. The second term (shrinking) is not viable in practical applications and the last term (squeeze) is the dynamic action (needed is the vertical component of the speed). Of the three terms only the first one is valid for statically loaded bearings and the last one, for dynamically loaded bearings. Possible methods of starting the wedge action are illustrated in Fig. 15.3.
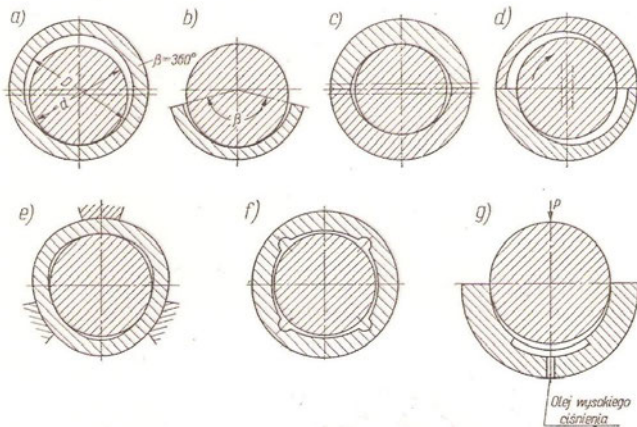
Fig. 15.3. Geometry of full-film journal bearings. Legend: olej wysokiego ciśnienia = jacking oil; płytki nastawne = tilting pads; płytki nienastawne = non-tilting pads; nieruchome = stationary [10]

A short description of Fig. 15.3: a) a standard situation,… c) a lemon type (heavy turbines, helps suppressing vibrations (the oil whirl), d) for CW rotation only, e) three lobe design, …g) a hydrostatic bearing (squeeze effect) or a so called oil jacking for the run up (starting) and run down (barring) phases of turbine operation.

15.2. Design of full film bearings

Bearing shells are mostly split-type designs (upper/lower shell). A thin layer of white metal sits on the steel/bronze /gun metal shell (Fig. 15.4).

Fig. 15.4. Bearing shells [10] Legend: Pasek bezpieczeństwa = emergency support collar; wylanie białym metalem = white metal coating; korpus – spiż = Bush – gun metal
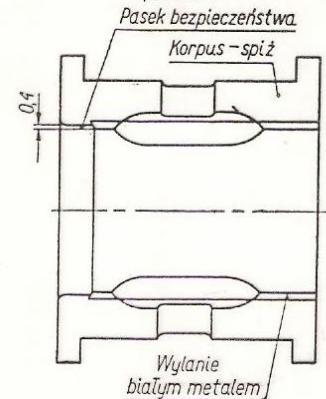
The shell assembly shall be provided with mechanical means helping in the alignment of the shaft within the shell (Fig. 15.5). The most employed solution shown in Fig b is used for the alignment of the shaft and the shell during assembly only.
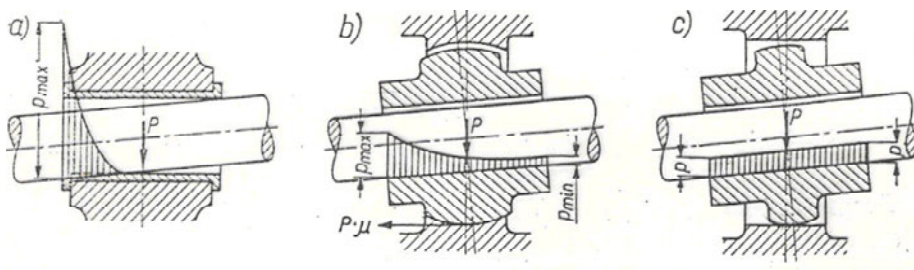
Fig. 15.5. Accommodation to the shaft misalignment [10]

Fig. 15.6 shows the design of a stand alone journal bearing that is externally fed with lubrication oil.

Fig. 15.6. A stand alone externally fed journal bearing [10]. Legend: podłączenie termometru = thermometer coupler; dopływ oleju – lubrication oil inlet; odpływ oleju; oil drain
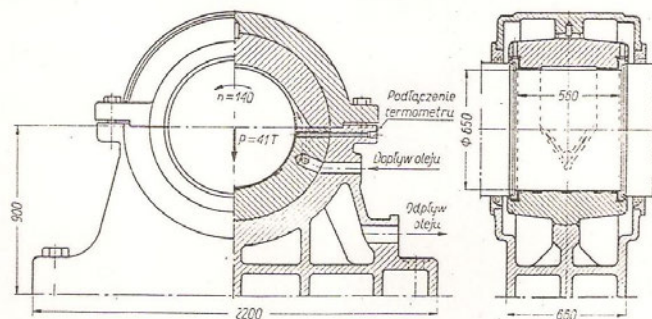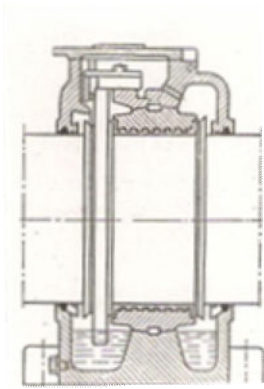
Fig. 15.7. A fixed ring bearing [10]

Fig. 15.7 shows a typical marine bearing with a stationary flange transporting oil to the upper casing, collected there by a scraper and directed to the lower shell.
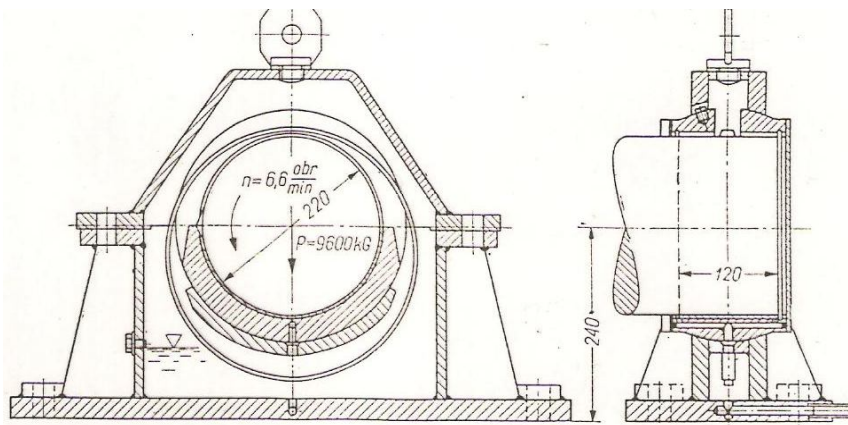
Fig. 15.8. A fabricated housing bearing with a loose lubricating ring for a water turbine application. [10]

Fig. 15.8 shows a bearing lubricated with a loose ring. Notice a fabricated housing (ecology!). As the capacity of this system depends on a good grip between the shaft and the ring, and the geometry of this pair meets all the conditions formulated by Reynolds to create the film, the inner surface of these rings is shaped such as to break this film (as in a treaded vehicle tire).
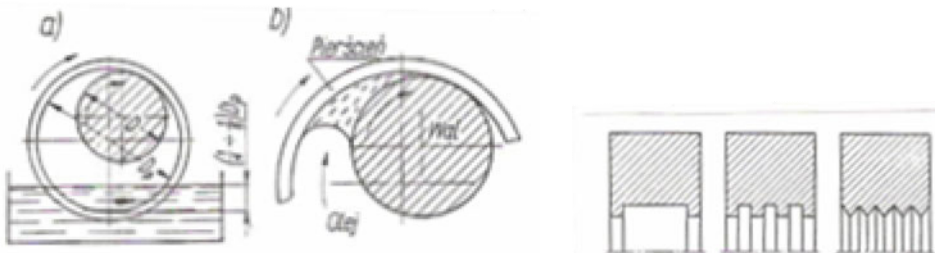
Fig. 15.9. Loose ring oil transportation system (left) and ma means to improve its performance (right) [10]
Legend: olej = oil; pierścień = ring; wał = shaft journal

15.3. Design and checkout calculations

All geometrical parameters involved in the design of full-film bearings are shown in Fig. 15.10 (the beginning of the oil film, the end, position of the maximum pressure etc.).The maximum pressure is distinctly higher than the average pressure. The design/checkout calculations are based upon a numerical solution of the Reynolds equation proposed by Raimondi and Boyd (Fig. 15.11).

Fig. 15.10. Bearing geometry Legend: rozkład ciśnienia…= distribution of oil pressure in the oil film [10]
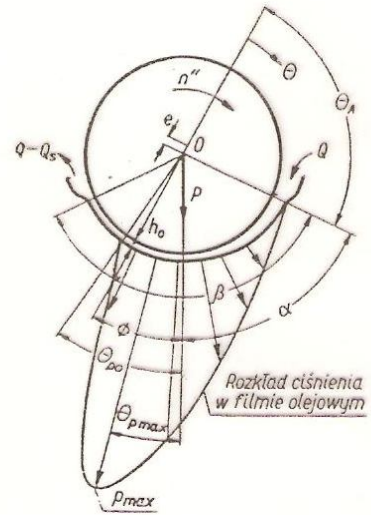
The idea is to select a fit, oil viscosity, oil delivery such that the minimum gap (h_o) is sufficiently large to accommodate surface irregularities both on the surface of the shaft and the bushing and the heat balance is secured. This will be illustrated with a numerical example. Heat balance and oil supply problems are excluded from our considerations! (Be careful with units! The full-film theory is a strange mixture of units. Some of them ($n^{''}$) had been obsolete still in the pre-ISO regulations in this matter.)
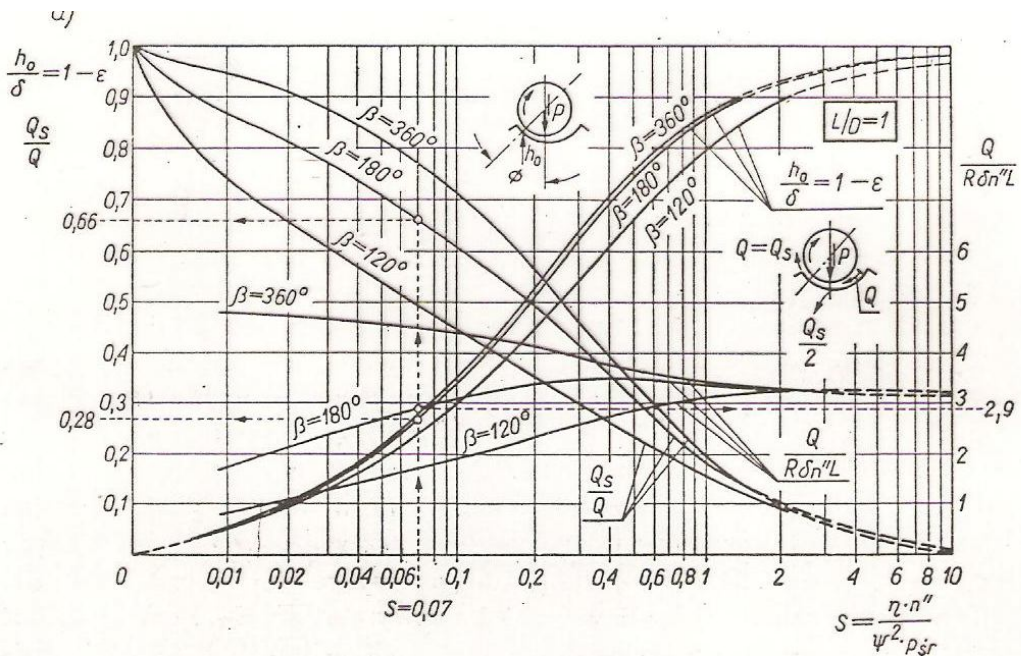
Fig. 15.11. Bearing graphs (excerpts) [10]

NP 15.1. For a journal bearing shown find a fit and oil viscosity to obtain full-film lubrication under geometrical and operating conditions specified in the drawing, i.e. $n = 375$ rpm ($n'' = n/60 = 6.75$ rev/s); $F = 153$ kN; $d = 300$ mm; $L/D = 1$. A temperature to be maintained is $t = 50$ °C.
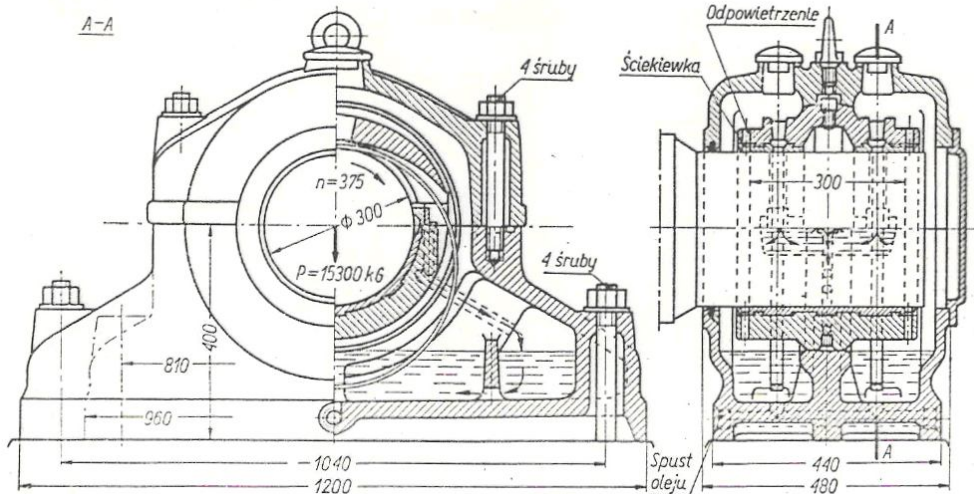
Legend: 4 śruby = 4 bolts; odpowietrzenie = vent; ściekiewka = oil drip; spust oleju = oil drain [10]

The mean pressure in the bearing: $p_m = \dfrac{F}{dL} = \dfrac{153 \cdot 10^3}{300 \cdot 300} = 1.7 \dfrac{\text{N}}{\text{mm}^2}$

The minimum oil gap for this type of bearing shall be $h_0 \geq 0.00025$ d. For d = 300 mm needed is an average amount of clearance in the range of 0.075 mm.

Let's try a Φ300 H11/c11 fit, for which EI = 0; ES = 320 μm; ei = -650 μm, es = -330 μm. The average clearance $L_m = \Delta = 650$ μm ($\delta = \Delta/2 = 325$ μm) and the relative average clearance $\Psi = \Delta/d = 650 \cdot 10^{-3}/300 = 0.002$

The film thickness ratio $h_0/\delta = 75/325 = 0.23$. Using the Raimondi's graph (Fig. 15. 11), the Sommerfeld number shall be 0.07.

Finally, the minimum viscosity of oil shall be: $\eta = \dfrac{S\Psi^2 p_m}{n''} = \dfrac{0.07 \cdot 0.002^2 \cdot 1.7 \cdot 10^6}{6.25} = 0.08 \dfrac{N}{m^2} s$ (see that p_m is in

Pascals!) Using a viscosity chart (Appendix 5) we can see that needed would be a very viscous oil. To increase the load carrying capacity of this bearing, the fit must be a little bit less loose. Let's try with Φ300 H9/d9 ($\Delta = 320$ μm ($\delta = \Delta/2 = 160$ μm) and the relative average clearance $\Psi = \Delta/d = 320 \cdot 10^{-3}/300 = 0.001$). Following the same logic we have: $h_0/\delta = 75/160 = 0.47$; S = 0.18 and $\eta = 0.048$ Ns/m². Light turbine oil might be good for this application.

15.4. Full-film bearings for axial load

With axially loaded bearing we need a large flange on the shaft and a large flange on the supported element. Here in one big problem: how to provide a variable height gap between the two flanges to conform to the wedge action necessary for the creation of full-film? A flange with constant sloped portions is good for specified operational conditions in terms of viscosity and loading only. Design recommendations for this type of bearing are shown in Fig. 15.12.

Fig. 15.12. Fixed profile thrust bearing [10]
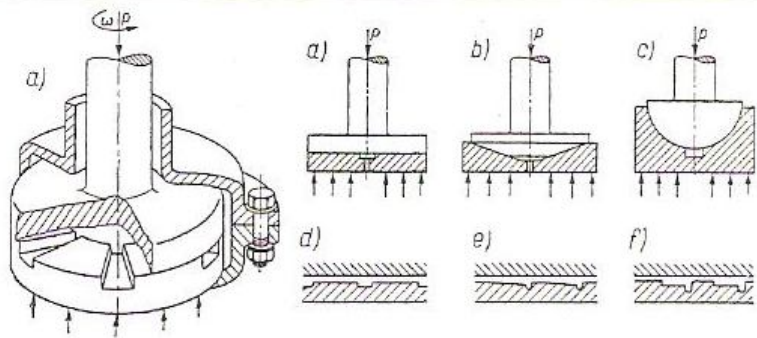
At the break of the 19th and 20th century Mitchell (Fig. 15.13c) and Kingsbury (Fig. 15.13d) proposed non-centrally supported tilting pads.
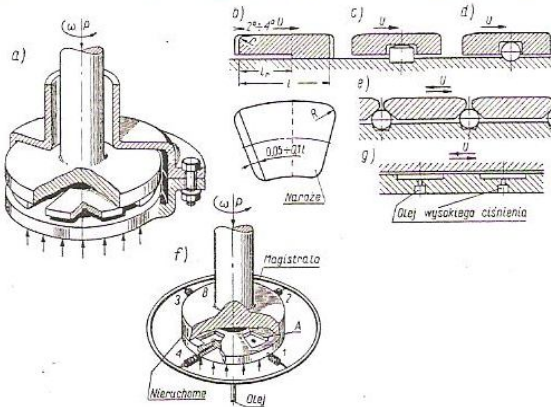
Fig. 15.13. Tilting pads [10]. Legend: olej wysokiego cisnienia = jacking oil; naroże = corner; nieruchome = stationary; magistrala = the main oil duct

Fig. 15.14 shows a typical radial double thrust turbine bearing.

Fig. 15.14   Double thrust turbine bearing [10] Legend: Odciążenie hydrostatyczne = oil jacking; olej wysokiego ciśnienia = high pressure oil; dopływ oleju = oil infeed
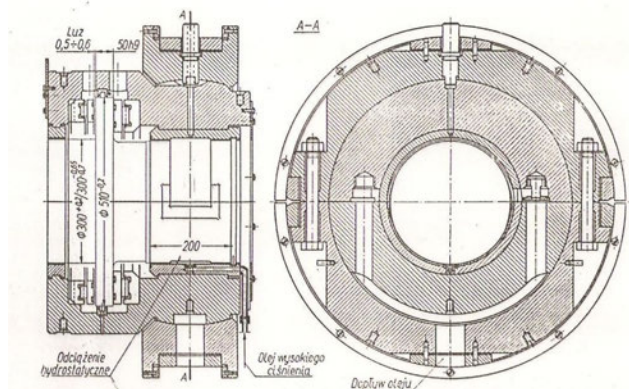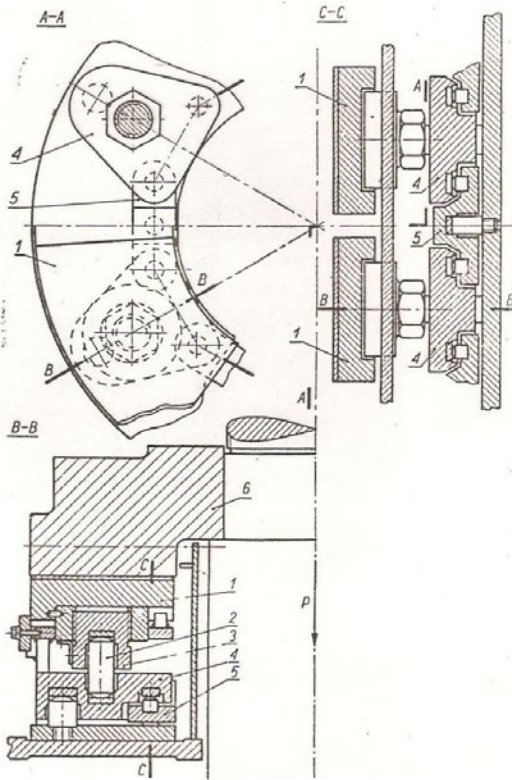
Fig. 15.15. Load balancing for a multi-pad thrust bearing [10]

An interesting feature shown in Fig. 15.15 is a load balancing system for a statically indeterminate assembly of friction pads (cross-section on C-C). Once any of the pads is subjected to an excessive load it yields, moves down and by a system of levers raises the two adjacent pads. As smaller clearance increases the load carrying capacity and the neighbouring plates take part of the load from the overloaded plate.

HW 15.1. A 100 mm in diameter and 100 long shaft journal is displaced by $e = 0.02$ mm from its central position under full load. Find this load if SAE 30W oil at a temperature of 80 ˚C is used. The rotational speed $n = 1000$ rpm; the relative clearance $\Psi = 0.001$

. Answer: $F = 10$ kN

Glossary

barring speed	prędkość obracania turbiny po zatrzymaniu (chłodzenie)
double thrust	dwustronny napór
fabricated	tu: spawane
oil jacking	lewarowanie olejowe
oil whirl	wir olejowy
run down	wybieg
shrinking:	tu kurczenie i rozkurczanie jednej z powierzchni
squeeze	wyciskanie
tilting pad	płytka przechylna
wedge action	efekt klina

Contents (part 2: units 16 to 30)

16. Transmission Systems

16.1. Function of a transmission

The purpose of any transmission is to adjust the characteristic of the driver (i.c. an engine, electrical motor etc.) to the characteristic of the driven machine (vehicle, machine tool, etc.). As a rule, nearly all driven machines require high torque at a low rotational speed and low torque at a high rotational speed (Fig. 16.1 - line a). This hyperbolic line represents the constant power line.
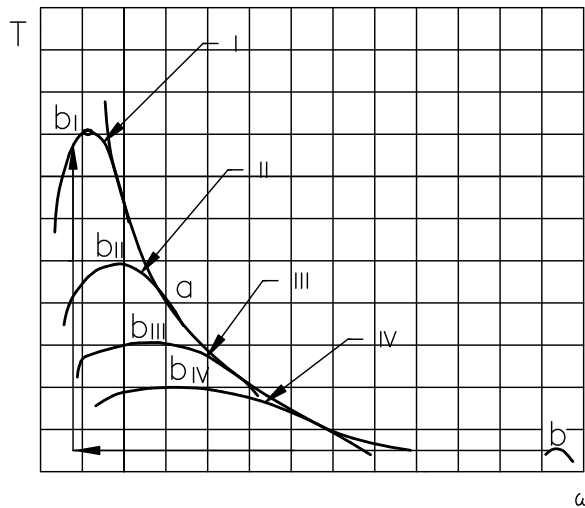
Fig. 16.1. Hyperbola of constant power

Unfortunately, most of the drivers (i.c. engines, AC motors) provide a characteristic that is depicted by line b in Fig. 16.1: the speed is too high and the torque to low to be matched with the line a. Some drivers, e.g. the steam engine, DC motors provide this type of characteristic, and in such cases there is no need for any transmission at all (needed is, however, a means to protect the engine against overspeeding).

The efficiency of any transmission is given by:

$$\eta = \frac{P_2}{P_1} = \frac{T_2 \; \omega_2}{T_1 \; \omega_1} = \frac{T_2}{T_1 u}$$

where $u = \omega_1/\omega_2$ is the transmission ratio.

If we neglect losses, an increase in the torque is inversely proportional to a reduction in the speed. A series system of the gearbox in the low gear and the final drive in the transmission system of any vehicle gives the transmission ratio equal to approx. 20. Each abscissa and ordinate of line b is to be transferred 20 times to the left and upwards respectively (line b_I). The same is done for the second, third and fourth gear in the gearbox giving lines bII, b_{III}, b_{IV}. The enveloping line is in a fairly good agreement with line a.

16.2. Infinitely variable transmissions

In some application needed is a strict conformity with the hyperbolic line. In a wire winding machine (Fig. 16.2) the pull force F is constant. With the drum diameter building up, the torque also builds up linearly. To maintain the same input power, the speed of the drum must decrease continuously.

Fig. 16.2 A wire drawing bench (XVIIIth century) [Actes Rencontres]

Among the many known devices for the continuous variation of speed the best known is P.I.V. (positively continuously variable) - Fig. 16.3.
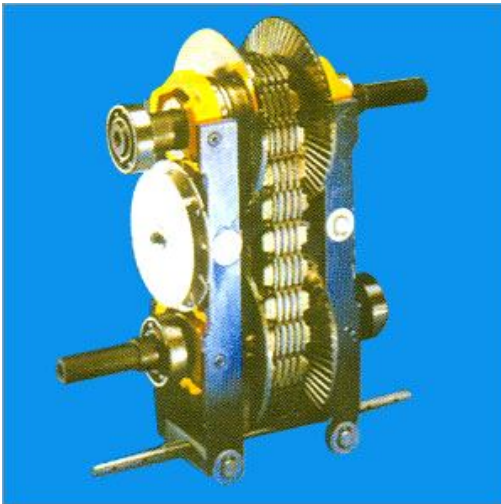
Fig. 16.3. A PIV infinitely variable chain transmission [Klew]

The two halves of each pulley are axially adjustable so that the chain may be moved from the minimum to the maximum position. Let's define the transmission ratio range R:

$$R = \frac{\omega_{max}}{\omega_{min}} = \frac{i_{max}}{i_{min}}$$

For symmetrical drives ($i_{max} = 1/i_{min}$) we have: $R = i_{max}^2$ (usually from 6 to 9).

NP 16.1. A variable speed transmission shown in Fig. 16.3 is designed for $R = 9$. Find the maximum and the minimum speed of the output shaft if the input speed $n_1 = 1500$ rpm. Calculate the maximum and the minimum output torque (neglect losses) if $T_1 = 100$ Nm.

$i_{min} = \dfrac{n_1}{n_{2\,max}}$ and $i_{max} = \dfrac{n_1}{n_{2\,min}}$; Since the drive is a symmetrical one:

$$\dfrac{n_1}{n_{2\,max}} = \dfrac{n_{2\,min}}{n_1} \; ; \; R = \dfrac{n_{2\,max}}{n_{2\,min}} \quad \text{hence}: n_{2\,max} = n_1\sqrt{R} = 1500\sqrt{9} = 4500 \text{ rpm}$$

and $n_{2\,min} = n_1/\sqrt{R} = 1500/\sqrt{9} = 500$ rpm

Torque: $T_{2,max} = T_1\sqrt{R} = 100\sqrt{9} = 300$ Nm ;

$T_{2\,min} = T_1/\sqrt{R} = 100/\sqrt{9} = 33.3$ Nm

Fig. 16.4 shows the first continuously variable transmission system CVT developed by van Doorne (the DAF Company, now a subsidiary of Volvo) for application in automobiles (DAF 55). Power from the driven sheaves was transferred by belt transmissions directly to the rear wheels eliminating the need for the transaxle and differential.

Fig. 16.4. DAF Power train using a continuously variable transmission [from Wikipedia]

Table 16.1 provides basic information needed to prepare a layout for your design assignment in this semester. These are limiting values of the transmission ratio and power transferred by different types of transmissions.

Table 16.1. Transmission types vs. transmission ratio and efficiency [2]

Transmission type	Transmission ratio		Efficiency
	standard	max.	
One stage spur gear	8	20	0.96 to 0.99
One stage planetary	8	13	0.98 to 0.99
Worm	60	100	0.45 to 0.97
Chain	6	10	0.97 to 0.98
Flat belt	5	10	0.96 to 0.98
V-belt	8	15	0.94 to 0.97
Frictional	6	10	0.95 to 0.98
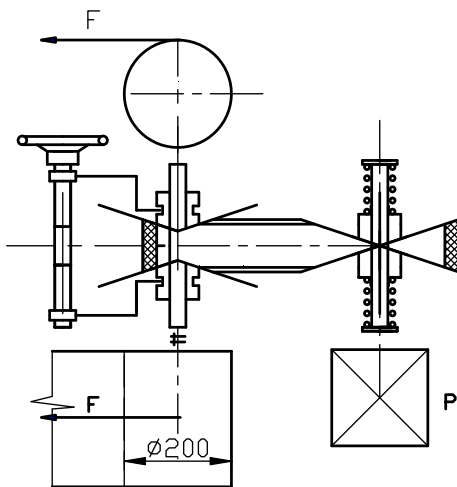
HW 16.1. Steel band is pulled with a constant force and wound around a 200 mm dia. drum. What should be the transmission range in a symmetrical variable transmission shown and the maximum diameter of the wound band if $P = 10$ kW; $n = 1500$ rpm; $F = 370$ N.

Answer: $R = 3$; $D_{max} = 600$ mm

Glossary

chain transmission	przekładnia łańcuchowa
drawing bench	urządzenie do przeciągania
driven	element napędzany
driver	element napędzający
envelope	tu: obwiednia
final drive	przekładnia główna
flat belt t.	przekładania pasowa z pasem płaskim
low gear	pierwszy bieg
machine tool	obrabiarka
overspeeding	rozbieganie
positively infinitely variable	zmienne w sposób ciągły ksztaltowy
sheave	koło pasowe
spur gear	koło zębate walcowe
V-belt transmisison	przekładnia pasowa (pas klinowy)
winding	nawijanie
wire drawing	przeciąganie drutu
worm transmission	przekładnia ślimakowa

17. Pulley Transmissions

17.1. Kinematics, transmission ratio

As you already did an experiment with a V-belt transmission in the previous semester, this chapter shall be considered as a guideline for the calculations and design of this semester's design project (a V-belt transmission) only. The geometrical calculations for a V-belt transmission are covered by a standard and shall be done accordingly (see [12] for help).

The theoretical transmission ration given by the ratio of the big pulley diameter to the small pulley diameter is slightly affected by the phenomenon of elastic slip: the elongation of a V-belt is different at different points due to a difference in the pull force. When a section of the belt on the slack side (large specific mass) enters into the arc of contact with the driven drum, its speed is still the same as that of the pulley. Due to an increasing pull force, belt elongations increases accordingly and this must be associated with a forward directed slip between the belt and the drum. Its maximum value is at the trailing edge (CW slip on the right pulley in Fig. 17.1).
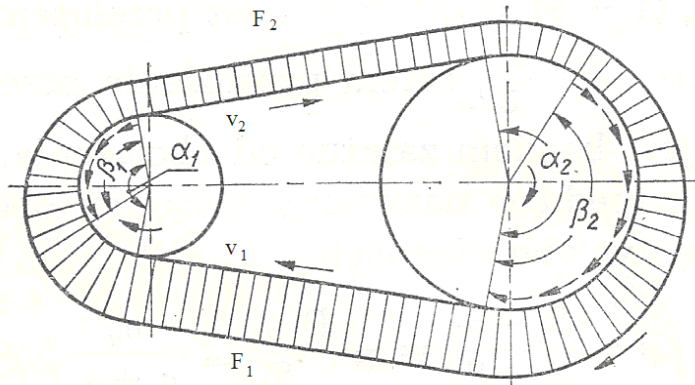
Fig. 17.1. The phenomenon of elastic slip [2]

On the left (driver) pulley, the situation is the opposite one: the belt shrinks with the maximum speed at the trailing side. The greater is the pull force, the greater is the arc of slip. Ultimately, the arc of slip covers the full arc of contact (the wrap angle) and the transmission of load is no more possible (permanent slip). The slip is defined as:

$$\xi = \frac{v_1 - v_2}{v_1}$$

The phenomenon of elastic slip affects the transmission ratio, and it is quantitatively described by the following formulas:

$$u = \frac{\omega_1}{\omega_2} = \frac{D_2}{D_1}\frac{v_1}{v_2} = \frac{D_2}{D_1(1-\xi)}$$

The greater is the slip, the greater is the transmission ratio (usually 1-2 %). You must account for this fact when assessing deviations in the overall transmission ratio of your transmission system (acceptable deviation = ± 4% from the calculated value).

17.2. Force analysis

The basic relationship between the pull force and slack forces and transmission rating was developed by Euler. See the formula that was given in chapter 12 (a band brake!):
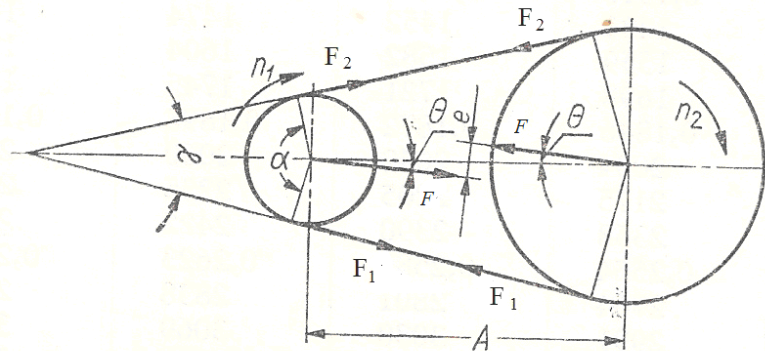
Fig. 17.2. Scheme of a pulley transmission, force and moment equilibrium [2]

$$\frac{F_1}{F_2} = e^{\mu'\alpha}$$

where α is the wrap angle in radians and μ' is the equivalent coefficient of friction.

The situation here is similar to that discussed in the previous semester for a screw-nut mechanism. (Due to an inclination of the thread surface, the normal force, which is responsible for friction losses, is by a cosine of the profile half-angle greater than the normal force). With a V-belt transmission there is a slight difference: the force normal to the surface of a groove is by a reciprocal of the sine of the half V-groove angle (usually 17°) greater than the pull force. This does make a difference! Unfortunately, this formula is helpful in the understanding of the superior friction coupling in V-belt transmissions but is of little use for the calculations of forces. Instead, to find forces loading the driven shaft (you are responsible for this shaft in your design assignment!), use the following two equations: The first is the same as in the band brake (static):

$$F_1 - F_2 = F = \frac{2T_1}{D_1}$$

The second equation is based upon experiments. The ultimate situation discussed in chapter 12 (a band brake) i.e., the full slip condition cannot happen in V-belt transmissions. If we define the drive coefficient φ as a ratio of the effective force over the summation of the two forces (tension and slack sides):

$$\varphi = \frac{F_1 - F_2}{F_1 + F_2}$$

then the graph of the transmission efficiency versus the drive coefficient is shown in Fig. 17.2 below.
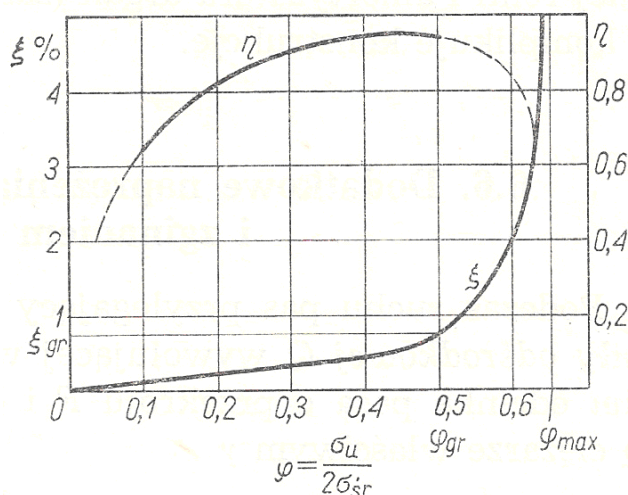
Fig. 17. 3. Efficiency of a V-belt transmission [2]

The maximum efficiency is at φ = 0.45 to 0.55 (assume 0.5). Having thus all the force components acting in the transmission we are able to calculate the resultant load. The resultant load shall be resolved, based upon your individual transmission layout, onto two planes: the horizontal and vertical ones. These are input forces for the calculation of the input shaft to the gear transmission.

17.3. Transmission of power

The belt is subjected to fluctuating tensile, bending and, in the case of high rotational speed, centrifugal loads which limit the amount of the transmitted power. As all belts are standardised in terms of dimensions, it is easy to calculate all the stress components and to establish the load carrying capacity of each belt. These are empirical formulas reflecting the testing of a 1500 mm length, 180˚ contact angle (1 to 1 transmission ratio) and uniformly loaded belt. Any deviation from these conditions shall be corrected by three factors k_L (belt length, i.e. the frequency of fluctuating load), kφ (arc of contact) and k_T (service life and service factor). This is in agreement with the first rule of construction, i.e. a recommendation

to distribute the load transferred into more than one path (an increased number of V-belts to transmit power).

The formulas and their graphical representations are given in the Polish standard PN-67/M-85203.

17.4. Belt tensioning systems

Depending upon the actual layout of the transmission system, again for the sake of our design project, I would recommend one of the following tensioning systems. For vertical (or quasi vertical) positions, a tilting platform/pedestal shown in Fig. 17.4a will do. This position includes also a so called "piggy back" layout (the motor sits on the top of a gear transmission).
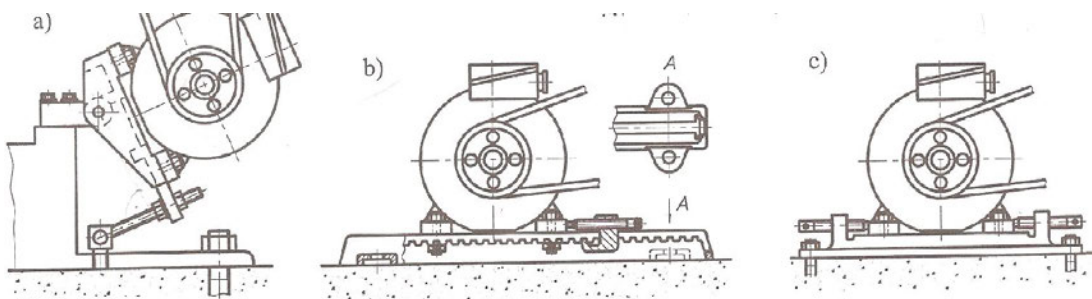
Fig. 17.4. Belt tensioning systems [12]

For horizontal or quasi horizontal positions, take the solution b or c. See that bolts in solution c are only two: one (the right side) is given from the motor front end side is used to provide tension in the belt whereas the second bolt (the left side) is given from the rear end side of the motor and is used to align the pulley with the belt. For long belts an additional dancer roll may be employed.

Glossary

dancer roll	rolka napinająca
elastic slip	poślizg sprężysty
guideline	przewodnik
permanent slip	poślizg trwały
piggy back	„na barana"
reciprocal	odwrotność (liczby)
ultimate	krańcowy
V-groove	rowek klinowy
wrap angle	kąt opasania

18. Gear Transmissions

18.1. Introduction

Fig 18.1 shows a typical layout of a water transportation system that has been in continuous use in Egypt for over 2000 yeas now (donkey/mule driven).
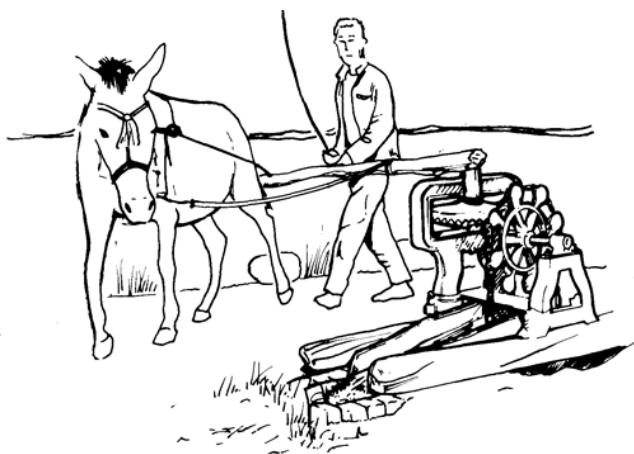
Fig. 18.1. An ancient water transportation system [FAO: this pictures depicts actually a system from ancient China)]

This is what we name in mechanical terms as a high torque, low speed prime mover transmission system. The transmission (speed increaser) is of a pin or a cog wheel type. Its planar equivalent may be represented by a pin and a plate (Fig. 18.2).

Fig. 18.2. A pin-plate meshing (▲)

$$\vec{v}_2 = \vec{v}_1 + \vec{v}_{21}$$

Using the rules of kinematics we set the speed v_1 as constant. The output speed (v_2) shall be perpendicular to radius O_2E. The relative speed is parallel to the plane of contact. You can see that the speed of the driven wheel is variable: its minimum is at the last point of engagement and its maximum, at point C. Since the speed of this transmission is relatively low, this disadvantageous phenomenon has a small impact on the operation of the system. With higher speeds and higher equivalent inertias, this would result with heavy vibrations and cannot be accepted in modern transmissions.
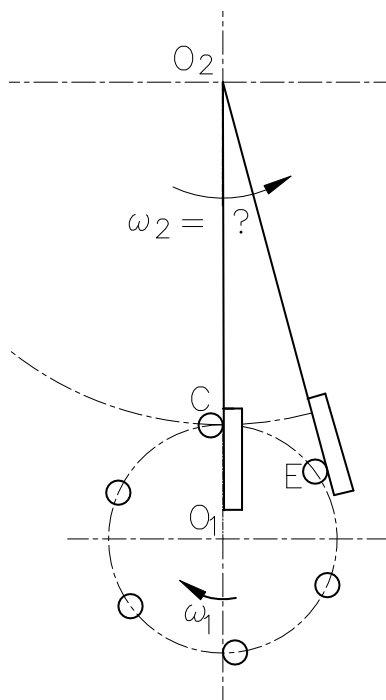
18.2. Fundamental law of toothed gearing

Fig. 18.3 shows two profiles (taken at random) in mesh.
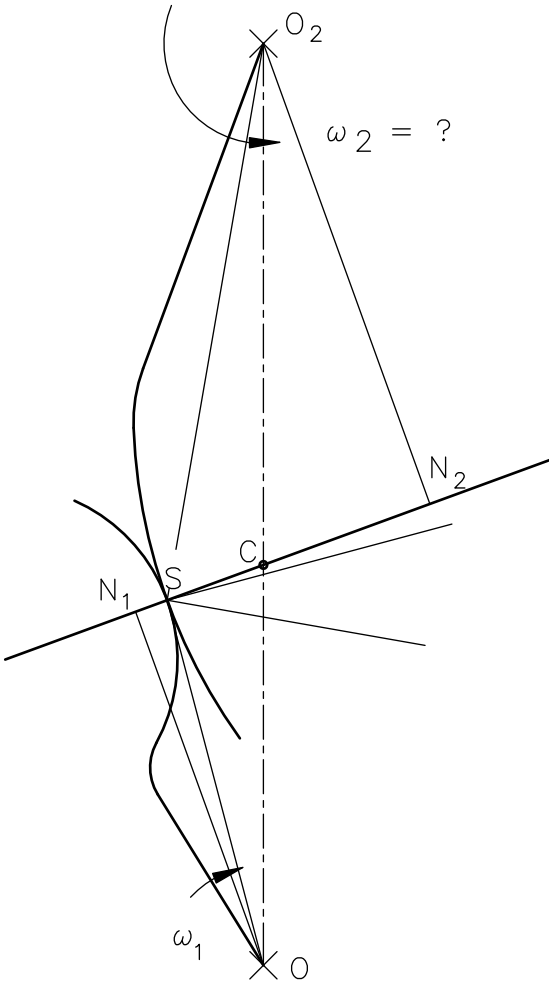
Fig. 18.3. Fundamental law of toothed gearing (▲)

To preserve the continuity of motion, the velocity normal to the mating surfaces (v) must be the same.

$$\omega_1 = \frac{v_1}{O_1 S} = \frac{v}{O_1 N_1} \; ; \; \omega_2 = \frac{v_2}{O_2 S} = \frac{v}{O_2 N_2}$$

So the transmission ratio:

$$u = \frac{\omega_1}{\omega_2} = \frac{O_2 N_2}{O_1 N_1}; \text{ but } \frac{O_2 N_2}{O_1 N_1} = \frac{O_2 C}{O_1 C}$$

Finally: $u = \dfrac{O_2 C}{O_1 C}$

Based upon formulas derived above, the fundamental law of gearing can be formulated in the following way:

To preserve the continuity and steadiness of motion, the line normal to the two meshing profiles must always pass through the fixed point C (pitch point), which divides the distance O₁O₂ into two sections proportional to the transmission ratio.

For a given tooth profile, it is possible to construct another profile (a so called conjugate profile), which will comply with this fundamental law. The first conjugate profile used in the history of gearing was a cycloidal profile.

18.3. Cycloidal meshing

This is how a cycloid is constructed. Consider a circle rolling along a straight line. Mark a fixed point on it – the curve created by that fixed point as the circle rolls is called a cycloid. Looking at the plot in Fig. 18.4, which depicts a circle rolling along a line at four different positions, you can see the cycloid traced out by the point A.
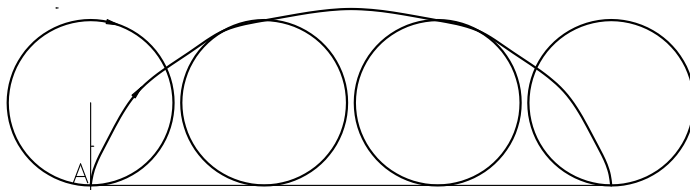
Fig. 18.4. Construction of a cycloid

How to construct two meshing cycloid profiles? Let's have two pitch circles. Each pitch circle has its own generating circle, usually with a radius equal to 0.333 of the pitch circle radius. Start rolling the first generating circle over the first pitch circle (external/internal = hypocycloid) and then on the second pitch circle (external/external = epicycloid).
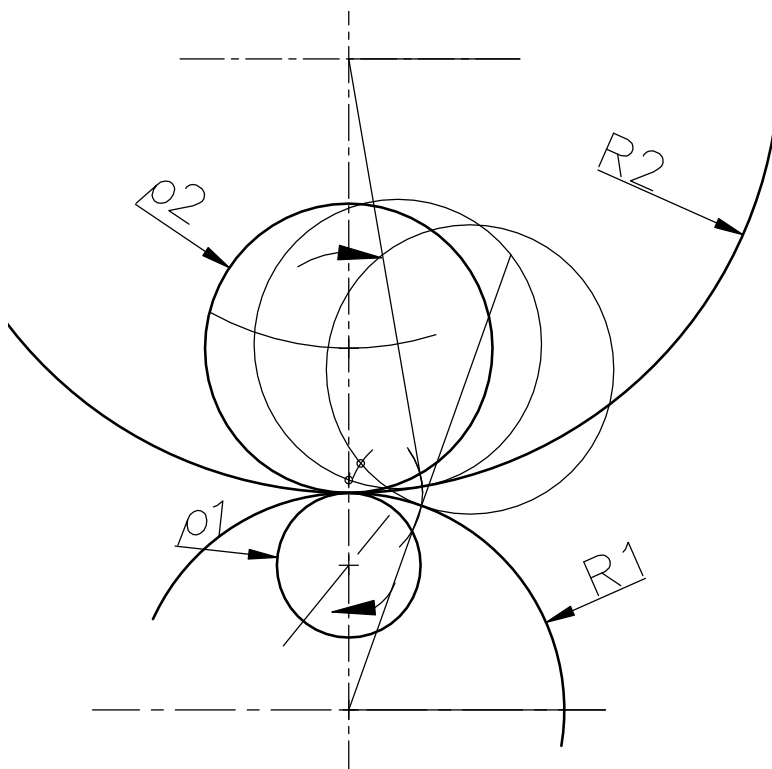
Fig. 18.5. Construction of meshing cycloid profiles (▲)

There are a few specific cases: Let's assume the generating radius equal to 0.5 R_1 or the same as the pitch radius. In the first case the dedendum is a straight line, whereas in the second case, it turns into a point.

As you can see the two meshing profiles are generated from two pitch circles. If these circles are no more tangent as a result of load related deformation, the fundamental law of toothed gearing is no more true. This type of gearing is therefore not fit for the transfer of load. On the other hand, the meshing of a concave surface with a convex surface produces low wear; thus this type of gearing has had many applications in fine mechanisms. Using the cycloid meshing rule, we may redesign the ancient cog transmission into a system preserving the fundamental law of toothed gearing. Its variant is a widely known Geneva wheel (Maltese wheel) for use in dwell mechanisms (Fig. 18.6).
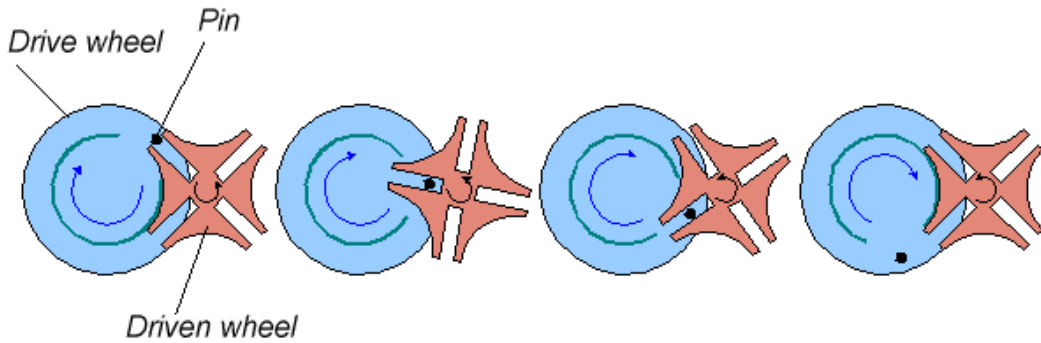
Fig. 18.6. A dwell mechanism (a Geneva wheel) [from the Automation Blog]

HW18.1. Construct two meshing cycloid profiles (addendum and dedendum) for the following data (assigned individually).

R_1 [mm]	R_2 [mm]	ρ_1 [mm]	ρ_2 [mm]

Glossary

addendum	głowa zęba
cog	kołek
concave/convex	wklęsły/wypukły
conjugate profiles	profile sprzężone
dedendum	stopa zęba
generating circle	koło odtaczające
mating surfaces	powierzchnie współpracujące
pitch point	punkt toczny
speed increaser	przekładnia zwiększająca prędkość, multiplikator

19. Involute, a Single Toothed Gear, Undercutting

19.1. The involute curve

The involute curve is formed by the end of a straight line (*YN*) that rolls without slip on a circle (the base circle). This is actually a special case of the cycloid curve. The involute function derived below will be used throughout the whole second part of the course.

Fig. 19.1. The involute curve and the involute function

$$\varphi = \alpha - \alpha_Y \; ; \text{ but } \alpha = \frac{ZN}{ON} \text{ and } \tan\alpha_Y = \frac{YN}{ON}$$

and $ZN = YN$ (*YN* is equal to the unwound arc *ZN*)

$$\varphi = \frac{ZN}{ON} - \alpha_Y = \frac{ON\tan\alpha_Y}{ON} - \alpha_Y = \tan\alpha_Y - \alpha_Y = \text{inv}\,\alpha_Y$$

It is worth memorizing, for the duration of this course only, that if $\alpha_Y = 20°$ then inv $\alpha_Y = 0.0149$.
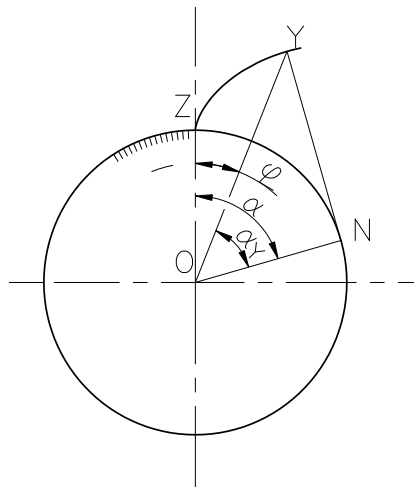
19.2. Gear terminology and basics
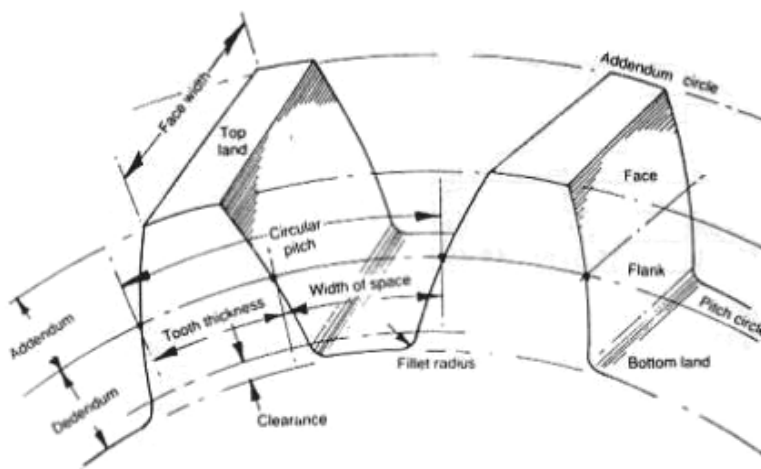
Fig.19.2. Gear basics [Yi Zhang, Finger S. Introduction to Mechanisms]

As you can see from this drawing, the circumference at the pitch circle is given by a product of the number of teeth and pitch. On the other hand it is also given by the ordinary definition (πd). The ratio of the pitch and π was defined as module: $zp = \pi d$ hence: $d = zp / \pi = zm$. Which of the above (pitch or module) shall be standardized? This decision had to be taken in the early days of gear engineering. The Americans decided for the pitch, actually a so-called Diametral Pitch (DP = a number of teeth per one inch of the pitch diameter). To keep the pitch diameter rational, the European decided for the module. So the total number of teeth: $z = DPzm / 25.4$ and $DP = 25.4 / m$.

The addendum diameter: $d_a = d + 2m$; the dedendum diameter: $d_f = d - 2.5m$;

and the base diameter (not shown in Fig. 19.2): $d_b = d \cos \alpha$.

19.3. Toothed gear manufacture

For simple applications a good tool is a milling cutter representing a tooth space (Fig. 19.3).

Fig. 19.3. Gear cutting tools, a milling cutter [United Tool Company]

A blank is prepared (addendum diameter), and the tool is fed into the material. This is a form method manufacture. As the number of tools is limited, one milling cutter is used for the manufacture of a certain set of gears, and only one of them will represent a true involute.

The dominant method of gear cutting is generation. The profile of a tooth is generated by consecutive positions of a tool, which is usually the basic rack. Fig. 19.4 shows standardized dimensions of the basic rack. The tool form is complementary to the basic rack, i.e. the tooth form takes the shape shown in Fig. 19.4 b.
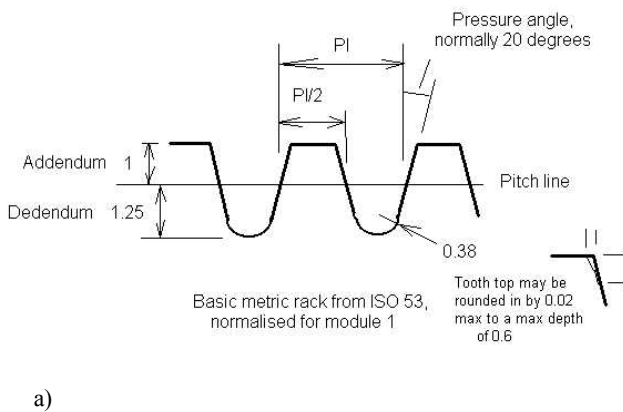
Fig. 19.4. Standard rack dimensions and the basic rack tool form [Doug Wright UWA]

a)   b)
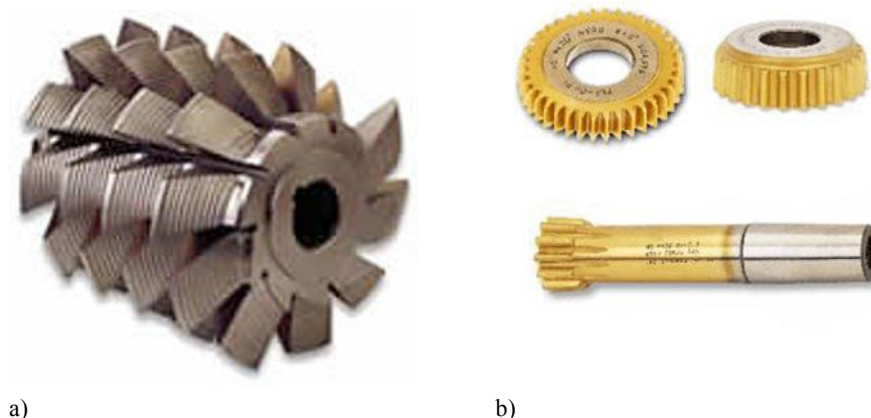
Fig. 19.5. Gear cutting tools a) a hob [Sandvik]; b) a pinion shaped cutters [Daritec]

A more efficient form of this tool is a hob shown in Fig. 19.5a. For internally toothed gearing we use a pinion shaped cutter (the Fellows cutter). An example is shown in Fig. 19.5b.

Let me explain the very idea of the generation process. Imagine a razor attached to the end of a horizontal stick and perpendicular to it (Fig. 19.6). In the first instance we need to provide the radial feed to get a tangency between the stick and the base circle.

Fig. 19. 6. Generation with the use of a "razor tool"

At this point the generation procedure starts. We raise the razor tool and roll it over the base circle. At the first point the tool goes down, removes a part of the flank, then it goes up, rolls to the second point and the procedure repeats until the whole tooth flank has been formed. Dimensions of the actual rack are different to those of the "razor blade". The cutting edge is inclined at an angle of 20˚. This will have some impacts on the generation procedure to be explained in the next chapter.
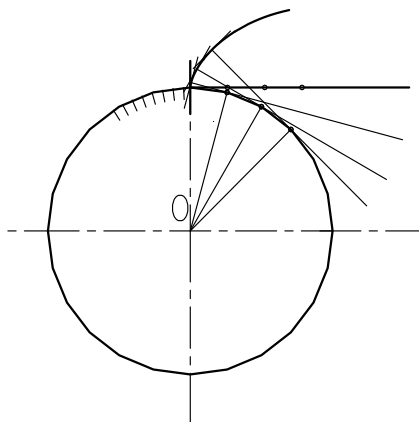
19.4. Generation of a small toothed gear

You must strictly follow my recommendations when tracing this drawing. Find the centre O_1 of the gear to be generated (the blank diameter, Fig. 19.7). Trace the pitch and addendum circles. See that the point N of this gear is situated outside of point F. The pitch circle shall be tangent to the middle line of the basic rack. Start rolling the middle line of the basic rack over the pitch circle (no slip!); first to the left, then to the right. Why to roll the middle line of the rack over the pitch line instead of the base line? Had the rack been manufactured with a rectangular shape, then it would have been rolled over the

base circle (as with the razor tool). As the cutting surface is inclined at an angle of 20 degrees, to preserve the same pitch, it must be rolled over the pitch circle.

Fig. 19.7. Generation of a standard toothed gear (▲)

The tooth thus obtained offers the involute line from the base circle to the addendum circle. Let's now repeat the same procedure but the size of the generated gear is defined by a point *N* located right to the point *F* (between *F* and *C*). To make the problem more illustrative, the basic rack has sharp corners at its top lands. Now we follow the same procedure as explained above.
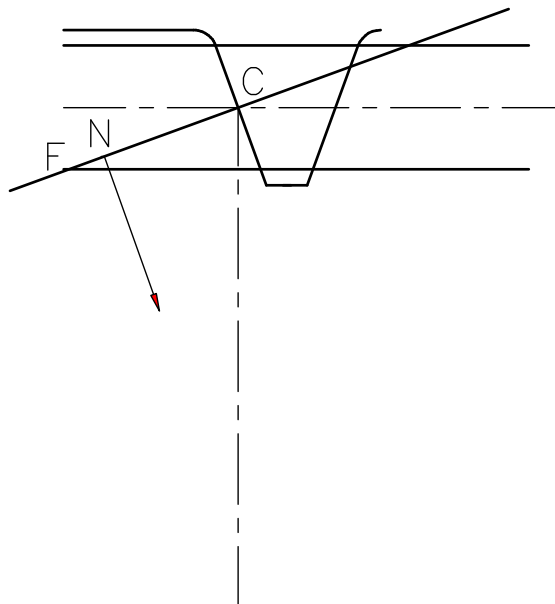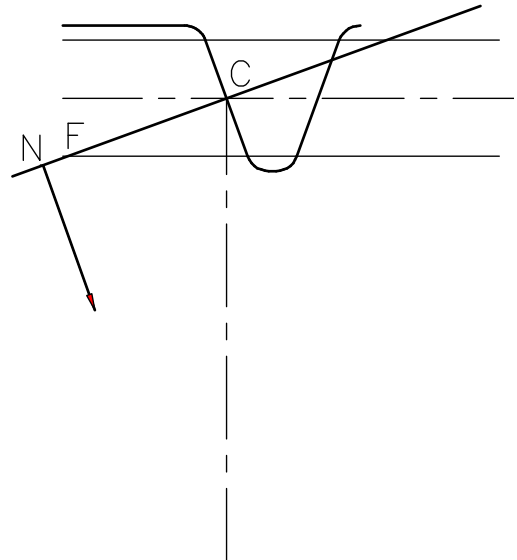
Fig. 19.8. Generation of a small toothed gear (▲)

You can see that the bottom part of the tooth was removed by the sharp tip of the tool when rolling the rack to the right. This phenomenon is termed as undercutting and shall be avoided. The limiting situation for an undercutting free gear is when point N coincides with point F.

$$FC = \frac{m}{\sin \alpha} \quad \text{but} \quad \frac{FC}{OC} = \sin \alpha$$

As $OC = z_{lim}m/2$ then: $z_{lim} = 2/sin^2\alpha$; for $\alpha = 20^o$ $z_{lim} = 17$

For $\alpha = 30^o$ $z_{lim} = 8$ and for $\alpha = 15^o$ $z_{lim} = 30$

HW 19.1. Undercutting (part one): Given is a number of teeth and a module (assigned individually). Determine the form of a tooth using the basic rack as a tool. Data: z =   ; α =   . Data assigned individually.

Procedure to be followed when solving your undercutting homework assignment: (part one)

1. Calculate the pitch, base and addendum diameters. Trace in scale 20:1 (if manually)
2. At the pitch point C trace the middle line of the basic rack. Trace the rack profile; make it sharp at the bottom corners.
3. At the pitch point C trace the pressure line at an angle of 20° to the middle line.
4. Find the point of intersection of the pressure line with the line traced one module below the middle line. You will find that this point is located between the pitch point C and the point of tangency of the pressure line with the base circle for your gear.
5. Start rolling the middle line of the rack over the pitch circle in both directions and trace the consecutive positions of the cutting edge.
6. Trace the enveloping curve for the addendum; trace the consecutive position of the sharp corner of the rack. It is supposed to remove a small portion of the tooth profile above the base circle (undercutting).
7. Since the tooth thickness at the pitch circle $(\pi m/2)$ is the same as that of the rack, trace the full tooth profile.

Glossary

blank	otoczka
flank	flanka, powierzchnia boczna
form method	metoda kształtowa
generation method	metoda obwiedniowa
hob	frez
involute	ewolwenta
milling cutter	frez modułowy
pinion shaped cutter	dłutak
pitch	podziałka
rational	wymierny
undercutting	podcięcie

20. Addendum Modification: part 1

20.1. How to avoid undercutting?

To avoid problems with undercutting, the intersection of the following two lines:

1) A horizontal line traced through the last point of the basic rack cutting edge, which is spaced by one module downwards from the middle line (basic rack above the blank), and

2) The pressure line shall intersect outside of the point of tangency of the base circle with the pressure line (N) (with respect to the pitch point C). If $z < z_{lim}$, then the only solution is to withdraw the rack from the material by the relevant distance $X = xm$. That means that the middle line of the rack shall be shifted by the same distance away from the pitch circle. The process is termed as addendum modification (correction, profile shift), since as a result of the process the addendum diameter increases its value (the same is with the dedendum; the pitch circle remains the same).
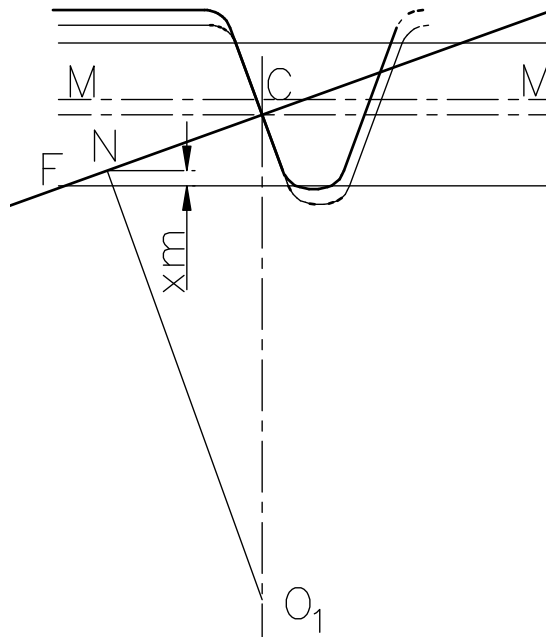
Fig. 20.1. Addendum modification (▲)

$$X = xm = \frac{z_{lim}m}{2} - \frac{z_{lim}m}{2}\cos^2\alpha - \frac{zm}{2}\sin^2\alpha$$

so $x = \frac{z_{lim}}{2}(1 - \cos^2\alpha) - \frac{z}{2}\sin^2\alpha$; as $z_{lim} = \frac{2}{\sin^2\alpha}$; so finally $x = \frac{z_{lim} - z}{z_{lim}}$

The necessary amount of shift for the standard value of the pressure angle (20˚) is given by a simple formula:

$$x = \frac{z_{\lim} - z}{z_{\lim}} = \frac{17 - z}{17} \text{ (for } \alpha = 20^o \text{)}; \textbf{(This formula is valid for } \textbf{\textit{z}}\textbf{<17 only!)}$$

A modified tooth changes its dimensions and form (Fig. 20.2). Its addendum and dedendum become bigger by the amount of the tool shift, i.e.:

$$d_a = d + 2 \cdot m(1 + x) \text{; and } d_f = d - 2 \cdot m(1.25 - x)$$

The tooth becomes thicker at the bottom, which is advantageous, and thinner at the addendum, which is disadvantageous. The minimum width of the top land shall be not less than 0.2 of the module. To calculate this thickness, we will use the involute function.

Fig. 20.2. The effect of modification on the tooth form (▲) [eassistant.eu]

Tooth thickness at the pitch diameter after modification: $s = \frac{\pi m}{2} + 2xm \tan \alpha$

(half of the pitch plus an amount by which the tooth space at the rolling line in the rack became larger).

To find the tooth thickness at the addendum diameter, needed is the addendum radius and the angle included between the two corners of the tooth.
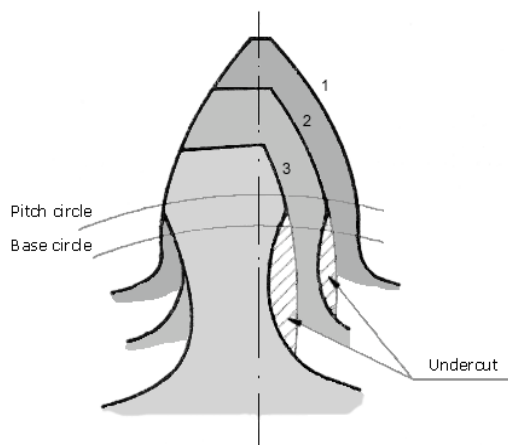
$$s_a = \frac{d_a}{2}\left[\frac{\pi}{z} + \frac{4x \tan \alpha}{z} - 2(inv\alpha_a - inv\alpha)\right]; \text{ where: } \cos \alpha_a = d_b / d_a$$

20.2. Gear transmissions (two meshing gears with $z > z_{lim}$)

Let's start with the simplest case of two meshing gears: these are with the number of teeth greater than 17. The small one is termed as "pinion" , the large one is termed as "gear". Follow carefully (step by step) my drawing.
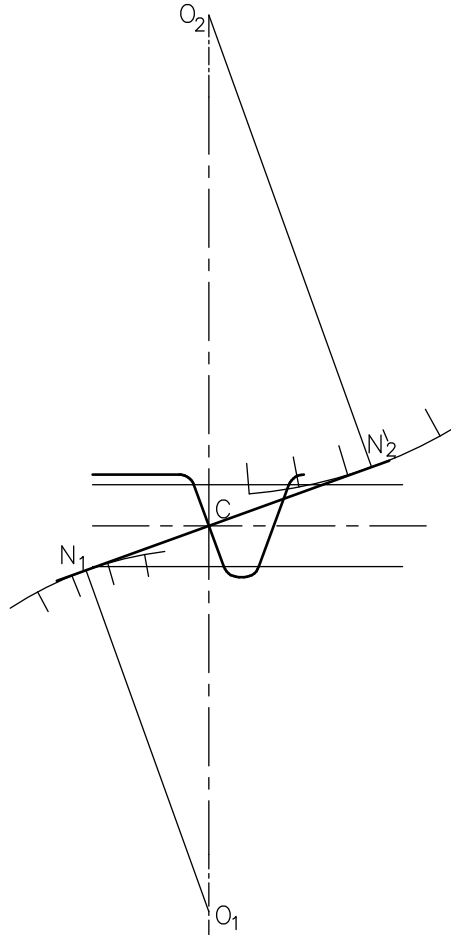
Fig. 20.3. Gear transmission basics (▲)

With the drawing ready, let's define some basic definitions of a gear transmission.
Transmission ratio: $u = z_2 / z_1$;

Centre distance: $a = \dfrac{d_1 + d_2}{2} = \dfrac{z_1 m + z_2 m}{2} = \dfrac{z_1 + z_2}{2} m$;

Force distribution: $F_t = \dfrac{2T}{d_1}$; $F_r = F_t \tan \alpha$

The overlap ratio: $\varepsilon_\alpha = \dfrac{AE}{p_b}$; it shall not be less than 1.1. If this ratio is, to different reasons,

less than 1, the transmission will experience a momentary violation of the fundamental law of toothed gearing! Finally, we shall sketch the distribution of linear velocities at any point within the pressure line. You can see that the slip velocity, which is crucial for the creation of full-film lubrication, is maximal at points A and E and zero at the pitch point C.

20.3. Two meshing gears with $z_1 < 17$ and $(z_2 + z_1) > 2 z_{lim}$

To avoid undercutting in the small gear, the rack shall be withdrawn from the blank by a distance $X_1 = x_1 m$. Let's move it downwards. If the above conditions are met, the 1 module line in the rack is still away from the dangerous point in gear 2. Thus, to avoid undercutting in the small gear we may assume $X_1 = -X_2$.
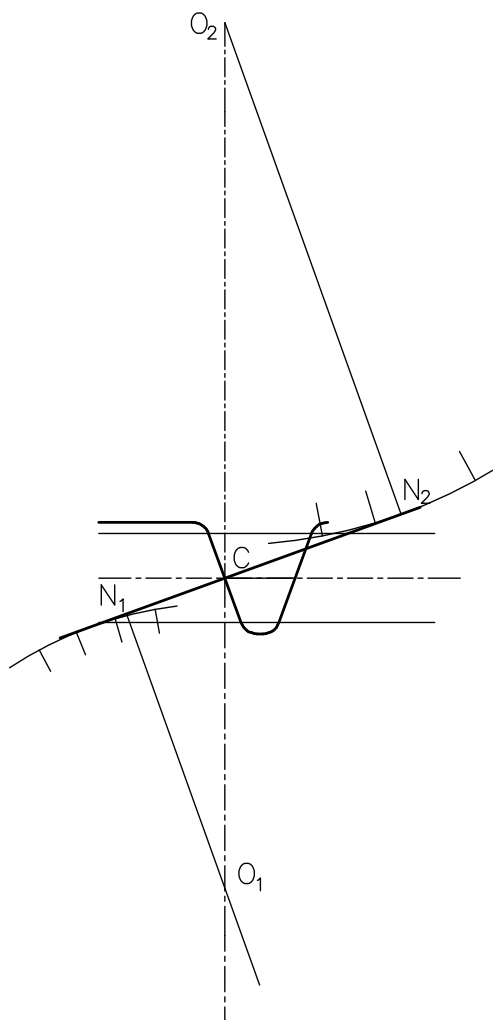
Fig. 20.4. The height addendum modification (P-0)(▲)

For this type of correction the centre distance remains the same. The approach contact ratio becomes shorter and the recess contact ratio becomes longer, which is beneficial to the level of noise in the transmission. An exemplary gear set that may be subjected to this type of modification: $z_1 = 12$; $z_2 > 21$. Dimension for the two gears shall be calculated using formulas from chapter 20.2.

HW 20.1 Continuation of the undercutting problem: calculate the necessary addendum modification for your tooth and construct a modified tooth form (see the attached drawing for help: symbols used in this drawing are obsolete now but the drawing is a good illustration of the procedure to be followed in this task).

Steps to be followed when solving part two of the assignment (see the attached drawing [15]).
1. Calculate the new addendum diameter (d + 2(x+1) m). Trace the new addendum diameter; the pitch and base diameters remain the same.
2. Trace the rack with its middle line (M'-M' in the drawing) shifted by a distance X away from the pitch circle.
3. The new line which is in contact with the pitch circle is called as the operating pitch line.
4. Start rolling the operating pitch line over the pitch circle
5. Repeat steps 6 and 7 of the first part

(▲)
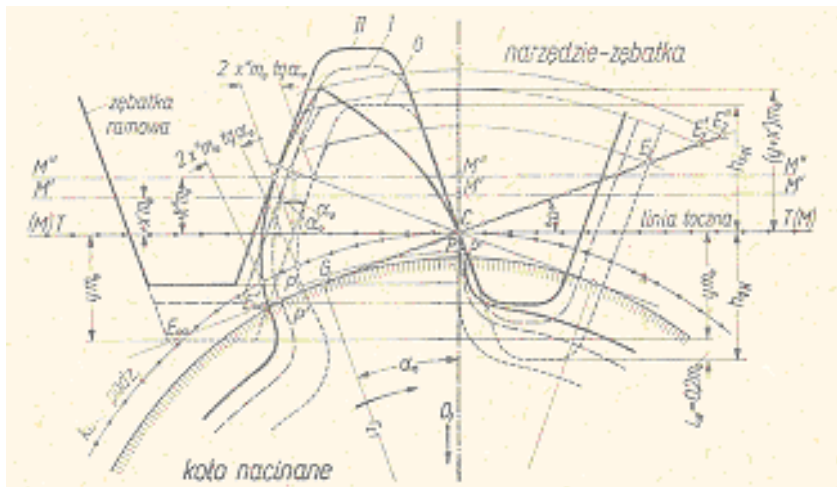
[15]. Legend: narzędzie zębatka = rack tool; koło nacinane = generated gear; linia toczna = operating pitch line; zębatka ramowa = reference rack

Glossary

addendum modification	korekcja zębienia
approach contact ratio	cząstkowy wskaźnik przyporu (wzębianie)
correction, profile shift	korekcja zazębienia
gear	koło duże (napędzane)
height correction	korekcja wysokosciowa (P-0)
operating (roll) line	linia toczna
overlap ratio	wskaźnik przyporu
pinion	zębnik
recess contact ratio	czstkowy wsk. przypory (wyzębianie)
top land	powierzchnia zęba na średnicy wierzch.
undercutting	podcięcie

21. Addendum Modification: part 2

21.1. Two meshing gears with $z_1 < 17$ and $(z_1 + z_2) < 2\, z_{lim}$

Let's define two gear centres such that both gears need addendum modification (the left drawing in Fig. 21.1).
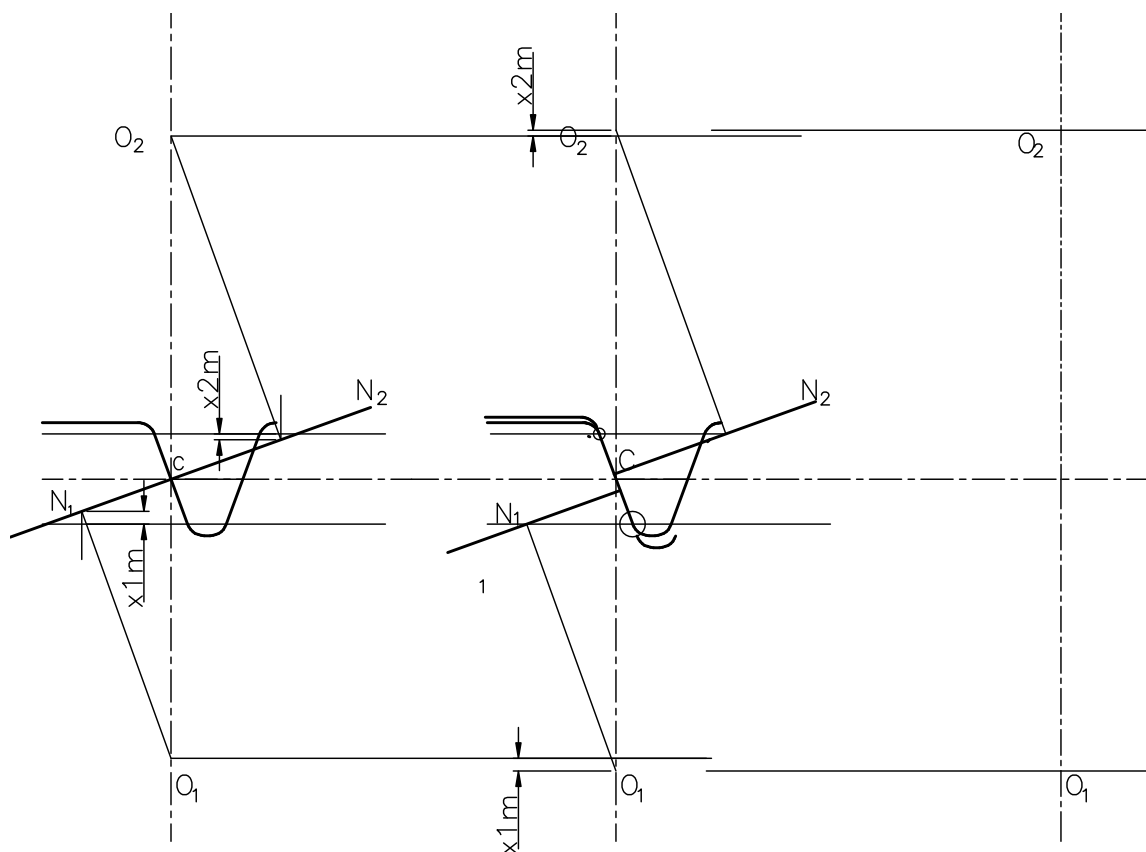
Fig. 21.1. Angular correction (▲)

Now we need to remove the rack from both gears. The approach employed in the previous case is no more possible. Let's us move the centres of both wheels by the necessary amount instead of moving the rack (the middle drawing). What's wrong with this gearing? See for the backlash: it is excessive. To eliminate this backlash, we move both gears towards each other. Conclusions:

- the pitch circles are no more tangent (there are two new circles (operating circles), which remain tangent,
- the operating centre distance a_w is no more equal to the base value a (it is a little bit greater)

- the effective, operating pressure angle becomes bigger,
- when moving both gears in the final stage, we need to control the bottom clearance.

21.2. Equations governing the angular correction

Based upon the last drawing in Fig. 21.2 we may derive the first equation that governs this type of correction:

$$a \cos \alpha = a_w \cos \alpha_w$$

The second one takes more time to be derived. Tooth and space thickness measured at the operating circle shall be equal to the pitch measured at this circle.

To obtain the second equation governing this type of addendum modification we need to discuss the tooth width and tooth space at the operating diameters. Let's start with the operating diameters. Fig. 21.2 is a view of a toothed pair after the angular correction.
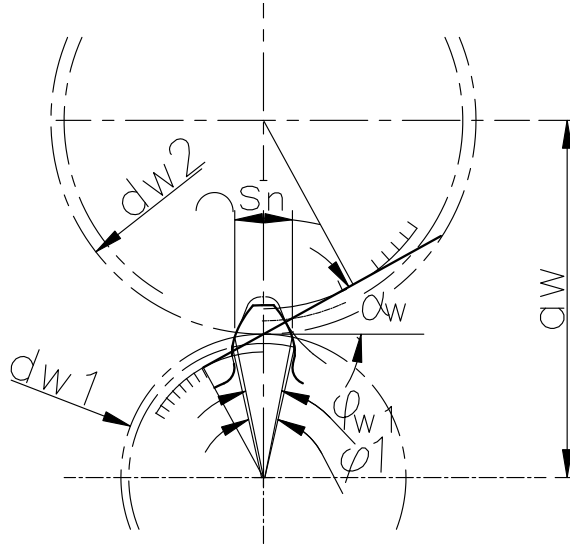
Fig. 21.2. A toothed pair after the angular correction

$$\frac{d_{w1} + d_{w2}}{2} = a_w \text{ and } \frac{d_{w2}}{d_{w1}} = u \text{ , hence: } d_{w1} = \frac{2a_w}{u+1} \text{ and } d_{w2} = \frac{2a_w u}{u+1}$$

Pitch at the operating diameter: $p_w = \pi d_{w1}/z_1$

Tooth thickness of gear 1 at the pitch diameter: $s_{n1} = \dfrac{\pi m}{2} + 2x_1 m \tan \alpha$

Tooth thickness (gear 2): $\qquad s_{n2} = \dfrac{\pi m}{2} + 2x_2 m \tan\alpha$

Included angles at the pitch circle ($2s_n/d_1$; $2s_{n2}/d_2$): $\varphi_1 = \dfrac{\pi}{z_1} + \dfrac{4x_1 \tan\alpha}{z_1}$; $\varphi_2 = \dfrac{\pi}{z_2} + \dfrac{4x_2 \tan\alpha}{z_2}$

Involute angle between the pitch and operating circles: $\varphi_{w1} = inv\alpha_w - inv\alpha$

So finally tooth thickness at the operating diameter:

$$\left[\varphi_1 - 2(inv\alpha_w - inv\alpha)\right]\frac{d_{w1}}{2} + \left(\varphi_2 - 2(inv\alpha_w - inv\alpha)\right)\frac{d_{w2}}{2} = p_w$$

Substituting all the above, rearranging we get the final, second formula for this modification:

$$\boldsymbol{inv\alpha_w - inv\alpha = \frac{2(x_1 + x_2)\tan\alpha}{z_1 + z_2}}$$

The two formulas printed in bold are of paramount importance to all correction problems!

The final problem to be settled is the bottom clearance. To maintain a constant value of the bottom clearance, the following approach was adopted: first we calculate the dedendum diameters for both gears:

$$d_{f1} = d_1 - 2m(1.25 - x_1)$$

$$d_{f2} = d_2 - 2m(1.25 - x_2)$$

The addendum, i.e. the diameter of blanks prepared for machining, is a difference between the centre distance, the dedendum radius of the opposite gear and the necessary amount of the bottom clearance:

$$d_{a1} = 2a_w - d_{f2} - 2c$$

$$d_{a2} = 2a_w - d_{f1} - 2c$$

where c is the bottom clearance c = 0.25 m.

NP 21.1. Propose the addendum modification for each of the four gears of a two-speed Fuller transmission ([8]). Data: $z_1 = 28$; $z_2 = 35$; $m_{1\text{-}2} = 5$; $z_3 = 15$; $z_4 = 33$; $m_{34} = 6.5$. Operational centre distance is equal to 160 mm.
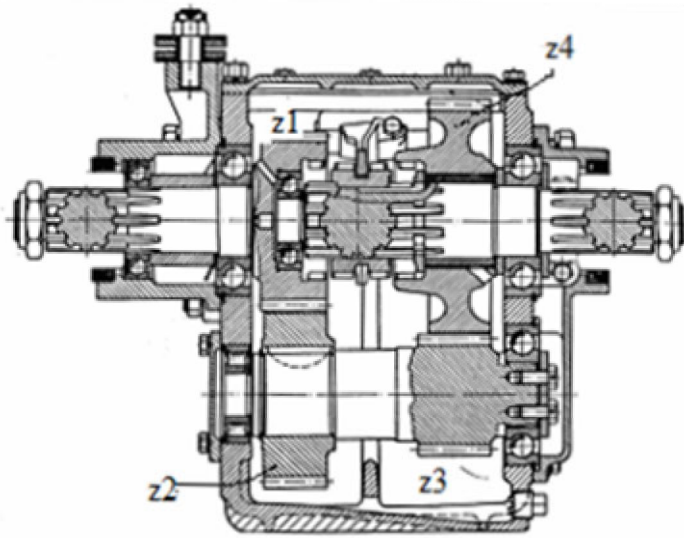
Let's control the underlying centre distance in the two meshing pairs:

$$a_{12} = \frac{z_1 + z_2}{2} m_{12} = \frac{28 + 35}{2} 5 = 157.5 \text{ mm}$$

$$a_{34} = \frac{z_3 + z_4}{2} m_{34} = \frac{15 + 33}{2} 6.5 = 156 \text{ mm}$$

As the underlying distance is by a few millimetres shorter than the operating distance, needed is the angular modification. We use the first formula to find the operating pressure angle in both toothed pairs.

$$\cos \alpha_{w12} = \frac{a_{12} \cos \alpha}{a_w} = \frac{157.5 \cdot \cos 20°}{160} = 0.925; \text{hence} : \alpha_w = 22.33015°$$

$$\cos \alpha_{w34} = \frac{a_{34} \cos \alpha}{a_w} = \frac{156 \cdot \cos 20°}{160} = 0.9162; \text{hence} : \alpha_w = 23.6232°$$

Notice! As the centre distance is toleranced to microns, due accuracy in the calculations of the pressure angle is a must. I'd recommend at least 4 to 5 trailing digits.

Using the second formula for the angular modification we can find the necessary summary addendum modification for both toothed pairs. Calculate first the involute function:

$$inv\alpha_{w12} = inv22.3301° = \tan 22.3301 - \frac{\pi \cdot 22.3301}{180} = 0.02101$$

$$inv\alpha_{w34} = inv23.6232° = \tan 23.6232° - \frac{\pi \cdot 23.6232}{180} = 0.02506$$

(For $\alpha = 20°$ the involute function is equal to 0.014909)

$$x_1 + x_2 = (inv\alpha_{w12} - inv\alpha)\frac{z_1 + z_2}{2 \tan \alpha} = (0.02101 - 0.014909)\frac{28 + 35}{2 \tan 20°} = 0.528$$

$$x_3 + x_4 = (inv\alpha_{w34} - inv\alpha)\frac{z_3 + z_4}{2 \tan \alpha} = (0.02506 - 0.014909)\frac{15 + 33}{2 \tan 20°} = 0.6704$$

Each of the above sums shall be split between the two relevant gears. A usual approach is to split it in inverse proportion to the number of teeth (to enhance the load carrying capacity of the pinion. Other methods will be explained in the design course. Consequently,

$$x_1 = x_{\Xi 12}\,\frac{z_2}{z_1 + z_2} = 0.528\,\frac{35}{35 + 28} = 0.293 \; ; \; x_2 = x_{\Xi 12} - x_1 = 0.528 - 0.293 = 0.234$$

Similarly, $x_3 = 0.461$ and $x_4 = 0.209$.

The addendum necessary to avoid undercutting in gear 3: $x_{3\,\min} = \dfrac{z_{\lim} - z_3}{z_{\lim}} = \dfrac{17 - 15}{17} = 0.118 \; ; \; x_3 > x_{3\min}$

HW 21.1. In a three speed gearbox shown (Fuller Transmission Division [8]).

a) Evaluate graphically the overlap ratio in the toothed pair $z_A - z_B$ ($z_A = 23$; $z_B = 27$; m = 5; no addendum modification)

b) Select z_C and z_D such that $u_{34} = 0.67 \pm 5\%$; m = 5 (trial and error procedure)

c) If $z_E = 15$ and $z_F = 33$; m = 5 calculate the necessary addendum modification
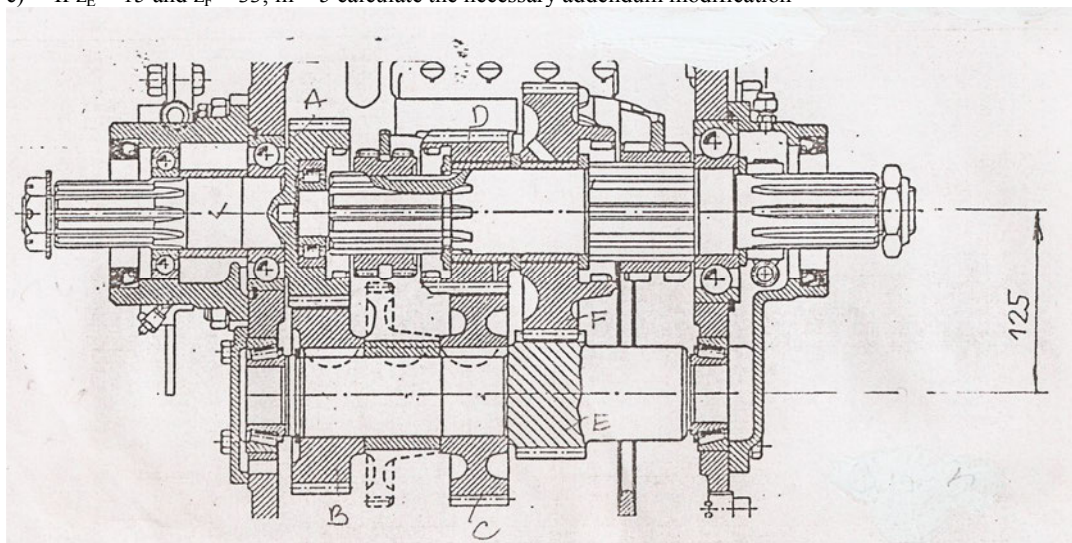
Answer: a) $\varepsilon_\alpha = 1.56$; c) $x_\Sigma = 1.138$

Glossary

angular correction	korekcja kątowa (P)
backlash	luz obwodowy
operating centre distance	rzeczywista odległość osi
bottom clearance	luz wierzchołkowy
space thickness	szerokość wrębu
underlying	tu: bazowy
trailing digits	miejsca po przecinku

22. Helical Gearing

22.1. Fundamentals of the geometry

The gradual meshing of helical gearing results with a smooth and silent operation of a toothed pair (greater overlap ratio). Consequently, it became a must in all gearing of practical importance. It is generated with the same tool as that used for spur gears, e.g. with a basic rack. The tool, therefore, must be inclined with respect to the horizontal line by angle β at the pitch circle. This will have some impacts on the geometry of a toothed pair. All dimensions that are in the normal cross-section are the same as for a spur gear. All dimensions that are in the plane perpendicular to the axis of rotation (transverse/radial plane) are to be modified in the following way:
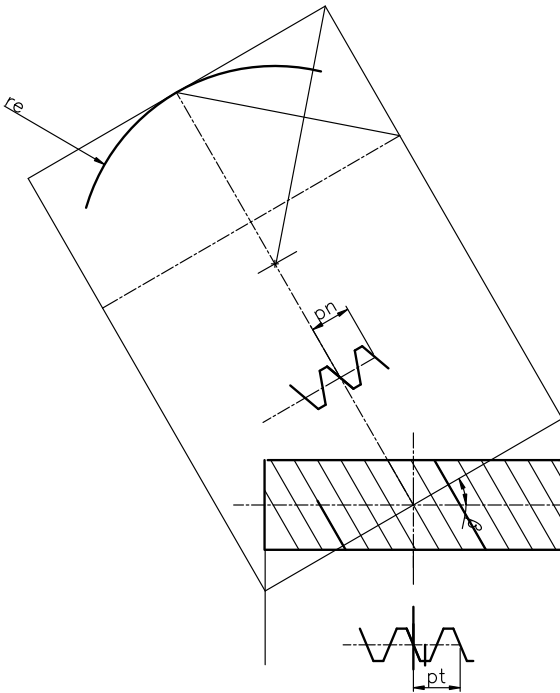
Fig.22.1. Geometry of a helical toothed gear

Module (see Fig. 22.1):

$$p_t = \frac{p_n}{\cos \beta} \text{ hence } m_t = \frac{m_n}{\cos \beta}$$

Helix angle: The helix angle is defined in gearing as an angle complementary to 90° with respect to the real inclination of the helix line (as defined in screws). As a result, contrary to relations valid in screws, the larger is the diameter, the larger is also the angle. A typical relationship (pitch diameter vs. operating diameter) is:

$$\tan \beta_w = \frac{d_{tw}}{d_t} \tan \beta$$

The equivalent spur gear with a radius r_e was constructed based on the major and minor axes of an ellipsis obtained in the normal plane of the gear. The number of teeth of this equivalent gear is equal to $z_e = z / \cos^3 \beta$.
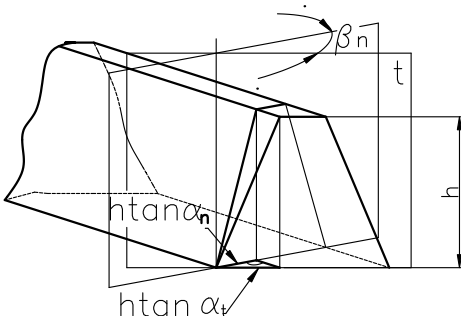
Fig. 22.2. Pressure angle in the transverse plane

$$\frac{h \tan \alpha_n}{h \tan \alpha_t} = \cos \beta \text{ hence} : \tan \alpha_t = \frac{\tan \alpha_n}{\cos \beta}$$

22.2. Toothed helical pair

The centre distance is defined in the transverse plane, i.e.:

$$a_t = \frac{z_1 + z_2}{2} m_t = \frac{z_1 + z_2}{2} \frac{m}{\cos \beta}$$

As you can see, the centre distance may be corrected here by mere changes in the helix angle. The two formulas that govern the angular (P) modification are also referenced to the transverse plane:

$$a_t \cos \alpha_t = a_{tw} \cos \alpha_{tw} \text{ ; and } \operatorname{inv} \alpha_{tw} - \operatorname{inv} \alpha_t = \frac{2(x_1 + x_2) \tan \alpha}{z_1 + z_2}$$

A numerical problem will explain a standard procedure for solving problems similar to that in problem HW 20.1 (part c) when gearing is helical. Part b of the same problem, i.e. design for a standard centre distance, will be explained in the design class.

NP 22.1 A summary of data: a_w = 125 mm; z_5 = 15; z_6 = 33; m = 5. Let's solve the problem without the addendum modification first (just by assuming helical gearing). The underlying centre distance a_t shall be the same as the operating centre distance, i.e. 125 mm.

The centre distance in a helical toothed pair is: $a_t = \frac{z_5 + z_6}{2} \frac{m}{\cos \beta}$

We need a value of the helix angle, so: $\cos \beta = \frac{(z_5 + z_6)m}{2a_t} = \frac{(15 + 33)5}{2 \cdot 125} = 0.96$ hence $\beta = 16.26°$

You can see that the output (secondary) shaft in this gearbox is supported in the input shaft (a cylindrical bearing, a floating support), and in the housing (a deep groove ball bearing, a fixed support). Deep groove ball bearings accept a small amount of axial load, but the helix angle, as a rule, shall not be greater than 15°. We assume $\beta = 10°$. Sought now is a value of the total addendum modification.

The transverse module $m_t = m / \cos \beta = 5 / \cos 10° = 5.0771$

The underlying centre distance $a_t = \frac{(z_5 + z_6)m_t}{2} = \frac{(15 + 33)5.0771}{2} = 121.8512$ mm

To employ the first of the two equations governing the addendum modification, we need the pressure angle in the transverse plane $\tan \alpha_t = \tan a / \cos \beta = \tan 20° / \cos 10° = 0.3696$ hence $\alpha_t = 20.2835°$

Now the operating pressure angle in the transverse plane is:

$$\cos \alpha_{tw} = \frac{a_t \cos \alpha_t}{a_{tw}} = \frac{121.8512 \cdot \cos 20.2835}{125} = 0.9144 \text{ hence } \alpha_{tw} = 23.8850°$$

To find the total addendum modification, continue as in problem NP 20.1.

22.3. Overlap ratio

We shall study now the effect of the inclined tooth line on the overlap ratio. There are two components of the overall overlap ratio: a radial one and an axial one. The first component is calculated using the same formula as that for a toothed spur pair. Instead of normal values of the module we shell introduce its value in the transverse plane. The radial component formula is:

$$\varepsilon_\alpha = \frac{z_1(\tan\alpha_{a1} - \tan\alpha_{tw}) + z_2(\tan\alpha_{a2} - \tan\alpha_{tw})}{2\pi}$$
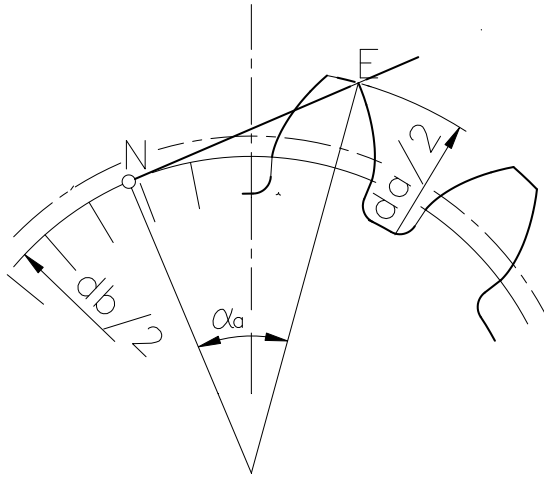
Fig. 22.3 The involute angle at the tip of a toothed gear

where: $\cos\alpha_a = d_b / d_a$ is the involute angle measured at the tip of a toothed gear.

The second (axial) component may be derived from Fig 22.4.
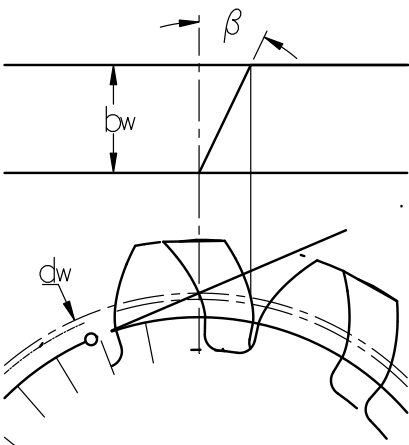
Fig. 22.4. Axial overlap ratio in helical gearing

$$\varepsilon_\beta = \frac{b_w \tan\beta}{p_t} = \frac{b_w \tan\beta}{\pi m / \cos\beta} = \frac{b_w \sin\beta}{\pi m}$$

Finally, the summary equation for the overlap ratio:

$$\varepsilon_\gamma = \varepsilon_\alpha + \varepsilon_\beta$$

22.4. Force distribution

There is one additional component in helical gearing when compared to spur gearing (the axial one). A starting point is as usual the tangential force (Fig. 22.5). It is one component of the resultant force in the contact plane, which is normal to the helix angle. The second component is the axial force. Let's cut the gear along the line normal to the helix line. Again, the resultant force acts along the pressure line at an angle of α. Its radial component is always directed towards the centre of the gear.

Fig. 22.5. Force distribution

Tangential and axial components:

$$F_t = \frac{2T_1}{d_{w1}}; \quad F_a = F_t \tan \beta_w; \quad \tan \beta_w = \frac{d_{w1}}{d_1} \tan \beta$$

The resultant force at the plane tangent to the operating diameter:

$$F_s = \frac{F_t}{\cos \beta_w}\ ;$$ The radial component of the resultant force:

$$F_r = F_s \tan \alpha_{nw} = F_t \tan \alpha_{tw}, \text{ but } \tan \alpha_{tw} = \frac{\tan \alpha_{nw}}{\cos \beta_w}$$
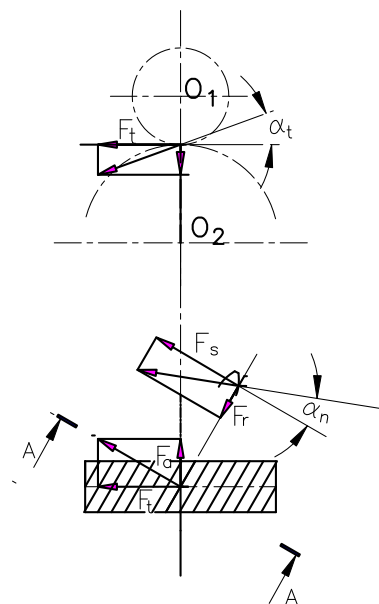
HW 22.1. In the double stage helical gear set shown determine the hand (left, right) and value of the helix angle in pinion 3 to balance the axial forces acting on the intermediary shaft.

Data: $z_1 = 18$; $z_2 = 83$; $m_{12} = 6$; $z_3 = 21$; $z_4 = 76$; $m_{34} = 8$; $\beta_{12} = 18.7598°$
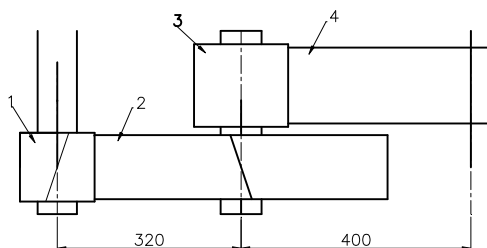
Glossary

helical gearing	zazębienie skośne
transverse/radial plane	płaszczyzna czołowa
axial overlap ratio	poskokowy wskaźnik przyporu

23. Internal Gearing

23.1. Pinion-shaped cutter

Internally toothed gears are generated mostly with pinion-shaped cutters, the shape of which depends upon the number of teeth and module (Fig. 19.1). The cutters are delivered in different pitch sizes (1", 2", 3" etc), so that for a given module, say 5 mm, a cutter 4" in dia. has 25 teeth.
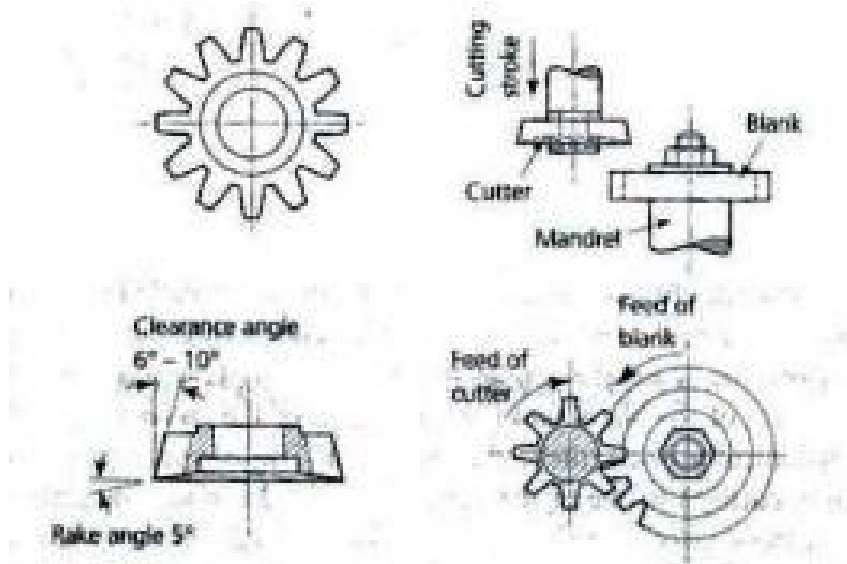
Fig. 23.1 Generation of an internally toothed gear [Suwa Precision]

There are many problems related to the generation and meshing processes in internal gearing. To begin with: any tool must be sharpened. With the basic rack there are no problems: this tool maintains its shape irrespective of its resharpening status. With a cutter, the situation is quite different: with each grinding the tooth form changes and the generation process is carried out by a different section of the involute profile (the cutter has different profile shift after each regrinding). Needed are therefore detailed calculations of the generating centre distance, generating pressure angle etc. The second, very complex problem consists in the so called interference. This is a situation when at the same time the tool and the generated gear (or the pinion and the gear) occupy the same place. If this happens during generation (the tool feed included), the cutter will remove a fraction of the tooth. If this happens during meshing, the transmission will be stopped or tooth breakage may result. Of the many possible interference occurrences, try to remember the most common: the interference that is due to a too small difference in the number of teeth in the pinion and the gear. This situation is illustrated in Fig. 23.2 (left side). With a proper modification (right side), the pair is free of interference.
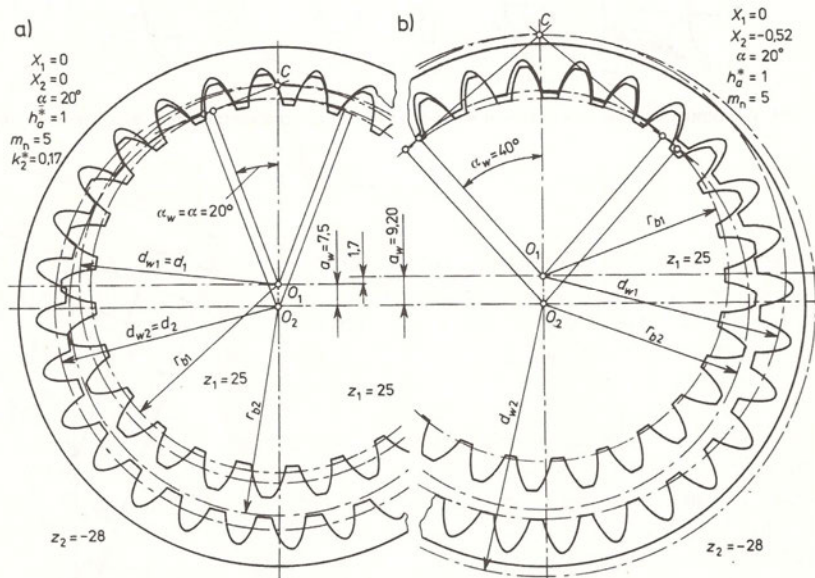
Fig. 23.2. Internal gearing with (a) and without (b) interference of tooth tips [5]

A minimum difference in the number of teeth in both gears shall be at least 9 to 10 (if mounted axially) and approx.15 (if mounted radially). A case study presented in the next chapter reflects some of the problems involved with the design of an internalloy toothed gear, which I experienced as a young engineer shortly after my graduation.

23.2. A case study

A meshing pair was composed of a pinion ($z = 10$) and gear ($z = -28$); $m = 5$. If the tooth count is negative we can employ the same formulas as those derived for external gearing. This toothed pair is illustrated in Fig. 23.3.
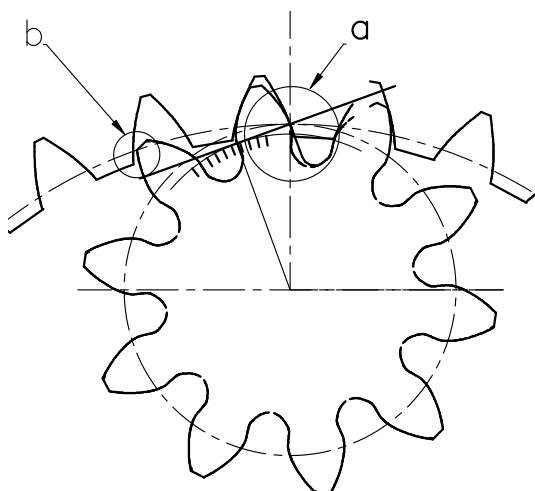
Fig. 23.3. The meshing scheme of a 10/28 internally toothed pair

23.2.1. The addendum diameter in the internal gear.

See an enlarged detail 'a' in Fig. 23.3 to find the addendum diameter in the internal gear. The external gear ($z = 10$) was protected against undercutting with the addendum modification $x = 0.235$ only, i.e. a practical formula ($x = 14 - 10$)/17 had been used. As a result, the tooth is a little bit undercut. You already know how to find an undercut profile.
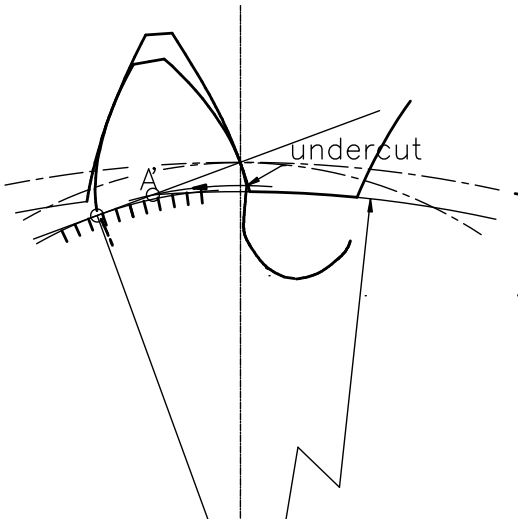
Fig. 23.4. An enlarged view of detail 'a' from Fig. 23.3.

Consequently, part of the involute is removed and meshing along the pressure line can start no sooner than at point $A^{'}$ (an arc with the radius from the centre of the external gear to the first involute point in the gear made to the intersection with the pressure line). The addendum in the internal gear cannot intersect the pressure line beyond point $A^{'}$, else there is a jam in meshing. This condition is termed as interference of the first order.

23.2.2. Interference checkout.

 Fig. 23.5 shows an enlarged view of the area marked as detail b in Fig. 23.3. It's, kind of, animation, i.e. coloured lines lines show consecutive positions of the two adjacent tooth tips passing freely each other when in mesh. So far so good.
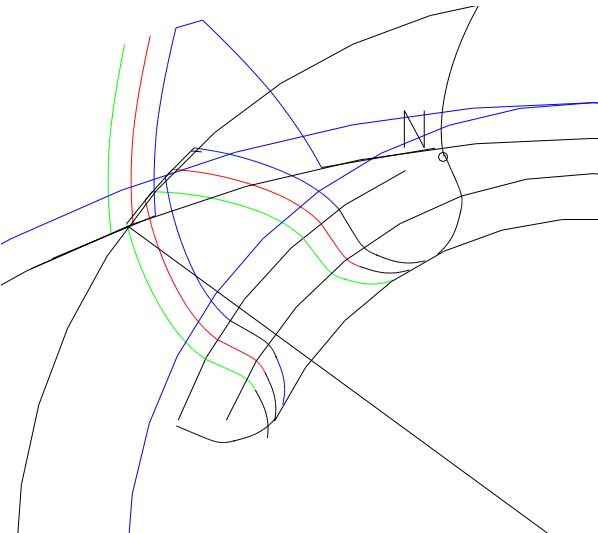
Fig. 23.5. Interference checkout

After due preparations a blank was delivered to BZUT (a gear transmission manufacturer, the biggest in Poland at that time) where the gear had been planned for generation.

23.2.3. Gear generation.

After a short checkout, a process engineer in the factory announced: we have a problem. The smallest tool for the generation of the gear was a 4" cuter with a tooth count equal to 20. This is seen in Fig. 23.6. I had not anticipated this situation.
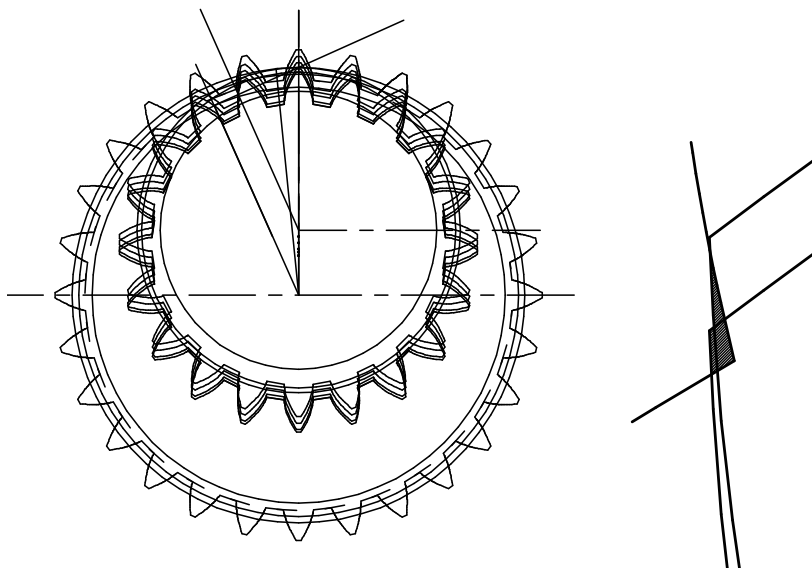
Fig. 23.6. Generation of a 28 tooth internal gear with a 20 tooth cutter (the radial feed)

The primary trouble is clearly seen in an enlarged view of the area marked with letter 'a'. (still missing!). When feeding the tool into the material, the second and third tooth to the left and right from the central tooth interferes with the tooth in the internal gear (still absent during this feed).The gear, however, was manufactured. How? You can see both gears in Fig. 23.7.
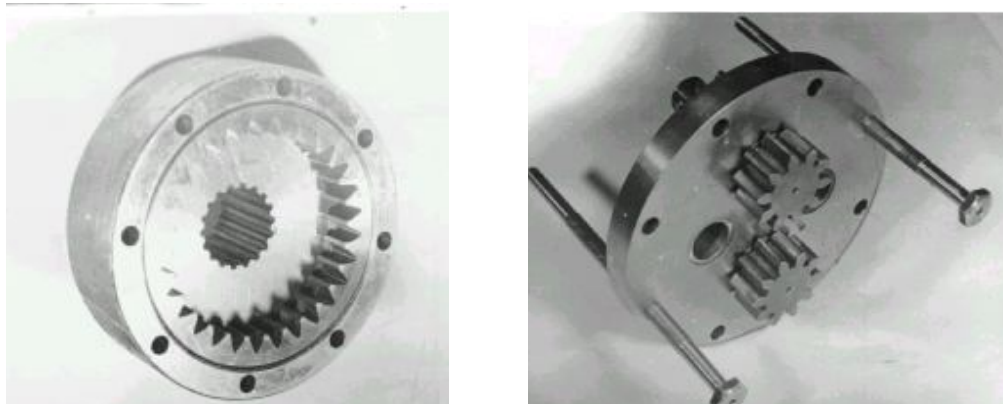
Fig. 23.7. Elements of a spur gear differential

Glossary

anticipated	tu: przewidziany
generating centre distance	obróbkowa odległość osi
interference	interferencja profili
pinion shaped cutter	dłutak modułowy

24. Strength Calculations: contact stresses

24.1. Modes of failure

Fig. 24.1 shows typical modes of failure for toothed gearing. From top (left to right): pitting, fatigue breakage, wear, scoring, rust, impact breakage.
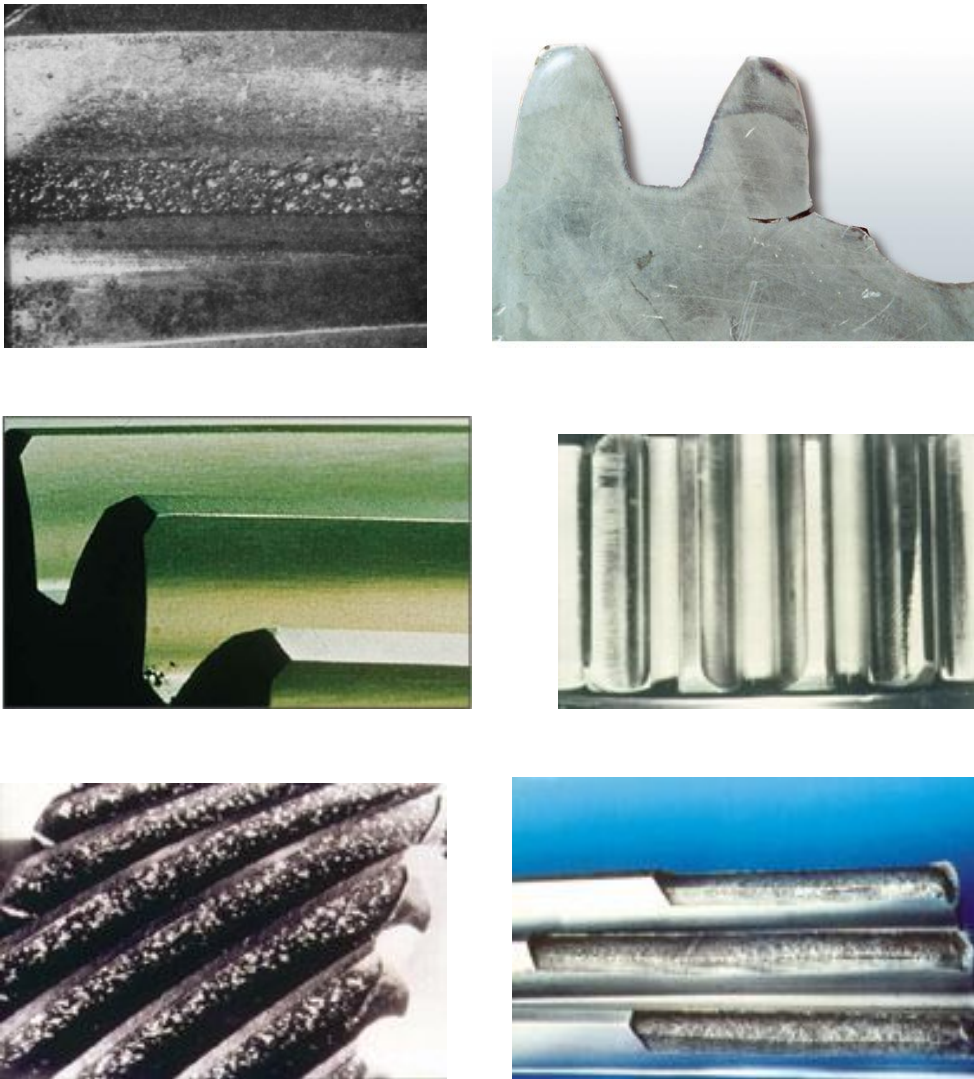
Fig. 24.1. Illustration of different modes of failure [Machinery Lubrication]
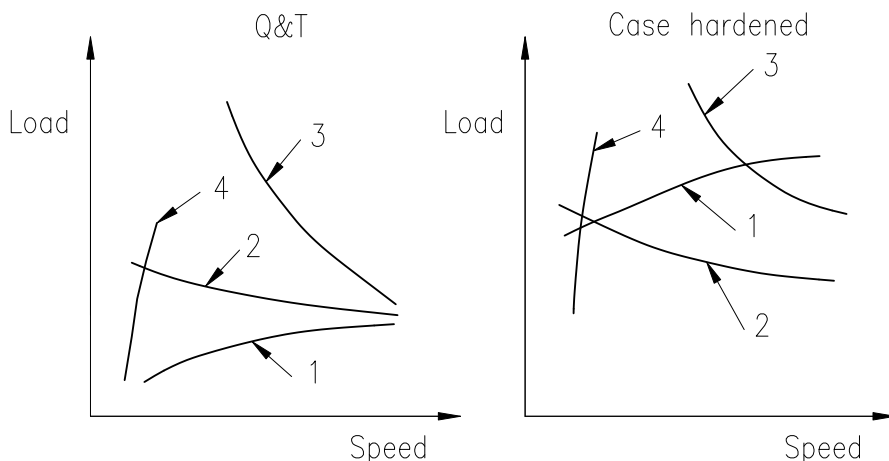
Fig. 24.2. Failure modes: 1 – contact stress (pitting); 2 – bending; 3 – seizure, scoring ; 4 – wear

The limiting load for Q&T gearing of general purpose results from allowable contact stresses. For case hardened teeth, it depends upon the allowable bending .Seizure (scoring) is dangerous at high rotational speeds (turbine systems), and wear is probable at low speed, in opened (no housing/case) transmissions.

24.2. Contact stresses (the underlying formula)

The result of surface fatigue are small flakes of material removed from the profile of a tooth, usually at the pitch circle. The phenomenon was named as pitting [pit: a hole in the ground] and has been since widely accepted and understood in Polish. This type of damage is associated mostly with so called "soft gearing", i.e. the gearing that is subjected to quenching and tempering (Q&T). The formula for contact pressure was derived by Herz.

Fig. 24.3. Contact stress [from: Cam Design Handbook]

$$p_H^2 = 0.35 E \frac{F_{bn}}{2\rho b} \, ;$$

where: $E = \dfrac{2E_1 E_2}{E_1 + E_2}$

is the equivalent modulus of elasticity (e.g. steel vs. cast iron etc.),
F_{bn} is the force normal to the contacting surfaces, and
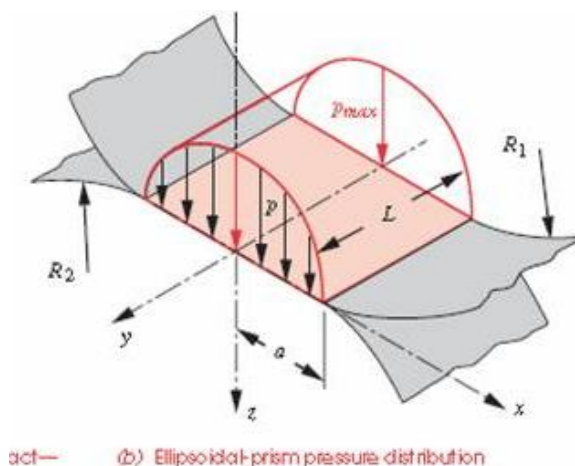
ρ (R in Fig. 24.3) is the equivalent radius at the contact point $\rho = \dfrac{\rho_1 \rho_2}{\rho_1 \pm \rho_2}$ (minus for internal gearing). Now the problem is to ssign all the element included in the Hertz's formula to a toothed pair.
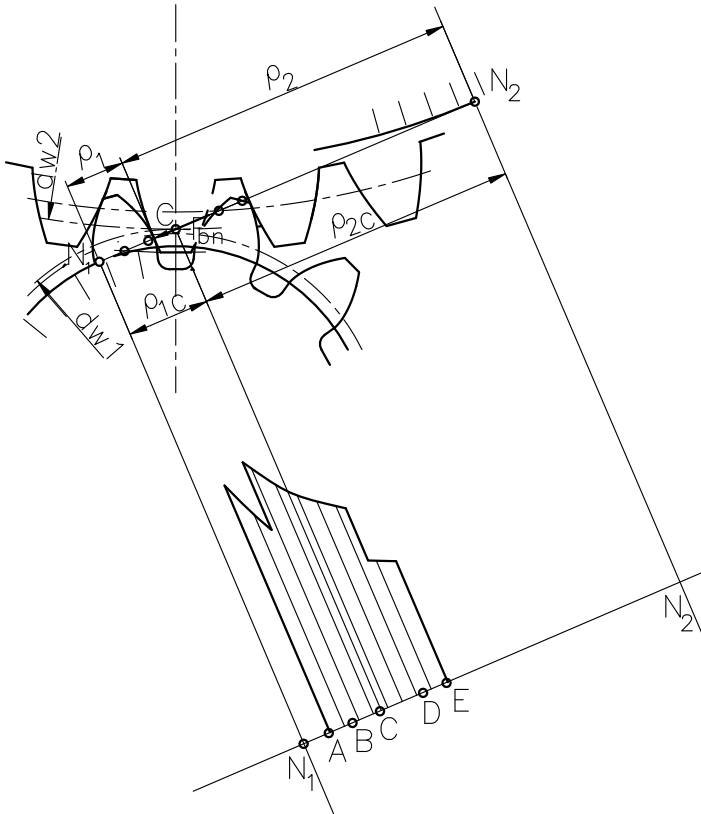
Fig. 24.4. Contact stresses along the pressure line

$$\rho_{1C} = \frac{d_{w1}}{2} \sin \alpha_w ;$$

$$\rho_{2C} = \frac{d_{w2}}{2} \sin \alpha_w \text{ and}$$

$$F_{bn} = \frac{F}{\cos \alpha_w} \text{ then}$$

$$p_{HC} = Z_E Z_H \sqrt{\frac{F}{bd_{w1}} \frac{u+1}{u}} ;$$

where: $Z_E = \sqrt{0.175E}$ and

$$Z_H = \sqrt{\frac{2}{\sin \alpha_w \cos \alpha_w}}$$

The pressure plot between points AB and DE is reduced by a square root of 2. This is due to the fact that the load within these two zones is divided by two (two toothed pair simultaneously in mesh). The standard point for the control of pressure is the pitch point C (the full load and no slip between the mating teeth: see again Fig. 20.3).

24.3. ISO-DIN formulas

The ISO-DIN standards recommend the use of the following formula:

$$s_H = \frac{\sigma_{H\lim} Z_N Z_L Z_R Z_v Z_w Z_x}{\sqrt{\dfrac{F_t}{b_w d_1} \dfrac{u+1}{u}} Z_E Z_H Z_\beta Z_\varepsilon \sqrt{K_A K_v K_{H\beta} K_{H\alpha}}} ;$$

The underlying formulas (Hertz) is embedded in the above formulas. Many coefficients were added. These can be divided into three groups.

24.3.1. Correction factors due to contact fatigue

These coefficients are similar to those discussed during our first semester discussion on fatigue: notch sensitivity, surface finish etc. A difference is that in general machine design we needed a transition from a cylindrical smooth specimen to real machine elements and in gearing, a specimen is similar to a toothed gear. It differs from an actual gear in size, surface finish a.s.o.

Let's discuss shortly all these coefficients:

Z_N – the influence of a limited number of cycles (smaller than the limiting one when establishing $\sigma_{Hlim.}$) An example: toothed gear of the first and reverse speed in the gearbox.

Z_L – viscosity and oil grade factor; Z_R – surface finish factor;

Zv – speed factor. Assume: ($Z_L Z_R Zv = 0.85$ to 1)

Zw – surface working factor (beneficial effect of plastic deformations on the contacting surfaces)

Zx – size (scale) factor. Assume both (Z_W, Z_x) = 1

24.3.2. Genewral influence factores - Operational coefficients

K_A – Application factor (the same as that when discussing the selection procedure for couplings, i.e. the prime mover vs. the driven machine): 1 to 2.25 (smooth vs. dynamic mode of operation); see Appendix 6.

K_v – Dynamic overload factor due to vibrations within the transmission only. It depends mostly on the speed and accuracy class of a transmission; see Appendix 7 for proper choice.

$K_{H\beta}$ – The face load factor accounts for the uneven distribution of load along the length of a tooth (different to contact pressure and bending). This is the most difficult coefficient to account for. The idea is to have uniform distribution of load under full load, so needed are small modifications in the tooth profile and tooth line, a highly specialised area of gearing. Make your choice based upon diagrams in Fig. 24.5 [12].

$K_{H\alpha}$ – Transverse load factor accounts for the distribution of load along the pressure line. For straight gearing $K_{H\alpha} = 1$. For helical gearing the limiting value of this coefficient is given by $K_{H\alpha} = \varepsilon_\gamma / (\varepsilon_\alpha Z_\varepsilon^2)$.

24.3.3. Design coefficients

Z_E – the equivalent modulus of elasticity, Poisson's ratio (see subchapter 24. 2)

Z_H – geometry (see subchapter 24.2);

Z_ε – the influence of the overlap ratio on the contact stresses:

$$Z_\varepsilon = \sqrt{\frac{4 - \varepsilon_\alpha}{3}\left(1 - \varepsilon_\beta\right) + \frac{\varepsilon_\beta}{\varepsilon_\alpha}} \text{ for spur gearing, and: } Z_\varepsilon = \sqrt{\frac{1}{\varepsilon_\alpha}} \text{ for helical gearing}$$

Z_β – additional influence of the helix line not included in Z_ε: $Z_\beta = \sqrt{\cos \beta}$
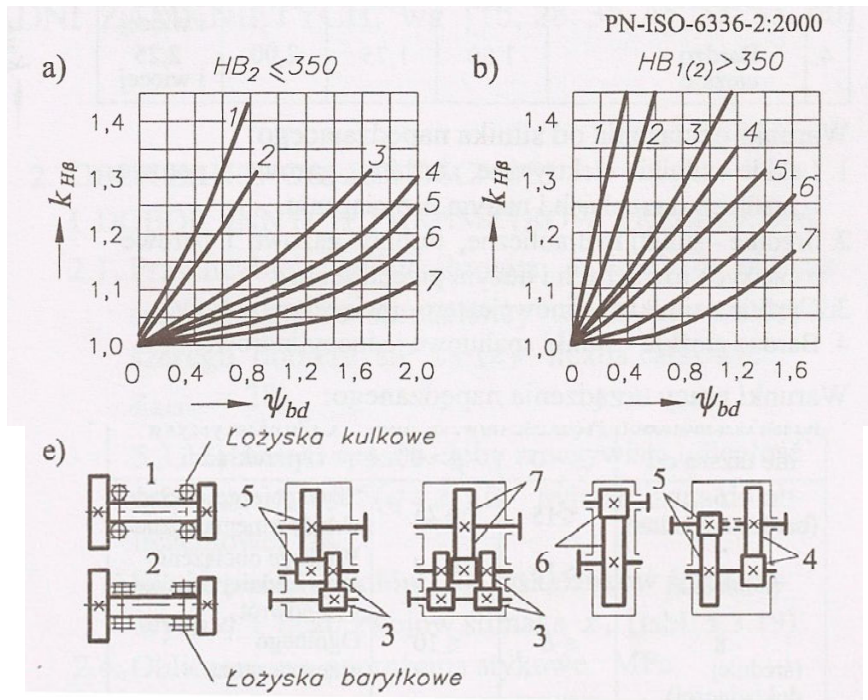
Fig. 24.5. Graphs (a and b) for the calculation of coefficients $K_{H\beta}$ [12]. Legend: łożysko kulkowe = deep groove ball bearing; łożyska baryłkowe = barrel roller bearings

The factor of safety s_H shall not be less than 1.2. Observe that this value is very small when compared to values in general machine design (1.7 min). Information on the actual loading conditions and on the material is very precise in gearing applications. It is one of the most researched machine elements.

HW 24.1. Sketch the distribution of stresses for a helical toothed pair. Take data from your design assignment 3 (a transmission system). Polish students: see problem 8.4 in [4].

Glossary

contact stress	nacisk stykowy
fatigue breakage	złamanie zmęczeniowe
form factor	współczynnik kształtu
impact breakage	złamanie doraźne
mode of failure	sposób uszkodzenia
pitting	złuszczenie powierzchni, pitting
scoring	zatarcie
surface working	dogniatanie powierzchni

25. Strength Calculations: bending

25.1. Bending capacity (the Lewis' formula)

Bending is dangerous for case hardened teeth (vehicle, machine tool, gearboxes). These are usually narrow and ground. Possible impacts of tooth breakage are far more dangerous than those resulting from pitting.

The first and so far the simplest model for the bending calculations was presented by Lewis at the end of the 19th century.
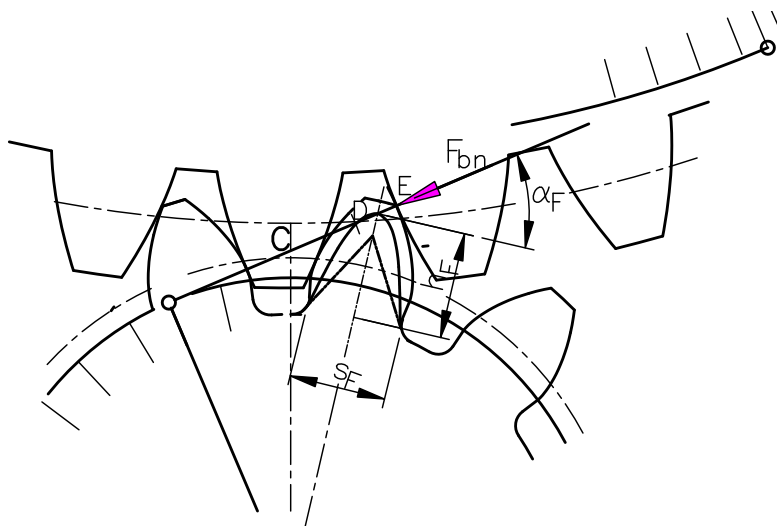
Fig. 25.1. A cantilever beam model proposed by Lewis

The most dangerous position for bending is the last point of one-pair meshing in the pinion (E_1). The force is applied at the addendum of the pinion. On the other hand, there is another toothed pair in meshing at the same time. This will be accounted for in the final formula. Of the three stress components (compression, shearing, bending) the most dangerous is the right side of the tooth even if the left side is statically more loaded. This is due to the fatigue mode of loading (tensile stress!).   Lewis considered bending only. The formula is:

$$\sigma = \frac{6F_{bn}\cos\alpha_F h_F}{bs_F^2} = \frac{F_t}{bm}q_w$$

where: q_w is an aggregated coefficient (a form factor) taking into account the geometry of one toothed pair. Fig. 25.2 shows this coefficient versus the equivalent number of teeth z_e and addendum coefficient.
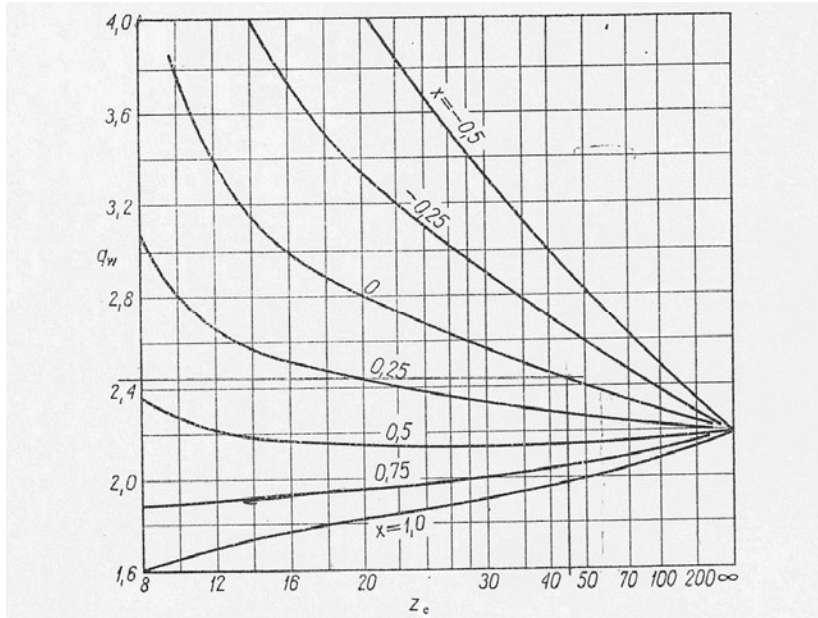
Fig. 25.2 The form factor vs. the tooth count [5]

The higher is the coefficient, the lower is the form factor, which witnesses to the beneficial effect of the addendum modification to bending capacity.

25.2. ISO-DIN Formulas

The ISO-DIN standards recommend the use of the following formula:

$$S_F = \frac{\sigma_{F\lim}}{\dfrac{F_t}{bm_n}} \frac{Y_N Y_\sigma Y_R Y_x}{\left(Y_{Fa} Y_{Sa} Y_\beta Y_\varepsilon\right)\left(K_A K_v K_{F\beta} K_{F\alpha}\right)}$$

Again, the underlying Lewis formula is embedded in the above formula. As for the contact pressure formula from the previous chapter, all additional coefficients can be divided into three groups.

25.2.1. Correction factors due to bending

These coefficients are similar to those discussed during our first semester discussion on fatigue: notch sensitivity, surface finish etc. A difference is that in general machine design we needed a transition from a cylindrical smooth specimen to a real machine elements and in gearing, a specimen is similar to a toothed gear. It differs from an actual gear in size, surface finish a.s.o.

Let me list shortly all these coefficients:

Y_σ – notch sensitivity factor
Y_N – the same as Z_N
Y_R – surface finish (the fillet area only)
Y_x – scale factor (assume all coefficients equal to 1 in your design calculations)

25.2.2. Operational coefficients

K_A, K_v – the same as in chapter 24 for contact pressure (Appendix 6 and 7)
$K_{F\beta}$ – The uneven distribution of load along the length of a tooth (related to contact pressure coefficient in the following way:

$$K_{F\beta} = \left(K_{H\beta}\right)^{NF}; \text{ where the exponent } NF = \frac{(b/h)^2}{(b/h)^2 + (b/h) + 1};$$

b = width of the gear (the pinion is usually wider);
$h = 2m_n/\varepsilon_\alpha$ for spur gearing and $h = 2m_n$ for helical gearing.
$K_{F\alpha}$ – the same as $K_{H\alpha}$.

25.2.3. Design coefficients

Y_{FS} – the form factor + stresses omitted by Lewis: $Y_{FS} = Y_{F\alpha}Y_{S\alpha}$ (see Fig. 25.3 and 25.4).
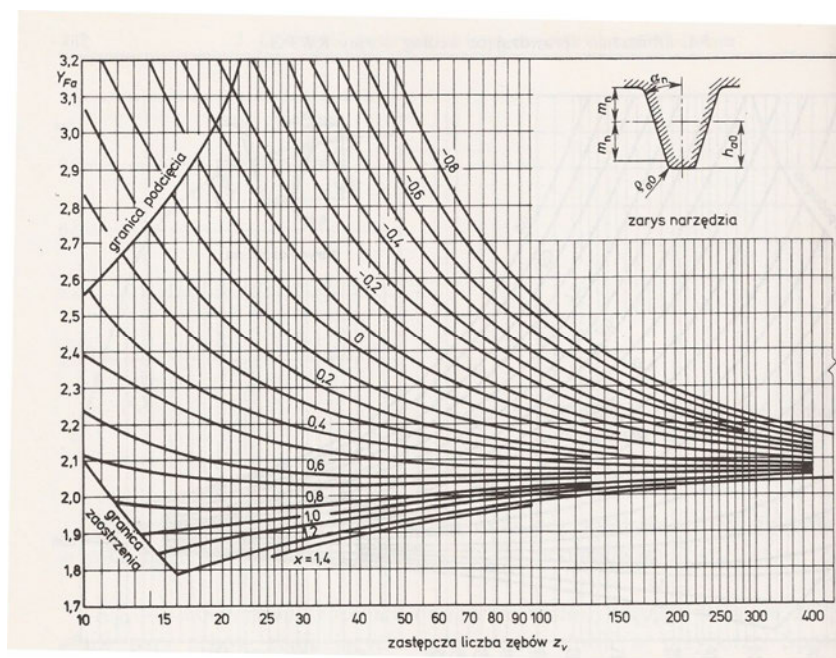
Fig. 25.3. The form factor [5]. Legend: zastępcza liczba zębów = equivalent number of teeth; granica podcięcia = undercut limit; granica zaostrzenia = sharp top land limit
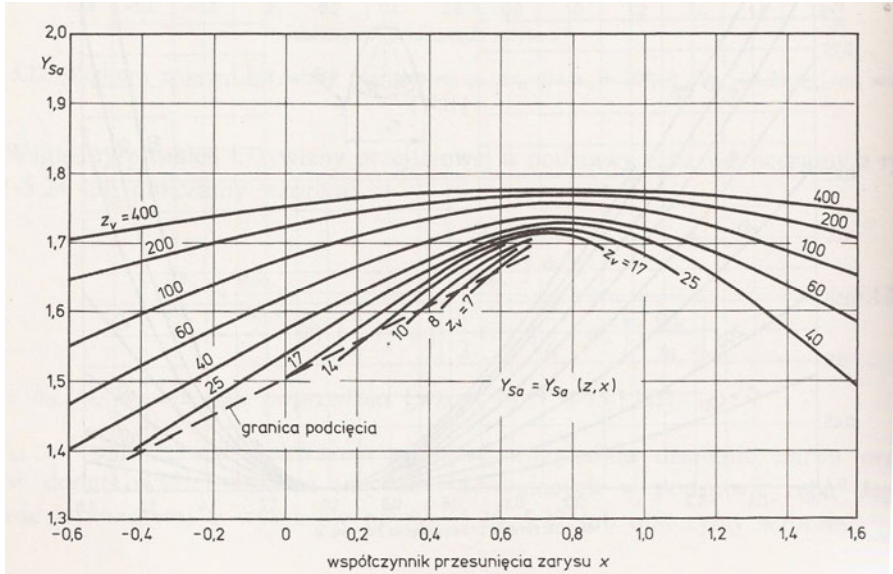
Fig. 25.4. Stress concentration factor [5]. Legend: współczynnik przesuniecia zarysu = addendum modification coefficient; granica podcięcia = undercut limit

Y_β – the influence of the helix line: the load in an equivalent spur gear is applied along a skew line, which is beneficial to the load carrying capacity of a tooth:

$$Y_\beta = 1 - \varepsilon_\beta \frac{\beta}{120} \geq Y_{\beta b\min} \text{ where: } Y_{\beta\min} = 1 - 0.25\varepsilon_\beta \geq 0.75$$

Y_ε – the influence of the overlap ratio (the full force does not act at point E but D):

$$Y_\varepsilon = 0.2 + \frac{0.8}{\varepsilon_\gamma}$$

The factor of safety s_F shall not be less than 1.5.

HW 25.1. Solve problem 24.1in terms of bending stresses (Lewis formula only).

Glossary

machine tool	obrabiarka
one-pair meshing	zazębienie jednoparowe
aggregated	tu: łączny
form factor	współczynnik kształtu
embedded	tu: zawarty, wpleciony

26. Bevel Gearing: part 1

26.1. Introduction

Bevel gearing is expensive! If not governed by other reasons, locate it always at the beginning of a transmission train, where torque, and consequently, transmission size is minimum. Unfortunately, the most known application is the final drive, where torque is relatively high, and transmission volume, large. This unfavourable situation triggered however a stream of inventions, mostly in the manufacturing process, which had made the process less expensive. But this will be discussed at the end of our lecture. Bevel gearing is a domain of a few world known manufactures; the best known of them, also in Poland (a licence agreement), is the Gleason Works in Rochester, USA. Some others are Klingelnberg (Germany), Renault (France), Fiat –Mammano (Italy) etc. As a result, the construction, machine tools, calculations etc. are manufacturer specific.

Fig. 26.1 shows the meshing scheme in a standard ($\delta_1 + \delta_2 = 90°$) bevel toothed pair. A spherical involute is created on the surface of a sphere. A trapezoidal tooth form at the equator, which converges to the sphere centre, is a reference gear (a crown gear). It plays the same role as the generating rack for a spur gear. Due to some reasons explained in the next drawing, it is a straight line when viewed from the frontal direction. We trace a vertical line tangent to the sphere and create so called complementary cones. With this simplification, the error is negligible and manufacturing difficulties avoided. To the right traced are complementary cones.
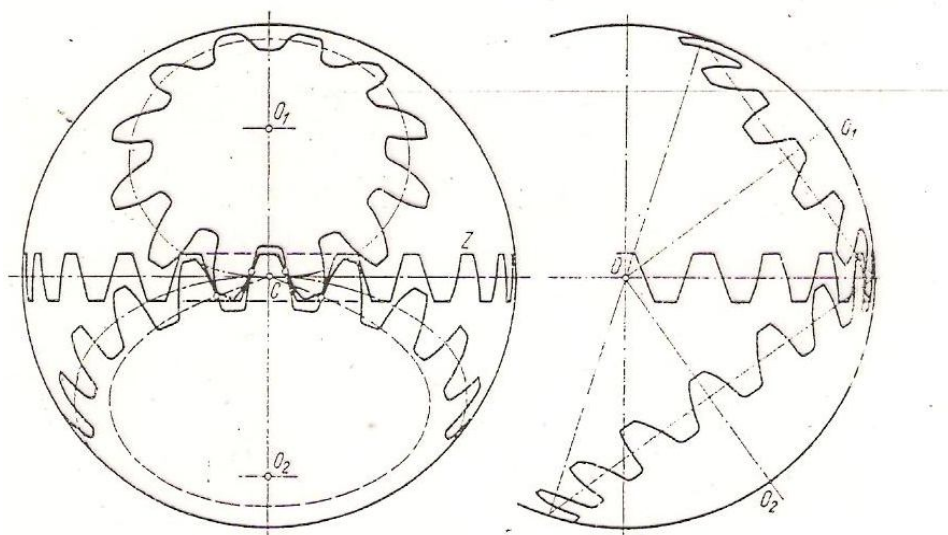
Fig. 26.1. The meshing scheme of a bevel toothed pair (complementary cones) [2] (▲)

Possible impacts of this simplification are shown in Fig. 26.2.
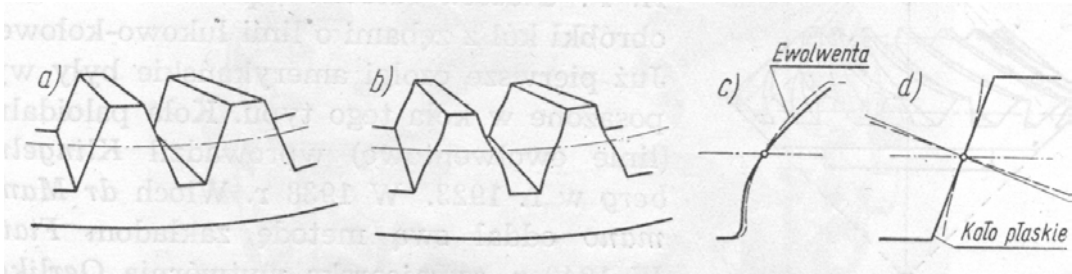
Fig. 26.2. A simplified tooth form of a common crown gear (a); the correct tooth form (b); an involute tooth form and a tooth form obtained with the simplified tooth form of the crown gear (c); the pressure line (d) [2].
Legend: ewolwenta = involute; koło płaskie = flat reference circle

The two cone angles may be found from simple formulas:

$$u = \frac{R_m \sin \delta_2}{R_m \sin \delta_1} = \frac{\sin \delta_2}{\sin \delta_1}. \text{ If } \delta_1 + \delta_2 = 90^o \text{ then to } u = \tan \delta_2 \text{ and } \frac{1}{u} = \tan \delta_1$$

Fig. 26.3 shows different orientation of tooth line (manufacturer specific). The mean helix angle is on average equal to 35°. All these gearing (save of a and d) is left hand (viewed form the pitch cone apex). A curved line provides for a localised contact irrespective of mounting errors.
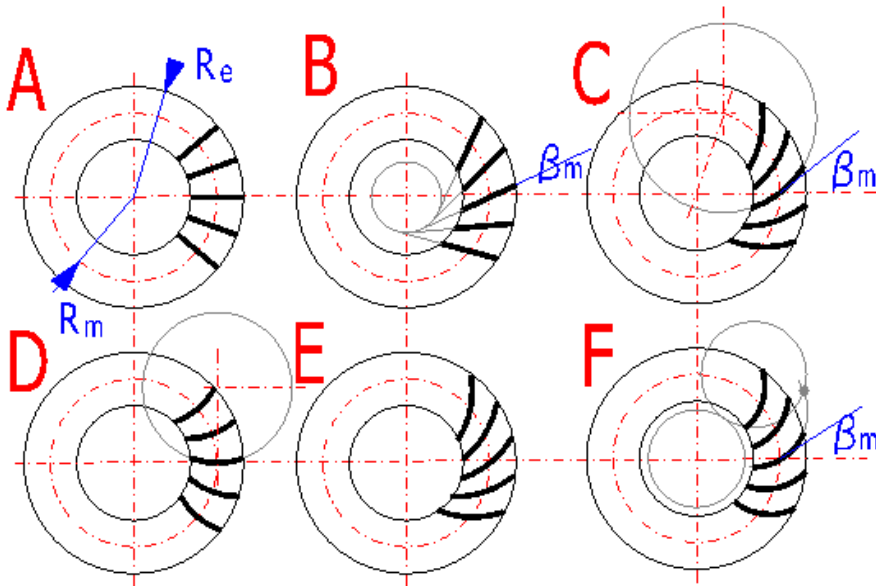
Fig. 26.3. Types of bevel gearing A = straight teeth; B = helical; C= spiral (Gleason); d = Zerol (Gleason); E = involute (Klingelnberg); F = cykloide (Oerlikon, Fiat) [Internet]

26.2. Geometry of a bevel toothed pair
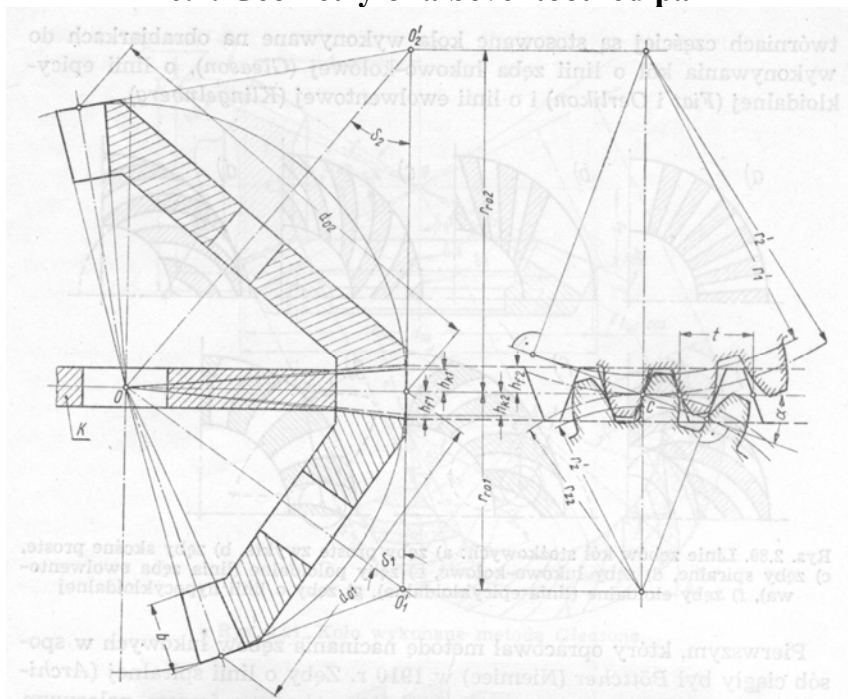
Fig. 26.4. Bevel gears, common flat crown gear (K) on the common reference plane [2]

$$z_{v1} = \frac{z_1}{\cos \delta_1} \; ; \; z_{v2} = \frac{z_2}{\cos \delta_2} \; ; \; u_v = \frac{z_{v2}}{z_{v1}} = u^2$$

Fig. 26.4 shows basic definitions for the geometry of a bevel toothed pair. These are: (subscript e is for the external diameter):

The pitch diameter: $d_{e1} = m_{te} \, z_1$; $d_{e2} = m_{te} z_2$;where m_{te} is the external transverse module to be calculated the same way as for helical gearing, i.e. $m_{te} = m_{nm} \dfrac{R_e}{R_m \cos \beta_m}$ and accounting for different values of the generator length.

Number of teeth in the crown gear: $z_c = \sqrt{z_1^2 + z_2^2}$

The length of the external cone generator: $R_e = 0.5 \; m_{te} z_c$

The face width of the gear: $b \le 0.3 \, R_e$

The mean cone radius: $R_m = R_e - 0.5b$

The mean circumferential module: $m_{ti} = m_{te} \dfrac{R_m}{R_e}$

Tooth proportions are a function of the transverse module (for straight gearing) or the medium module (for helical and spiral gearing of all types). Different approach is also for tooth height proportions and the bottom clearance. Explained in Fig. 26.4 is also the notion of the equivalent spur gear (similarly to helical gearing).

26.3. The generation process

As mentioned in the introduction, the generation process is manufacturer specific. Fig. 26.5 shows the Gleason process and Fig. 26.6, a Gleason face mill cutter in operation.
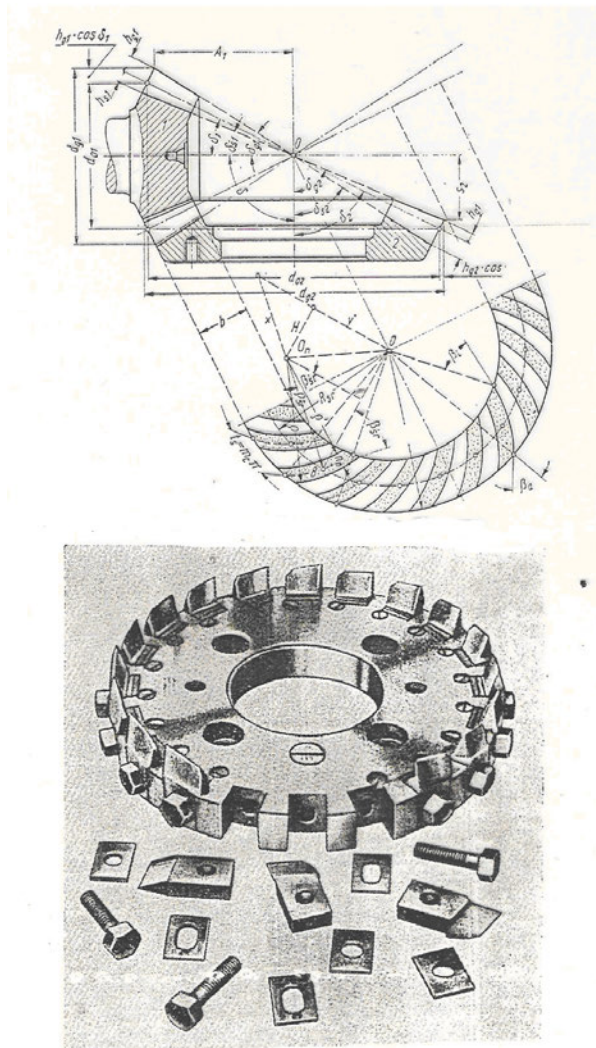
Fig. 26.5. The Gleason process, a blade milling cutter [2]

Fig. 26.6. A Gleason face mill cutter in operation [The Gleason Works]

26.4. Profile correction

Apart of the standard P-0 correction (mostly to level the relative sliding velocities in the meshing toothed pair), it is possible to employ a so called tangential correction.

As each side of a tooth flank is machined separately, it is possible to modify the width of a tooth, i.e. to increase the width of the pinion tooth and to decrease (to the same amount) the width of the gear tooth levelling thus the load carrying capacity of this pair. The reference profile is shown in Fig. 26.7.
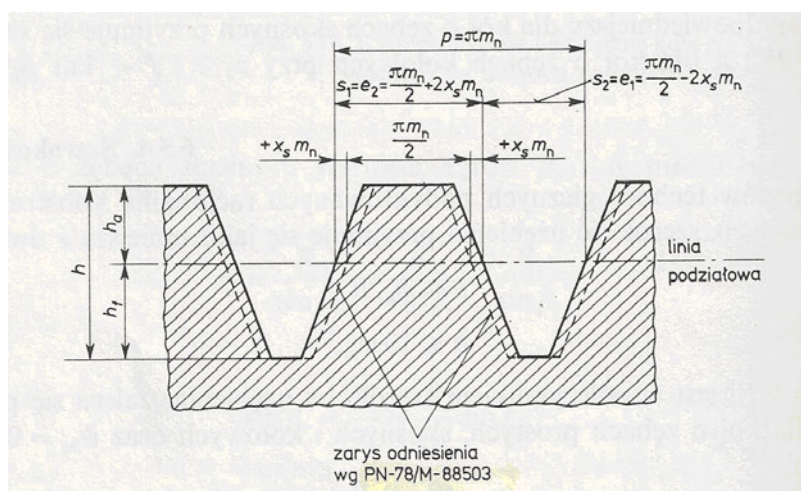
Fig. 26.7. The tangential correction in bevel gearing [5]. Legend: zarys odniesienia = reference profile; linia podziałowa = pitch line

NP 26.1. ([4]) (Use this example and attached graphs for the calculations of the first stage of your design class assignment). Calculate the diameter of a spiral bevel pinion subjected to a permanent torque load of 100 Nm. The transmission ratio $u = 4$; material of the pinion and gear: case hardened steel with $\sigma_{Hlim} = 1375\ MPa$; relative tooth width ($\psi_{be} = b/R_e = 0.3$). Using the graph we find the coefficient of non-uniform load $K_{H\beta} = 1.18$. Allowable stress $\sigma_{HP} = 0.8\ \sigma_{Hlim} = 0.8 \cdot 1375 = 1100$ MPa.

The diameter of the pinion [5]:
$$d_{e1} = 89\sqrt[3]{\frac{T_1 K_{H\beta}}{(1 - \Psi_{be})\Psi_{be} u \sigma_{HP}^2}} = 89\sqrt[3]{\frac{100 \cdot 10^3 \cdot 1.18}{(1 - 0.3)0.3 \cdot 4 \cdot 1100^2}} = 48.6\ \text{mm}$$

The selection of the tooth count, module etc. will be discussed in the design class.
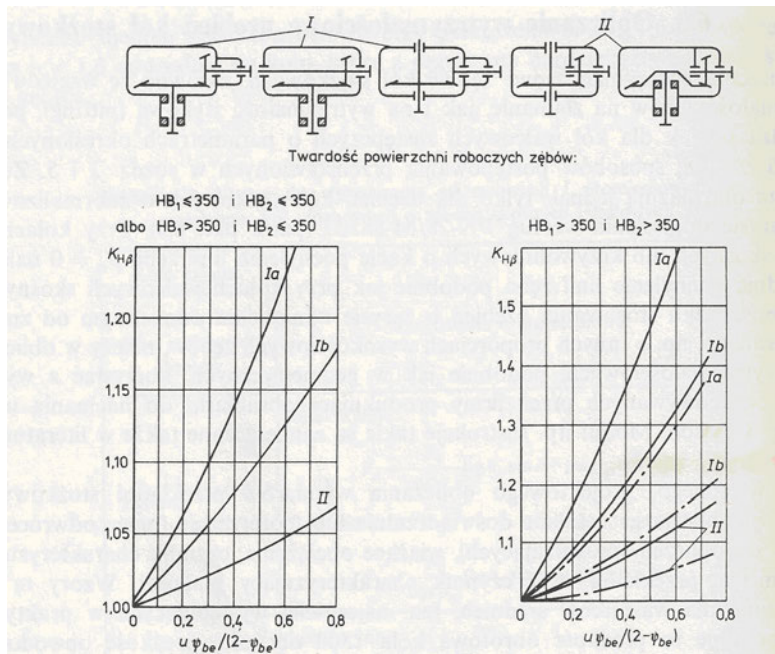
Legend: twardość powierzchni roboczych = surface hardness of the contacting tooth surfaces

HW 26.1. ([4]) A bevel toothed pair is composed of $z_1 = 23$; $z_2 = 60$ $m = 6$; $\alpha = 20°$; rim width $w = 58$ mm; straight teeth. Convert this toothed pair into an equivalent spur toothed pair (a graphical solution).

Glossary

bevel gearing	koła zębate stożkowe
case hardened	utwardzany powierzchniowo
crown gear	koło koronowe
final drive	przekładnia główna
generator	pobocznica stożka
manufacturer specific	specyficzna dla danego wytwórcy
mounting error	błąd montażu
reference gear	koło odniesienia
spherical involute	ewolwenta kołowa
spiral	kołowo-łukowe

27. Bevel Gearing: part 2

27.1. Force distribution

Let's make a summary of force distributions in helical gearing before we start discussing this problem in bevel gearing (a copy from chapter 22)

Helical gearing

Fig. 27.1. A summary of force distribution in helical gearing

Tangential and axial components:

$$F_t = \frac{2T_1}{d_{w1}}; \quad F_a = F_t \tan \beta_w;$$

$$\tan \beta_w = \frac{d_{w1}}{d_1} \tan \beta$$

The resultant force at the plane tangent to the operating diameter:

$$F_s = \frac{F_t}{\cos \beta_w}$$

The radial component of the resultant force:

$$F_r = F_s \tan \alpha_{nw} = F_t \tan \alpha_{tw}, \text{ but}$$

$$\tan \alpha_{tw} = \frac{\tan \alpha_{nw}}{\cos \beta_w}$$
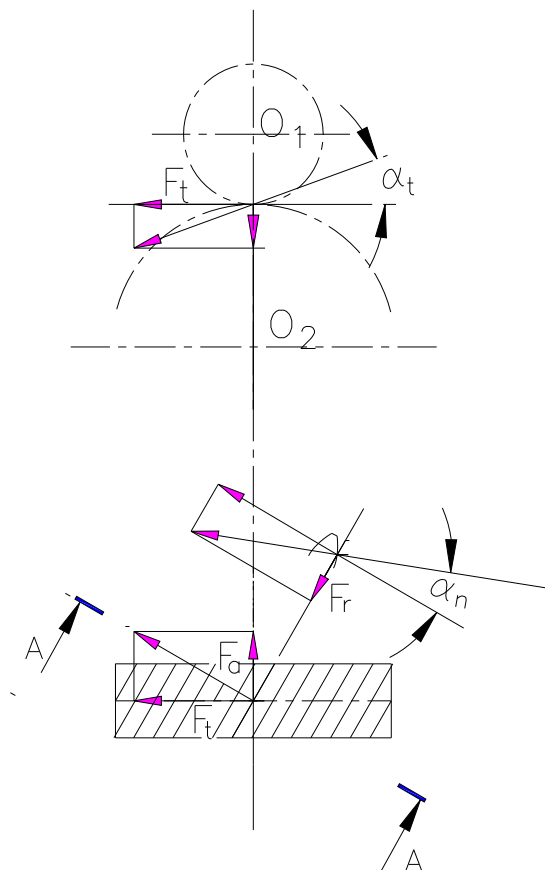
Remember: the underlying formula is always for the tangential force. Next comes the formula for the radial force as the tangent (in terms of trigonometry) or the tangent one (in terms of direction). There is no need for the resultant force as all forces must be resolved into the horizontal and vertical planes. With the tangent force known, you can find the axial force and its sense (helical gearing). The resultant of the tangent and axial forces produces the radial load, which is always directed towards the centre of the gear. This force is best seen in a cross-section normal to the helix line. And now a bevel gearing set (helical or spiral, Fig. 27.2).
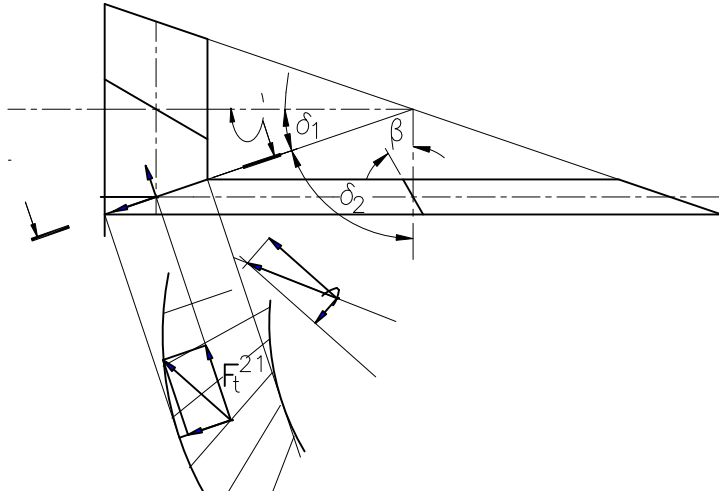
Fig. 27.2. Force distribution in a bevel toothed pair (▲)

There are two variables: the direction of the helix line and direction of rotation. You establish them viewing from the pitch cone apex. Depending upon a combination of these two, the results will be quite different. Let's try to establish the loading of the pinion gear shaft. As usually, we start with the tangential force. As the tooth line is inclined, we need to view it from top to find the force which acts along the cone generator line. The resultant of the two, when sectioned along the normal line, when resolved into axial and radial planes, will give the overall axial and radial load for the pinion. When tracing force layout for the shaft calculations, do not forget about the tangential force, which is perpendicular to the radial and axial ones. The upper sign in the formulas are for situations when the helix line agrees with the sense of rotation (i.e. the right one with the CW direction). The lower one is for opposed directions.

$$F_a^{21} = \frac{F_t}{\cos \beta_m} \left[\tan \alpha_n \cos \delta_2 \pm \sin \beta_m \cos \delta_1 \right]$$

$$F_r^{21} = \frac{F_t}{\cos \beta_m} \left[\tan \alpha_n \cos \delta_1 \mp \sin \beta_m \cos \delta_2 \right]$$

NP 27.1. ([4]). Find forces in the meshing of a straight teeth bevel transmission: Data: $z_1 = 23$; $z_2 = 60$; $m = 6$; width $w = 58$ mm; $T_1 = 0.4$ kNm.

The pitch diameter: $d_1 = mz_1 = 6 \cdot 23 = 138$ mm; $d_2 = mz_2 = 6 \cdot 60 = 360$ mm

Cone angles: $\delta_1 = \arctan \frac{z_1}{z_2} = \arctan \frac{23}{60} = 20.973°$; $\delta_2 = 90° - \delta_1 = 90° - 20.973° = 69.027°$

The mean diameter of the pinion: $d_m = d_1 - w \sin \delta_1 = 138 - 58 \cdot \sin 20.973° = 117.24$ mm

The tangential force: $F_t = \dfrac{2T_1}{d_{m1}} = \dfrac{2 \cdot 0.4 \cdot 10^6}{117.24} = 6823.61\,\text{N}$

The axial force ($\beta = 0$): $F_a = F_t \tan\alpha_n \cos\delta_2 = 6823.6116197 \cdot \tan 20° \cos 69.027° = 888.95\,\text{N}$

The radial force: $F_r = F_t \tan\alpha_n \cos\delta_1 = 6823.61 \cdot \tan 20° \cos 20.973° = 2319.05\,\text{N}$

27.2. Peculiarities of the final drive design
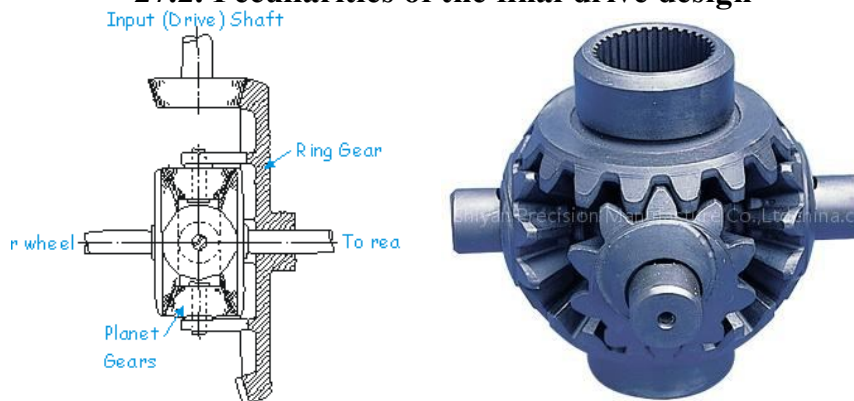
Fig. 27.3. A differential gear (the Revacycle method) [Shiyan Precision Manufacturing]

Differential gears are manufactured not by a generation process but are broached. Tooth profile is not a true involute but it does not matter as the relative speed of differential gearing is relatively small. An off-topic remark would be to mention that this type of violation was employed on purpose in a special differential design for off-road vehicles by the Timken Company. The idea was to enhance the traction capabilities of a vehicle under adverse road conditions.

As to the pinion and crown gears, the Gleason Company invented an ingenious method in which the pinion is generated but the gear is form cut (Formate®). This approach balances time necessary to produce a bevel pair. A trade-off between accuracy and economy.

The position of the pinion depends upon application: where high clearance is necessary (off road vehicles), the pinion is located above the axis of the gear. If you want to design a low floor bus for easy entry, locate the pinion below the gear centre line. The size of the pinion varies accordingly. Why? The size of the pinion depends upon the number of teeth and the transverse module. For a left hand pinion (right hand gear) the tooth is nearly horizontal, meaning that the module is roughly the same as the normal module. The lower is the pinion, the higher is the angle and, consequently the higher is the transverse module and pinion size. This situation is beneficial to the load carrying capacity of the pinion. On the other hand, if the pinion is right hand, the situation is inversed. You can check that final drive pinions are usually left handed.
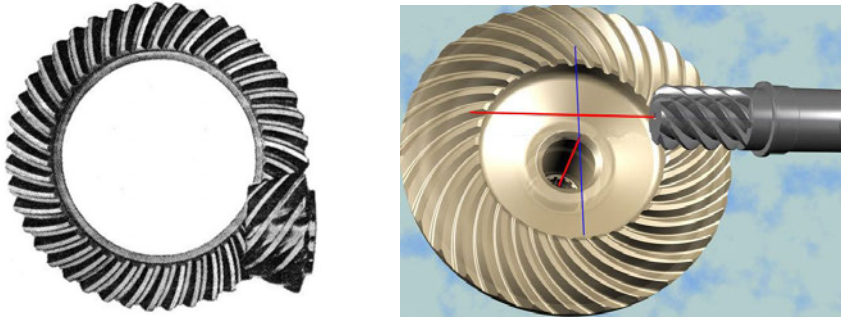
Fig. 27.4. Bottom and top pinion layouts for a final drive [Zakgear technology]

27.3. Assembly of a bevel toothed pair

The assembly of a bevel toothed pair is one of the most difficult tasks in mechanical engineering. Needed are technical means (shims) to move axially both the pinion and the crown gear without compromising the axial clearance (preload) in the rolling contact bearings (mostly tapered roller bearings). Fig. 27.5 shows a typical bearing arrangement of the final drive with necessary means for the control of both gears.
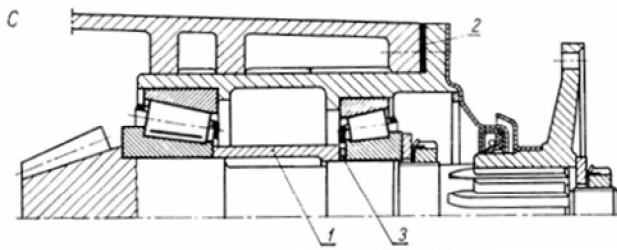
Fig. 27.5. Bearing arrangements in the final drive and regulation means (shims 2 and 3) [8]

HW 27.1 (modified after [4]). For a spiral bevel transmission gear find the resultant axial and radial load for the pinion and gear if: $z_1 = 19$; $z_2 = 50$; $\alpha = 20°$; $w = 60$ mm; transverse external module $m_t = 7$; mean helix angle $\beta_m = 35°$. The pinion torque $T_1 = 2$ kNm; the helix line is a) the same as the sense of rotation; b) the helix line is opposite to the sense of rotation.

Answer: a) $F_a^{21} = F_r^{12} = 23.4$ kN; $F_r^{21} = F_a^{12} = 5.96$ kN
b) $F_a^{21} = F_r^{12} = -17.8$ kN; $F_r^{21} = F_a^{12} = 23.8$ kN

Glossary

broached	przeciągany
form-cut	nacinanie kształtowe
high clearance	tu: duży prześwit
off- road vehicles	pojazdy terenowe
pitch cone apex	wierzchołek stożka podziałowego
shim	podkładka regulacyjna
spiral bevel gear	koło stożkowe kołowo-łukowe
trade-off	kompromis

28. Worm Gearing: part 1

28.1. General, application areas

Worm gearing is a dual purpose gearing: a change in the direction of rotation and a high transmission ratio (up to 60 in one stage). The worm meshes with the worm gear (a bull gear) like a screw with its nut. Both transmissions feature the same formulas for efficiency. The application area includes both high and low transmission ratio applications. With a high transmission ratio, the efficiency is usually low, and a transmission is self-locking. A good application is a winch (no need for a backstop brake - Fig. 28.1a) or a tuning mechanism (Fig. 28.1 b).
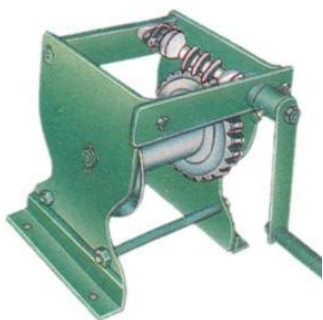
a) [Globe]   b) [from: find_target]   c) [A EC Regal Mark bus]
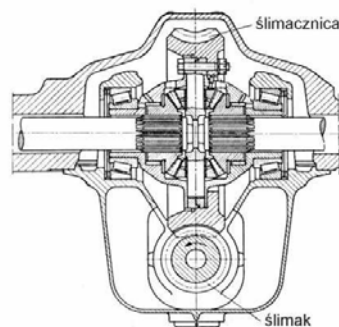
Fig. 28.1 High (a, b) and low (c) transmission ratio worm gear sets

A worm gear may also replace a bevel gear in the final drive of an automobile. In this case the transmission ratio is low, and efficiency is very high (Fig. 28.1 c)

A variable pitch worm (Fig. 28.2 a) is very useful for the regulation of the end play in the steering gear of an automobile. A frequent application there is an hour-glass (Hindley) worm (Fig. 28.2 b).
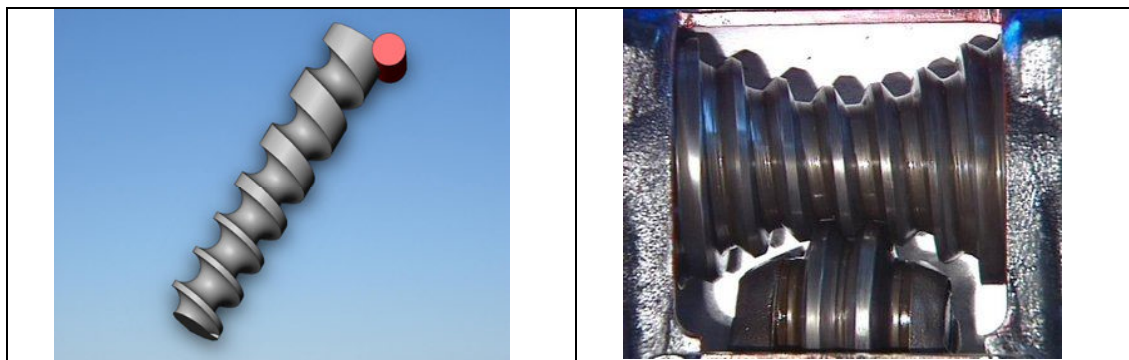
Fig. 28.2. A variable pitch worm (a) [from: Eng.Tips] and a worm gearing used in steering systems (b) [Global]

28.2. Worm design

The worm surface is actually a helical surface. In the general case, any helical surface is a product of the combined translation and rotation of a straight line. The line is inclined at a given angle α_b to the horizontal and tangent to a helical line wound around a cylinder (radius r_b) with a lead angle γ. In the most common case of a screw surface, the radius r_b is equal to zero and the surface thus generated is called after Archimedes as an A type (Fig. 28.3, a standard in Germany). If r_b is equal to cosine 20° of the pitch circle, then the worm surface is of the involute type E (Fig. 28.3, a standard in the U.K.).
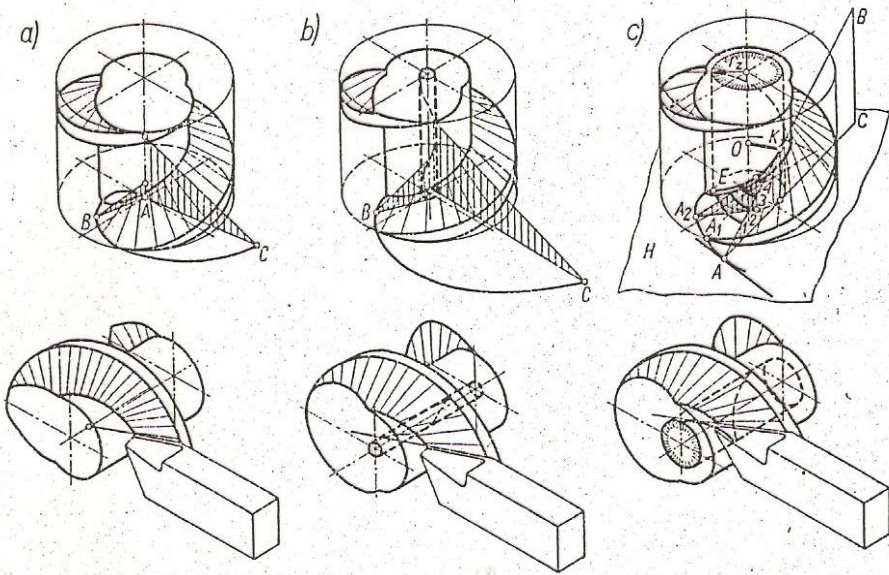
Fig. 28.3 Helical surfaces [2]

The A type worm is easy for manufacture and control. To avoid undercutting in the bull gear, a typical relationship between the helix angle and the pressure angle in an A-type of worm transmission is given in the following table:

Table 28.1. Typical relationship between the pressure and helix angle in A-type worms

α	14.5°	20°	25°	30°
γ	16°	25°	35°	45°

This pressure angle is defined in the axial plane of the worm (contrary to other types of worm gear profiles (the normal plane). As in screw mechanisms, the smaller is the helix angle, the higher is the transmission ratio. With an increased value of the helix angle, the worm may have 2 or more starts.
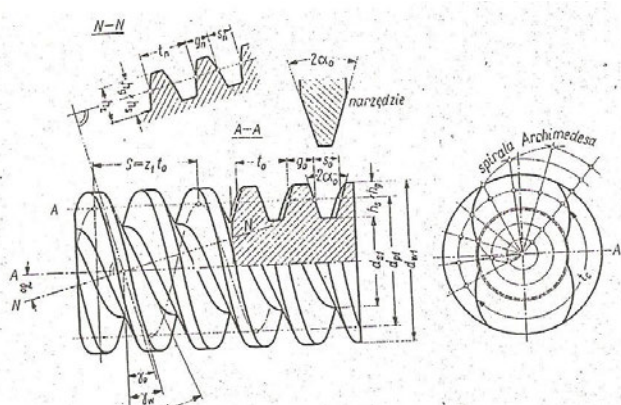
Fig. 28.4. A two-start worm
(Legend: narzędzie = tool) [2]

$$p_x = z_1 p = \pi d_1 \tan \gamma$$

$$d_1 = \frac{z_1 p}{\pi \tan \gamma} = m \frac{z_1}{\tan \gamma} = mq$$

where: q is the worm diameter factor (also subject to standardisation (5.5 to 20).

An eternal dilemma in the gear transmissions: a standard pitch vs. the standard module is absent in worm transmissions. The addendum and dedendum diameters (the A type) are given by:

$$d_{a1} = d_1 + 2 \cdot m_n$$

$$d_{f1} = d_1 - 2.4 \cdot m_n$$

28.3. The worm (bull) gear

The generation process in a worm gear is done by a hob, which reflects the surface of this worm. A distinct difference in the design of a worm gear is that its meshing surface is a torus and all cross-sections which are shifted from the central position are in a natural way positively shifted. This may result with sharp top lands in extreme left and right cross-sections. Fig. 28.5 shows different rim shapes; from the most vulnerable (a) to the least vulnerable (d).
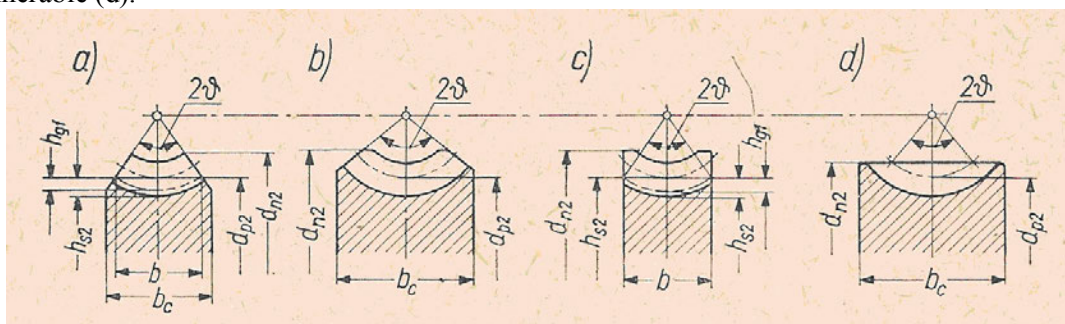
Fig. 28.5. Rim design in a worm wheel [2]

Merrit recommends the following formula for the width of a worm gear: $b = 2m\sqrt{q+1}$.
Other formulas are similar to those in helical gearing, i.e.:

The pitch diameter (worm gear): $d_2 = z_2 m$;

The addendum diameter $d_{a2} = 2a_w - d_{f1} - 2c$

28.4. Worm transmissions

Fig. 28.6 shows base relationships in a worm gear set traced both in the axial and normal planes.
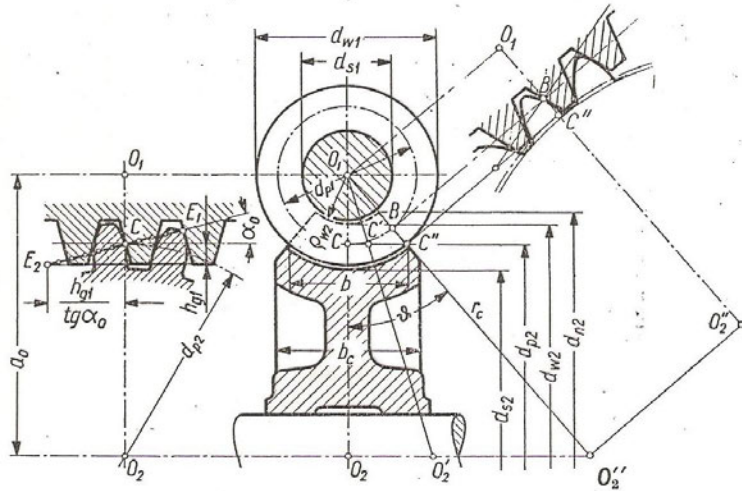
Fig. 28.6. Base relationships in a worm gear transmission [15]

The main parameter, i.e. the centre distance is given by the following formula:

$$a = \frac{q + z_2}{2} m$$

Other meshing parameters (together with addendum modification) will be discussed in the next chapter.

Glossary

worm gearing	przekładnie ślimakowe
worm	ślimak
worm gear/bull gear	ślimacznica
backstop brake	hamulec zwrotny
tuning mechanism	mechanizm do strojenia
an hour-glass worm	ślimak globoidalny
hob	frez
rim	wieniec

29. Worm Gearing: part 2

29.1. Meshing parameters

Contrary to helical gearing, worm gearing remains in constant contact over a certain area, the pressure area. To establish its limits, needed are either complex analytical considerations or a graphical method. The first step in this method consists in the determination of the pressure line. This is illustrated in Fig. 29.1. For a given tooth profile we trace a few lines perpendicular to this profile (e.g. AA'). When transferring this line to the pitch point P, the first point of the pressure line is found (A_1), to maintain the fundamental law of toothed gearing, the line normal to the contacting surfaces must pass through the pitch point P).

Fig. 29.1. Determination of the pressure line [11].
Legend: linia toczna ślimaka = operating line of the worm
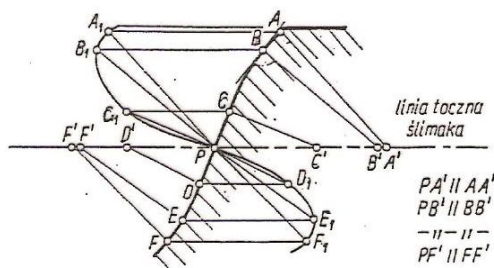
For 5 longitudinal cross-sections in the worm constructed are 5 pressure lines (see Fig. 29.2). The limiting points are defined by intersections of the pressure lines with the addendum of the worm gear (the first point, an equivalent to point A in spur gearing) and of the worm (the last point, E in spur gearing).
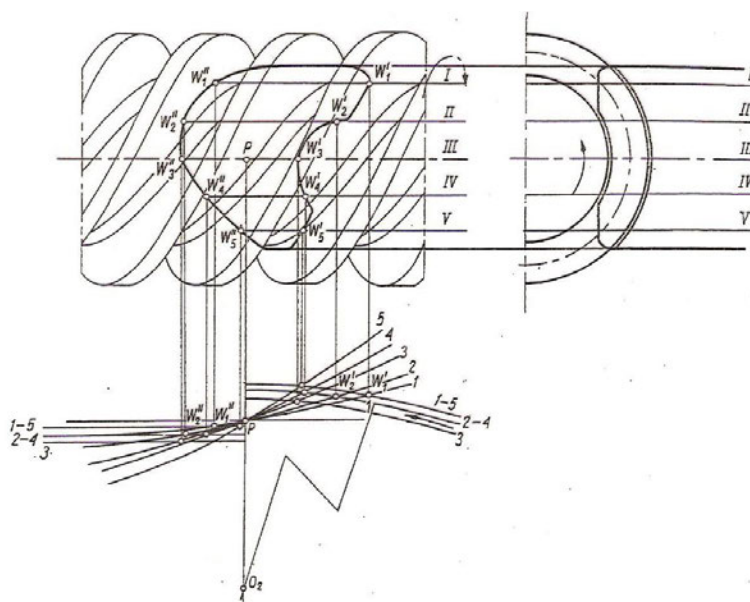
Fig. 29.2. Construction of the pressure area [11]

With the pressure area and the pressure lines constructed, we are able to construct contact lines. The procedure is shown in Fig. 29.3.
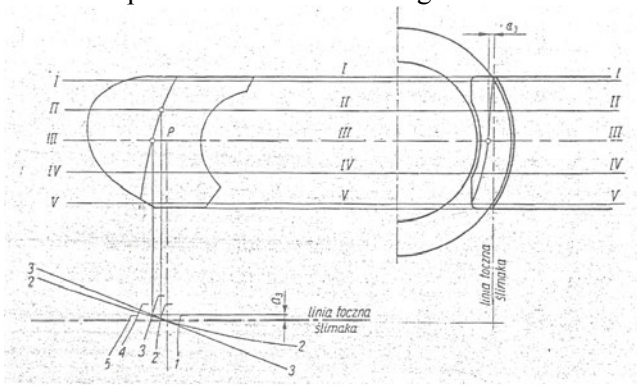
Fig. 29.3. Construction of a contact line [11]. Legend: linia toczna ślimak = operating pitch line of the worm

29.2. Addendum modification

A major problem with worm gearing is a poor arrangement of contact lines between the worm and the worm gear. These lines are located very close, in terms of direction, to the lines of relative velocities between the two gears. See Fig. 29.4 (left side).
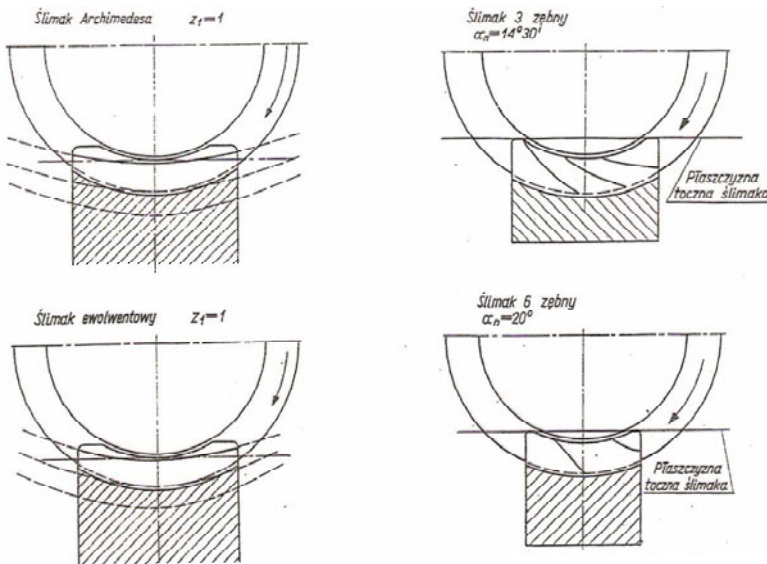
Fig. 29.4. The effect of correction on the position of contact lines [2]. Legend: Slimak Archimedesa = Archimedes worm; ślimak 3/6 zębny = three/six start worm; ślimak ewolwentowy = involute worm; płaszczyzna toczna ślimaka = operating pitch plane of the worm

This situation is very disadvantageous (no chance for the oil film). A remedy is to apply an ample amount of P-O profile shift to the transmission. This results in recess only meshing (meshing starts in point C and goes to point E in the worm gear). Contact lines in meshing form larger angles with the sliding velocity lines making the formation of full-film lubrication easier. (Fig. 29.4, right side).

Yet another solution is a convex-concave gearing developed by prof. Nieman and shown in Fig. 29.5 together with the pattern of contact lines.
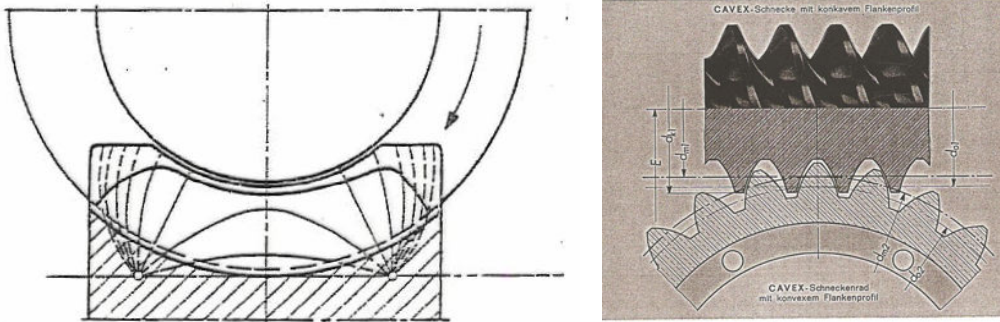
Fig. 29.5. The Cavex worm gearing [2, Flender]

29.3. Force distribution, efficiency

The situation here is the same as in power screws discussed in the previous semester. Formulas offered by textbooks account for the pressure angle. (If you remember, in power screws we assumed a rectangular shape of the thread profile; therefore one component force was lost). With small helix angles, high axial thrust is present in the worm. Needed are therefore strong bearing arrangements designed for this type of loading. The double action axial thrust ball bearing is best adapted to this task. The worm wheel is usually supported by a face to face arrangement of tapered roller bearings (Fig. 29.6).
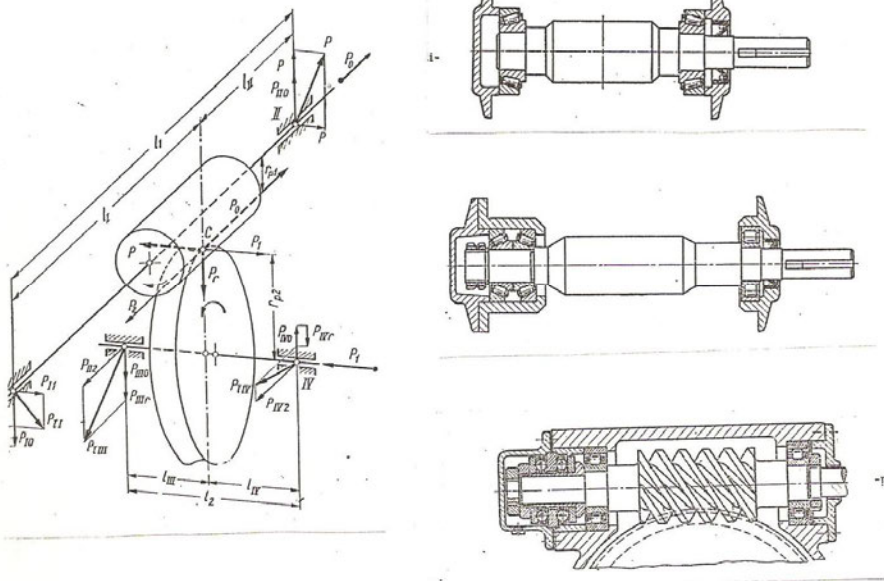
Fig. 29.6. Force distribution and bearing arrangements for the worm [2]

Efficiency formulas are the same as those for power screws (Chapter 3): $\eta = \dfrac{\tan\gamma}{\tan(\gamma + \rho^{'})}$.

For high transmission ratios the helix angle is close to the friction angle, a transmission is self-locking and fficiency is close to 50% or even less. Heat balance considerations are then of great importance. Apart of usual means for better heat transfer (ribbed casings, additional cooling fans) a good solution is an intermittent mode of operation, as in a central pivot irrigation shown in Fig. 29.7. The transmission system of each tower consists of two series connected worm transmissions with a total transmission ratio of 1800 (30x60). To move the pivot arm at a constant rotational speed (approximately one full turn every 24 hours), it is composed of articulated spans. At a preset value of the misalignment angle the leding span is stopped and the lagging span is activated. The arm moves in a zig-zag line.
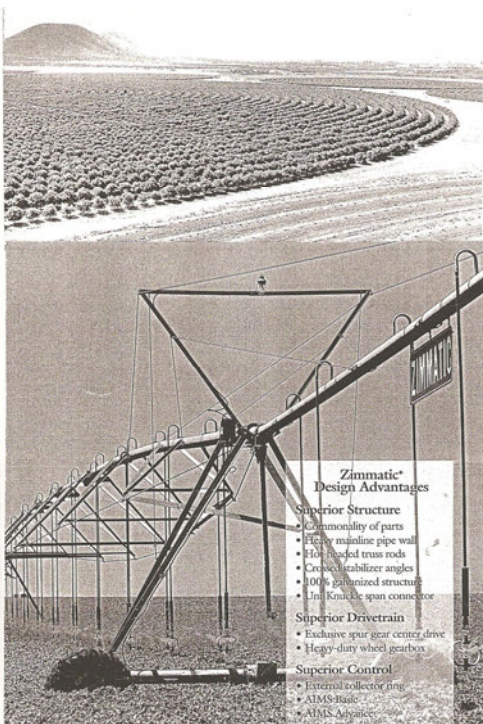
Fig. 29.7. A central pivot irrigation system (a series system of two worm gear transmissions) [Zimmatic]

HW 29.1. [4] Calculate the output torque in a worm gear transmission transmitting power of 9 kW at a speed of 742 rpm. Data: pitch diameter of the worm $d_1 = 80$ mm; tooth count: $z_1 = 2$ (a two start worm); $z_2 = 39$; $m = 8$; the normal pressure angle $\alpha_n = 20°$. The two shafts are supported with 2 roller contact bearings each ($\eta = 0.995$); the coefficient of friction in meshing $\mu = 0.04$. Neglect oil splash losses.

Answer: 1.8 kNm

Glossary

recess only worm gear	przekładnia pracująca tylko w okresie wyzębiania
central pivot irrigation system	obrotowy system irygacyjny

30. Planetary Gear Trains

30.1. Kinematical analysis

I assume that you can calculate the transmission ratio for any given planetary arrangement (the Theory of Mechanisms course, the Polish students). A short summary for our foreign students: let's have a simple one-row epicyclic (planetary) transmission gear train. The tooth count is $z_1 = 40$; $z_2 = 20$, and $z_3 = 80$.
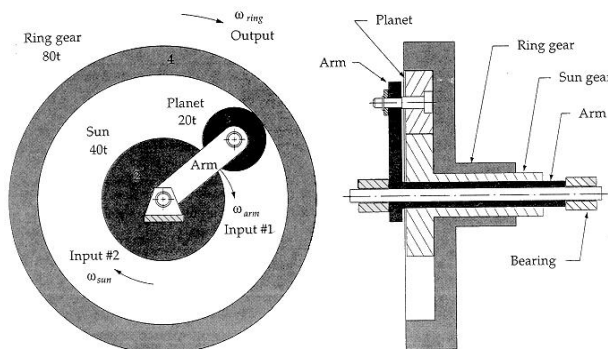
Fig. 30.1 The layout of a simple planetary gear train (▲) [Internet]

At the moment, the mobility of this system is redundant (it is a differential gear). Usually we reduce it by one by making the ring gear stationary. All methods for the calculation of the transmission ratio account for the fact that the motion of the planet gears is a combination of rotation and translation (rotation with respect to an instantaneous centre of rotation). So let's do the first step (the first line in table 30.1): a rotation of the whole transmission by ω_A. The arm has reached its final speed, so let's make it stationary now. With the fixed arm, the transmission becomes a standard, stationary axis transmission. In the second step (the second line in the table), we rotate the ring gear back by $-\omega_A$ (its speed must be equal to zero after summation of the two steps). **The sign shall reflect the sense of meshing!** If it is the same (internal gearing), we keep the same sign. If it is opposite (external gearing), we change also the sign. Finally, the summation of the two rows will give the final speed.

Table 30.1. The table method

Sun = 1	Arm = A	Planet = 2	Ring = 3
ω_A	ω_A	ω_A	ω_A
$\omega_A z_3/z_1$	0	$-\omega_A z_3/z_2$	$-\omega_A$
$\omega_A(1+z_3/z_1)$	ω_A	$\omega_A(1-z_3/z_2)$	0

$$i_{1A} = \frac{\omega_1}{\omega_A} = \frac{\omega_A(1+\frac{z_3}{z_1})}{\omega_A} = 3$$

For proportions given in Fig.25.1, i.e. $z_3/z_1 = 2$, the transmission ratio is by one greater, i.e. 3. If the input is to the sun gear, the arm will rotate three times slower.

If we take power directly from the planet gear (a situation that may happen when the ratio of z_3/z_2 is close to one (a high reduction gear), than needed is a mechanism similar to a universal joint to take power from an off-set shaft.

30.2. Force analysis

Let's assume that the torque applied to the sun gear is equal to one unit ($T_1 = 1$), the length of the sun gear radius is equal to $R_S = 2$ units; $R_P = 1$ unit; $R_R = 4$ units. The tangential force on the sun gear: $F_{12} = T_1 / R_1 = 1/2 = 0.5\,\text{unit}$.

Needed are static equations of equilibrium for the planet gear 2. Mark all external forces acting on this gear in Fig. 15.1. The force F_{12} is directed to the right and its magnitude is equal to 0.5 of a unit. The force F_{32} has the same magnitude as F_{12} and the same sense. To make the balance, the force applied to the arm must be twice as large and of the opposite sense. The output torque is equal to the product of this force and the relevant arm: here 3 units. So the output torque is three times as large as the input. Well, no difference with fixed-axis transmissions. A question is: what amount of torque is necessary to stop the ring gear (this gear in automatic transmission is held stationary by a band brake). A simple product of force F_{32} and the relevant radius (4) yields 2 units.

A general formula is:

$$T_A = -T_1 i_{1A}^3 = -T_1 \frac{\omega_1 - \omega_3}{\omega_A - \omega_3} = -T_1 \frac{\omega_A(1+\frac{z_3}{z_1})}{\omega_A} = -3T_1$$

The torque necessary to stop the annulus gear:

$$T_3 = -T_1 i_{13}^A = -T_1 \frac{\omega_1 - \omega_A}{\omega_3 - \omega_A} = -T_1 \frac{\omega_A + \omega_A \frac{z_3}{z_1} - \omega_A}{-\omega_A} = T_1 \frac{z_3}{z_1} = 1 \cdot \frac{80}{40} = 2\,\text{units}$$

30.3. Power analysis, efficiency

The flow of power in planetary transmission is a complex problem. You must be aware that in some situations the way the power is transmitted in a transmission is beneficial to its overall efficiency. In some layouts, unfortunately, it is disastrous.

Let's start with our transmission and go back to the first table (the transmission ratio). The process expressed by the first line of this table (rotation of the whole gear set) is free of any losses. This part of power is termed in English as the power of coupling. The power associated

with the second row in the table is termed as the power of meshing. This part of the power flow is associated with mechanical losses. In some situations the whole power is split into two parts (or transmission) and only the power of engagement is subject of mechanical losses.

The input power splits into two parts:

$$P_1 = T_1\omega_A + T_1(\omega_1 - \omega_A)\eta_{12}$$

The first term represents the power of coupling (no losses), the second, the power of meshing (subject to mechanical losses). Assume $\eta_{12} = 0.98$ (meshing losses only for the external toothed pair 1 to 2). For our numerical data:

$$P_1 = 1 \cdot 1/3 + 1(1 - 1/3)0.98 = 0.987$$

Power at the ring gear (the two types of power are the same by amount but with the opposite signs). Efficiency in an internal toothed gear $\eta_{23} = 0.99$ (higher than in an externally toothed pair!).

$$P_3 = T_3\omega_A + T_3(\omega_3 - \omega_A)\eta_{23} = 2 \cdot 1/3 + 2(0 - 1/3)0.99 = 0.007$$

The power lost in the first meshing is 0.013 and in the second meshing 0.007, so the overall loss is equal to 0.020, i.e. $\eta = 0.98$. In a fixed axis transmission this efficiency would be 0.99x0.98 = 0.97, so by 1% less.

The general formula for this layout is: $\eta = \dfrac{1 + \dfrac{z_3}{z_1}\eta_{13}}{1 + \dfrac{z_3}{z_1}} = \dfrac{1 + 2 \cdot 0.97}{1 + 2} = 0.98$

The least advantageous situations are in double row planetary units, unfortunately the most widespread, where the effective torque developed on the planet gear is a difference between two opposing torques of significantly greater magnitude.

30.4. Assembly constraints

For the one row planetary gear unit discussed a sufficient condition for successful assembly (in terms of meshing) is that a sum of the number of teeth in both central gears, i.e. in the sun and in the ring gear, is divisible by a number of planets (mostly 3). This condition is met by the transmission shown in Fig. 30.1. Certainly, this condition is met by all transmissions where both the sun gear and ring gear tooth count is divisible by 3.

HW 30.1. Find the speed of the roller L (v_L) if: a) The system is driven by the primary motor. The annulus gear 3 is locked (the worm gear is self locking!), b) The system is driven by the secondary motor (the sun gear 1 is locked with the band brake.) Data: $z_1 = 17$; $z_2 = 35$; $z_3 = 87$. The worm gear transmission ratio: $u = 102$. Determine the sense (CW, CCW?) of the motor rotation when lifting the weight (as viewed from the clutch) for both cases.
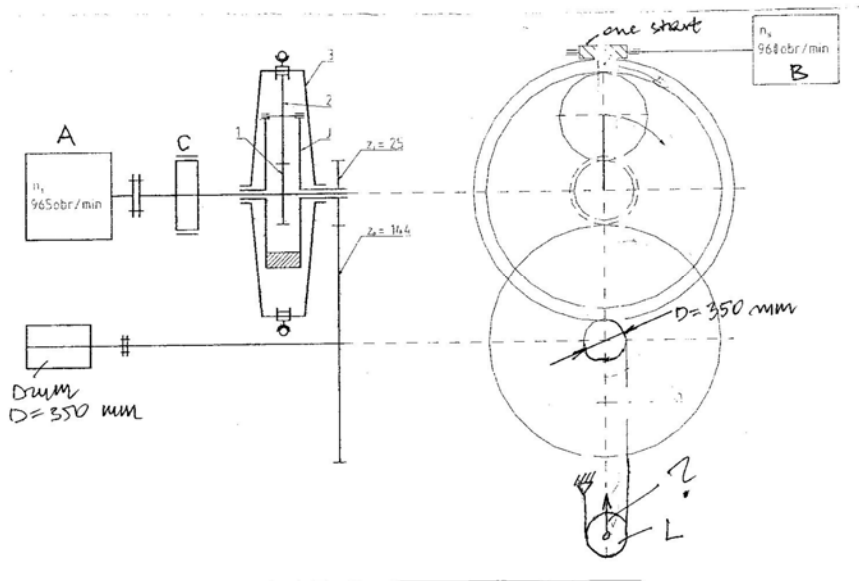
Answer: a) $v = 0,25$ m/s; b) $v = 0.0125$ m/s

Glossary

epicyclic gear	przekładnia planetarna
instantaneous centre of rotation	chwilowy środek obrotu
power of coupling	moc sprzężenia
power of meshing	moc zazębienia
redundant	nadmiarowy
ring/annulus gear	koło pierścieniowe
stationary axis transm.	przekładnia o osiach stałych
sun gear	koło słoneczne
tooth count	liczba zębów

Thank you for registering to this course. I wish you luck in the final examination!

References (incl. illustration material sources)

[1] DIETRYCH J., KOCAŃDA S. KOREWA W.: Podstawy Konstrukcji Maszyn cz. 1, WNT Warszawa 1971

[2] DIETRYCH J., KOREWA W., KORNBERGER Z.: Podstawy Konstrukcji Maszyn, cz. 3, WNT, Warszawa 1971

[3] DZIAMA A.: Metodyka Konstruowania Maszyn, PWN, Warszawa 1985

[4] DZIAMA A.: Podstawy Konstrukcji Maszyn – Zbiór Zadań, Wyd. Politechniki Wrocławskiej, Wrocław, 1973

[5] DZIAMA A., MICHNIEWICZ M., NIEDŹWIEDZKI A.: Przekładnie Zębate, PWN, Warszawa 1995

[6] GIESECKE E.E., MITCHEL A. et all.: Technical Drawing, Macmillan Publishing, New York, 13th edition, 2003

[7] IVANOV M.N., IVANOV B.H.: Detali Maszyn, Izd. Vysszaja Szkola, Moscou, 1975

[8] JAŚKIEWICZ Z.: Mechaniczne Napędy Samochodów. Skrzynki przekładniowe, WKiŁ, Warszawa, 1967

[9] JAŚKIEWICZ Z.: Mosty napędowe, WNT, Warszawa 1977

[10] KOREWA W., ZYGMUNT K.: Podstawy Konstrukcji Maszyn, cz. 2 WNT Warszawa 1965

[11] KORNBERGER Z.: Przekładnie Ślimakowe, WNT, Warszawa 1971

[12] KURMAZ L. W., KURMAZ O.L.: Projektowanie węzłów i części maszyn, Wyd. Politechniki Świętokrzyskiej, Kielce 2004

[13] MOTT R.L,: Machine Element in Mechanical Design, Prentice Hall, 2003

[14] OSIŃSKI Z., pr. zbiorowa: Podstawy Konstrukcji Maszyn, PWN, Warszawa 1999

[15] OCHĘDUSZKO K.: Koła Zębate, WNT, Warszawa 1965

[16] RYDZANICZ I.: Zapis Konstrukcji, Zbiór zadań, WNT, Warszawa, 2004

[17] SHIGLEY E. MISCHKE C.R.: Standard Handbook of Machine Design, Mc Graw-Hill Book Company, 1996

Illustrations pasted from the Internet (jpg) are referenced directly in the relevant captions. These are:

Fig. 1.5. Jiaxin Datong Manufacturing Co. Ltd	Fig. 16.2. Actes Rencontres Harmoniques, Lausanne
Fig. 2.1. Aircraaft Accident Report, Aloha Flight 243	Fig. 16.3. Engineering Works Klew
Fig. 3.9. Nook Industries	Fig. 16.4. Wikipedia (source unkonown)
Fig. 6.1. corusconstruction.com	Fig. 18.1. FAO Corporated Depository
Fig. 6.2. Roymech	Fig. 18.6. The Automation Blog
Fig. 7.6. SKF Kugellager-Vertriebsgesellschaft m.b.H.	Fig. 19.2. Yi Zhang, Finger S.: Intr. to Mechanisms
Fig. 10.2. Stattford Manufacturing Company	Fig. 19.3. United Tool Company
Fig. 10.3 Brance-Kraevy Co	Fig. 19.4. Doug Wright Company
Fig. 10.4. Royersford	Fig. 19.5. Daritec
Fig. 10.5. Ruland Mfg Co.	Fig. 20.2. eassistance website
Fig. 10.6. Rexnord Industries	Fig. 23.1. Suva Precision
Fig. 10.7. Engine Mechanics	Fig. 24.1. Machine Lubrication
Fig. 10.9. Wikipedia	Fig. 24.3. Cam Design
Fig. 10.10. Hangzhou Ever-Power Transmissions Ltd	Fig. 26.3. Internet (source unknown)
Fig. 10.12. Swastica Industries	Fig. 26.6. The Gleason Works
Fig. 10.11. Biby Transmissions	Fig. 27.3. Shyin Precision Manufacturing
Fig. 11.1. Wallace	Fig. 27.4. Zakgear Technology
Fig. 11.7. The Hillard Corporation	Fig. 29.5. Flender GmbH Bocholt
Fig. 11.8. Cross + Morse Power Transmission Solution	Fig. 29.7. Zimmatic leaflet
Fig. 11.10. Hangzhou Ever-Power Transmissions Ltd	Fig. 30.1. Internet (source unknown)
Fig. 13.5. Roymech	
Fig. 14.3. BHR website	

Appendix 1: Fatigue diagrams [1]
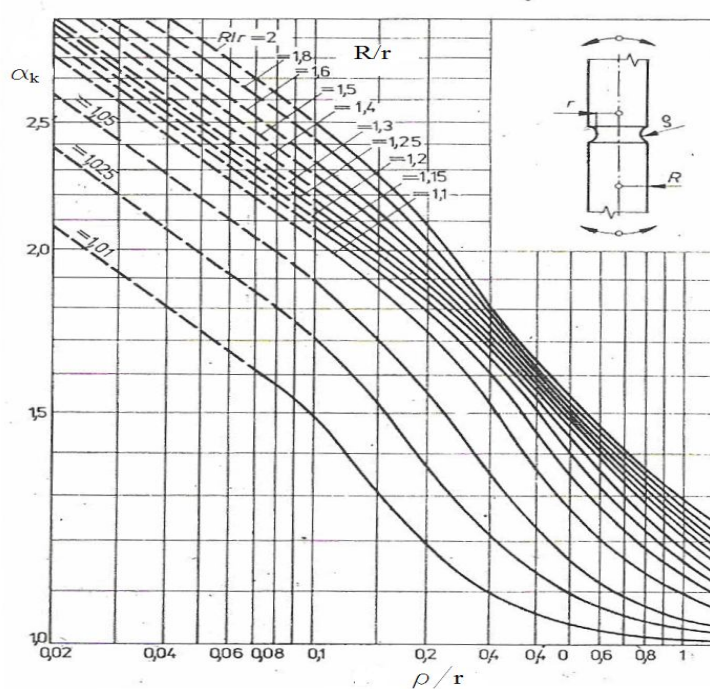
Fig. A1.1. Theoretical stress concentration factor α_k (grooved round bar in bending)
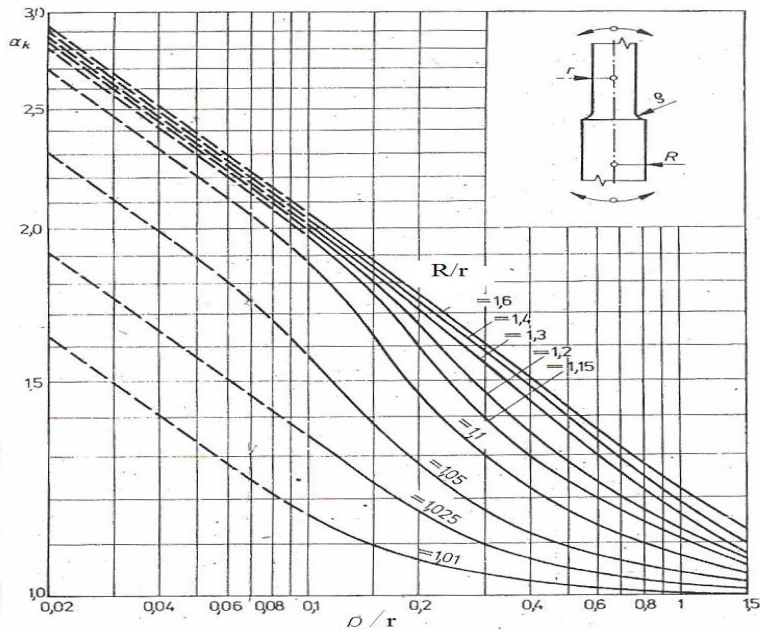
Fig. A1.2. Theoretical stress concentration factor α_k (shoulder fillet in bending)
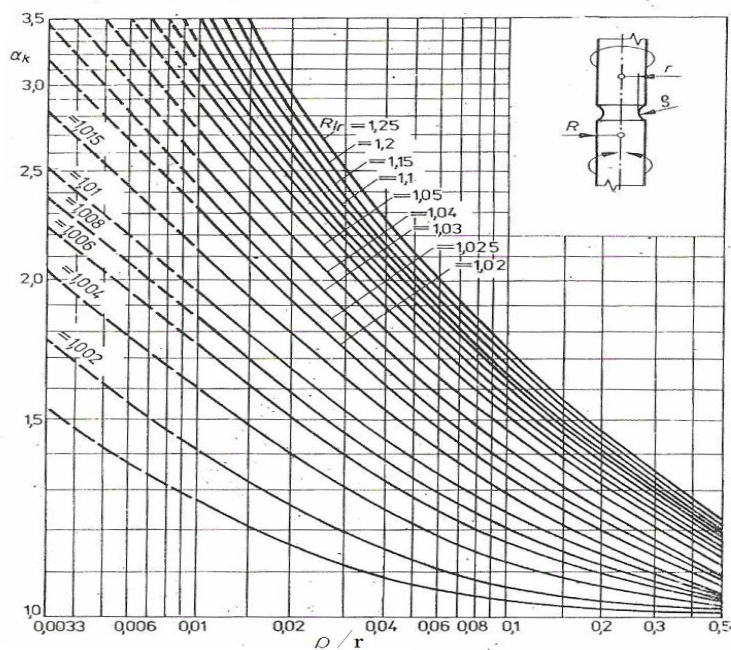
Fig. A1.3. Theoretical stress concentration factor α_k (grooved round bar in torsion)
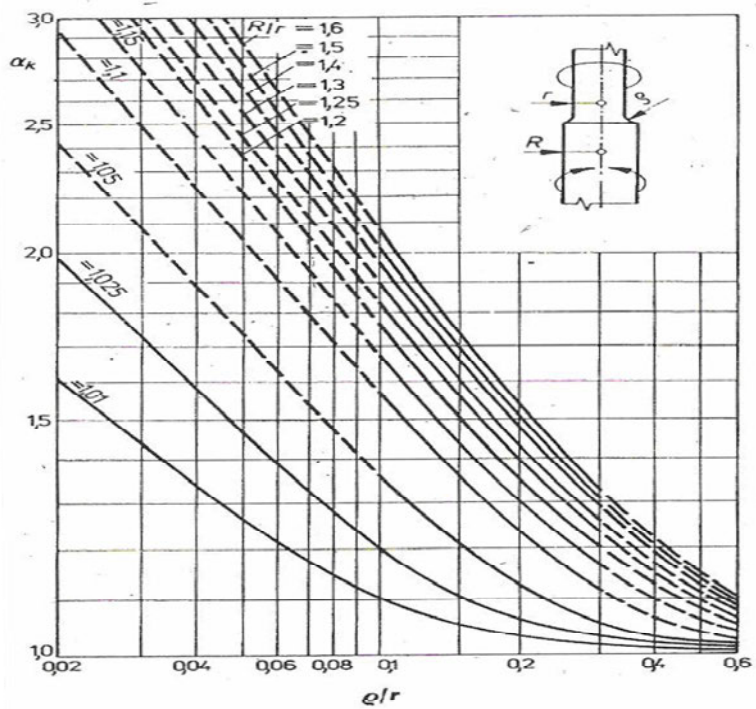
Fig. A1.4. Theoretical stress concentration factor α_k (shoulder fillet in torsion)
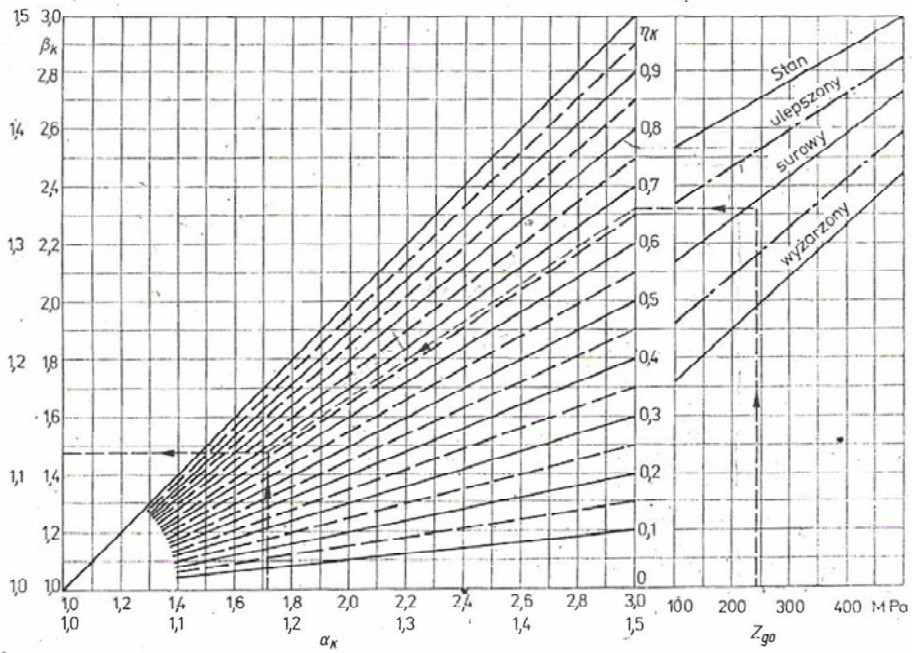
Fig. A1.5. The sensitivity factor (index) η_k and actual stress concentration factor β_k versus the theoretical stress concentration factor α_k. Legend: stan ulepszony = quenched and tempered; surowy = raw material; wyżarzony = annealed
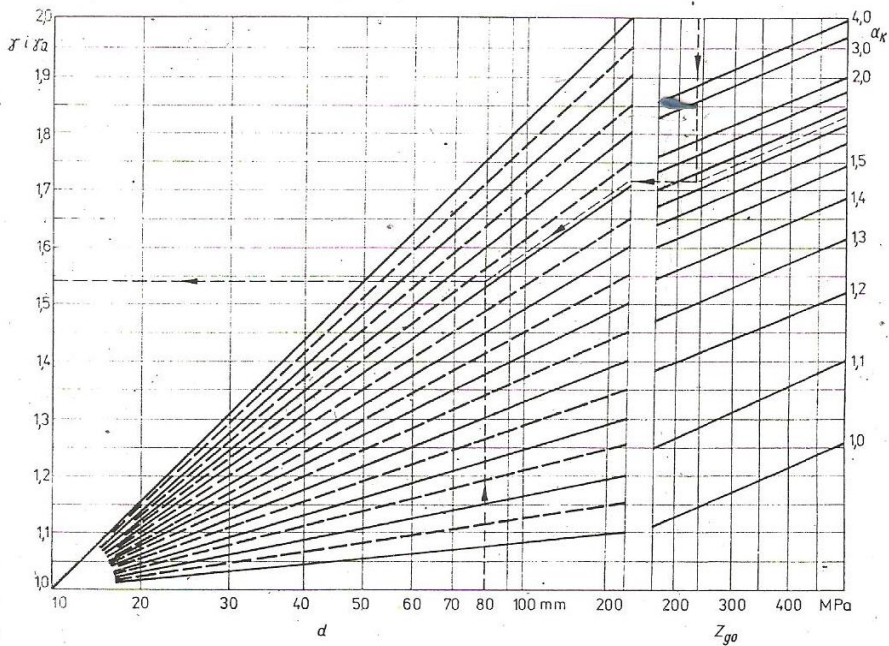
Fig. A1.6. The size factor (illustration for an item made of material with Z_{go} = 240 MPa; α_k = 1.72; d = 80 mm

Fig. A 1.7. Type of machining vs. surface finish factor. Legend: 1 = ground; 2 = fine turning; 3 = course turning; 4 (as depicted); 5 = as rolled; 6 = etched with brine
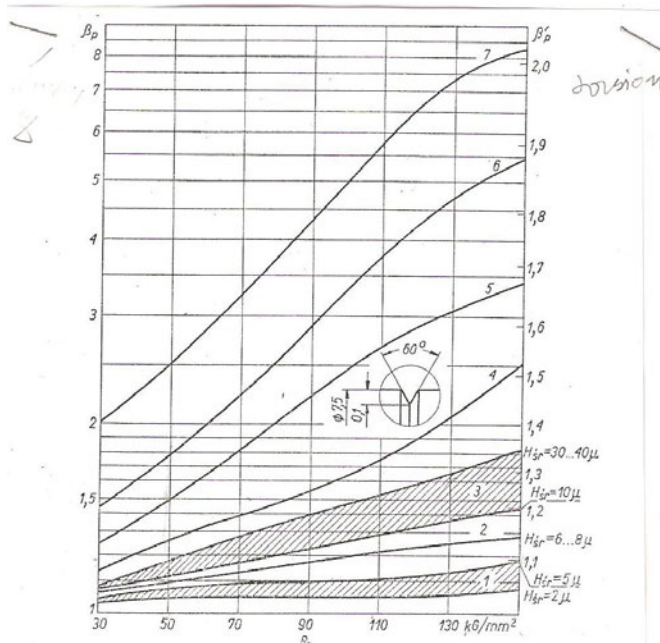
Appendix 2: Fits and tolerances (excerpts [PN-EN 20286-2:1996])

Table A2.1. Base tolerances for shafts and holes

Tablica 3. Tolerancje podstawowe wałków i otworów

D mm		Klasy dokładności																
		01	0	1	2	3	4	5	6	7	8	9	10	11	12	13	14	15	16
po-nad	do	IT01	IT0	IT1	IT2	IT3	IT4	IT5	IT6	IT7	IT8	IT9	IT10	IT11	IT12	IT13	IT14	IT15	IT16
		Wartości w mikronach																
0	3	0,3	0,5	0,8	1,2	2,0	3	4	6	10	14	25	40	60	100	140	250	400	600
3	6	0,4	0,6	1,0	1,5	2,5	4	5	8	12	18	30	48	75	120	180	300	480	750
6	10	0,4	0,6	1,0	1,5	2,5	4	6	9	15	22	36	58	90	150	220	360	580	900
10	18	0,5	0,8	1,2	2,0	3,0	5	8	11	18	27	43	70	110	180	270	430	700	1100
18	30	0,6	1,0	1,5	2,5	4,0	6	9	13	21	33	52	84	130	210	330	520	840	1300
30	50	0,6	1,0	1,5	2,5	4,0	7	11	16	25	39	62	100	160	250	390	620	1000	1600
50	80	0,8	1,2	2,0	3,0	5,0	8	13	19	30	46	74	120	190	300	460	740	1200	1900
80	120	1,0	1,5	2,5	4,0	6,0	10	15	22	35	54	87	140	220	350	540	870	1400	2200
120	180	1,2	2,0	3,5	5,0	8,0	12	18	25	40	63	100	160	250	400	630	1000	1600	2500
180	250	2,0	3,0	4,5	7,0	10	14	20	29	46	72	115	185	290	460	720	1150	1850	2900
250	315	2,5	4,0	6,0	8,0	12	16	23	32	52	81	130	210	320	520	810	1300	2100	3200
315	400	3,0	5,0	7,0	9,0	13	18	25	36	57	89	140	230	360	570	890	1400	2300	3600
400	500	4,0	6,0	8,0	10,0	15	20	27	40	63	97	155	250	400	630	970	1550	2500	4000

Legend: ponad =over; do = up to (including); klasy dokładności = accuracy class; wartości w mikronach = values in micrometers

Table A2.2. Base deviations for shafts (upper deviations: *es)*

Tablica 5. Odchyłki podstawowe wałków

D mm		Górne odchyłki (G_w) wałków ruchowych									
		a	b	c	cd	d	e	ef	f	fg	g	h
ponad	do	dla wszystkich klas dokładności									
		Wartości w mikronach									
0	3	—270	—140	— 60	—34	— 20	— 14	—10	— 6	— 4	— 2	0
3	6	—270	—140	— 70	—46	— 30	— 20	—14	—10	— 6	— 4	0
6	10	—280	—150	— 80	—56	— 40	— 25	—18	—13	— 8	— 5	0
10	14	—290	—150	— 95		— 50	— 32		—16		— 6	0
14	18	—290	—150	— 95		— 50	— 32		—16		— 6	0
18	24	—300	—160	—110		— 65	— 40		—20		— 7	0
24	30	—300	—160	—110		— 65	— 40		—20		— 7	0
30	40	—310	—170	—120		— 80	— 50		—25		— 9	0
40	50	—320	—180	—130		— 80	— 50		—25		— 9	0
50	65	—340	—190	—140		—100	— 60		—30		—10	0
65	80	—360	—200	—150		—100	— 60		—30		—10	0
80	100	—380	—220	—170		—120	— 72		—36		—12	0
100	120	—410	—240	—180		—120	— 72		—36		—12	0
120	140	—460	—260	—200		—145	— 85		—43		—14	0
140	160	—520	—280	—210		—145	— 85		—43		—14	0
160	180	—580	—310	—230		—145	— 85		—43		—14	0
180	200	—660	—340	—240		—170	—100		—50		—15	0
200	225	—740	—380	—260		—170	—100		—50		—15	0
225	250	—820	—420	—280		—170	—100		—50		—15	0
250	280	—920	—480	—300		—190	—110		—56		—17	0
280	315	—1050	—540	—330		—190	—110		—56		—17	0
315	355	—1200	—600	—360		—210	—125		—62		—18	0
355	400	—1350	—680	—400		—210	—125		—62		—18	0
400	450	—1500	—760	—440		—230	—135		—68		—20	0
450	500	—1650	—840	—480		—230	—135		—68		—20	0
D mm		a	b	c	cd	d	e	ef	f	fg	g	h

Legend: górne odchyłki wałków ruchowych = upper deviations of running shafts; dla wszystkich klas = valid for all accuracy classes; wartości w mikronach = values in micrometers

Table A2.2. cont. Base deviations for shafts (lower deviationsfor *ei*)

cd. tabl. 5

D mm		Dolne odchyłki (F_w) wałków mieszanych i wtłaczanych							
		js	j			k		m	n	p
ponad	do	dla wszystkich klas dokładności	dla klas dokładności					dla wszystkich klas dokładności		
			5 i 6	7	8	4 do 7	pozostałych			
			Wartości w mikronach							
0	3		— 2	— 4	—6	0	0	+ 2	+ 4	+ 6
3	6		— 2	— 4		+1	0	+ 4	+ 8	+12
6	10		— 2	— 5		+1	0	+ 6	+10	+15
10	14		— 3	— 6		+1	0	+ 7	+12	+18
14	18		— 3	— 6		+1	0	+ 7	+12	+18
18	24		— 4	— 8		+2	0	+ 8	+15	+22
24	30		— 4	— 8		+2	0	+ 8	+15	+22
30	40		— 5	—10		+2	0	+ 9	+17	+26
40	50		— 5	—10		+2	0	+ 9	+17	+26
50	65		— 7	—12		+2	0	+11	+20	+32
65	80		— 7	—12		+2	0	+11	+20	+32
80	100	—0,5 IT	— 9	—15		+3	0	+13	+23	+37
100	120		— 9	—15		+3	0	+13	+23	+37
120	140		—11	—18		+3	0	+15	+27	+43
140	160		—11	—18		+3	0	+15	+27	+43
160	180		—11	—18		+3	0	+15	+27	+43
180	200		—13	—21		+4	0	+17	+31	+50
200	225		—13	—21		+4	0	+17	+31	+50
225	250		—13	—21		+4	0	+17	+31	+50
250	280		—16	—26		+4	0	+20	+34	+56
280	315		—16	—26		+4	0	+20	+34	+56
315	355		—18	—28		+4	0	+21	+37	+62
355	400		—18	—28		+4	0	+21	+37	+62
400	450		—20	—32		+5	0	+23	+40	+68
450	500		—20	—32		+5	0	+23	+40	+68
D mm		js	j			k		m	n	p

Legend: dolne odchyłki wałków ruchowych = lower deviations for shafts in transition and press fits; dla wszystkich klas = valid for all accuracy classes; wartości w mikronach = values in micrometers

Table A2.2. cont. Base deviations for shafts (lower deviations for *ei*)

cd. tabl. 5

D mm		Dolne odchyłki (F_w) wałków mieszanych i wtłaczanych										
		'r	s	t	u	v	x	y	z	za	zb	zc
ponad	do	dla wszystkich klas dokładności										
		Wartości w mikronach										
0	3	+ 10	+ 14		+ 18		+ 20		+ 26	+ 32	+ 40	+ 60
3	6	+ 15	+ 19		+ 23		+ 28		+ 35	+ 42	+ 50	+ 80
6	10	+ 19	+ 23		+ 28		+ 34		+ 42	+ 52	+ 67	+ 97
10	14	+ 23	+ 28		+ 33		+ 40		+ 50	+ 64	+ 90	+ 130
14	18	+ 23	+ 28		+ 33	+ 39	+ 45		+ 60	+ 77	+ 108	+ 150
18	24	+ 28	+ 35		+ 41	+ 47	+ 54	+ 63	+ 73	+ 98	+ 136	+ 188
24	30	+ 28	+ 35	+ 41	+ 48	+ 55	+ 64	+ 75	+ 88	+ 118	+ 160	+ 218
30	40	+ 34	+ 43	+ 48	+ 60	+ 68	+ 80	+ 94	+ 112	+ 148	+ 200	+ 274
40	50	+ 34	+ 43	+ 54	+ 70	+ 81	+ 97	+ 114	+ 136	+ 180	+ 242	+ 325
50	65	+ 41	+ 53	+ 66	+ 87	+102	+122	+ 144	+ 172	+ 226	+ 300	+ 405
65	80	+ 43	+ 59	+ 75	+102	+120	+146	+ 174	+ 210	+ 274	+ 360	+ 480
80	100	+ 51	+ 71	+ 91	+124	+146	+178	+ 214	+ 258	+ 335	+ 445	+ 585
100	120	+ 54	+ 79	+104	+144	+172	+210	+ 254	+ 310	+ 400	+ 525	+ 690
120	140	+ 63	+ 92	+122	+170	+202	+248	+ 300	+ 365	+ 470	+ 620	+ 800
140	160	+ 65	+100	+134	+190	+228	+280	+ 340	+ 415	+ 535	+ 700	+ 900
160	180	+ 68	+108	+146	+210	+252	+310	+ 380	+ 465	+ 600	+ 780	+1000
180	200	+ 77	+122	+166	+236	+284	+350	+ 425	+ 520	+ 670	+ 880	+1150
200	225	+ 80	+130	+180	+258	+310	+385	+ 470	+ 575	+ 740	+ 900	+1250
225	250	+ 84	+140	+196	+284	+340	+425	+ 520	+ 640	+ 820	+1050	+1350
250	280	+ 94	+158	+218	+315	+385	+475	+ 580	+ 710	+ 920	+1200	+1550
280	315	+ 98	+170	+240	+350	+425	+525	+ 650	+ 790	+1000	+1300	+1700
315	355	+108	+190	+268	+390	+475	+590	+ 730	+ 900	+1150	+1500	+1900
355	400	+114	+208	+294	+435	+530	+660	+ 820	+1000	+1300	+1650	+2100
400	450	+126	+232	+330	+490	+595	+740	+ 920	+1100	+1450	+1850	+2400
450	500	+132	+252	+360	+540	+660	+820	+1000	+1250	+1600	+2100	+2600
D mm		r	s	t	u	v	x	y	z	za	zb	zc

Legend: dolne odchyłki wałków ruchowych = lower deviations for shafts in transition and press fits; dla wszystkich klas = valid for all accuracy classes; wartości w mikronach = values in micrometers

Table A2.3. Base deviations for holes (lower deviations *EI*)

Tablica 6. Odchyłki podstawowe otworów

D mm		Dolne odchyłki (F_o) otworów ruchowych										
		A	B	C	CD	D	E	EF	F	FG	G	H
ponad	do	dla wszystkich klas dokładności										
		Wartości w mikronach										
0	3	+ 270	+ 140	+ 60	+34	+ 20	+ 14	+10	+ 6	+4	+ 2	0
3	6	+ 270	+ 140	+ 70	+46	+ 30	+ 20	+14	+10	+6	+ 4	0
6	10	+ 280	+ 150	+ 80	+56	+ 40	+ 25	+18	+13	+8	+ 5	0
10	14	+ 290	+ 150	+ 95		+ 50	+ 32		+16		+ 6	0
14	18	+ 290	+ 150	+ 95		+ 50	+ 32		+16		+ 6	0
18	24	+ 300	+ 160	+110		+ 65	+ 40		+20		+ 7	0
24	30	+ 300	+ 160	+110		+ 65	+ 40		+20		+ 7	0
30	40	+ 310	+ 170	+120		+ 80	+ 50		+25		+ 9	0
40	50	+ 320	+ 180	+130		+ 80	+ 50		+25		+ 9	0
50	65	+ 340	+ 190	+140		+100	+ 60		+30		+10	0
65	80	+ 360	+ 200	+150		+100	+ 60		+30		+10	0
80	100	+ 380	+ 220	+170		+120	+ 72		+36		+12	0
100	120	+ 410	+ 240	+180		+120	+ 72		+36		+12	0
120	140	+ 460	+ 260	+200		+145	+ 85		+43		+14	0
140	160	+ 520	+ 280	+210		+145	+. 85		+43		+14	0
160	180	+ 580	+ 310	+230		+145	+ 85		+43		+14	0
180	200	+ 660	+ 340	+240		+170	+100		+50		+15	0
200	225	+ 740	+ 380	+260		+170	+100		+50		+15	0
225	250	+ 820	+ 420	+280		+170	+100		+50		+15	0
250	280	+ 920	+ 480	+300		+190	+110		+56		+17	0
280	315	+1050	+ 540	+330		+190	+110		+56		+17	0
315	355	+1200	+ 600	+360		+210	÷125		+62		+18	0
355	400	+1350	+ 680	+400		+210	+125		+62		+18	0
400	450	+1500	+ 760	+440		+230	+135		+68		+20	0
450	500	+1650	+ 840	+480		+230	+135		+68		+20	0
D mm		A	B	C	CD	D	E	EF	F	FG	G	H

Legend: dolne odchyłki otworów ruchowych = lower deviations for holes in running fits; dla wszystkich klas = valid for all accuracy classes; wartości w mikronach = values in micrometers

Table A2.3. cont. Base deviations for holes (upper deviations *ES*)

D mm		JS	J			K		M	
		dla wszystkich klas dokładności	dla klas dokładności						
ponad	do		6	7	8	do 8	pow. 8	do 8	pow. 8
			Wartości w mikronach						
0	3		+ 2	+ 4	+ 6	0	0	— 2	— 2
3	6		+ 5	+ 6	+10	$-1+\Delta_n$	0	$-4+\Delta_n$	— 4
6	10		+ 5	+ 8	+12	$-1+\Delta_n$	0	$-6+\Delta_n$	— 6
10	14		+ 6	+10	+15	$-1+\Delta_n$	0	$-7+\Delta_n$	— 7
14	18		+ 6	+10	+15	$-1+\Delta_n$	0	$-7+\Delta_n$	— 7
18	24		+ 8	+12	+20	$-2+\Delta_n$	0	$-8+\Delta_n$	— 8
24	30		+ 8	+12	+20	$-2+\Delta_n$	0	$-8+\Delta_n$	— 8
30	40		+10	+14	+24	$-2+\Delta_n$	0	$-9+\Delta_n$	— 9
40	50	+ 0,5 IT	+10	+14	+24	$-2+\Delta_n$	0	$-9+\Delta_n$	— 9
50	65		+13	+18	+28	$-2+\Delta_n$	0	$-11+\Delta_n$	—11
65	80		+13	+18	+28	$-2+\Delta_n$	0	$-11+\Delta_n$	—11
80	100		+16	+22	+34	$-3+\Delta_n$	0	$-13+\Delta_n$	—13
100	120		+16	+22	+34	$-3+\Delta_n$	0	$-13+\Delta_n$	—13
120	140		+18	+26	+41	$-3+\Delta_n$	0	$-15+\Delta_n$	—15
140	160		+18	+26	+41	$-3+\Delta_n$	0	$-15+\Delta_n$	—15
160	180		+18	+26	+41	$-3+\Delta_n$	0	$-15+\Delta_n$	—15
180	200		+22	+30	+47	$-4+\Delta_n$	0	$-17+\Delta_n$	—17
200	225		+22	+30	+47	$-4+\Delta_n$	0	$-17+\Delta_n$	—17
225	250		+22	+30	+47	$-4+\Delta_n$	0	$-17+\Delta_n$	—17
250	280		+25	+36	+55	$-4+\Delta_n$	0	$-20+\Delta_n$*	—20
280	315		+25	+36	+55	$-4+\Delta_n$	0	$-20+\Delta_n$*	—20
315	355		+29	+39	+60	$-4+\Delta_n$	0	$-21+\Delta_n$	—21
355	400		+29	+39	+60	$-4+\Delta_n$	0	$-21+\Delta_n$	—21
400	450		+33	+43	+66	$-5+\Delta_n$	0	$-23+\Delta_n$	—23
450	500		+33	+43	+66	$-5+\Delta_n$	0	$-23+\Delta_n$	—23
D mm		JS	J			K		M	

Legend: górne odchyłki otworów mieszanych i wtłączanych = upper deviations for holes in transition and press fits; dla wszystkich klas = valid for all accuracy classes; wartości w mikronach = values in micrometers

Table A2.3. cont. Base deviations for holes (upper deviations *ES*)

D mm		Górne odchyłki (G_o) otworów mieszanych i wtłaczanych								
ponad	do	N		P do ZC	P	R	S	T	U	V	X
		do 8	pow. 8	do 7	pow. 7*						
		dla klas dokładności — Wartości w mikronach									
0	3	— 4	— 4		— 6	— 10	— 14		— 18		— 20
3	6	— 8+Δ_n	0		—12	— 15	— 19		— 23		— 28
6	10	—10+Δ_n	0		—15	— 19	— 23		— 28		— 34
10	14	—12+Δ_n	0		—18	— 23	— 28		— 33		— 40
14	18	—12+Δ_n	0		—18	— 23	— 28		— 33	— 39	— 45
18	24	—15+Δ_n	0		—22	— 28	— 35		— 41	— 47	— 54
24	30	—15+Δ_n	0		—22	— 28	— 35	— 41	— 48	— 55	— 64
30	40	—17+Δ_n	0		—26	— 34	— 43	— 48	— 60	— 68	— 80
40	50	—17+Δ_n	0		—26	— 34	— 43	— 54	— 70	— 81	— 97
50	65	—20+Δ_n	0		—32	— 41	— 53	— 66	— 87	—102	—122
65	80	—20+Δ_n	0		—32	— 43	— 59	— 75	—102	—120	—146
80	100	—23+Δ_n	0		—37	— 51	— 71	— 91	—124	—146	—178
100	120	—23+Δ_n	0		—37	— 54	— 79	—104	—144	—172	—210
120	140	—27+Δ_n	0		—43	— 63	— 92	—122	—170	—202	—248
140	160	—27+Δ_n	0		—43	— 65	—100	—134	—190	—228	—280
160	180	—27+Δ_n	0		—43	— 68	—108	—146	—210	—252	—310
180	200	—31+Δ_n	0		—50	— 77	—122	—166	—236	—284	—350
200	225	—31+Δ_n	0		—50	— 80	—130	—180	—258	—310	—385
225	250	—31+Δ_n	0		—50	— 84	—140	—196	—284	—340	—425
250	280	—34+Δ_n	0		—56	— 94	—158	—218	—315	—385	—475
280	315	—34+Δ_n	0		—56	— 98	—170	—240	—350	—425	—525
315	355	—37+Δ_n	0		—62	—108	—190	—268	—390	—475	—590
355	400	—37+Δ_n	0		—62	—114	—208	—294	—435	—530	—660
400	450	—40+Δ_n	0		—68	—126	—232	—330	—490	—595	—740
450	500	—40+Δ_n	0		—68	—132	—252	—360	—540	—660	—820
D mm		N		P do ZC	P	R	S	T	U	V	X

(P do ZC column, rotated text spanning all rows: Odchyłka jest taka sama jak dla klas dokładności większych od siódmej, lecz powiększona algebraicznie o wartość liczbową Δ_n)

Legend: górne odchyłki otworów mieszanych i wtłaczanych = upper deviations for holes in transition and press fits; dla wszystkich klas = valid for all accuracy classes; wartości w mikronach = values in micrometers

Appendix 3: V-thread data (PN-ISO 2904 A:1966)
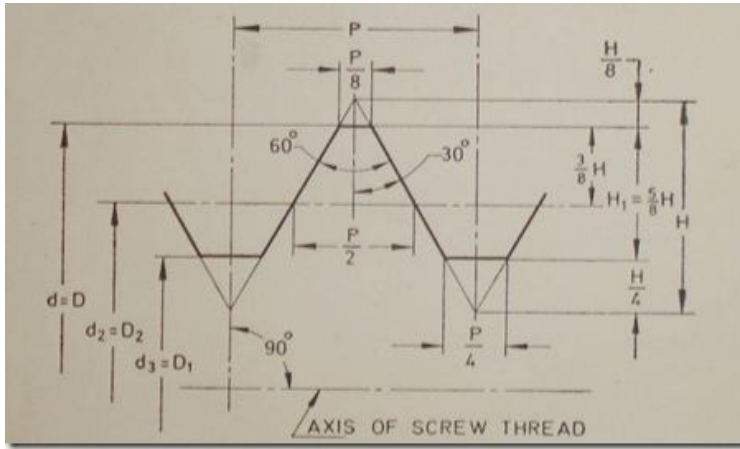
Fig. A3.1. V-thread dimensions

Table A.3.1.V-thread data

d	p	$D_2=d_2$	$D_1=d_1$	d_3
8	1.25	7.19	6.65	6.47
	1.0	7.35	6.92	6.77
	0.75	7.51	7.19	7.08
10	1.5	9.03	8.38	8.16
	1.25	9.19	8.65	8.47
	1.0	9.35	8.92	8.77
	0.75	9.51	9.19	9.08
12	1.75	10.86	10.11	9.85
	1.5	11.03	10.38	10.16
	1.25	11.19	10.65	10.47
	1.0	11.35	10.92	10.77
16	2	14.7	13.84	13.55
	1.5	15.03	14.38	14.16
	1.0	15.35	14.92	14.73
20	2.5	18.38	17.29	16.93
	2	17.7	17.84	17.55
	1.5	19.03	18.38	18.16
	1	19.35	18.92	18.77

Appendix 4: Deep Groove Ball Bearings [12]
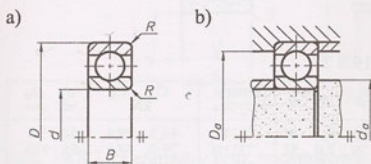
Rys. 19.8.1. a) podstawowe wymiary łożyska;
b) obudowa łożyska

Tabl. 19.8.1. Parametry oraz podstawowe wymiary
łożysk kulkowych zwykłych, mm

d	D	B	R	Oznacz. łożyska	C (kN)	C_o (kN)	d_a min	D_a max
20	32	7	0,3	61804	2,8	1,6	22	30
	42	8	0,3	16004 *	7,0	3,4	22	40
	42	12	0,6	6004 *	9,3	4,4	22	40
	47	14	1,0	6204 *	12,7	6,1	25	42
	52	15	1,1	6304 *	16,3	7,8	26	45
	72	19	1,1	6404	30,5	16,0	27	63
25	37	7	0,3	61805	3,4	2,8	27	35
	47	8	0,3	16005	7,2	4,6	27	43
	47	12	0,6	6005 *	11,0	5,5	27	43
	52	15	1,0	6205 *	14,0	6,9	30	47
	52	18	1,0	62205 *	14,0	6,9	30	47
	62	17	1,1	6305 *	22,4	11,0	31	55
	80	21	1,5	6405 *	35,9	19,0	34	70
30	42	7	0,3	61806	4,1	3,3	32	40
	55	9	0,3	16006 *	11,2	6,2	32	53
	55	13	1,0	6006 *	13,3	6,8	32	53
	62	16	1,0	6206 *	19,5	10,0	35	57
	72	19	1,1	6306 *	28,5	14,5	36	65
	90	23	1,5	6406 *	43,3	24,0	39	80
35	47	7	0,3	61807	4,3	3,6	37	45
	62	9	0,3	16007 *	12,3	7,2	37	60
	62	14	1,0	6007 *	15,9	8,5	37	60
	72	17	1,1	6207 *	25,5	13,7	42	65
	80	21	1,5	6307 *	33,2	18,0	42	71
	100	25	1,5	6407 *	55,0	30,0	44	90
40	52	7	0,3	61808	4,6	4,2	42	50
	68	9	0,3	16008	13,2	9,0	42	66
	68	15	1,0	6008 *	16,8	9,3	42	66
	80	18	1,1	6208 *	30,0	16,0	47	73
	90	23	1,5	6308 *	41,5	22,0	47	81
	110	27	2,0	6408 *	63,0	35,0	50	97
45	58	7	0,3	61809	6,0	4,3	47	56
	75	10	0,6	16009 *	15,6	10,8	49	71
	75	16	1,0	6009 *	21,2	12,2	49	71
	85	19	1,1	6209 *	33,2	17,8	52	73
	100	25	1,5	6309 *	53,0	30,0	52	81
	120	29	2,0	6409 *	76,2	45,0	55	97
50	65	7	0,3	61810	6,3	4,7	52	63
	80	10	0,6	16010	16,2	10,8	54	76
	80	16	1,0	6010 *	21,7	13,2	54	75
	90	20	1,1	6210 *	36,3	19,8	57	83
	110	29	2,0	6310 *	62,0	35,0	60	100
	130	31	2,1	6410 *	87,0	52,0	63	116
55	72	9	0,3	61811	8,4	6,2	57	70
	90	11	0,6	16011 *	19,5	13,5	59	86
	90	18	1,1	6011 *	28,0	17,0	59	86

Cd. tabl. 19.8.1

d	D	B	R	Oznacz. łożyska	C (kN)	C_o (kN)	d_a min	D_a max
55	100	21	1,5	6211 *	43,3	25,0	62	91
	120	29	2,0	6311 *	73,5	41,0	65	110
	140	33	2,1	6411 *	99,5	62,0	68	126
60	78	10	0,3	61812	9,0	6,5	62	76
	95	11	0,6	16012	20,0	14,0	64	91
	95	18	1,1	6012 *	29,6	18,2	64	91
	110	22	1,5	6212 *	48,5	29,0	67	101
	130	31	2,1	6312 *	81,5	46,0	72	118
	150	35	2,1	6412 *	109	69,5	73	136
65	85	10	0,6	61813	11,7	9,1	69	81
	100	11	0,6	16013	21,2	16,6	69	96
	100	18	1,1	6013 *	30,6	19,6	69	96
	120	23	1,5	6213 *	56,9	34,8	72	111
	140	33	2,1	6313 *	92,5	55,0	76	128
	160	37	2,1	6413 *	119	78,0	78	146
70	90	10	0,6	61814	12,2	10,0	74	86
	110	13	0,6	16014	28,0	25,0	74	116
	110	20	1,1	6014 *	38,0	24,5	74	106
	125	24	1,5	6214 *	62,0	37,2	77	116
	150	35	2,1	6314 *	104	61,0	81	138
	180	42	3,0	6414 *	143	100	85	164
75	95	10	0,6	61815	12,5	10,8	79	91
	115	13	0,6	16015	28,6	27,0	79	121
	115	20	1,1	6015 *	39,8	28,5	79	111
	130	25	1,5	6215 *	66,0	41,0	82	121
	160	37	2,1	6315 *	112	72,0	86	148
	190	45	3,0	6415	153	112	90	174
80	100	10	0,6	61816	12,5	10,8	84	96
	125	14	0,6	16016	32,5	31,0	84	121
	125	22	1,1	6016 *	47,5	31,8	84	121
	140	26	2,0	6216 *	71,0	45,0	90	130
	170	39	2,1	6316 *	124	86,0	91	158
	200	48	3,0	6416	163	125	95	184
85	110	13	1,0	61817 *	18,2	15,5	90	105
	130	14	1,0	16017	34,0	33,5	89	126
	130	22	1,1	6017 *	49,5	43,0	89	126
	150	28	2,0	6217 *	83,0	53,0	95	140
	180	41	2,0	6317 *	132	82,0	98	166
	210	52	4,0	6417 *	174	130	105	190
90	115	13	1,0	61818	20,0	16,7	96	110
	125	18	1,1	61918 *	33,2	31,5	96	119
	140	16	1,0	16018	41,6	39,0	95	135
	140	24	1,5	6018 *	58,5	39,2	95	135
	160	30	2,0	6218 *	95,7	62,0	100	150
	190	43	3,0	6318 *	142	96,0	103	176
	225	54	4,0	6418	186	146	110	215
95	120	13	1,0	61819	22,0	19,2	100	115
	145	16	1,0	16019	41,5	40,5	100	140
	145	24	1,5	6019 *	60,5	41,7	100	140
	170	32	2,1	6219 *	108	69,0	107	158
	200	45	3,0	6319 *	153	108	109	186
100	125	13	1,0	61820	23,0	21,0	105	120
	150	16	1,0	16020	44,2	44,0	105	145
	150	24	1,5	6020 *	60,5	54,0	105	145
	180	34	2,1	6220 *	124	78,0	112	168
	215	47	3,0	6320 *	174	130	113	201
...								

Legend: a) podstawowe wymiary .. = basic dimensions; b) obudowa łożyska = bearing housing;
oznaczenie łożyska = bearing designation

F_a/C_0	e	$F_a/F_r \leq Fe$		$F_a/F_r \leq Fe$	
		X	Y	X	Y
0.025	0.22	1	0	0.56	2
0.04	0.24	1	0	0.56	1.8
0.07	0.27	1	0	0.56	1.6
0.13	0.31	1	0	0.56	1.4
0.25	0.37	1	0	0.56	1.2
0.5	0.44	1	0	0.56	1

Appendix 5: Viscosity Chart [10]

Centi-stokes	Saybolt	Redwood	Engler	η Ns/m²
				100
76000	365000	310500	10000	70
38000	182500	155200	5000	35
				20
15200	73000	62100	2000	
				10
7600	36500	31050	1000	7
				5
3800	18250	15525	500	3
2280	10950	9315	300	
1520	7300	6210	200	2
				1
760	3650	3105	100	0,7
532	2555	2173,5	70	0,5
304	1460	1242	40	0,3
228	1095	931,5	30	0,2
152	730	621	20	
				0,1
76	365	310,5	10	0,07
61	292	248,1	8	0,05
45,1	218	185,1	6	
				0,03
29,3	142,1	122	4	0,025
21,1	104,5	90,8	3	0,02
16,6	85,2	73,9	2,5	0,018
				0,016
				0,015
11,8	65,3	57,9	2	0,014
9,6	56,9	51,2	1,8	0,013
				0,012
7,4	49,4	44,9	1,6	0,011
6,2	45,4	41,6	1,5	
5	41,5	38,5	1,4	0,01
3,9	38	35,4	1,3	0,009

Approximate characteristics of lubrication oils

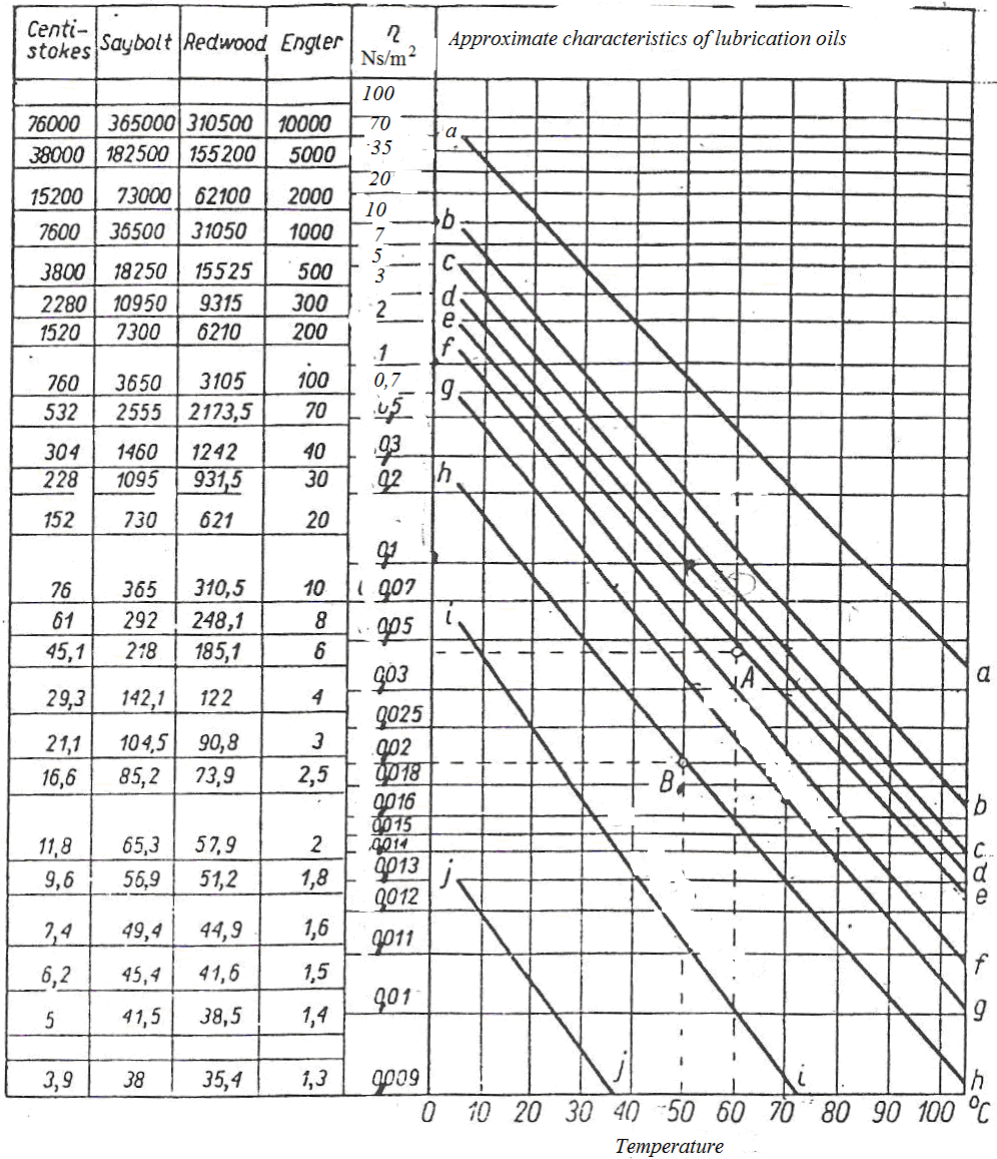Temperature: 0 10 20 30 40 50 60 70 80 90 100 °C

Fig. A5.1. Viscosity of machine oils: a) oil for superheated steam; b) very viscous engine oil; c) medium viscous oil; d) viscous engine oil; e) – f) light engine oils; g) turbine oil (SAE 20); h) light turbine oil (SAE 10); i)spindle oil; j) very light spindle oil.

Appendix 6: Application factor K_a [after 12]

Load duty				
Driver side	Driven/load side			
	Light	Medium	Heavy	Very heavy
Light	1.00	1.25	1.50	1.75
Medium	1.10	1.35	1.6	1.85
Heavy	1.25	1.50	1.75	2 and more
Veryh heavy	1.5	1.75	2.00	2.25 ad more

Driver side: Light: electrical moters, gas and steam turbines (occasional starting)
        Medium: hydraulic motors; sta and gas turbines with frequent staring
        Heavy" internal combustion engines (four and more cylinders)
        Very heavy: one cylinder inernal combustion engines

Load side: Light: uniformly fed conveyors, centrifugl pumps
        Medium: non-uniformly fed conveyors, machine tools, centrifugal compressors, mixsers,
        Heavy: cement mixers; agricultural machinery,3 cylindeer reciprocating pumps,
        Very heavy: mills, crushers, one cylinder eciprocting pumps, drilling equipment

Appendix 7: Dynamic factor K_v [12]]

Accuracy class[*]	Tooth hardness	K_v	Circumferential speed v, in m/s				
			1	3	5	8	10
6	HB<350	K_{Hv}	1.03/1.01	1.09/1.03	1.16/1.06	1.25/1.09	1.32/1.13
		K_{Fv}	1.06/1.03	1.18/1.09	1.32/1.13	1.50/1.20	1.64/1.26
	HRC>45	K_{Hv}	1.02/1.01	1.06/1.03	1.10/1.04	1.16/1.06	1.20/1.08
		K_{Fv}	1.02/1.01	1.06/1.03	1.10/1.04	1.16/1.06	1.20/1.08
7	HB<350	K_{Hv}	1.04/1.02	1.12/1.06	1.20/1.08	1.32/1.13	1.40/1.16
		K_{Fv}	1.08/1.03	1.24/1.09	1.40/1.16	1.64/1.25	1.80/1.32
	HRC>45	K_{Hv}	1.02/1.01	1.06/1.03	1.12/1.05	1.19/1.08	1.25/1.10
		K_{Fv}	1.02/1.01	1.06/1.03	1.12/1.05	1.19/1.08	1.20/1.10
8	HB<350	K_{Hv}	1.05/1.02	1.15/1.06	1.24/1.10	1.38/1.15	1.48/1.19
		K_{Fv}	1.10/1.04	1.30/1.12	1.48/1.19	1.77/1.30	1.96/1.38
	HRC>45	K_{Hv}	1.03/1.01	1.09/1.03	1.15/1.06	1.24/1.09	1.30/1.12
		K_{Fv}	1.03/1.01	1.09/1.03	1.15/1.06	1.24/1.09	1.30/1.12
9	HB<350	K_{Hv}	1.06/1.02	1.12/1.06	1.28/1.11	1.45/1.18	1.56/1.22
		K_{Fv}	1.11/1.04	1.33/1.12	1.56/1.22	1.90/1.36	2.25/1.45
	HRC>45	K_{Hv}	1.03/1.01	1.09/1.03	1.17/1.07	1.28/1.11	1.35/1.14
		K_{Fv}	1.03/1.01	1.09/1.03	1.17/1.07	1.28/1.11	1.35/1.14

* Circumferential speed (m/s) /accuracy/accuracy class:
> 15 m/s = 6; 10 to 15 m/s = 7; 6 to 10 m/s = 8; less than 2 = 9